Institute

Working Paper 146 | **July 2023**

From Climate Stress Testing to Climate Value-at-Risk: A Stochastic Approach

Document for the exclusive attention of professional clients, investment services providers and any other professional of the financial industry

From Climate Stress Testing to Climate Value-at-Risk: A Stochastic Approach

Abstract

Baptiste DESNOS
Amundi Institute
baptiste.desnos@amundi.com

Théo LE GUENEDAL
Amundi Technology
theo.leguenedal-ext@amundi.com

Philippe MORAIS
Amundi Technology
philippe.morais@amundi.com

Thierry RONCALLI
Amundi Institute
thierry.roncalli@amundi.com

This paper proposes a comprehensive climate stress testing approach to measure the impact of transition risk on investment portfolios. Unlike most climate stress testing models, which are designed for the banking industry and follow a top-down approach, our framework considers a bottom-up approach and is mainly relevant for the asset management industry. In this paper, we model the distribution function of the carbon tax, provide an explicit specification of indirect carbon emissions in the supply chain, introduce pass-through mechanisms of carbon prices, and compute the probability distribution of potential (economic and financial) impacts in a Monte Carlo setting. Rather than using a single or limited set of scenarios, we use a probabilistic approach to generate thousands of simulated pathways. We can then examine the impact of transition risk at the economic level and analyze inflation, growth and earnings risks at the sector and country level. We also propose a framework for modeling earnings-at-risk and asset-return shocks at the issuer level. Finally, by combining value-at-risk and stress testing approaches, we define appropriate risk measures for managing climate risk in investment portfolios and asset allocation.

Keywords: Climate change, stress testing, value-at-risk, carbon tax, input-output analysis, cost-push price model, dual Leontief matrix, pass-through, indirect emissions, inflation risk, risk contribution, substochastic matrix, Neumann series, directed graph, copula, Monte Carlo simulation.

JEL classification: C6, G11, Q5.

Acknowledgement

The authors are grateful to Guillaume Coqueret, Yassine Derbel and Frédéric Lepetit for their helpful comments. The opinions expressed in this research are those of the authors and are not meant to represent the opinions or official positions of Amundi Asset Management.

About the authors

Baptiste DESNOS

Baptiste Desnos joined Amundi in January 2023 as an intern in the Quant Portfolio Strategy team of Amundi Institute. He is currently a graduate student at Ecole Centrale de Nantes and Audencia Business School where he studied signal processing and financial markets.

Théo LE GUENEDAL

Théo Le Guenedal joined Amundi's Quantitative Research team in December 2018, after completing his internship, which focused on the performance of ESG investing in the equity market. Since then, he has been involved in an extensive research project on the incorporation of ESG factors and climate risks into asset allocation strategies. He completed his Ph.D. thesis entitled "Financial Modeling of Climate-related Risks" in Applied Mathematics at the Institut Polytechnique in December 2023. This research covers both transition and physical risks. On this occasion, Théo co-authored a paper entitled "Credit Risk Sensitivity to Carbon Price". This work was recognized with the GRASFI Best Paper Prize for Research on Climate Finance, a distinguished honor sponsored by Imperial College London, in 2020. On the subject of physical risks, Théo made significant contributions to the academic domain by creating the Tropical Cyclone Generation Algorithm. This innovative tool incorporates a THERmodynamic module for Integrated National Damage Assessment, known as CATHERINA. More recently, Théo he has been focusing on the integration of advanced climate metrics, stress-tests, and analytics in investment tools at the Amundi Technology's Innovation Lab.

Philippe MORAIS

Philippe Morais joined the Responsible Investments Management team of Amundi Technology in 2022 after his internship dedicated to climate stress test that included the cascading effects caused by the implementation of a carbon price. As part of this role, he contributed to the development of tools and a visualization dashboard on investment portfolios, which allows users to evaluate their portfolio's exposure to transition risk. Since completing his internship, he has taken on an operational and functional role from software development to product line management for ALTO* Sustainability platform. This solution consolidates all ESG and Climate-related metrics and analytics for portfolio managers and investors, thus helping them achieve their sustainable investment goals. Philippe holds an Engineer's Degree in Applied Mathematics and Computer Science from Grenoble INP - Ensimag and a Master's Degree in Quantitative Finance from Grenoble IAE.

Thierry RONCALLI

Thierry Roncalli is the Head of Quant Portfolio Strategy within Amundi Institute. In this role, he steers the quantitative research towards the best interests and ambitions of Amundi and its clients. He is also involved in the development of client relationships and innovative investment solutions.

Prior to his current position, he was the Head of Research and Development at Lyxor Asset Management (2009-2016), Head of Investment Products and Strategies at SGAM AI, Société Générale (2005-2009), and Head of Risk Analytics at the Operational Research Group of Crédit Agricole SA (2004-2005). From 2001 to 2003, he was also a member of the Industry Technical Working Group on Operational Risk (ITWGOR). Thierry began his professional career at Crédit Lyonnais in 1999 as a financial engineer. Before that, Thierry was a researcher at the University of Bordeaux and then a Research Fellow at the Financial Econometrics Research Centre at Cass Business School. During his five-year academic career, he also served as a consultant on option pricing models for different banks.

Since February 2017, he has been a Member of the Scientific Advisory Board of AMF, the French Securities & Financial Markets Regulator, while he was a Member of the Group of Economic Advisers (GEA), ESMA's Committee for Economic and Market Analysis (CEMA) and European Securities and Market Analysis from 2014 to 2018. Thierry is also an Adjunct Professor of Economics at the University of Paris-Saclay (Evry), Department of Economics. He holds a PhD in Economics from the University of Bordeaux, France. He is the author of numerous academic articles in scientific reviews and has published several books on risk and asset management. His last two books are "Introduction to Risk Parity and Budgeting" published in 2013 by Chapman & Hall and which was translated into Chinese in 2016 by China Financial Publishing House, and "Handbook of Financial Risk Management" published in 2020 by Chapman & Hall.

1 Introduction

In the face of escalating greenhouse gas emissions, countries have adopted climate policies to facilitate the transition to a low-carbon economy. However, it is widely acknowledged that these policies, although implemented with the will of limiting climate change, are insufficient to effectively limit global warming to within the 1.5°C threshold by the end of this century (IPCC, 2018). Strengthening existing policies is therefore essential, even though it may entail some economic and financial risks. In addition, the intersection of transition and physical risks may lead to consequential spillovers that spread across different countries and sectors and subtly infiltrate areas of the economy previously thought to be unaffected (Raymond *et al.*, 2020; Naqvi and Monasterolo, 2021). According to the Financial Stability Board, "*a systemic event is the disruption to the flow of financial services that is (i) caused by an impairment of all or parts of the financial system and (ii) has the potential to have serious negative consequences on the real economy*" (FSB, 2009, page 6). With this statement, it becomes incontrovertible that climate-related risk is indeed a systemic risk raising the need for stress testing methodologies.

In response to this need, the literature on climate stress testing has grown considerably in recent years. Indeed, significant attention has been given to the development of financial climate stress tests, particularly in the banking sector. The pioneering work of Battiston *et al.* (2017) proposed the first stress test to consider cascading effects within the banking sector. Roncoroni *et al.* (2021) extended this approach to include investment funds. In the same vein, a number of stress testing models have been proposed by central bankers and academics[1]. However, most of this research is devoted to the banking industry. In the light of these developments, ESMA (2022) has underlined the need for innovative operational stress testing models applicable to the asset management sector.

Several methodological approaches can be distinguished for climate stress testing and, more generally, for assessing transition risk (Le Guenedal, 2022). In asset management, systematic risk is generally measured using the capital asset pricing model or a multi-factor risk model. This approach, adaptable to ESG criteria and transition risk (Bennani *et al.*, 2018; Drei *et al.*, 2019; Roncalli *et al.*, 2020, 2021), has been used to estimate systemic climate risk exposure. For example, Jourde and Moreau (2022) constructed both transition and physical risk factors. However, the factor approach is subject to large variations in exposure and the estimated betas may be too dynamic (Fama and Stern, 2016). As they remain mostly backward-looking, they may not efficiently capture transition risk, especially in the context of a disorderly transition. It is therefore more common to introduce forward-looking scenarios to conduct climate stress tests.

Transition risk methodologies primarily use scenario analysis based on integrated assessment models that embed climate factors into macroeconomic modeling. Most models take a cost-benefit approach, balancing future damage costs against current mitigation efforts. Models vary in technological precision, complexity of macroeconomic feedbacks and market realism. To provide a standard source of information, the network for greening the financial system has selected a set of models and variables that best describe the transition to a greener economy (NGFS, 2022). The six selected scenarios represent all outcomes with their underlying hypothesis, which adds complexity to asset pricing in the context of scenario uncertainty. The main variable of interest used to perform the transition stress test is the carbon price, although it is recognised that other variables should be taken into account. The carbon price provided by these models is not necessarily comparable to effective prices,

[1]See, for example, Allen *et al.* (2020), Alogoskoufis *et al.* (2021), Dunz *et al.* (2021), Gourdel and Sydow (2022), Grippa and Mann (2020), Reinders *et al.* (2023) and Nguyen *et al.* (2021).

and the distinction between the social cost of carbon and the effective carbon pricing mechanism needs to be made, which is also a barrier to understanding effective transition risk. Therefore, we must differentiate implicit costs of carbon, explicit carbon taxes and carbon market prices.

There are two main ways to consider the impact of these scenarios on investment portfolios. First, top-down methods directly use economic variables from integrated valuation models to approximate potential losses at the portfolio level. To illustrate, the study by Vermeulen *et al.* (2018) examined the impact of a \$100/tCO_2 carbon price on sectoral value added and financial indices. To be relevant in asset management, top-down approaches need to rely on precise and granular results at the sector $\times$ country level. Bottom-up approaches, on the other hand, assess the impact at the issuer level and aggregate losses to calculate overall portfolio exposure. For example, the Bank of France's 2020 stress test was a bottom-up analysis (Allen *et al.*, 2020; ACPR, 2021).

The design of these methodologies differs in several aspects (time horizon, climate scenario, risk factors, balance sheet assumptions, etc.). Nevertheless, most of them underestimate the contagion effects in the real economy and the multi-level uncertainty regarding how a shock may cascade between issuers (Cartellier, 2022; Acharya *et al.*, 2023). Indeed, in terms of economic interdependence, most bank stress tests have primarily emphasised the interconnectedness of the financial system rather than the interdependencies within the physical supply chain (Battiston *et al.*, 2017; Roncoroni *et al.*, 2021). Adenot *et al.* (2022) introduced the use of input-output matrices for portfolio stress testing, taking into account cascading effects. Their model builds on several contributions and an extensive literature on price cascading effects measuring the diffusion of carbon and pollutant tax costs across sectors (Gemechu *et al.*, 2014; Mardones and Mena, 2020; Cahen-Fourot *et al.*, 2021).

However, when conducting climate transition stress tests, it is important to recognise the limited information available on the proportion of the carbon price that is passed on to consumers through product prices. To address this, it is necessary to introduce a pass-through mechanism. This reflects how changes in costs faced by firms are reflected in price changes for consumers or downstream markets. A pass-through parameter typically ranges from 0% when the agent bears the full cost burden to 100% when the full amount is passed on to direct customers (Bouchet and Le Guenedal, 2020; Adenot *et al.*, 2022). One of the difficulties is that pass-through rate is not homogeneous across sectors and can vary across industries, markets and firms. Calculating it therefore remains a challenge. There are several approaches to estimating pass-through parameters. A comprehensive report commissioned by the Office of Fair Trading discussed the fundamental aspects of pass-through mechanisms (RBB Economics, 2014). According to this report, pass-through parameters are theoretically influenced by various factors, including supply and demand elasticities, international trade exposure and market structures. Nevertheless, estimation methods are still in their infancy and reveal significant asymmetries at the firm level. Several empirical studies have been carried out to examine the effects of changes in the tax system. These studies compare prices before and after the introduction of a tax. The survey of Sautel *et al.* (2022) showed that the uncertainty of pass-through rates is large. Therefore, the impact of a carbon tax in a climate stress test cannot be summarised by a single figure, but requires a probabilistic approach.

The methodology developed in this paper is based on the various methods listed above. The starting point is an analysis of the NGFS scenarios. The six economic paths are representative of six climate scenarios. Therefore, the uncertainty of a stress test comes from the uncertainty of the occurrence of the given scenario. To run a stochastic stress test program, we could use a probability distribution of the six scenarios. This creates uncertainty as to which climate scenario will be followed. In this case, the stress test is a between-scenario analysis and there is no conditional uncertainty within a scenario[2]. To perform a within-scenario exercise, we could use all the models in the NGFS database and not just the scenario × model selected by NGFS. However, the number of models is limited[3]. Another solution is to use the IPCC database, but the results are not standardised and homogeneous for a given climate scenario (Roncalli, 2023). The real challenge of stress testing is then to model the economic uncertainty and random consequences of a given climate scenario. Another issue in conducting a stress testing program is the definition of the stress scenario. In general, the stress scenario is complex and mixes transition and physical risks. In this context, it is not always obvious to understand the underlying assumptions: the climate policy response function, the change in consumer preferences, the severity/frequency risk of natural disasters, etc. In addition, some variables may be endogenous. For example, the carbon price is an output of integrated assessment models and not an input. In this research project, we prefer to use a very simple framework. We consider only the transition risk and assume that a flat carbon tax is introduced. The stress test scenario is then described by the level of the carbon tax and its scope. For instance, the implementation by the EU of a \$100/tCO_2e carbon tax across all sectors of the economy is a stress scenario.

Our model adopts an environmentally extended input-output framework. Using the value added approach to describe price dynamics, we are able to diffuse the carbon tax across the global value chain. We also introduce a pass-through mechanism and show how it modifies the Leontief multiplier matrix. For a given level of carbon tax, we can then assess the economic cost, the increase in inflation and the impact on different sectors. Having defined the downscaling process, we can assess the transition risk at the firm level, measure the loss distribution of an investment portfolio and propose a risk decomposition. As explained by Roncalli (2020), the scenario design of the stress test is important, in particular the choice of risk factors. Our model has two main sources of risk: the carbon tax and the pass-through rates. We can then introduce several layers of uncertainty. The vector of pass-through rates is a stochastic risk factor and follows a multivariate distribution with beta-distributed margins and a Gaussian copula. We can then estimate the probability distribution function of the output variables given a level of carbon tax. This conditional approach can be extended to the unconditional approach, where the carbon tax is also random. To do this, we use a calibrated log-normal distribution. Thus, our model for estimating the impact of transition risk can be seen as a probabilistic approach with multiple stress scenarios. Our methodology belongs to the stress testing framework because the introduction of a carbon tax of 100 or 250 \$/tCO_2e is indeed a huge economic shock. However, it also belongs to the value-at-risk framework as we obtain a probability distribution of the loss, but without specifying a holding period (Schweimayer and Stoyanova, 2022). Given the great uncertainty of climate change, we believe that the combination of the two frameworks is necessary to obtain a comprehensive range of possible outcomes.

This research paper is organised as follows. Section Two describes the NGFS climate scenarios. Section Three sets the stage for a good understanding of the main source of transition risk and focuses on the price of carbon, whether explicit (market price and carbon tax) or implicit (social cost of carbon). Section Four shows how multi-regional input-output (MRIO) analysis can be used to estimate indirect emissions through the supply chain. Section Five describes the diffusion of the carbon tax and price dynamics, and defines pass-through mechanism and its calibration. Section Six presents the methodology for defining the value-at-risk of investment portfolios. We consider a probabilistic approach with different uncertainties and apply this Monte Carlo simulation approach to investment portfolios. Finally, section Seven draws some conclusions.

[2]Given a scenario, the economic path is deterministic.

[3]The three models are GCAM, MESSAGEix-GLOBIOM and REMIND-MAgPIE.

2 Climate scenarios

As greenhouse gases emissions have been increasing since the industrial revolution, climate policies have been set by countries in order to organize the transition to a low-carbon economy. Actually, we know that they are not sufficient to limit global warming to 1.5°C by the end of this century (IPCC, 2018). Therefore, there is a high uncertainty about the future trajectory of the global economy. In this context, a climate stress testing exercise is not obvious since it depends on many assumptions, and relationships between climate change and the economy are uncertain and unclear. For instance, the transition risk depends on future innovations such as the development of carbon dioxide removal (CDR) technologies, the coordination between countries' climate policies, green preferences of consumers, etc. Moreover, the scientific community has stressed that physical risks may materialize sooner than expected before 2050. Since it is impossible to analyze the different sources of uncertainty, we discuss several major issues for illustrative purpose. The first one concerns the design of climate scenarios. Indeed, the choice of climate scenarios is an important issue. For instance, we can use the net zero emissions by 2050 scenario (NZE) provided by the International Energy Agency (IEA), the 1.5°C scenarios calculated by IPCC (2018) or the AR6 scenarios presented in IPCC (2022). These scenarios have the drawback to be non-homogeneous, meaning that the output variables and the region coverage highly depend on the integrated assessment model that is used and are not always consistent (Roncalli, 2023). Therefore, the investment industry prefer to use the NGFS scenarios that have become a common standard in finance and have been defined for the purpose of stress testing (NGFS, 2020). In particular, the goal of the NGFS scenarios is to help central banks and supervisors to assess both transition and physical risks, and their possible impacts on the economy and the financial system (NGFS, 2022).

2.1 Definition of the NGFS scenarios

The NGFS scenarios framework is a set of six alternative scenarios that can be grouped into three families (Figure 1):

- Orderly scenarios aim at reducing transition and physical risks at a maximum level. Therefore, they assume that climate policies are introduced early and become gradually more stringent.
  - #1 Net zero 2050 (NZ) limits global warming to 1.5°C.
  - #2 Below 2°C (B2D) gradually increases the stringency of climate policies, giving a 67% chance of limiting global warming to below 2°C.
- Disorderly scenarios assume higher transition risk due to a global delay or divergence of climate policies to mitigate global warming.
  - #3 Divergent net zero (DNZ) reaches net zero around 2050.
  - #4 Delayed transition (DT) assumes annual emissions do not decrease until 2030.
- Hot house world scenarios assume more severe physical risk and low transition risk, because global efforts are insufficient to halt global warming.
  - #5 Nationally determined contributions (NDC) includes all pledged targets.
  - #6 Current policies (CP) assumes that only current policies are implemented.

Figure 1: NGFS scenarios framework

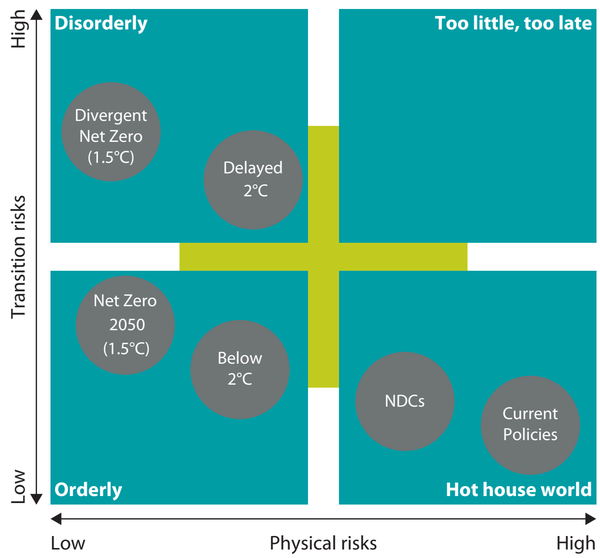

Source: Richters *et al.* (2022).

2.2 Severity of the NGFS scenarios

Despite being based on the same economic background assumptions, all scenarios reflect various combinations of assumptions pertaining to technological situations, climate policies, and the impact of climate change. First, physical risks affect the economy because of event-driven hazards (acute risk) and life condition changes (chronic risk). For instance, the increased severity of extreme weather events (cyclones, floods, etc.) induce more insurance risks and economic losses. In a similar way, chronic impacts on temperature and precipitation may change the labor and agricultural productivity. Second, managing transition risks implies to accelerate the transition to a low-carbon economy. According to NGFS (2022), several factors can then be considered: policy reaction, technology change, carbon dioxide removal and regional differences. Climate policies can be implemented by introducing a carbon tax, setting limits on GHG emissions, increasing public investments, facilitating private investments, etc. This policy dimension of the transition risk must be completed by the technological dimension. Indeed, the decarbonization pathway of the global economy strongly depends on future technologies and solutions. There is a high uncertainty on this second dimension, which also depends on current climate policies and the investment amount in green capex and R&D. Finally, the third dimension is complex to take into account, because it depends on geopolitical issues and coordination between countries. For instance, we know that technology transfer and financial support of developed countries to poor and vulnerable countries is a key challenge to fight global warming and limit physical risks everywhere.

We can assess the severity of the NGFS scenarios by using several metrics, which concern both physical and transition risks. Nevertheless, there is a trade-off between the two dimensions, meaning that a high physical risk is generally associated to a low transition risk. Therefore, a severity measure based on physical/transition dimensions is not always relevant and useful when the two dimensions are combined. It would be better to consider an economic variable that summarizes the stress severity. In Table 2, we report the change (in

Table 1: Risk severity of the NGFS scenarios

Scenario	Physical risk	Transition risk			
		Policy reaction	Technology change	CO_2 removal	Regional differences
B2D	Medium	Medium	Medium	Medium	Low
CP	High	Low	Low	Low	Low
DNZ	Low	High	High	Low	Medium
DT	Medium	High	High	Low	High
NDC	High	Low	Low	Low	Medium
NZ	Low	Medium	High	Medium	Medium

Source: NGFS (2022, page 8).

%) on the world GDP between the baseline scenario and each NGFS scenario[4]. We notice that the severity depends on the time horizon. For instance, if we consider a short-term horizon (2025), we obtain the following ranking in terms of stress severity:

$$\text{DNZ} \succ \text{NZ} \succ \text{B2D} \succ \text{NDC} \succ \text{CP} \succ \text{DT}$$

If we prefer a long-term horizon (2050), the ranking becomes:

$$\text{DT} \succ \text{DNZ} \succ \text{NDC} \succ \text{CP} \succ \text{NZ} \succ \text{B2D}$$

The time horizon is then an important variable when we want to perform a stress testing exercise. While the Net Zero 2050 scenario induces higher economic costs before 2030, its impact is very small between 2030 and 2050. This is not the case for the delayed transition scenario, whose economic costs increase over time.

Table 2: Impact of climate change on GDP (% change wrt baseline)

Year	B2D	CP	DNZ	DT	NDC	NZ
2025	−1.37	−0.76	−8.15	−0.60	−1.12	−4.24
2030	−2.11	−1.43	−9.87	−2.70	−2.14	−4.99
2035	−2.60	−2.27	−10.43	−9.21	−3.17	−4.91
2040	−3.00	−3.24	−10.78	−11.30	−4.26	−4.94
2045	−3.26	−4.17	−10.91	−12.09	−5.15	−4.92
2050	−3.51	−5.26	−11.53	−13.37	−6.16	−4.84

Source: `www.ngfs.net` & `https://data.ene.iiasa.ac.at/ngfs`.

We can perform the same analysis by considering other economic variables and/or regions. For instance, we have reported some figures in Table 3 for USA, Europe and China. The figures measures the impact by 2050. If we consider GDP, the impact highly depends on the country or the region. For the DT scenario, the GDP loss is about 18% for the USA, 11% for Europe and less than 7% for China. We observe similar patterns for the productivity. The impact on the inflation is not significant, because most of the effects are located between 2025 and 2040 while we observe a normalization in the long-run whatever the NGFS scenario we use (Roncalli, 2023). In a similar way, the impact on the unemployment rate is relatively low. This is not the case of public investment and the debt, which depend on the scenario.

[4]We consider the MESSAGEix-GLOBIOM model because it produces differentiated figures between scenarios (Roncalli, 2023).

Table 3: Impact of climate change on economic variables by 2050 (% change wrt baseline)

Region	Variable	B2D	CP	DNZ	DT	NDC	NZ
USA	GDP	−2.67	−4.38	−15.37	−17.66	−6.31	−4.36
	Inflation	−0.02	0.19	−0.50	0.02	0.16	−0.07
	Productivity	−2.79	−4.41	−15.64	−17.45	−6.32	−4.78
	Public investment	9.06	−4.04	−9.93	−10.77	−5.62	8.56
	Unemployment	−0.12	−0.17	−0.18	0.18	−0.10	−0.29
Europe	GDP	−1.02	−2.84	−9.64	−11.02	−4.01	−1.62
	Inflation	0.04	0.15	−0.42	0.09	0.13	−0.00
	Productivity	−0.79	−2.43	−8.66	−9.33	−3.68	−1.25
	Public investment	14.20	−2.71	−8.97	−8.53	−3.87	13.62
	Unemployment	−0.03	−0.09	0.02	0.12	−0.07	−0.07
China	GDP	−2.33	−4.97	−5.13	−6.73	−4.67	−2.76
	Inflation	−0.06	0.25	−0.64	−0.34	0.22	−0.24
	Productivity	−2.26	−5.02	−5.15	−6.67	−4.69	−2.74
	Public investment	3.31	−4.60	−3.37	−4.01	−4.28	3.28
	Unemployment	−0.04	−0.29	0.01	−0.03	−0.23	−0.02

Source: www.ngfs.net & https://data.ene.iiasa.ac.at/ngfs.

Remark 1. *In Appendix B on pages 153–156, we present the heatmaps of GDP impact by 2030 and 2050. If we focus on the 2030 time horizon, two scenarios are relatively severe (DT and NZ), while three scenarios show very low impact (CP, DNZ and NDC). The comparison between 2030 and 2050 scenarios show clearly that the cost of climate change is time-dependent. Moreover, we notice that all regions are not equal. On average, the economic cost will be higher in Africa and Middle East than in the rest of the world.*

2.3 Impact on asset pricing

In the case of an investor, measuring the impact on the economic sphere is not sufficient and must be complemented by an analysis of the financial markets. With the NGFS scenarios, we have access to three financial variables: the central bank intervention rate, which is a proxy for short-term interest rates, the stock price index and the long-term interest rate. We can therefore analyze the impact of climate change on the equity and sovereign bond markets.

Results on equity prices are reported in Figures 2 and 3. On average, the highest impacts are obtained when we consider the DNZ and DT scenarios. The NZ scenario implies negative returns in the stock market on the short run, but the impact could be close to zero on the long run. The B2D scenario presents similar patterns. We could expect the CP and NDC scenarios to have the same behavior, but this is not the case. However, these global results depends on the country. For instance, we observe that the Japanese stock market may face more risk than Chinese, European and US stock markets, especially in the case of B2D, DNZ, DT and NZ scenarios. One explanation is that the Japanese economy may be hurt by more physical risks than the others (DNZ and DT), and the cost to mitigate them may also be higher (B2D and NZ). The Chinese equity market is at risk when we consider the CP and NDC scenarios, but it is more resilient for the other four scenarios. If we consider long-term interest rates, climate change generally induces higher financing costs (Figure 4) and a steeper yield curve in the short term (Figure 5). These results question the sustainability of the private debt, and shows that the impact of climate change on sovereign bond markets may be large.

Figure 2: Evolution of equity prices (% change from baseline)

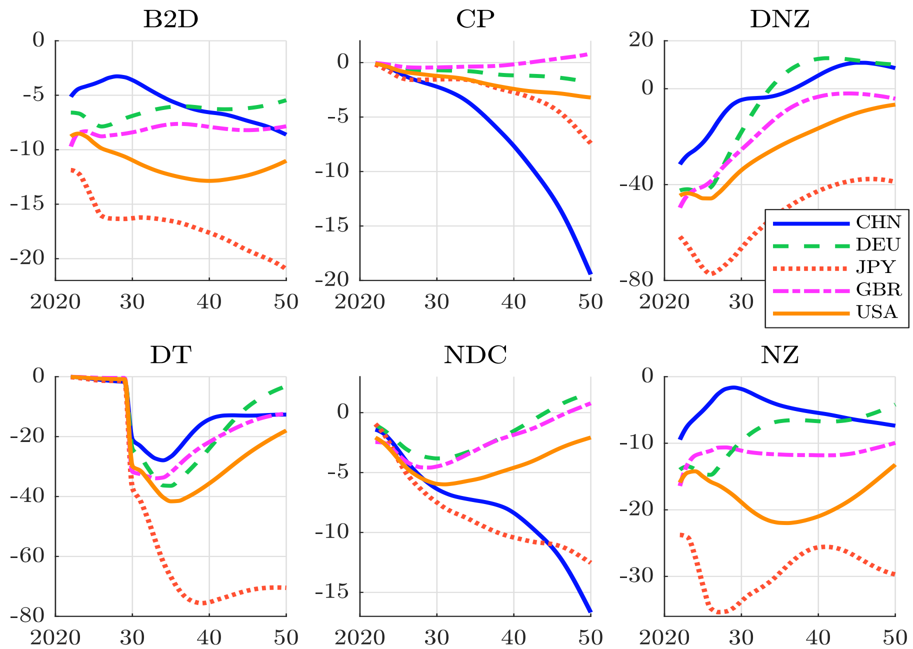

Source: www.ngfs.net & https://data.ene.iiasa.ac.at/ngfs.

Figure 3: Confidence interval of equity prices (% change from baseline)

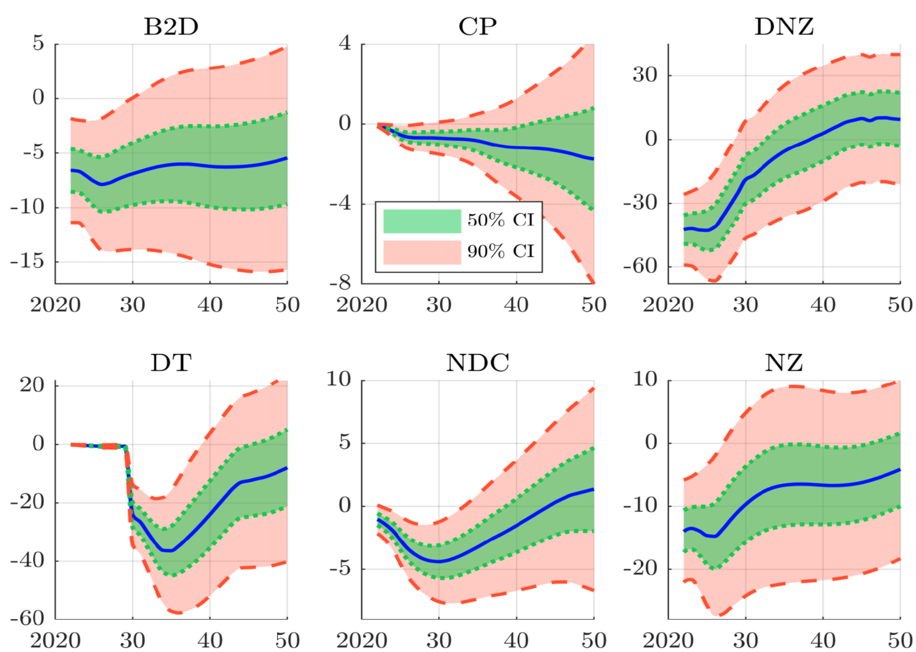

Source: www.ngfs.net, https://data.ene.iiasa.ac.at/ngfs & Authors' calculations.

Figure 4: Confidence interval of long-term interest rates (% change from baseline)

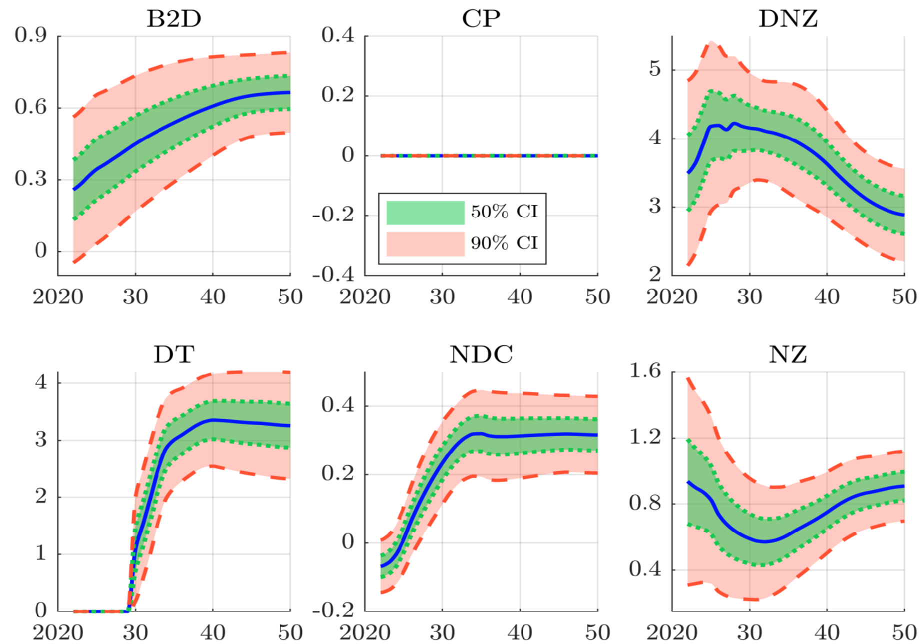

Source: www.ngfs.net, https://data.ene.iiasa.ac.at/ngfs & Authors' calculations.

Figure 5: Confidence interval of the yield curve slope (% change from baseline)

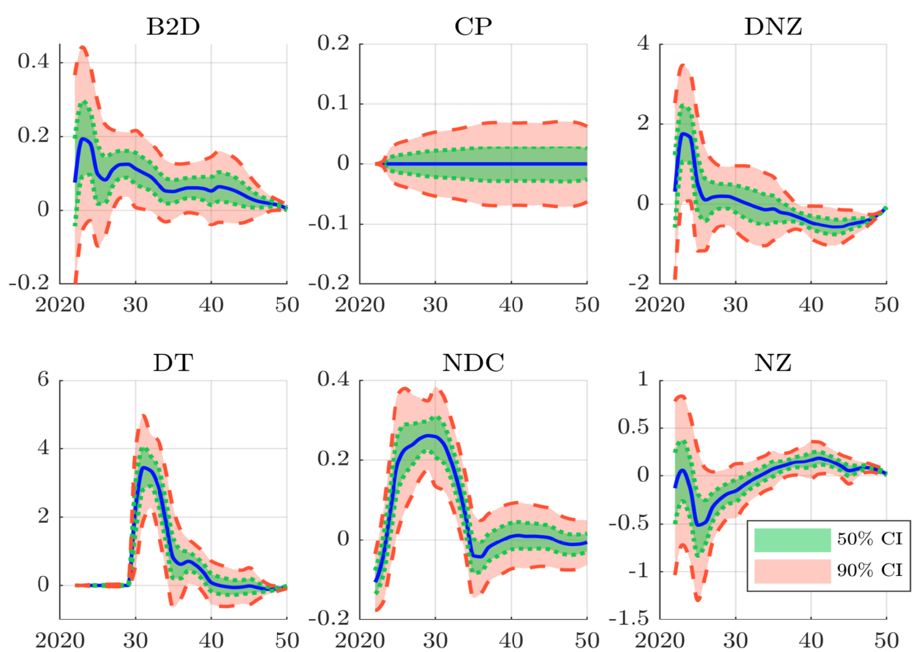

Source: www.ngfs.net, https://data.ene.iiasa.ac.at/ngfs & Authors' calculations.

3 Carbon pricing

One of the major uncertainties in climate stress testing is the climate policy, which is also a control variable in most integrated assessment models. Carbon pricing is the main tool to implement a public policy whose objective is to reduce CO_2 emissions:

> "*Carbon pricing is an instrument that captures the external costs of greenhouse gas (GHG) emissions — the costs of emissions that the public pays for, such as damage to crops, health care costs from heat waves and droughts, and loss of property from flooding and sea level rise — and ties them to their sources through a price, usually in the form of a price on the carbon dioxide emitted.*"
> World Bank (2021), `carbonpricingdashboard.worldbank.org`.

Carbon pricing takes different forms, *e.g.*, carbon tax, ETS, and carbon credit mechanism. The underlying idea is that the biggest emitters of greenhouse gases pay higher taxes or face higher costs. Therefore, they are encouraged to transform their activities, and then lower their emissions. By increasing the price of brown activities, these mechanisms also promote the development of green businesses and stimulate market innovations. Carbon pricing also generates revenues for governments that can be used to finance the transition to a low-carbon economy. Generally, we distinguish two forms of carbon pricing:

1. External carbon pricing
   External pricing is made up of carbon taxes and emissions trading system (ETS). These methods are managed by governments, in order to quantify the external carbon costs, *i.e.* costs related to damages from GHG emissions that people will have to pay. They reflect the price of a tonne of CO_2e emitted.

2. Internal carbon pricing
   Internal prices are set at the corporation level, and can take three different forms (Ahluwalia, 2017; Harpankar, 2019). The first one is an internal carbon fee. It represents the monetary value of each tonne of carbon emissions that arise from the company's business activities. Since the collected amount stays within the company, it thus creates a revenue that can be used to finance the emissions reduction efforts. The second form is a shadow price, which is the theoretical price on carbon that aims at helping long-term business planning and investment strategies. By construction, they are an estimate of carbon pricing that will arise from future regulations. Therefore, shadow prices put incentives on prioritizing low-carbon investments and must help companies to prepare themselves for incoming regulations. The third form of internal carbon pricing is by setting an implicit price, based on how much money a company spends to reduce GHG emissions. This implicit price is calculated retroactively based on the measures implemented to mitigate emissions (*e.g.*, investments in renewable energy) and costs that arise from the efforts made to comply with climate regulations and public policies.

In Figure 6, we report the different explicit carbon prices. According to Poupard *et al.* (2022), there are 68 explicit carbon pricing mechanisms as of 1st August 2022, with the following breakdown: 32 emission trading systems and 36 carbon taxes. We notice that some countries have chosen to implement simultaneously the two carbon pricing tools. For example, this is the case of the Canada federal mechanism, New Brunswick, Newfoundland and Labrador, and Switzerland. In some European countries (*e.g.*, Austria and Germany), a national ETS complements the EU ETS.

Figure 6: Map of explicit carbon prices around the world in 2022

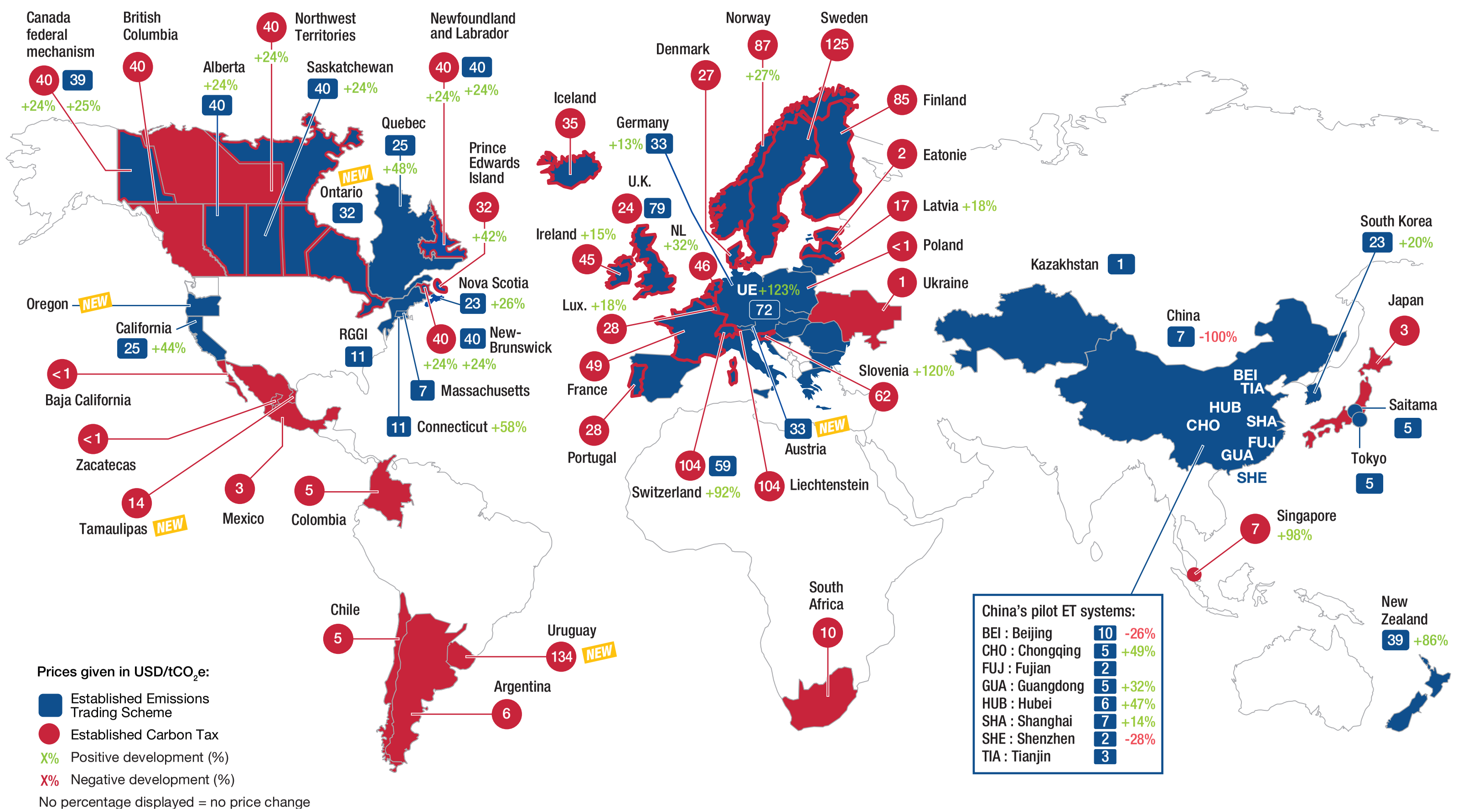

Source: Poupard *et al.* (2022, page 2) based on data from I4CE, ICAP, World Bank and public information.

3.1 Emission trading system

An emission trading system (ETS) allows corporations (and countries) to trade carbon emissions to meet their targets. This system is based on a global amount of emissions that can be traded by the different entities on a carbon market. There are two main types of ETS. The first one is a cap-and-trade system, which sets an absolute emission cap. Emissions allowances, which are partly distributed and auctioned, are then traded by the entities in the emissions allowance market. The second one is a baseline-and-credit system. Baseline levels of emissions are set for individual entities. Then, emission credits are issued by entities that have lowered their emissions below the baseline level, and these credits are traded by entities that have exceeded their baseline level.

Figure 7: Evolution of the EU ETS carbon allowance price

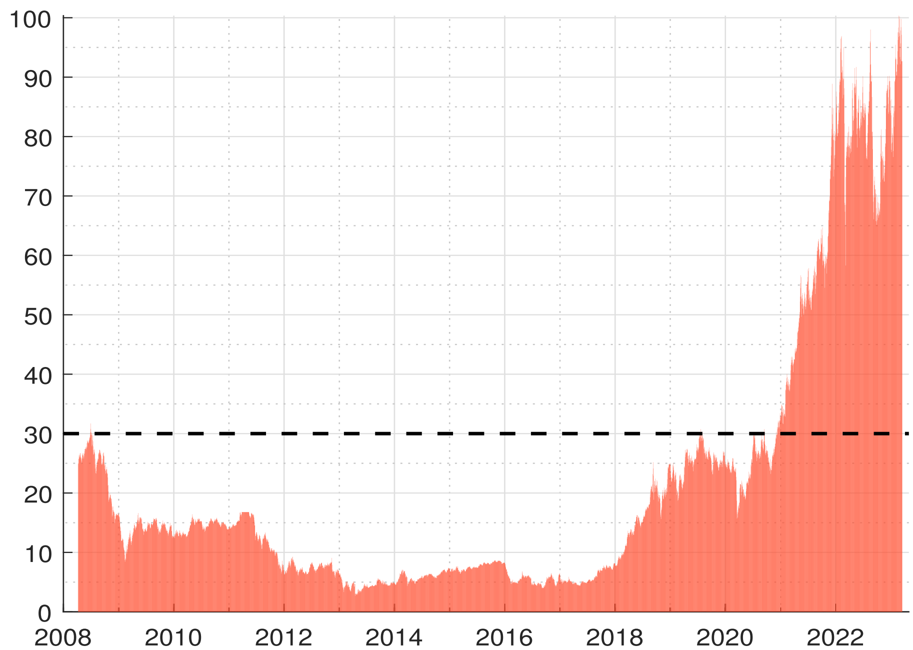

Source: Factset (2023).

The European Union ETS was created in 2005, with the goal of pricing emissions that can be accurately estimated[5]. In Figure 7, we report the carbon price of the EU cap-and-trade ETS. It is worth noting that for a considerable period of time, the carbon price remained below €30/tCO_2e. In particular, the carbon price saw a sharp decline after the Global Financial Crisis from €30 in 2008 to a mere €2.75 in April 2013. Phase 4 started in 2021

[5]Today, EU ETS accounts for:

- Carbon dioxide (CO_2) emissions that come from electricity and heat generation, and energy-intensive industry sectors (oil refineries, steel works, production of iron, aluminum, metals, cement, lime, glass, ceramics, pulp, paper, cardboard, acids and bulk organic chemicals);
- Nitrous oxide (N_2O) from production of nitric, adipic and glyoxylic acids and glyoxal;
- Perfluorocarbons (PFCs) from the production of aluminium.

Even though participation in the EU ETS is mandatory for the companies from theses sectors, some companies below a certain size can be exempted. Concerning the aviation sector, only flights between European Economic Area airports are concerned.

with the goal of reducing GHG emissions by 40%, compared to 1990 levels. But the last review of the EU ETS aims at reducing net emissions by 55%. As a result, the carbon price went from €34 in January 2021 to nearly €100 in February 2023.

Let us assume that the carbon price $\mathcal{CP}(t)$ follows a geometric Brownian motion (GBM):

$$\mathrm{d}\mathcal{CP}(t) = \mu\mathcal{CP}(t)\,\mathrm{d}t + \sigma\mathcal{CP}(t)\,\mathrm{d}W(t)$$

where $W(t)$ is a standard Wiener process. In order to test this assumption, we compute the empirical volatility $\hat{\sigma}(h)$ of the relative variation of $\mathcal{CP}(t)$ using the previous EU ETS data[6]. We consider different time horizons h and plot the standard deviation $\hat{\sigma}(h)$ with respect to h (Figure 8). We notice that we can easily fit the non-parametric curve with the square-root-of-time rule: $\hat{\sigma}(h) \approx \beta_0 + \beta_1\sqrt{h}$. We conclude that we can approximate the carbon price by a GBM process. The ML estimation gives $\hat{\mu} \approx 20\%$ and $\hat{\sigma} \approx 50\%$. In Figure 9, we report the distribution of $\mathcal{CP}(t)$ by assuming an initial carbon price of \$100. We observe the high kurtosis of the carbon price, which is due to the high volatility of the relative variation. Indeed, an empirical volatility of 50% typically corresponds to the volatility of commodities, which is higher than that of single stocks. In Table 4, we compute the exceedance probability[7] $\Pr\left\{\mathcal{CP}(t) \geq x \mid \mathcal{CP}(0) = \mathcal{CP}_0\right\}$ by assuming that $\mathcal{CP}_0 = 100$, $\mu = 20\%$ and $\sigma = 50\%$. Based on this model, there is a probability of 27% to observe a carbon tax greater than \$5 000 in 30 years. Even if we set $\mu = 0$, the probability is not equal to zero. This demonstrates the high uncertainty when modeling the carbon price.

Table 4: Exceedance probability $\Pr\left\{\mathcal{CP}(t) \geq x \mid \mathcal{CP}(0) = 100\right\}$ in % ($\sigma = 50\%$)

μ	x	t (in years) 1	2	5	10	20	30
20%	200	10.82	22.12	38.80	51.43	64.09	71.51
	500	0.11	1.95	13.48	29.34	48.05	59.25
	1 000	0.00	0.12	4.23	16.31	35.98	49.23
	5 000	0.00	0.00	0.08	2.28	14.04	27.20
0%	200	5.09	9.11	11.92	10.95	7.66	5.24
	500	0.03	0.43	2.28	3.53	3.30	2.52
	1 000	0.00	0.02	0.44	1.23	1.59	1.35
	5 000	0.00	0.00	0.00	0.05	0.21	0.26

Remark 2. *We generally obtain lower values with other emission trading systems, except with the UK ETS carbon price (Figure 93 on page 157). In this case, the correlation between the two systems is equal to 75%.*

[6] We define the relative variation as follows:

$$R(t,h) = \frac{\mathcal{CP}(t) - \mathcal{CP}(t-h)}{\mathcal{CP}(t-h)}$$

and compute the standard deviation $\hat{\sigma}(h)$:

$$\hat{\sigma}(h) = \frac{1}{n-1}\sum_t \left(R(t,h) - \frac{1}{n}\sum_t R(t,h)\right)^2$$

where n is the number of non-missing observations.

[7] It is equal to:

$$\Pr\left\{\mathcal{CP}(t) \geq x \mid \mathcal{CP}(0) = \mathcal{CP}_0\right\} = \Phi\left(\frac{1}{2}\sigma\sqrt{\tau} - \frac{1}{\sigma\sqrt{\tau}}\ln\frac{x}{e^{\mu t}\mathcal{CP}_0}\right)$$

Figure 8: Volatility of carbon prices satisfies the square-root-of-time rule

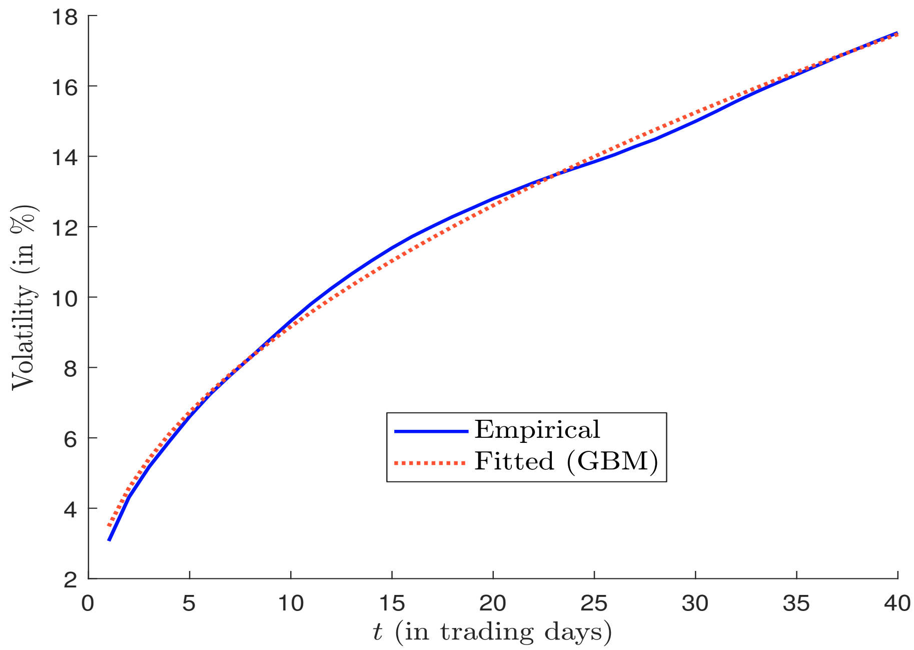

Figure 9: Probability density function of the carbon price

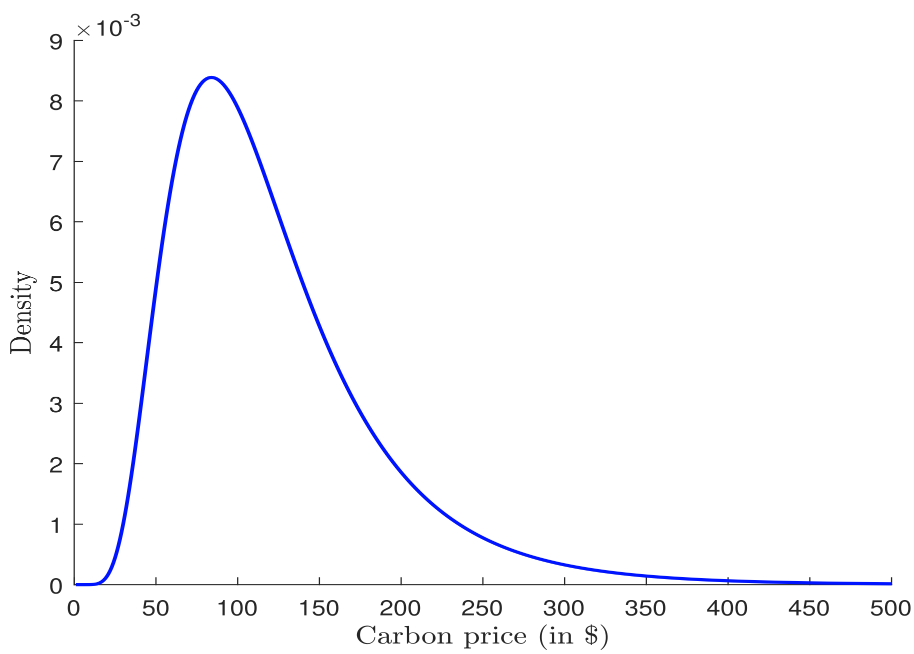

3.2 Social cost of carbon

The social cost of carbon (SCC) is defined as the present value of the impact of an additional tonne of CO_2 emitted in the atmosphere. It is a measure of the externality of future carbon emissions. For instance, a SCC of \$100 means that emitting one extra tonne of CO_2 today has the same consequence on the social welfare as a reduction of consumer's consumption by \$100. In this sense, the social cost of carbon differs from the effective price that reflects the market trading price. Following Bouchet and Le Guenedal (2020), the SCC can be computed by two main approaches:

- The cost-benefit approach consists in finding the optimal trajectory of carbon emissions and computing the optimal carbon price, which is obtained by equalizing the marginal cost of reducing GHG emissions and the marginal benefit of the avoided damage (Nordhaus, 1991).
- The cost-efficiency approach tends to estimate the optimal price of carbon that will allow to meet emission reduction targets. For instance, which carbon price a country must implement to reach a 20% reduction of GHG emissions by 2030?

Cost-benefit analysis are often used by integrated assessments models (IAMs). For instance, the social cost of carbon in the DICE model is computed as follows:

$$\text{SCC}\,(t) = -\frac{\dfrac{\partial\, W}{\partial\, \boldsymbol{\mathcal{CE}}(t)}}{\dfrac{\partial\, W}{\partial\, C(t)}} = -\frac{\partial\, C(t)}{\partial\, \boldsymbol{\mathcal{CE}}(t)}$$

where W denotes the social welfare function, $\boldsymbol{\mathcal{CE}}(t)$ is the total GHG emissions at time t and $C(t)$ is the consumption at time t. The term $\dfrac{\partial\, W}{\partial\, \boldsymbol{\mathcal{CE}}(t)} \leq 0$ is the marginal social welfare with respect to GHG emissions, while $\dfrac{\partial\, W}{\partial\, C(t)} \geq 0$ is the marginal utility of consumption. Therefore, the social cost of carbon is the opposite of the marginal variation of the consumption with respect to a marginal variation of GHG emissions. In fact, there are several ways to compute the SCC. For instance, Wang *et al.* (2019) reviewed the different formulas to estimate the SCC from the academic literature based on the cost-benefit analysis. Nevertheless, as noticed by Clarkson and Deyes (2002), its estimation is subject to deep uncertainties that can be scientific (current and futures level of GHG emissions, damage function, etc.) or concerns the economic valuation (economic impact, abatement cost, discount rate, etc.). The Stern-Nordhaus controversy is one illustration of these uncertainties.

What is the typical level of the social cost of carbon? In fact, there is no obvious answer since it depends on many parameters. For instance, in Table 5, we report the SCC estimated for the standard DICE model computed by Nordhaus (2017). Under the baseline scenario assumption[8], the SCC value is \$31.2/tCO_2 in 2015 and reaches \$102.5/tCO_2 in 2050, implying a compound annual growth rate of 3.46%. The optimal scenario gives SCC figures that are similar to the baseline scenario. Nordhaus (2017) also evaluated two alternative scenarios: the 2.5°C-max scenario constraints the temperature to be below 2.5°C, whereas the 2.5°C-mean imposes an average temperature of 2.5°C for the next 100 years. The impact of these two alternative scenarios is significant. In this case, the social cost of carbon can reach the value \$1 000/tCO_2 in 2050.

[8]The baseline scenario corresponds to the current policy.

Table 5: Global SCC under different scenario assumptions (in $\$/tCO_2$)

Scenario	2015	2020	2025	2030	2050	CAGR
Baseline	31.2	37.3	44.0	51.6	102.5	3.46%
Optimal	30.7	36.7	43.5	51.2	103.6	3.54%
2.5°C-max	184.4	229.1	284.1	351.0	1 006.2	4.97%
2.5°C-mean	106.7	133.1	165.1	203.7	543.3	4.76%

Source: Nordhaus (2017, Table 1, page 1520).

The SCC is currently used by the US government to inform climate change policies. In 2009, US President Barack Obama established the interagency working group on social cost of greenhouse gases, whose objective is the following:

> "*The interagency working group (IWG) on the social cost of greenhouse gases is committed to ensuring that the estimates agencies use when monetizing the value of changes in greenhouse gas emissions resulting from regulations and other relevant agency actions continue to reflect the best available science and methodologies.*" (IWG, 2021, page 1).

The first estimates were published in 2010 and were around $\$30/tCO_2$ (Wagner, 2021) for the year 2020. Then, IWG proposed a price of $\$50/tCO_2$ in 2013 and made several revisions in 2015 and 2016. According to Wagner *et al.* (2021, page 546), "*former president Donald Trump changed the terms for the SCC from 2017. He limited damages to those within the United States, omitting impacts that will be felt in other countries. And he gave an unrealistically low estimate of the costs of future damages as counted in today's dollars. Together, these changes slashed the SCC to $1-7 per tonne: too low to influence policy*". In February 2021, IWG published a new analysis with computed SCC values for CO_2, CH_4 and N_2O. Figures are reported in Table 6 for three different values of the discount rate. For instance, if the discount rate is set to 5%, the social cost of carbon is equal to $19, while the social cost of methane is equal to $940 for GHG emissions emitted in 2030. Currently, the Biden administration uses a value of $\$51/tCO_2$, which corresponds to a discount rate of 3% and the 2020 emission year (Rennert *et al.*, 2021). In September 2022, the US Environmental Protection Agency published a controversial report for two main reasons. First, the EPA is a member of the IWG and has participated in the works of IWG (2021) one year earlier. Second, the EPA report presents new and updated results that are highly different from those we can find in the IWG report. Table 6 gives some figures with respect to the Ramsey discount rate (1.5%, 2% and 2.5%). For instance, if we consider the 2% case, the social cost of carbon is equal to $193 instead of $51, implying a multiplication factor of 3.75.

The previous results show the high uncertainty around the computation of the SCC. Of course, it strongly depends on the modeling of the discount rate. For example, using a constant Ramsey discount rate is equivalent to use a stochastic discount rate. Nevertheless, the uncertainty does not only concerns the model parameters. It is also related to the integrated assessment model. IWG and the EPA uses three models: DICE, FUND and PAGE (Roncalli, 2023). Generally, the most conservative results are obtained with the PAGE model followed by the DICE model, while FUND is viewed as the less conservative model. In Figure 10, we report the histograms of the SCC estimates, which are obtained by IWG[9] in July 2015. Each histogram is based on a Monte Carlo simulation with 10 000 replications and five different climate scenarios (IMAGE, MERGE Optimistic, MESSAGE,

[9] The data are available at https://obamawhitehouse.archives.gov/omb/oira/social-cost-of-carbon.

Table 6: Comparison of IWG and EPA SCC values (in 2020 dollars per tonne)

Agency	Year	CO_2			CH_4			N_2O		
		5%	3%	2.5%	5%	3%	2.5%	5%	3%	2.5%
IWG (2021)	2020	14	51	76	670	1 500	20 00	5 800	18 000	27 000
	2030	19	62	89	940	2 000	25 00	7 800	23 000	33 000
	2040	25	73	103	1 300	2 500	31 00	10 000	28 000	39 000
	2050	32	85	116	1 700	3 100	38 00	13 000	33 000	45 000
		2.5%	2.0%	1.5%	2.5%	2.0%	1.5%	2.5%	2.0%	1.5%
EPA (2022)	2020	117	193	337	1 300	1 600	2 300	35 000	54 000	87 000
	2030	144	230	384	1 900	2 400	3 200	45 000	66 000	100 000
	2040	173	267	431	2 700	3 300	4 200	55 000	79 000	120 000
	2050	205	308	482	3 500	4 200	5 300	66 000	93 000	140 000

Source: IWG (2021, Tables 1–3, pages 5–6) & EPA (2022, Table 4.2.1, page 120).

Figure 10: Histogram of the 150 000 US Government SCC estimates for 2020 with a 3% discount rate

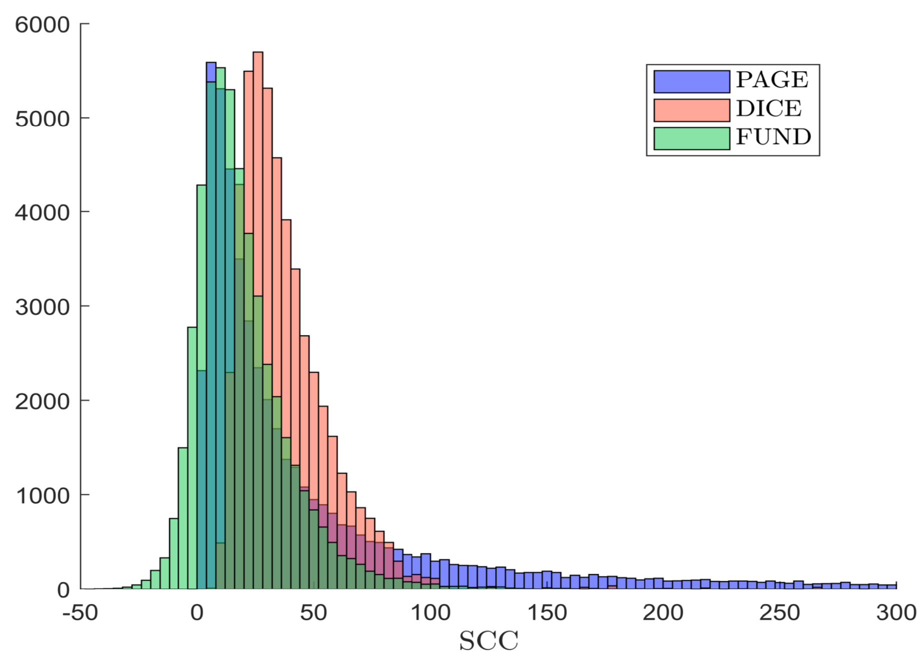

The figure combines the 50 000 2020 3% discount rate estimates from each of the three US Government models to illustrate their influence on the aggregate histogram that determines the official USG SCC for 2020 at 3%, which is equal to \$41.6 (average) and \$123.4 (95th percentile).

Source: IWG (2015), Rose *et al.* (2017, page 3) & Authors' calculations.

MiniCAM Base, 5th Scenario). Below, we also report the average and the 95th percentile:

Model	Average	95th percentile
DICE	37.8	74.0
FUND	19.3	56.4
PAGE	67.7	289.8
IWG	41.6	123.4

We notice that the probability distribution of SCC values is right-skewed. In fact, we may consider that the SCC follows a log-normal distribution:

$$\text{SCC} \sim \mathcal{LN}\left(\mu, \sigma^2\right)$$

As for the case of the carbon price, we can calibrate the parameters of the probability distribution with the traditional estimators: $\hat{\mu} = n_S^{-1} \sum_{i=1}^{n_S} \ln(\text{SCC}_i)$ and $\hat{\sigma}^2 = n_S^{-1} \sum_{i=1}^{n_S} \ln^2(\text{SCC}_i) - \hat{\mu}^2$ where $\left\{\text{SCC}_1, \ldots, \text{SCC}_{n_S}\right\}$ is a sample of n_S simulated values of the SCC. Another approach consists in using the following scaling rule: $\text{SCC}(\alpha) \approx k_\alpha \mathbb{E}[\text{SCC}]$ where $\text{SCC}(\alpha)$ is the quantile at the confidence level α, $\mathbb{E}[\text{SCC}]$ is the expected value and k_α is the scaling factor. For instance, we observe that:

$$\text{SCC}(95\%) \approx 3 \times \mathbb{E}[\text{SCC}]$$

In Appendix A.2 on page 144, we present another calibration procedure to estimate the parameters (μ, σ). Using this method with the SCC values generated in IWG (2015), we obtain Figure 11. We notice the big impact of the discount rate (2.5%, 3% and 5%). We also observe the "*randomness characteristics*" of the SCC. Using a constant value for the SCC is really challenging.

Figure 11: Probability distribution of the SCC

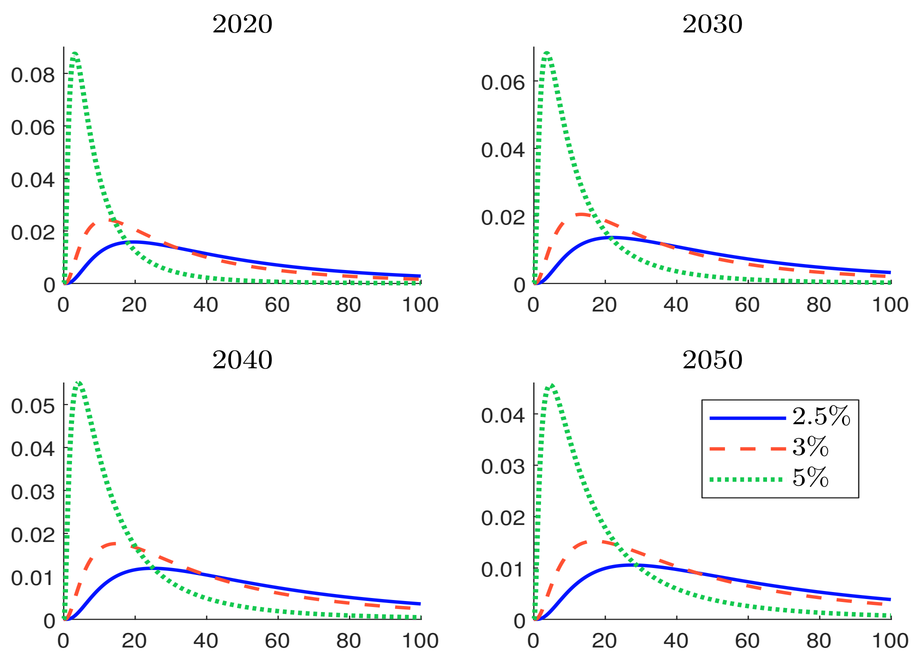

3.3 Carbon tax

Another approach of carbon pricing is through a carbon tax system. In this case, a specific amount has to be paid and is a linear function of the carbon emitted. It differs from an emission trading system since the carbon price is fixed and constant, but not the amount of saved GHG emissions. Therefore, issuers can still decide to pay and not make efforts to reduce their emissions.

Table 7: Carbon tax $\mathcal{CT}$ in the world (in \$/tCO_2)

Country	2017	2018	2019	2020	2021	2022	Share
Sweden	139.84	139.11	126.78	119.43	137.24	129.89	40%
Liechtenstein	86.95	100.90	96.46	99.44	101.47	129.86	81%
Switzerland	86.95	100.90	96.46	99.44	101.47	129.86	33%
Norway	56.25	64.29	59.22	52.89	69.33	87.61	63%
Finland	73.23	76.87	69.66	67.80	72.83	85.10	36%
France	36.03	55.30	50.11	48.77	52.39	49.29	35%
Ireland	23.62	24.80	22.47	28.43	39.35	45.31	40%
Canada			15.00	21.10	31.83	39.96	22%
Iceland	22.57	35.71	31.34	29.88	34.83	34.25	55%
Denmark	27.38	28.82	26.39	25.93	28.14	26.62	35%
Portugal	8.09	8.49	14.31	25.83	28.19	26.44	36%
United Kingdom	23.78	25.46	23.59	22.28	24.80	23.65	21%
Slovenia	20.43	21.45	19.44	18.92	20.32	19.12	52%
Latvia	5.32	5.58	5.06	9.84	14.10	16.58	3%
Spain		24.80	16.85	16.40	17.62	16.58	2%
South Africa				7.06	9.15	9.84	80%
Colombia	5.00	5.67	5.17	4.24	5.00	5.01	23%
Chile	5.00	5.00	5.00	5.00	5.00	5.00	29%
Argentina			6.24	5.94	5.54	4.99	20%
Mexico	2.89	3.01	2.99	2.42	3.18	3.72	44%
Singapore			3.69	3.51	3.71	3.69	80%
Japan	2.62	2.74	2.60	2.69	2.61	2.36	75%
Estonia	2.36	2.48	2.25	2.19	2.35	2.21	6%
Ukraine	0.01	0.02	0.37	0.38	0.36	1.03	71%
Poland	0.08	0.09	0.08	0.07	0.08	0.08	4%

Source: World Bank Carbon Pricing Dashboard (2023),
`carbonpricingdashboard.worldbank.org/map_data`.

Table 7 shows the global carbon tax evolution at the country level[10]. These figures are very difficult to compare, because they do not cover the same sectors. In 2022, the carbon tax was equal to \$129.89 in Sweden, \$16.58 in Spain and \$2.36 in Japan, but the target share of GHG emissions covered was different: 40% in Sweden, 2% in Spain and 75% in Japan. Therefore, there is no global homogeneity within countries. For some countries, this is the main instrument, while it complements other mechanisms such as an ETS in other countries. For example, the Portugal carbon tax serves as a complementary policy measure to the EU ETS. It applies to CO_2 emissions from mainly the industry, buildings and transport sectors, and sectors that are covered under the EU ETS. Sectors that do not use fossil fuels are

[10]We do not consider carbon taxes from regional or federal states, which are mainly implemented in Canada or Mexico (*e.g.*, Baja California, New Brunswick, Newfoundland and Labrador, Northwest Territories, Prince Edward Island, Zacatecas)

Figure 12: Implied carbon prices

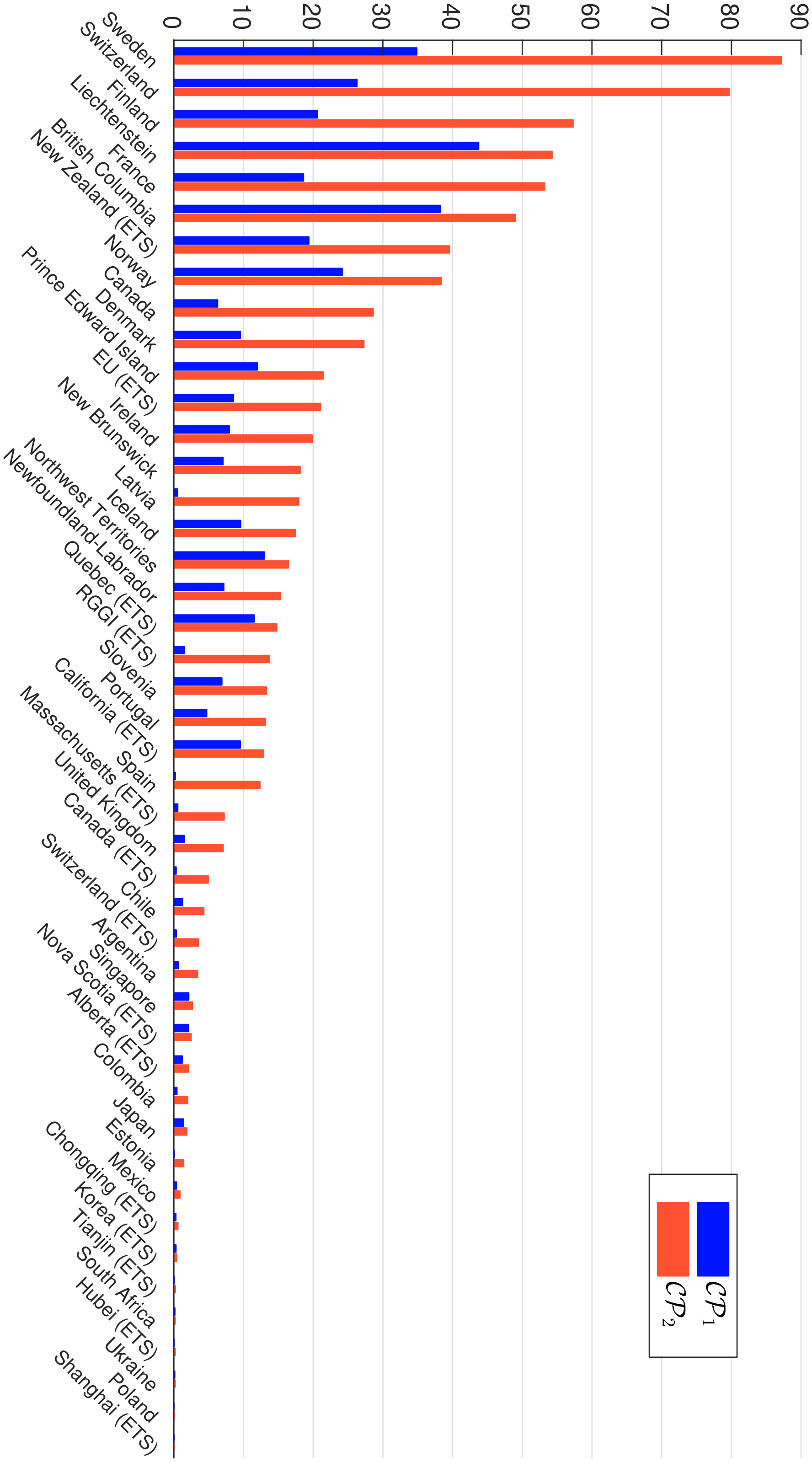

Source: World Bank Carbon Pricing Dashboard (2023), carbonpricingdashboard.worldbank.org/map_data & Authors' calculations.

exempt from paying the carbon tax. Another big difference is that the carbon tax can be paid by producers or consumers. In France, the carbon tax[11] is paid by individuals and businesses and added to the final price of petrol, diesel, heating oil or natural gas. In this context, it is difficult to compare the carbon tax level across countries.

Nevertheless, we can estimate the implied carbon price generated by the government revenues collected from the carbon tax. If we consider the global level of GHG emissions, the carbon price is equal to:

$$\mathcal{CP}_1 = \frac{\mathcal{R}}{\mathcal{CE}}$$

where $\mathcal{R}$ corresponds to the revenues generated by the carbon tax and $\mathcal{CE}$ is the GHG emissions of the country. If we restrict the analysis to the covered GHG emissions, the formula of the carbon price becomes:

$$\mathcal{CP}_2 = \frac{\mathcal{R}}{s^\star \cdot \mathcal{CE}}$$

where $s^\star$ is the target share of GHG emissions. In Figure 12 we report the two implied carbon prices $\mathcal{CP}_1$ and $\mathcal{CP}_2$. By construction, we have[12] $\mathcal{CT} \geq \mathcal{CP}_2 \geq \mathcal{CP}_1$. We observe a difference between $\mathcal{CT}$ and $\mathcal{CP}_2$, because the target share of covered GHG emissions is different from the effective share of covered GHG emissions[13]. Carbon prices $\mathcal{CP}_2$ greater than \$50/tCO_2 are exceptional (Sweden, Switzerland, Finland, Liechtenstein and France). If we consider the global GHG emissions (and not only the target share), the maximum carbon price $\mathcal{CP}_2$ is observed for Liechtenstein with a price of \$54.3/tCO_2. These implemented carbon taxes are far below the last values of the social cost of carbon computed by academics (Rennert *et al.*, 2021).

3.4 Impact of a flat carbon tax

Let us assume that a flat-rate tax $\mathcal{CT}$ is applied on direct carbon emissions. The direct cost (expressed in \$) is equal to:

$$\mathcal{C}ost = \mathcal{CT} \cdot \mathcal{CE}_1$$

where $\mathcal{CE}_1$ is the scope 1 emissions expressed in tCO2e. For instance, if we consider the universe of corporations in the MSCI World index at the end of December 2021, a carbon tax of \$100/tCO_2 generates a direct cost of \$373.64 bn. This represents 30.35% of the dividends distributed by these corporates in 2021, and respectively 10.57% and 1.15% of their net profit and sales. In Table 8, we report these ratios by sector[14]. We notice a high discrepancy between sectors. For instance, a tax of \$100 implies a direct cost, which represent less than 1% of the dividends for Communication Services, while it is greater than two times the amount of dividends for Utilities. In fact, the three main contributors are Utilities, Materials and Energy, which represent respectively 35.91%, 26.80% and 19.77% of the total cost amount. The total contribution of these three sectors is then equal to 82.5% while their weight in the MSCI World index is less than 10%.

Another way to illustrate the high heterogeneity between sectors is to compute the break-even price $\mathcal{CT}^\star$, which is the solution of the equation $\mathcal{C}ost = \mathcal{P}rofit$. Since the direct cost

[11] Known as taxe intérieure de consommation sur les produits énergétiques (TICPE).

[12] Indeed, if there is no tax exemption, the revenues generated by the carbon tax are equal to $\mathcal{R} = \mathcal{CT} \cdot (s^\star \cdot \mathcal{CE})$, because $s^\star \cdot \mathcal{CE}$ measures the covered GHG emissions.

[13] The reason is that there are generally many tax exemptions.

[14] DY is the dividend yield, $\mathcal{CT}/\mathcal{D}ividend$ is the ratio of the carbon tax and the distributed dividend, $\mathcal{CT}/\mathcal{P}rofit$ is the ratio between the carbon tax and the net profit, $\mathcal{CT}/\mathcal{S}ales$ is the ratio between the carbon tax and the net sales and $\mathcal{MC}$ is the market capitalization.

Table 8: Carbon tax ratios (in %) by sector (MSCI World index, December 2021, $\mathcal{CT}$ = \$100/tCO_2)

Sector	DY	$\mathcal{Cost}/\mathcal{Dividend}$	$\mathcal{Cost}/\mathcal{Profit}$	$\mathcal{Cost}/\mathcal{Sales}$	Breakdown	
					$\mathcal{Cost}$	MC
Communication Services	1.22	0.93	0.22	0.03	0.20	8.37
Consumer Discretionary	0.87	8.15	1.80	0.14	1.83	12.28
Consumer Staples	2.54	6.80	3.96	0.25	2.28	6.93
Energy	4.60	81.64	42.38	3.11	19.77	2.98
Financials	2.76	3.02	0.85	0.15	2.07	13.20
Health Care	1.58	1.80	0.71	0.07	0.66	12.65
Industrials	1.64	30.45	10.82	0.85	9.90	10.24
Information Technology	0.73	1.42	0.41	0.07	0.45	23.67
Materials	3.73	94.05	40.36	4.97	26.80	4.17
Real Estate	2.39	0.99	0.57	0.13	0.13	2.79
Utilities	3.10	210.64	153.90	9.71	35.91	2.73

Source: Factset (2023) & Authors' calculations.

is an increasing function of the carbon tax, $\mathcal{CT}^{\star}$ indicates the maximum level of the carbon tax that can be supported in order to guarantee that the net profit of corporations is not offset by the direct cost of the carbon tax. On a global basis, $\mathcal{CT}^{\star}$ is equal to \$946 per tonne of CO_2e. The results of our sector analysis are given in Figure 13. We obtain the following ranking. The break-even price is minimum for the Utilities sector with a value of \$65. Then, we obtain the Energy and Materials sectors, whose break-even price is about \$250. The fourth sector is Industrials with a price close to \$1 000. It is followed by Consumer staples and Consumer discretionary. Finally, five sectors present a price greater than \$10 000: Financials, Health Care, Real Estate, Information Technology and Communication Services.

Figure 13: Break-even carbon tax in \$/tCO_2 (MSCI World index, December 2021)

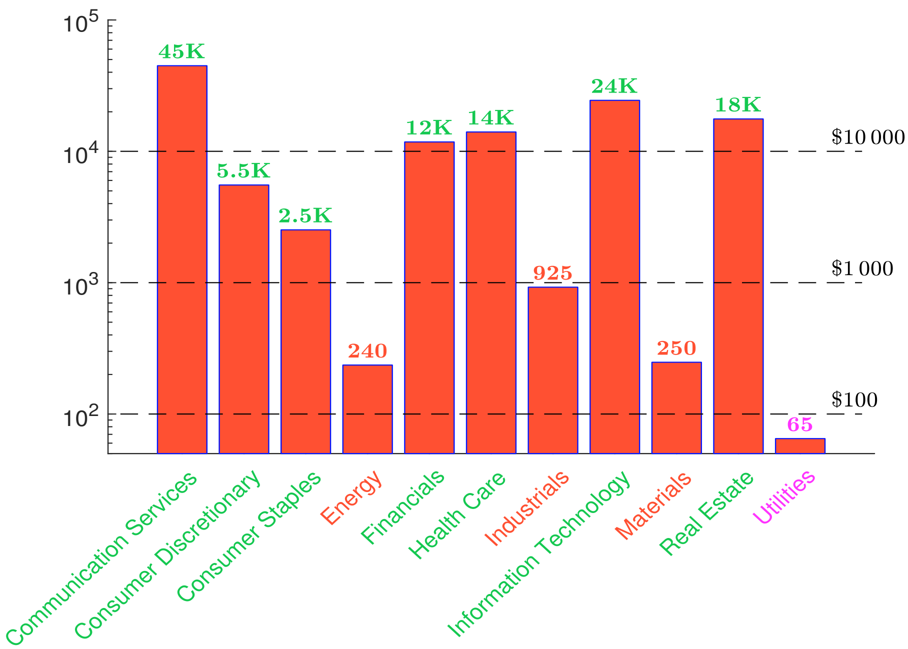

Source: Factset (2023) & Authors' calculations.

Figure 14: Boxplot of the $\mathcal{C}ost/\mathcal{D}ividend$ ratio in % (MSCI World index, December 2021, $\mathcal{CT} = \$100/\text{tCO}_2$)

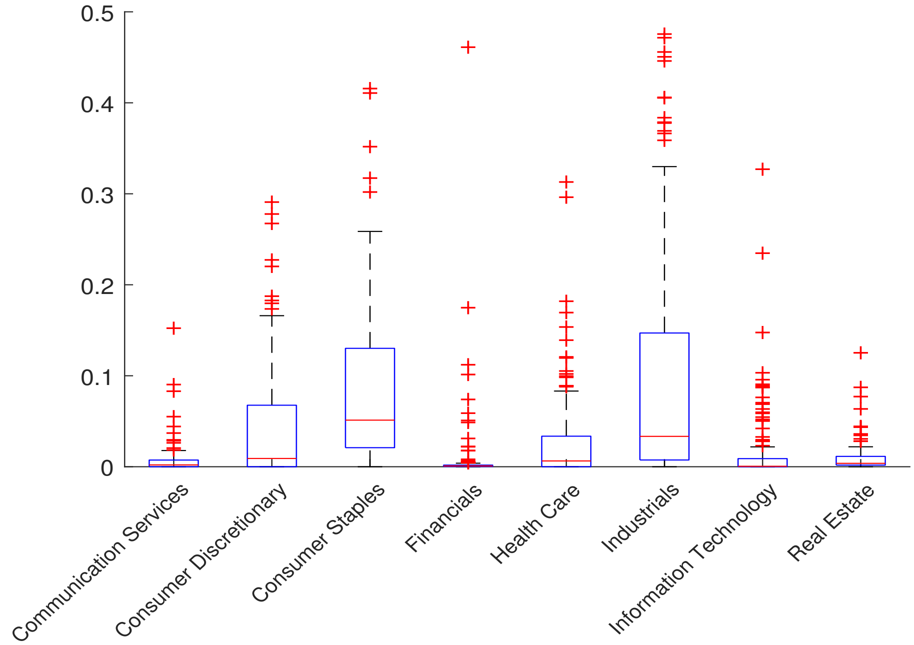

Source: Factset (2023) & Authors' calculations.

Figure 15: Boxplot of the $\mathcal{C}ost/\mathcal{D}ividend$ ratio in % (MSCI World index, December 2021, $\mathcal{CT} = \$100/\text{tCO}_2$)

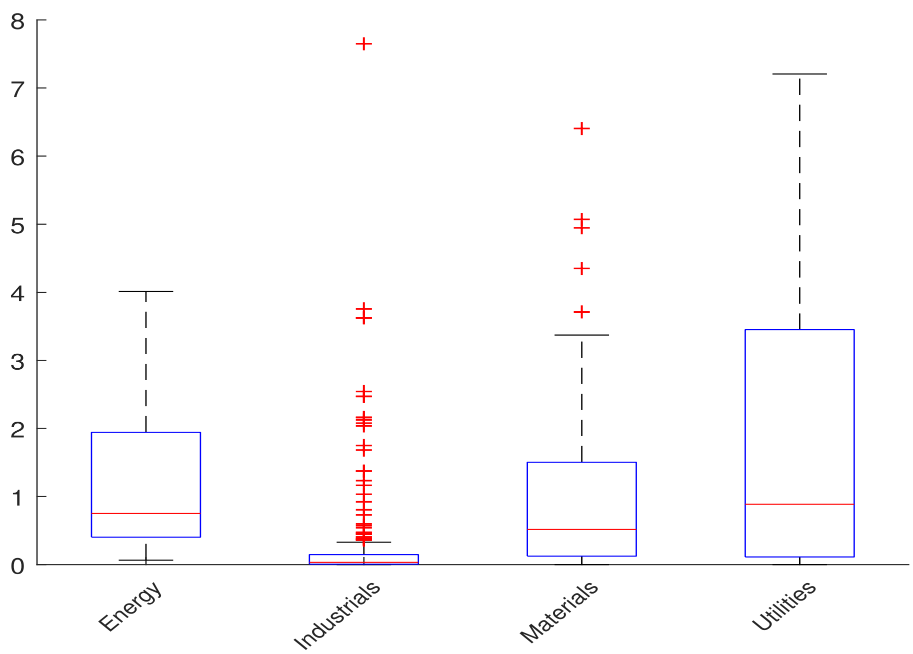

Source: Factset (2023) & Authors' calculations.

Remark 3. *We observe the heterogeneity not only between sectors, but also within sectors. For instance, we report the boxplots of the ratio* $\mathcal{C}ost/\mathcal{D}ividend$ *computed at the issuer level in Figures 14 and 15. For each sector, the boxplot indicates the statistical quantiles* 5%, 25%, 50%, 75% *and* 95% *of the ratio. Within a sector, the impact can be different from one firm to another. This type of heterogeneity can also be found at a higher level of the GICS classification. For instance, if we consider the level 2, the break-even price is equal to* \$2 600 *for Capital Goods,* \$780 *for Commercial & Professional Services and* \$370 *for Transportation, although these three industry groups belong to the same sector (Industrials).*

4 Indirect emissions and supply chain modeling

When performing transition stress tests, another major uncertainty concerns the estimation of upstream and downstream emissions. Since the reporting of indirect emissions is not mandatory and the models for applying the GHG protocol are not standardized, indirect emissions are generally estimated using input-output models. In this section, we develop the mathematical tools for performing such analysis and apply this framework to the MSCI World index.

4.1 Indirect emissions

We reiterate that there are several gases causing global warming, and regulations target them differently[15]. In general, GHG emissions are expressed in CO_2e to simplify the accounting process. The GHG Protocol provides a standardized framework to classify a company's greenhouse gas emissions in three scopes[16]. It also identifies fifteen categories of upstream and downstream emissions. Generally, upstream scope 3 emissions are indirect emissions resulting from purchased goods and services, while downstream scope 3 emissions are indirect emissions caused by sold goods and services. The diversity of the fifteen sub-scopes facilitates the reporting process, but also adds complexity to the estimation process, since indirect emissions are less frequently disclosed. In fact, an increasing number of companies are required to publicly disclose their scope 1 and 2 emissions. Conversely, scope 3 emissions are disclosed on a voluntary basis. In practice, the quality and coverage of information related to direct emissions (scope 1) are continually improving through mandatory and declarative reporting. The estimation of scope 2 emissions often follows, as it merely requires the energy mix of the region (location-based) or the GHG emissions of the energy supplier (market-based). Although several methodological initiatives like the Carbon Disclosure Project (CDP) are describing the issues inherent to indirect emissions computation (Shrimali, 2022) or propose machine learning techniques to estimate the missing information (Nguyen *et al.*, 2021), there is a clear lack of quantitative framework allowing to provide a transparent and interpretable estimation of scope 3 emissions. Consequently, multiple (engineering-based) proprietary methodologies emerged, and many companies develop their own computational models. This may generate bias in investment portfolio if the assumptions used by the different stakeholders differ. In the context of climate stress testing, modeling the uncertainty of scope 3 emissions is necessary but a also a difficult task.

[15] We classify greenhouse gases into two types. The first category corresponds to natural greenhouse gases, such as water vapor, CO_2, CH_4, N_2O, and O_3, which existed before humans but can be worsened by human activity. The second category corresponds to man-made greenhouse gases, created by human industrial activity. Some of these gases are sulfur hexafluoride (SF6) and chlorofluorocarbons (CFCs).

[16] Scope 1 emissions are direct GHG emissions from sources owned and controlled by the issuer, while Scope 2 emissions are indirect GHG emissions from purchased electricity. Scope 3 emissions are all other indirect emissions of the issuer's value chain.

4.2 Environmentally extended input-output model

An input-output model is a mathematical tool that represents the macroeconomic relationships between different entities or industries. It can be used for modeling the supply chain of a product, the sectoral structure of an economy, the production network of a country or the foreign exchange between regions. Most of these models are monetary-based. When applying to the economic transactions between different sectors, they can be used to compute the contribution or the value added of each sector to the final output of an economy. Environmentally extended input-output (EEIO) analysis is an extension of the input-output framework when including environmental externalities such as pollution and GHG emissions. In particular, we can use EEIO models to estimate upstream scope 3 emissions.

4.2.1 Input-output analysis

The input-output model was first introduced by Leontief (1936, 1941). It quantifies the interdependencies between various sectors in a single or multi-regional economies, based on the product flows between sectors (Miller and Blair, 2009). The underlying idea is to model the interconnectedness between sectors and to describe the relations from each of the producer/seller sectors to each of the purchaser/buyer sectors. Following Miller and Blair (2009), we consider n different sectors and we note $Z_{i,j}$ the value of transactions from Sector i to Sector j. We can interpret $Z_{i,j}$ in different ways:

1. It is the production that Sector i sells to Sector j;
2. It is the input of Sector i required by Sector j for its production (or output).

Let y_i be the final demand for products sold by Sector i. This final demand is composed of the external sales to households, government purchases, and demand resulting from investment capacities and foreign trade. Then, the total production x_i of Sector i is equal to:

$$\underbrace{x_i}_{\text{Supply}} = \underbrace{\sum_{j=1}^{n} Z_{i,j} + y_i}_{\text{Demand}} \tag{1}$$

In this equation, x_i and $\sum_{j=1}^{n} Z_{i,j} + y_i$ are the supply and demand related to products of Sector i, and $z_i = \sum_{j=1}^{n} Z_{i,j}$ represents the intermediary demand. The interdependence relation between sectors is usually expressed as a ratio between $Z_{i,j}$ and x_j:

$$A_{i,j} = \frac{Z_{i,j}}{x_j}$$

We denote by $A = \left(A_{i,j}\right) = Z \operatorname{diag}(x)^{-1}$ the input-output matrix of the technical coefficients $A_{i,j}$. In a matrix form, we have $x = Z\mathbf{1}_n + y$ and $Z \equiv A \operatorname{diag}(x) = A \odot x^{\top}$, and we deduce that:

$$x = Ax + y$$

where $x = (x_1, \ldots, x_n)$ and $y = (y_1, \ldots, y_n)$. Assuming that the final demand is exogenous, technical coefficients are fixed and the output is endogenous, we obtain:

$$x = (I_n - A)^{-1} y \tag{2}$$

$\boldsymbol{\mathcal{L}} = (I_n - A)^{-1}$ is known as the Leontief inverse (or multiplier) matrix and represents the amount of total output from Sector i that is needed by Sector j to satisfy its final demand. Equation (2) describes a *demand-pull quantity* model.

Let m be number of primary inputs (*e.g.*, labor, capital, etc.). We note $V = \left(V_{k,j}\right)$ the value added matrix where $V_{k,j}$ represents the amount of primary input k required to produce the output of Sector j. Since the total input of each sector is equal to its total output, we have $x_j = \sum_{i=1}^{n} Z_{i,j} + \sum_{k=1}^{m} V_{k,j}$. Therefore, $\upsilon_j = \sum_{k=1}^{m} V_{k,j} = x_j - \sum_{i=1}^{n} Z_{i,j}$ represents the other expenditures of Sector j or the total primary inputs used in Sector j. We have $\upsilon = (\upsilon_1, \ldots, \upsilon_n) = V^\top \mathbf{1}_m$. Let $p = (p_1, \ldots, p_n)$ and $\psi = (\psi_1, \ldots, \psi_m)$ be the vector of sector prices and primary inputs. p_j and ψ_k are then the prices per unit of Sector j and primary input k. As in the quantity model, the interdependence relationship between primary inputs and sectors is expressed as a ratio between $V_{k,j}$ and x_j:

$$B_{k,j} = \frac{V_{k,j}}{x_j}$$

We denote by $B = \left(B_{k,j}\right) \equiv V \operatorname{diag}(x)^{-1}$ the input-output matrix of the technical coefficients $B_{k,j}$. Following Gutierrez (2008), the value of output must be equal to the value of its inputs:

$$\underbrace{p_j x_j}_{\text{Value of the output}} = \underbrace{\sum_{i=1}^{n} Z_{i,j} p_i + \sum_{k=1}^{m} V_{k,j} \psi_k}_{\text{Value of the inputs}}$$

We deduce that:

$$\begin{aligned} p_j &= \sum_{i=1}^{n} \frac{Z_{i,j}}{x_j} p_i + \sum_{k=1}^{m} \frac{V_{k,j}}{x_j} \psi_k \\ &= \sum_{i=1}^{n} A_{i,j} p_i + \sum_{k=1}^{m} B_{k,j} \psi_k \end{aligned}$$

In a matrix form, we obtain $p = A^\top p + B^\top \psi$. $\upsilon = B^\top \psi$ is the vector of value added ratios. Finally, the output prices are equal to:

$$p = \left(I_n - A^\top\right)^{-1} \upsilon \tag{3}$$

$\tilde{\boldsymbol{\mathcal{L}}} = \left(I_n - A^\top\right)^{-1}$ is known as the dual inverse matrix[17] and represents the cost amount from Sector j that is passed to Sector i. Equation (3) describes a *cost-push price* model. By adding the income identity[18], Gutierrez (2008) proposed the following complete version of the full basic input-output model:

$$\left\{ \begin{array}{l} x = (I_n - A)^{-1} y \\ \upsilon = V^\top \mathbf{1}_m \\ \upsilon = B^\top \psi \\ p = \left(I_n - A^\top\right)^{-1} \upsilon \\ x^\top \upsilon = y^\top p \end{array} \right. \tag{4}$$

It mixes both the quantity and price models. In this system, A, B and V are the model parameters, ψ, υ and y are the exogenous variables, and x and p are the endogenous variables. By changing the model parameters or the exogenous variables, we can measure the impacts Δx and Δp on the quantities and prices of the economy.

[17] Since we have $\left(I_n - A^\top\right)^{-1} = \left((I_n - A)^\top\right)^{-1} = \left((I_n - A)^{-1}\right)^\top$, we deduce that $\tilde{\boldsymbol{\mathcal{L}}} = \boldsymbol{\mathcal{L}}^\top$.

[18] Since the input-output analysis assumes an equilibrium model, the total value of the revenues $y^\top p$ is equal to the total value of costs $x^\top \upsilon$.

Remark 4. *The previous analysis has been derived for physical input-output tables, whose flows are expressed in product units. However, the analysis remains valid when considering monetary input-output tables. The only difference is the computation of the vector of primary costs. In a monetary input-output analysis, ψ is set to $\mathbf{1}_m$ by construction, implying that $\upsilon = B^\top \mathbf{1}_m = \left(v_1/x_1, \ldots, v_n/x_n\right)$ (Miller and Blair, 2009, Section 2.6.3, pages 43-44).*

The matrix $\boldsymbol{\mathcal{L}}$ admits the following Neumann series[19] (Schechter, 1996, chapter 23, pages 627-628):

$$\begin{aligned}\boldsymbol{\mathcal{L}} &= (I_n - A)^{-1} \\ &= I_n + A + A^2 + A^3 + \ldots \\ &= \sum_{k=0}^{\infty} A^k\end{aligned}$$

Then, we obtain the following decomposition:

$$\begin{aligned}x &= \sum_{k=0}^{\infty} A^k y \\ &= y + Ay + A^2 y + \ldots \\ &= \sum_{k=0}^{\infty} y_{(k)}\end{aligned}$$

where $y_{(0)} = y$ is the final demand (or zeroth-tier intermediary demand), $y_{(1)} = Ay$ is the first-tier intermediary demand, $y_{(2)} = A^2 y$ is the second-tier intermediary demand, and $y_{(k)} = A^k y$ is the k^{th}-tier intermediary demand. Moreover, we have:

$$\frac{\partial\, x}{\partial\, y} = (I_n - A)^{-1} \equiv \boldsymbol{\mathcal{L}}$$

We better understand why the matrix $\boldsymbol{\mathcal{L}}$ is also called the multiplier matrix because it is an analogy of the Keynesian consumption theory and the impact of a change in aggregate demand on the output[20].

4.2.2 Application to environmental problems

At the end of the sixties, several authors proposed to connect economic and ecologic systems by using generalized input-output models. For instance, Daly (1968) proposed to augment the technical coefficients with additional rows/columns to reflect non-human sectors such as animals, plants, and bacteria, and non-living sectors such as atmosphere, hydrosphere, and lithosphere. Leontief (1970) himself explained how externalities such as environmental pollution can be incorporated into a basic input-output model. Since these first contributions, the input-output analysis has been extended to many environmental problems[21].

In order to understand how input-output analyses can be used for measuring carbon emissions, we consider the mathematical problem of computing the contribution of carbon

[19] We have $I_n - A^k = (I_n - A)\left(I_n + A + A^2 + \ldots + A^{k-1}\right)$. Since A is a substochastic matrix ($A_{i,j} \geq 0$ and $\sum_{i=1}^n A_{i,j} \leq 1$), the eigendecomposition of A is $A = V \Lambda V^{-1}$ where V is the matrix of eigenvectors, $\Lambda = \operatorname{diag}(\lambda_1, \ldots, \lambda_n)$ and $|\lambda_i| \leq 1$. In the case where $|\lambda_i| < 1$ (this is generally the case, especially when $\sum_{i=1}^n A_{i,j} < 1$), we deduce that $\lim_{k\to\infty} A^k = V \Lambda^k V^{-1} = \mathbf{0}_{n,n}$.

[20] Let c be the marginal propensity to consume. The Keynesian multiplier is equal to $m = 1 + c + c^2 + \ldots = (1-c)^{-1}$.

[21] See Chapters 9 and 10 of Miller and Blair (2009).

emissions per product. Following Miller and Blair (2009), we note $C^{(x)} = \left(C^{(x)}_{g,j}\right)$ the matrix of pollution output where $C^{(x)}_{g,j}$ is the total amount of the g^{th} pollutant generated by the output of the j^{th} sector. In a similar way, we define $D^{(y)} = C^{(x)} \operatorname{diag}(x)^{-1} = \left(D^{(y)}_{g,j}\right)$ the matrix of direct impact coefficients where $D^{(y)}_{g,j} = c^{(y)}_{g,j}/x_j$ is the amount of the g^{th} pollutant generated by 1\$ of the output of the j^{th} sector. Let $\varpi = (\varpi_1, \ldots, \varpi_m)$ be the vector of pollution level. We have:

$$\begin{aligned}\varpi &= D^{(x)} x \\ &= D^{(x)} (I_n - A)^{-1} y \\ &= D^{(y)} y\end{aligned}$$

where $D^{(y)} = D^{(x)} (I_n - A)^{-1}$ is the pollutant multiplier matrix with respect to the final demand y. $D^{(y)}$ also measures the product carbon footprint (PCF). Since we have the following identity $\varpi_g = \left(D^{(y)} y\right)_g = \sum_{j=1}^{n} D^{(y)}_{g,j} y_j$, we deduce that the total contribution of Sector j to the g^{th} pollutant is equal to:

$$C^{(x)}_{g,j} = \frac{\partial\, \varpi_g}{\partial\, y_j} y_j = D^{(y)}_{g,j} y_j$$

Again, we can decompose the pollutant level according to the k^{th} tier. We have:

$$\begin{aligned}\varpi &= D^{(y)} y \\ &= \sum_{k=0}^{\infty} D^{(x)} A^k y \\ &= \sum_{k=0}^{\infty} \varpi_{(k)}\end{aligned}$$

where $\varpi_{(0)} = D^{(x)} y$ is the pollutant level due to the final demand (or the zeroth-tier pollutant level), $\varpi_{(1)} = D^{(x)} A y$ is the pollutant level due to the first-tier supply chain, and $\varpi_{(k)} = D^{(x)} A^k y$ is the k^{th}-tier pollutant level. The matrix $D^{(y)}_{(k)} = D^{(x)} A^k$ is called the k^{th}-tier multiplier matrix and satisfies the identity $D^{(y)} \equiv \sum_{k=0}^{\infty} D^{(y)}_{(k)}$.

Table 9: Environmentally extended monetary input-output table (Example #1)

		To			Final demand	Total output
		$\mathcal{S}_1$	$\mathcal{S}_2$	$\mathcal{S}_3$	y	x
From	$\mathcal{S}_1$	100	300	100	500	1 000
	$\mathcal{S}_2$	250	150	200	1 600	2 000
	$\mathcal{S}_3$	25	200	75	200	500
	Value added	625	1 350	125		
	Total outlays	1 000	2 000	500		
GHG	CO_2	50	20	5	75	
	CH_4	3	1	0	4	

We consider the example given in Table 9. This basic economy has three sectors: $\mathcal{S}_1$, $\mathcal{S}_2$ and $\mathcal{S}_3$. In this example, businesses in Sector $\mathcal{S}_1$ purchase \$100 goods and services from other businesses in Sector $\mathcal{S}_1$, \$250 goods and services from Sector $\mathcal{S}_2$, and \$25 goods and services from Sector $\mathcal{S}_3$. The final demand for goods and services produced in Sector $\mathcal{S}_1$ is equal to \$500, while their intermediary demand is equal to \$500. We deduce that the matrix of technical coefficients is equal to:

$$A = Z \operatorname{diag}(x)^{-1} = \begin{pmatrix} 10.0\% & 15.0\% & 20.0\% \\ 25.0\% & 7.5\% & 40.0\% \\ 2.5\% & 10.0\% & 15.0\% \end{pmatrix}$$

It follows that the multiplier matrix is equal to:

$$\boldsymbol{\mathcal{L}} = (I_3 - A)^{-1} = \begin{pmatrix} 1.1871 & 0.2346 & 0.3897 \\ 0.3539 & 1.2090 & 0.6522 \\ 0.0766 & 0.1491 & 1.2647 \end{pmatrix}$$

The direct impact matrix corresponds to the GHG emissions divided by the output:

$$D^{(x)} = \begin{pmatrix} 50/1000 & 20/2000 & 5/500 \\ 3/1000 & 1/2000 & 0/500 \end{pmatrix} = \begin{pmatrix} 0.05 & 0.01 & 0.01 \\ 0.003 & 0.0005 & 0 \end{pmatrix}$$

The unit of $D^{(x)}$ is expressed in kilogram of the gas per dollar. For instance, the GHG intensities of the products manufactured in Sector $\mathcal{S}_1$ are equal to 0.05 $kgCO_2$/\$ and 0.003 $kgCH_4$/\$. Finally, we obtain:

$$D^{(y)} = D^{(x)} \boldsymbol{\mathcal{L}} = \begin{pmatrix} 0.0637 & 0.0253 & 0.0387 \\ 0.0037 & 0.0013 & 0.0015 \end{pmatrix}$$

While $D^{(x)}$ corresponds to the production-based inventory, $D^{(y)}$ measures the carbon footprint from the viewpoint of the consumption-based inventory (Kitzes, 2013). Therefore, we obtain the following decomposition:

$$C^{(y)} = \begin{pmatrix} 31.83 & 35.44 & 7.73 \\ 1.87 & 1.83 & 0.30 \end{pmatrix} \neq \begin{pmatrix} 50 & 20 & 5 \\ 3 & 1 & 0 \end{pmatrix} = C^{(x)}$$

We notice that the two contribution matrices are different. For instance, while Sector $\mathcal{S}_1$ is responsible of 50 $kgCO_2$, the products manufactured by this sector are responsible of only 31.83 $kgCO_2$, meaning that 18.17 $kgCO_2$ are emitted by Sector $\mathcal{S}_1$ for the other sectors. The difference between $C^{(x)}$ and $C^{(y)}$ depends on the structure of the matrix A. In particular, we can show that $C^{(x)} = C^{(y)}$ implies that A is a diagonal matrix. We conclude that the supply chain and the interconnectedness between sectors can give a false perception of the sectoral carbon footprint.

The previous framework can be applied to many problems that involve the computation of carbon footprint. Miller and Blair (2009) examined three categories of EEIO analysis: generalized input-output, economic-ecologic and commodity-by-industry models. An overview of generalized input-output models can be found in Minx *et al.* (2009) and Wiedmann (2009). These models are generally used for computing the carbon footprint of nations, sectors, supply chains, etc., and analyzing the impact of foreign trade. The use of economic-ecologic models is less popular since it involves building an input-output table for the ecologic sectors (species, plants, etc.). Commodity-by-industry models are more studied because it is easier to collect data for the commodity sector (Jackson, 2006).

The use of environmental extended input-output models requires credible database. According to Han *et al.* (2022), most of studies are based on four input-output databases[22]:

[22]The corresponding websites are `www.exiobase.eu`, `www.worldmrio.com`, `www.gtap.agecon.purdue.edu` and `www.rug.nl/ggdc/valuechain/wiod`.

Eora, Exiobase, GTAP and WIOD. These four multi-regional input-output models have been developed by academic institutes. In the case of the Eora global supply chain database, the model uses more than 15 000 sectors across 190 countries, and contains about 2 700 environmental indicators covering GHG emissions, air pollution, energy use, water requirements, land occupation, etc. Exiobase is a multi-regional environmentally extended supply-use and input-output model with 44 countries, 163 industries, and 417 emission categories. The global trade analysis project (GTAP) is a global database describing bilateral trade patterns, production, consumption and intermediate use of commodities and services. Finally, the world input-output database (WIOD) is another famous multi-regional input-output model. Although this database is extensively used by academia and professionals, the last version was released in 2016 and there is no plan to update it.

4.3 Estimation of indirect emissions

4.3.1 Mathematical framework

Basic formula We assume that the carbon footprint is assessed in CO_2e, implying that the input-output analysis will consider only one pollutant, all greenhouse gases being converted into the carbon based on their warming potential. In this case, $D^{(x)}$ is a row vector of dimension n, and $D_j^{(x)}$ measures the direct emission intensity of Sector j. We reiterate that the total emission intensities are equal to $D^{(y)} = D^{(x)}\boldsymbol{\mathcal{L}} = D^{(x)}\left(I_n - A\right)^{-1}$. $D^{(y)}$ is a row vector of dimension n, and $D_j^{(y)}$ measures the direct and indirect emission intensity of Sector j. Using the usual notation $\boldsymbol{\mathcal{CI}}$ for the carbon intensity, we have[23]:

$$\begin{aligned}\boldsymbol{\mathcal{CI}}_{\text{total}} &= \boldsymbol{\mathcal{CI}}_{1-3} \\ &= \boldsymbol{\mathcal{L}}^\top \boldsymbol{\mathcal{CI}}_1 \\ &= \left(I_n - A^\top\right)^{-1} \boldsymbol{\mathcal{CI}}_1 \end{aligned} \tag{5}$$

where $\boldsymbol{\mathcal{CI}}_1 = \boldsymbol{\mathcal{CI}}_{\text{direct}}$ is the vector of scope 1 (direct) carbon intensities and $\boldsymbol{\mathcal{CI}}_{1-3} = \boldsymbol{\mathcal{CI}}_{\text{total}}$ is the vector of scope $1+2+3$ (direct plus indirect) carbon intensities. It follows that the indirect carbon intensities are given by:

$$\begin{aligned}\boldsymbol{\mathcal{CI}}_{\text{indirect}} &= \boldsymbol{\mathcal{CI}}_{1-3} - \boldsymbol{\mathcal{CI}}_1 \\ &= \left(\left(I_n - A^\top\right)^{-1} - I_n\right) \boldsymbol{\mathcal{CI}}_{\text{direct}} \end{aligned} \tag{6}$$

In particular, we can decompose $\boldsymbol{\mathcal{CI}}_{\text{indirect}}$ using the Neumann series:

$$\boldsymbol{\mathcal{CI}}_{\text{indirect}} = \underbrace{A^\top \boldsymbol{\mathcal{CI}}_1}_{\text{First-tier}} + \underbrace{\left(A^\top\right)^2 \boldsymbol{\mathcal{CI}}_1}_{\text{Second-tier}} + \ldots + \underbrace{\left(A^\top\right)^k \boldsymbol{\mathcal{CI}}_1}_{k^{th}\text{-tier}} + \ldots \tag{7}$$

and we have:

$$\boldsymbol{\mathcal{CI}}_{\text{total}} = \underbrace{\underbrace{\boldsymbol{\mathcal{CI}}_1}_{\text{Scope 1}}}_{\text{Direct intensity}} + \underbrace{\underbrace{A^\top \boldsymbol{\mathcal{CI}}_1}_{\text{First-tier}} + \underbrace{\left(A^\top\right)^2 \boldsymbol{\mathcal{CI}}_1}_{\text{Second-tier}} + \ldots + \underbrace{\left(A^\top\right)^k \boldsymbol{\mathcal{CI}}_1}_{k^{th}\text{-tier}} + \ldots}_{\text{Indirect intensities}} \tag{8}$$

Equations (5–8) are the core formulas of the consumption-based inventory approach.

[23] Because $D^{(x)} = \boldsymbol{\mathcal{CI}}_1^\top$ and $D^{(y)} = \boldsymbol{\mathcal{CI}}_{1-3}^\top$.

Illustration We consider a toy example with four sectors: $\mathcal{S}_1$ is the energy sector, $\mathcal{S}_2$ the materials sector, $\mathcal{S}_3$ the industrials sector and $\mathcal{S}_4$ the sector of services. The input-output matrix of the technical coefficients is given in Table 10. The interpretation of A is the following. To produce \$1, the energy sector has to purchased \$0.10 of output from other businesses in the energy sector, \$0.10 of materials, \$0.05 of output from the industrials sector and \$0.02 of services. If we focus on the sector of services, the output of \$1 requires the purchase of \$0.10 from the energy sector, \$0.05 of materials, \$0.10 of industrials, and \$0.35 from other businesses in the sector of services. The carbon emissions are expressed in ktCO_2e, and the carbon intensities are measured in tCO_2e/\$ mn. Energy is the most polluting sector with 500 ktCO_2e, followed by materials and industrials with 200 ktCO_2e. Energy and services have respectively the highest and lowest carbon intensity (100 tCO_2e/\$ mn vs. 10 tCO_2e/\$ mn).

Table 10: Environmentally extended monetary input-output table (Example #2)

Sector	A				$\mathcal{CE}$	$\mathcal{CI}$
Energy	0.10	0.20	0.20	0.10	500	100
Materials	0.10	0.10	0.20	0.05	200	50
Industrials	0.05	0.20	0.30	0.10	200	25
Services	0.02	0.05	0.10	0.35	125	10

Using the previous figures, we obtain the following dual inverse matrix:

$$\tilde{\mathcal{L}} = \left(I_4 - A^\top\right)^{-1} = \begin{pmatrix} 1.1881 & 0.1678 & 0.1430 & 0.0715 \\ 0.3894 & 1.2552 & 0.4110 & 0.1718 \\ 0.4919 & 0.4336 & 1.6303 & 0.2993 \\ 0.2884 & 0.1891 & 0.3044 & 1.6087 \end{pmatrix}$$

Using these multipliers, we obtain the direct and indirect carbon intensities given in Table 11. While the scope 1 carbon intensity of the energy sector is equal to 100 tCO_2e/\$ mn, its total carbon intensity is equal to 131.49 tCO_2e/\$ mn. The difference 31.49 tCO_2e/\$ mn corresponds to the indirect emissions. In the case of the energy sector, direct and indirect emissions represent respectively 76.05% and 23.95% of the total emissions. In fact, this sector has the lowest ratio of indirect carbon emissions. On the contrary, 83.87% of the total emissions are indirect for the sector of services.

Table 11: Direct and indirect carbon intensities (Example #2)

Sector	$\mathcal{CI}_1$	$\mathcal{CI}_{\text{total}}$ (in tCO_2e/\$ mn)	$\mathcal{CI}_{\text{direct}}$	$\mathcal{CI}_{\text{indirect}}$	$\mathcal{CI}_{\text{direct}}$ (in %)	$\mathcal{CI}_{\text{indirect}}$	$\frac{\mathcal{CI}_{\text{total}}}{\mathcal{CI}_1}$
Energy	100.00	131.49	100.00	31.49	76.05%	23.95%	1.31
Materials	50.00	113.69	50.00	63.69	43.98%	56.02%	2.27
Industrials	25.00	114.62	25.00	89.62	21.81%	78.19%	4.58
Services	10.00	61.99	10.00	51.99	16.13%	83.87%	6.20

We note $\mathcal{CI}_{(k)} = \left(A^\top\right)^k \mathcal{CI}_1$ the indirect carbon intensity when we consider the k^{th} tier, and $\mathcal{CI}_{(1-k)} = \sum_{h=1}^{k} \left(A^\top\right)^h \mathcal{CI}_1$ the cumulative indirect carbon intensity for the first k tiers. Results are given in Table 12. For the sector of services, the first- and second-tier rounds add 18.50 and 13.50 tCO_2e/\$ mn to the indirect carbon intensity. If we limit the analysis to the first two tiers, the indirect carbon intensity is equal to 32. The tree represented in Figure 16 explains this computation. To produce \$1 of services, we need to

Figure 16: Upstream tree of the first- and second-tier rounds for the sector of services (Example #2)

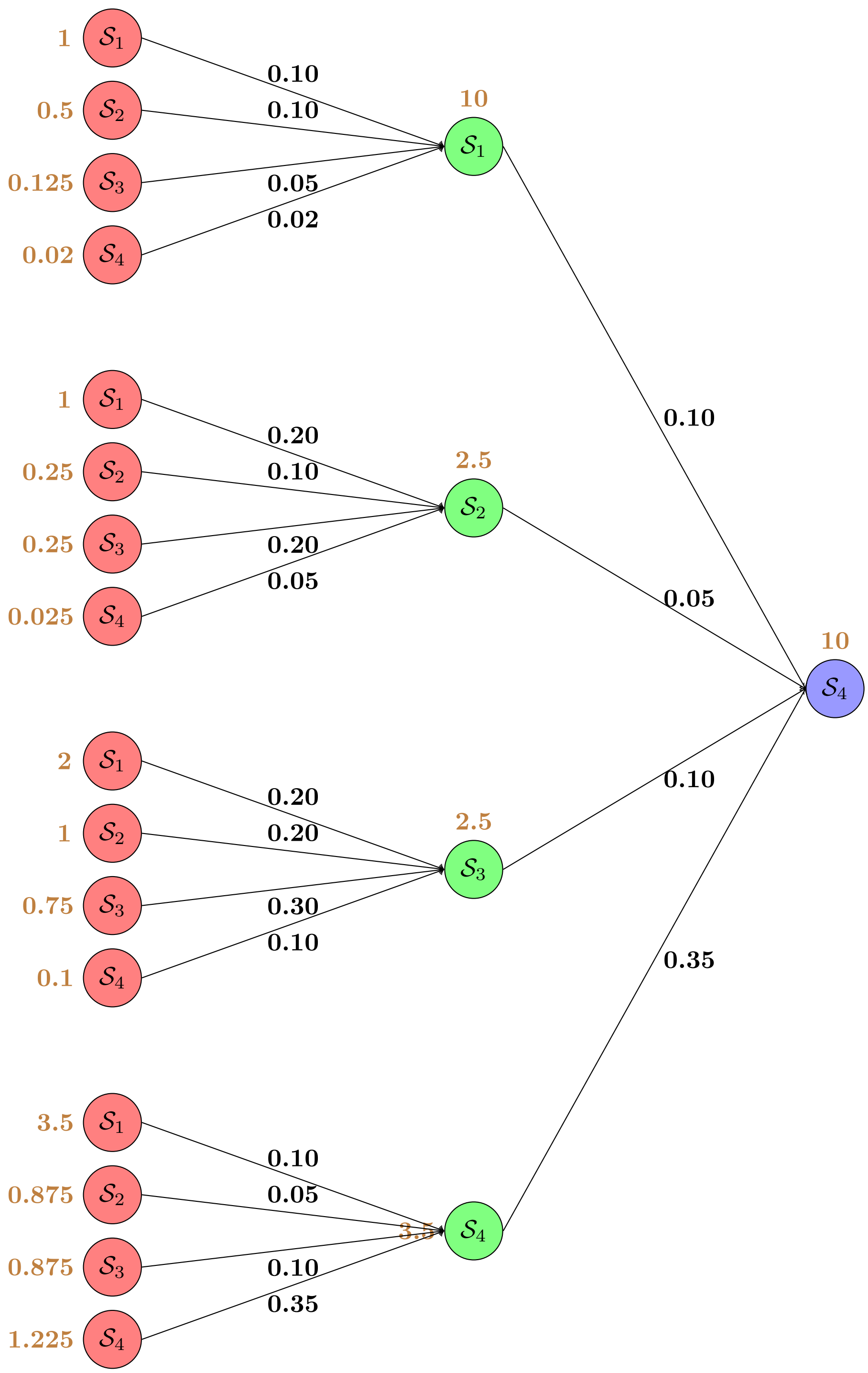

Table 12: Tier decomposition of carbon intensities (Example #2)

	Sector	1	2	3	4	5	10	15	∞
$\mathcal{CI}_{(k)}$	Energy	16.45	6.99	3.60	1.97	1.09	0.06	0.00	0.00
	Materials	30.50	14.97	8.13	4.47	2.48	0.14	0.01	0.00
	Industrials	38.50	22.79	12.58	6.96	3.88	0.21	0.01	0.00
	Services	18.50	13.50	8.45	4.98	2.86	0.16	0.01	0.00
$\mathcal{CI}_{(1-k)}$	Energy	16.45	23.44	27.04	29.02	30.11	31.41	31.48	31.49
	Materials	30.50	45.47	53.59	58.06	60.55	63.52	63.68	63.69
	Industrials	38.50	61.29	73.87	80.83	84.71	89.35	89.61	89.62
	Services	18.50	32.00	40.44	45.43	48.29	51.79	51.98	51.99

purchase 0.10$ of energy, \$0.05 of materials, etc. It follows that the first-tier indirect carbon intensities for the sector of services is equal to:

$$\begin{aligned}\mathcal{CI}_{(1)}(\mathcal{S}_4) &= 0.10 \times 100 + 0.05 \times 50 + 0.10 \times 25 + 0.35 \times 10 \\ &= 10 + 2.5 + 2.5 + 3.5 \\ &= 18.50\end{aligned}$$

We can continue the analysis and consider the second tier. Indeed, the businesses involved in the first-tier round also purchase goods and services that emit new indirect emissions. We have:

$$\begin{aligned}\mathcal{CI}_{(2)}(\mathcal{S}_4) = \; & 0.10 \times \underbrace{(0.10 \times 100 + 0.10 \times 50 + 0.05 \times 25 + 0.02 \times 10)}_{\text{Indirect emissions from businesses of the energy sector}} + \\ & 0.05 \times \underbrace{(0.20 \times 100 + 0.10 \times 50 + 0.20 \times 25 + 0.05 \times 10)}_{\text{Indirect emissions from businesses of the materials sector}} + \\ & 0.10 \times \underbrace{(0.20 \times 100 + 0.20 \times 50 + 0.30 \times 25 + 0.10 \times 10)}_{\text{Indirect emissions from businesses of the industrials sector}} + \\ & 0.35 \times \underbrace{(0.10 \times 100 + 0.05 \times 50 + 0.10 \times 25 + 0.35 \times 10)}_{\text{Indirect emissions from businesses of the services sector}} + \\ = \; & 13.495\end{aligned}$$

We can pursue the analysis, and we verify that $\mathcal{CI}_{(3)}(\mathcal{S}_4) = 8.45$, $\mathcal{CI}_{(4)}(\mathcal{S}_4) = 4.98$, etc. Finally, the cumulative sum converges to $\mathcal{CI}_{(1-\infty)}(\mathcal{S}_4) = 51.99$.

The previous analysis concerns the carbon intensity. To estimate total emissions, we just multiply by the output and we have the following identities:

$$\frac{\mathcal{CE}_{\text{total}}}{\mathcal{CE}_1} = \frac{\mathcal{CI}_{\text{total}}}{\mathcal{CI}_1} \Leftrightarrow \mathcal{CE}_{\text{total}} = \mathcal{CI}_{\text{total}} \odot \frac{\mathcal{CE}_1}{\mathcal{CI}_1} = x \odot \mathcal{CI}_{\text{total}} \tag{9}$$

Therefore, the indirect emissions are given by:

$$\begin{aligned}\mathcal{CE}_{\text{indirect}} &= \mathcal{CE}_{\text{total}} - \mathcal{CE}_{\text{direct}} \\ &= (\mathcal{CI}_{\text{total}} - \mathcal{CI}_1) \odot \frac{\mathcal{CE}_1}{\mathcal{CI}_1}\end{aligned} \tag{10}$$

The breakdown of the total carbon emissions is reported in Table 13. We notice that indirect carbon emissions are subject to double counting. Indeed, the total direct carbon emissions are equal to 1 025 $ktCO_2e$ and indirect emissions add 1 779 $ktCO_2e$. Based on direct emissions, we have the following distribution: 49% for energy, 20% for materials, 20% for industrials and 12% for the sector of services. If we include the indirect emissions, we obtain another picture. For instance, the sector of services represents more than 25% of total emissions because the direct emissions have been multiplied by a factor of 6.2, while energy has now a contribution lower than 25%.

Table 13: Breakdown of carbon emissions (Example #2)

Sector	$\mathcal{CE}_{\text{direct}}$	$\mathcal{CE}_{\text{indirect}}$ (in $ktCO_2e$)	$\mathcal{CE}_{\text{total}}$	$\mathcal{CE}_{\text{direct}}$	$\mathcal{CE}_{\text{indirect}}$ (in %)	$\mathcal{CE}_{\text{total}}$
Energy	500	157.44	657.44	48.78	8.85	23.45
Materials	200	254.76	454.76	19.51	14.32	16.22
Industrials	200	716.97	916.97	19.51	40.30	32.70
Services	125	649.92	774.92	12.20	36.53	27.64
Total	1 025	1 779.10	2 804.10	100.00	100.00	100.00

Remark 5. *It would be wrong to diffuse directly the carbon emissions instead of the carbon intensities:* $\mathcal{CE}_{\text{total}} = \left(I_n - A^\top\right)^{-1} \mathcal{CE}_1$. *Indeed, carbon emissions are not comparable from one sector to another sector, because they are not normalized and monetary input-output tables give the technical coefficients for $1 output of each sector.*

Upstream vs. downstream analysis The previous analysis is an output-based analysis. This is obvious if we consider Figure 16, which illustrates the requirement impacts to produce $1 in one sector. Once we have produced $1 in a given sector, we may wonder how it is used by the value chain. In this case, we obtain an input-based analysis. Indeed, instead of moving up the supply chain, we move down the value chain (Figure 17). Therefore, this approach is also called the downstream analysis while the output-based approach is known as the upstream analysis.

To perform a downstream analysis, we first need to define the technical coefficients for $1 input (and not output):

$$\breve{A}_{i,j} = \frac{Z_{i,j}}{x_i}$$

$\breve{A}_{i,j}$ indicates the proportion of $1 produced by Sector i that is used by Sector j. We denote by $\breve{A} = \left(\breve{A}_{i,j}\right) = \operatorname{diag}(x)^{-1} Z$ the matrix of input impacts. We notice that:

$$\breve{A}_{i,j} = \frac{Z_{i,j}}{x_j} \cdot \frac{x_j}{x_i} = A_{i,j} \cdot T_{i,j}$$

In a matrix form, we have $\breve{A} = A \odot T$ where $T = \left(T_{i,j}\right) = \left(x_i^{-1} x_j\right)$. Using the same rationale as in the previous paragraphs, we can show that:

$$\mathcal{CI}_{\text{total}}^{\text{down}} = \left(I_n - \breve{A}\right)^{-1} \mathcal{CI}_1 \tag{11}$$

where $\mathcal{CI}_{\text{total}}^{\text{down}}$ is the vector of scope $1+2+3$ downstream (direct plus downstream indirect) carbon intensities. It follows that the indirect downstream carbon intensities are given by:

$$\mathcal{CI}_{\text{indirect}}^{\text{down}} = \mathcal{CI}_{\text{total}}^{\text{down}} - \mathcal{CI}_1 = \left(\left(I_n - \breve{A}\right)^{-1} - I_n\right) \mathcal{CI}_{\text{direct}} \tag{12}$$

Figure 17: Downstream tree of the first- and second-tier rounds for the sector of services (Example #2)

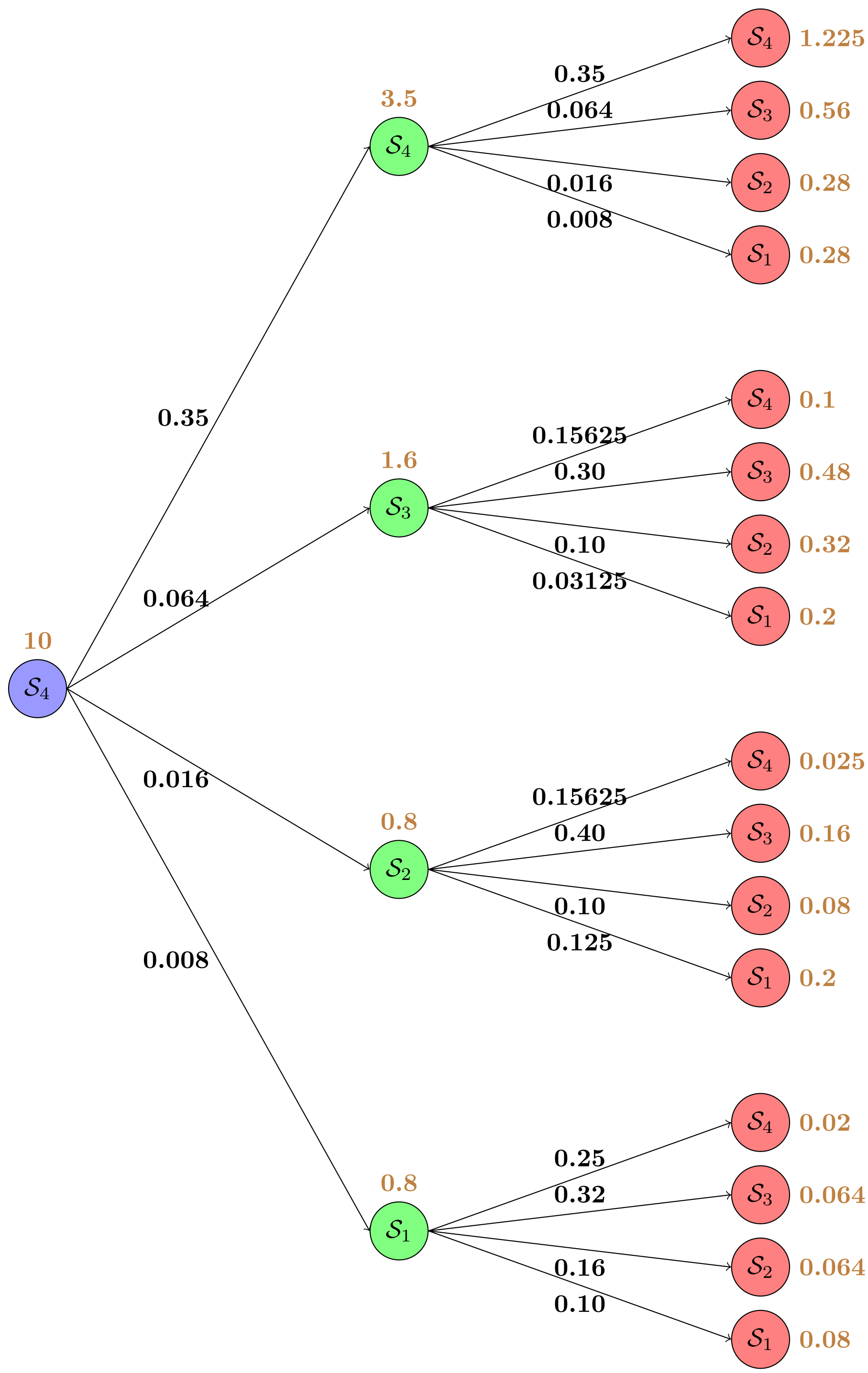

In particular, we can decompose $\mathcal{CI}_{\text{indirect}}^{\text{down}}$ as follows:

$$\mathcal{CI}_{\text{indirect}}^{\text{down}} = \underbrace{\breve{A}\mathcal{CI}_1}_{\text{First-tier}} + \underbrace{\breve{A}^2\mathcal{CI}_1}_{\text{Second-tier}} + \ldots + \underbrace{\breve{A}^k\mathcal{CI}_1}_{k^{th}\text{-tier}} + \ldots \tag{13}$$

and we have:

$$\mathcal{CI}_{\text{total}}^{\text{down}} = \underbrace{\underbrace{\mathcal{CI}_1}_{\text{Scope 1}}}_{\text{Direct downstream}} + \underbrace{\underbrace{\breve{A}\mathcal{CI}_1}_{\text{First-tier}} + \underbrace{\breve{A}^2\mathcal{CI}_1}_{\text{Second-tier}} + \ldots + \underbrace{\breve{A}^k\mathcal{CI}_1}_{k^{th}\text{-tier}} + \ldots}_{\text{Indirect downstream}} \tag{14}$$

Again, to compute the carbon emissions, we use the proportionality rule. We have:

$$\mathcal{CE}_{\text{total}}^{\text{down}} = \mathcal{CI}_{\text{total}}^{\text{down}} \odot \frac{\mathcal{CE}_1}{\mathcal{CI}_1} \tag{15}$$

and:

$$\mathcal{CE}_{\text{indirect}}^{\text{down}} = \mathcal{CE}_{\text{total}}^{\text{down}} - \mathcal{CE}_{\text{direct}}^{\text{down}} = \left(\mathcal{CI}_{\text{total}}^{\text{down}} - \mathcal{CI}_1\right) \odot \frac{\mathcal{CE}_1}{\mathcal{CI}_1} \tag{16}$$

Remark 6. *In order to avoid any confusion, we can use the notations $\mathcal{CI}_{\text{total}}^{\text{up}}$, $\mathcal{CI}_{\text{indirect}}^{\text{up}}$, $\mathcal{CI}_{(k)}^{\text{up}}$ and $\mathcal{CI}_{(1-k)}^{\text{up}}$ to define total, indirect, k^{th}-tier and first k tier intensities when we consider the upstream analysis described in Equations (5)–(8). The total/indirect upstream carbon emissions defined in Equations (9) and (10) are denoted by $\mathcal{CE}_{\text{total}}^{\text{up}}$ and $\mathcal{CE}_{\text{indirect}}^{\text{up}}$.*

Using our previous example, we obtain the results reported in Appendix A.3 on page 146. We obtain a downstream indirect emissions of 1 232 ktCO_2e, while the upstream indirect emissions was equal to 1 779 ktCO_2e. In order to better understand the difference between the downstream and the upstream, we represent the downstream tree of the first two tiers for the sector of services in Figure 17. If we compare this tree with Figure 16, we notice that downstream trees are growing to the right, while upstream trees are growing to the left.

Equivalence with GHG protocol taxonomy We must be careful with the upstream and downstream concepts of the input-output analysis, because they do not correspond to the upstream and downstream concepts of the GHG Protocol. Indeed, it is tempting to propose the following mapping:

GHG Protocol	$\mathcal{CE}_2 + \mathcal{CE}_3^{\text{up}}$	$\mathcal{CE}_1$	$\mathcal{CE}_2 + \mathcal{CE}_3^{\text{down}}$
EEIO	$\mathcal{CE}_{\text{indirect}}^{\text{up}}$	$\mathcal{CE}_{\text{direct}}$	$\mathcal{CE}_{\text{indirect}}^{\text{down}}$

but this mapping is wrong. By construction, we have $\mathcal{CE}_{\text{direct}} = \mathcal{CE}_1$, $\mathcal{CE}_{\text{indirect}}^{\text{up}} \neq \mathcal{CE}_2 + \mathcal{CE}_3^{\text{up}}$ and $\mathcal{CE}_{\text{indirect}}^{\text{down}} \neq \mathcal{CE}_2 + \mathcal{CE}_3^{\text{down}}$. The reason is the following. First, an input-output analysis does not make the difference between scopes 2 and 3 emissions. They are both embedded in the indirect emissions. If the mapping is true, we have:

$$\mathcal{CE}_{\text{direct}} + \mathcal{CE}_{\text{indirect}}^{\text{up}} + \mathcal{CE}_{\text{indirect}}^{\text{down}} = \mathcal{CE}_1 + 2\,\mathcal{CE}_2 + \mathcal{CE}_3^{\text{up}} + \mathcal{CE}_3^{\text{down}}$$

Therefore, we notice that the location of the scope 2 emissions is not clear, and they may be counted twice. In fact, an input-output analysis estimates both $\mathcal{CE}_2^{\text{up}}$ and $\mathcal{CE}_2^{\text{down}}$, and not directly $\mathcal{CE}_2$. A second mapping can be proposed:

GHG Protocol	$\mathcal{CE}_2^{\text{up}} + \mathcal{CE}_3^{\text{up}}$	$\mathcal{CE}_1$	$\mathcal{CE}_2^{\text{down}} + \mathcal{CE}_3^{\text{down}}$
EEIO	$\mathcal{CE}_{\text{indirect}}^{\text{up}}$	$\mathcal{CE}_{\text{direct}}$	$\mathcal{CE}_{\text{indirect}}^{\text{down}}$

but this mapping is also wrong. The GHG Protocol splits the scope 3 emissions into 8 upstream categories and 7 downstream categories. The downstream of the GHG Protocol concerns the carbon emissions once goods and services are produced. It includes their use by other sectors, but also the final demand. In the input-output analysis, the downstream carbon emissions due to the final demand are not taken into account. The downstream concept in the input-output analysis is then not consistent with the definition of the GHG Protocol. Moreover, input-output tables do not capture all the economic activities and their resolution is low. These issues weaken an input-output analysis. Another problem is the high correlation between upstreamness and downstreamness of input-output results (Antràs and Chor, 2018; Bartolucci *et al.*, 2023). In fact, we can notice that there are a lot of double counting items in the two analyses. Let us assume for instance that the matrix A is diagonal. In this case, we can show that $\mathcal{CE}_{\text{indirect}}^{\text{up}} = \mathcal{CE}_{\text{indirect}}^{\text{down}}$. In this particular case, upstream and downstream analyses refer to the same carbon emissions, and we do not really know whether these emissions are in the upstream or downstream of the value chain.

Mathematical properties The two main equations of the EEIO analysis are based on the matrix A: $\mathcal{CI}_{\text{indirect}}^{\text{up}} = \left(\left(I_n - A^\top\right)^{-1} - I_n\right)\mathcal{CI}_1$ and $\mathcal{CI}_{(k)}^{\text{up}} = \left(A^\top\right)^k \mathcal{CI}_1$. In fact, these two equations are equivalent since we have $\sum_{k=1}^{\infty}\left(A^\top\right)^k = \left(\left(I_n - A^\top\right)^{-1} - I_n\right)$. Therefore, we only need to study the mathematical properties of $\left(A^\top\right)^k$.

First, we notice that the matrix $A^\top$ is nonnegative: $A^\top \succeq \mathbf{0}_{n,n}$. Since the powers of nonnegative matrices are nonnegative and the elements of the vector $\mathcal{CI}_1$ are all positive, we deduce that $\mathcal{CI}_{(k)}^{\text{up}} \succeq \mathbf{0}_n$ and $\mathcal{CI}_{\text{indirect}}^{\text{up}} \succeq \mathbf{0}_n$. Moreover, the cumulative upstream indirect intensities $\mathcal{CI}_{(1-k)}^{\text{up}}$ are non-decreasing with respect to k. We verify that $\left(I_n - A^\top\right)^{-1} - I_n \succeq \mathbf{0}_n$, which implies that $\left(I_n - A^\top\right)^{-1} \succeq I_n$. This is obvious because we have $\mathcal{CI}_{\text{total}}^{\text{up}} \succeq \mathcal{CI}_1$.

We also notice that $A^\top$ is a row substochastic matrix: $A_{i,j} \geq 0$ and $\sum_{i=1}^{n} A_{i,j} < 1$. If we assume that $A^\top$ is irreducible[24], the Perron-Frobenius theorem states that the spectral radius $\varrho\left(A^\top\right)$ is strictly lower than 1 and corresponds to the largest positive eigenvalue λ_1. This implies that all the eigenvalues $\lambda_1 \geq \lambda_2 \geq \ldots \geq \lambda_n$ satisfies $|\lambda_i| < 1$. Using the eigendecomposition $A^\top = V\Lambda V^{-1}$, we have $\left(A^\top\right)^k = V\Lambda^k V^{-1}$ and we deduce that $\lim_{k\to\infty}\left(A^\top\right)^k = \mathbf{0}_{n,n}$. The sum $\sum_{k=1}^{\infty}\left(A^\top\right)^k$ converges then to a finite matrix, which implies that the multiplier matrix $\tilde{\mathcal{L}}$ is nonsingular.

Since $\mathcal{CI}_{(k)}^{\text{up}}$ converges to $\mathbf{0}_n$, we may wonder whether this convergence is monotone. In particular, do we verify that $\mathcal{CI}_{(k)}^{\text{up}} \succeq \mathcal{CI}_{(k+1)}^{\text{up}}$? The answer to this question is no. Indeed, we can easily find counter examples. The reason lies in the fact that $\left(A^\top\right)^k \not\succeq \left(A^\top\right)^{k+1}$. For instance, we have $\left(A^\top\right)_{4,2} = 0.05 < \left(A^\top\right)^2_{4,2} = 0.0525$ in Example #2. Nevertheless, we observe empirically that the relationship $\mathcal{CI}_{(k)}^{\text{up}} \succeq \mathcal{CI}_{(k+1)}^{\text{up}}$ is satisfied for $k \geq k^\star$. This means that if k is sufficiently large, the k^{th}-tier contribution decreases with respect to k. A sufficient (but not necessary) condition is that $\left(A^\top\right)^k \succeq \left(A^\top\right)^{k+1}$ for $k = k^\star$. Let us assume that $\left(A^\top\right)^k \succeq \left(A^\top\right)^{k+1}$ holds for $k = k^\star$. We note $B = \left(A^\top\right)^k$, $C = \left(A^\top\right)^{k+1}$ and $D = A^\top$. Property NN1 (Appendix A.8 on page 150) implies that $BD \succeq CD$. This means that if $\left(A^\top\right)^k \succeq \left(A^\top\right)^{k+1}$, then $\left(A^\top\right)^{k+1} \succeq \left(A^\top\right)^{k+2}$. We conclude that if $\left(A^\top\right)^k \succeq \left(A^\top\right)^{k+1}$ for $k = k^\star$, then $\left(A^\top\right)^k \succeq \left(A^\top\right)^{k+1}$ for $k \geq k^\star$ and the relationship $\mathcal{CI}_{(k)}^{\text{up}} \succeq \mathcal{CI}_{(k+1)}^{\text{up}}$ is

[24] This is the case if $A_{i,j} > 0$ for all i, j.

satisfied[25] for $k \geq k^{\star}$.

We recall that:

$$\mathcal{CI}_{\text{total}}^{\text{up}} = \left(I_n - A^{\top}\right)^{-1} \mathcal{CI}_1 = \sum_{k=0}^{\infty} \left(A^{\top}\right)^{k} \mathcal{CI}_1 = \sum_{k=0}^{\infty} \mathcal{CI}_{(k)}^{\text{up}}$$

Let $w_{(k)}^{\text{up}}$ be the relative contribution vector of the k^{th} tier. We have:

$$w_{(k),j}^{\text{up}} = \frac{\mathcal{CI}_{(k),j}^{\text{up}}}{\sum_{h=0}^{\infty} \mathcal{CI}_{(k),j}^{\text{up}}}$$

Following Antràs *et al.* (2012), we define the upstreamness index as the weighted average of the tiers with respect to their relative contributions:

$$\begin{aligned}
\boldsymbol{\tau}_j^{\text{up}} &= \sum_{k=0}^{\infty} k \cdot w_{(k),j}^{\text{up}} \\
&= 0 \times \frac{\mathcal{CI}_{(0),j}^{\text{up}}}{\mathcal{CI}_{\text{total},j}^{\text{up}}} + 1 \times \frac{\mathcal{CI}_{(1),j}^{\text{up}}}{\mathcal{CI}_{\text{total},j}^{\text{up}}} + 2 \times \frac{\mathcal{CI}_{(2),j}^{\text{up}}}{\mathcal{CI}_{\text{total},j}^{\text{up}}} + \ldots \\
&= \frac{\left(\sum_{k=0}^{\infty} k \cdot \mathcal{CI}_{(k)}^{\text{up}}\right)_j}{\left(\sum_{k=0}^{\infty} \mathcal{CI}_{(k)}^{\text{up}}\right)_j}
\end{aligned}$$

In Appendix A.4 on page 147, we show that[26]:

$$\boldsymbol{\tau}_j^{\text{up}} = \frac{\left(A^{\top} \left(I_n - A^{\top}\right)^{-2} \mathcal{CI}_1\right)_j}{\left(\left(I_n - A^{\top}\right)^{-1} \mathcal{CI}_1\right)_j}$$

If we consider Example #2, the upstreamness index is respectively equal to 0.49, 1.21, 1.79 and 2.13 for the four sectors. If we consider the downstreamness index:

$$\boldsymbol{\tau}_j^{\text{down}} = \frac{\left(\breve{A} \left(I_n - \breve{A}\right)^{-2} \mathcal{CI}_1\right)_j}{\left(\left(I_n - \breve{A}\right)^{-1} \mathcal{CI}_1\right)_j}$$

the figures become 0.84, 1.20, 1.40 and 1.48.

4.3.2 Application to Exiobase and WIOD input-output tables

Data In order to illustrate the use of input-output models, we estimate the indirect carbon emissions and compare these figures with those computed by Trucost in the next section. For that, we consider two input-output databases[27]: WIOD and Exiobase. WIOD is very

[25] We assume of course that the scope 1 carbon intensities are not negative.

[26] This expression is not exactly the formula proposed by Antràs *et al.* (2012), because they do not weight the tiers in the same way.

[27] As said previously, there are several input-output tables and databases available to analyze the economic and environmental impacts of production and consumption. Table 14 provides their main features and differences. Exiobase offers a detailed and highly disaggregated MRIO database, encompassing com-

famous among economists and extensively used by academics[28] (Dietzenbacher *et al.*, 2023; Timmer *et al.*, 2015). We use the 2016 release, which contains the 2014 input-output table for 44 regions (28 EU countries, 15 other major countries and a global region that corresponds to a rest-of-the-world aggregate[29]) and 56 industries. While WIOD is a traditional input-output table, Exiobase is an environmentally extended input-output table (Tukker *et al.*, 2013; Stadler *et al.*, 2018). It has been less used by economists and academics, but it has the advantage to include data for most recent years. Therefore, we use the last table for the year 2022, and also the 2014 matrix in order to compare with the WIOD matrix. The version 3 database has 49 regions (44 countries and 5 rest-of-the-world aggregates) and 163 industries. The Exiobase countries are almost the same than those we find in the WIOD model[30].

Table 14: Comparison of input-output databases

Database	Coverage	Classification	Strengths and limitations
Eora	Over 200 countries 15 000 sectors	Eora input-output	Highly disaggregated, global coverage Some data gaps, inconsistencies due to harmonization
Exiobase	49 countries 163 industries	Eora input-output	Detailed environmental, social and economic data Limited sector coverage, data integration challenges
GTAP	141 countries 65 sectors	GTAP/ISIC	Comprehensive trade data, trade policy analysis Less detailed sector/country coverage, trade focus
OECD	OECD countries 34 industries	ISIC Rev. 4	Focus on OECD economic transactions, reliable data Limited non-OECD coverage, less detailed sectors
WIOD	44 countries 56 industries	NACE Rev. 2	Detailed economic transactions, globalization effects Limited country coverage, data until 2014

prehensive environmental, social, and economic data for countries and regions worldwide. It employs the flexible Eora input-output classification system, which harmonizes industry and product classifications into a unified framework. In contrast, GTAP is a proprietary global economic model that captures production, consumption, and trade interactions. It primarily serves as a tool for trade policy analysis, examining the effects of policy changes on various sectors and regions. Lastly, the OECD provides extensive data and analysis on diverse topics such as economics, environment, education, and social issues. Its databases encompass multiple countries and industries, making them widely utilized by policymakers, researchers, and analysts. Nevertheless, the OECD input-output tables mainly focus on OECD countries and contain few non-OECD countries.

[28] After GTAP, WIOD is certainly the second most known input-output table with more than 10 000 citations according to Google Scholar.

[29] The list of countries and their ISO codes are given in Table 45 on page 175. ROW is the ISO code for the rest-of-the-world region.

[30] The differences are the following: South Africa is included in Exiobase, but not in WIOD. Moreover, the rest-of-the-world aggregate is split into five regions: Africa, Americas, Asia and Pacific, Europe and Middle East.

Estimation of the matrix A When dealing with monetary input-output databases, a direct estimation of the technical coefficient $A_{i,j} = Z_{i,j}/x_j$ may not be robust because the intermediary demand may be greater than the output for some sectors: $\sum_{j=1}^{n} Z_{i,j} > x_i$. This implies that some values of $A_{i,j}$ may be greater than one or A may be not substochastic. The reason lies in the definition of the final demand y_i, which includes accounting items that can take a negative value. In the case of the WIOD table, the final demand y_i is split into 5 items:

1. Final consumption expenditure by households;
2. Final consumption expenditure by non-profit organisations serving households (NPISH);
3. Final consumption expenditure by government;
4. Gross fixed capital formation;
5. Changes in inventories and valuables.

Changes in inventories are defined as the difference between additions to and withdrawals from inventories. They can take a positive or negative value. A high negative evolution of stocks can then produce a situation where output is lower than the intermediary demand. In fact, this type of situation can also be observed for the other items, in particular the gross fixed capital formation and the final consumption expenditure by households. To obtain a better estimate of the matrix A, we replace the net output x_i by the total intermediary demand when the condition $\sum_{j=1}^{n} Z_{i,j} > x_i$ is satisfied[31]:

$$x_i \longleftarrow \max \left(x_i, \sum_{j=1}^{n} Z_{i,j}, \sum_{j=1}^{n} Z_{j,i} \right)$$

The WIOD input-output matrix A has then $44 \times 56 = 2\,464$ rows and columns and requires 46 MB of RAM to be stored. If we consider the Exiobase table, A is a $7\,987 \times 7\,987$ matrix and takes 487 MB of RAM. The matrix A is very sparse and is less relevant to perform an upstream exercise. Moreover, the results obtained with WIOD and Exiobase are difficult to compare, because the two datasets use different sector classification systems: Eora for Exiobase and NACE Rev. 2 for WIOD. Therefore, we map the 163 Exiobase industries into the WIOD classification[32], and we aggregate South Africa and the 5 rest-of-the-world regions[33]. We then obtain a matrix A, which has exactly the same industries and regions than WIOD.

To illustrate the mapping process, we consider the *Mining and quarrying* sector, which gathers 14 Exiobase sectors[34]. Performing the aforementioned aggregation thus allows us to compare the main upstream and downstream relationships depicted by the two databases.

[31] Another approach would be to consider the accounting identity: $x_i = \sum_{j=1}^{n} Z_{i,j} + y_i$ where $y_i = \sum_{k=1}^{m} y_{i,k}$ is the total final demand and m is the number of items of the final demand. The issue may occur when some items $y_{i,k}$ are negative. In this case, the idea is to replace x_i by $\sum_{j=1}^{n} Z_{i,j} + \sum_{k=1}^{n} \max\left(y_{i,k}, 0\right)$.

[32] Some Exiobase sectors can be mapped to two WIOD candidate sectors. For example, the Exiobase sector *Chemicals nec* can go in the WIOD sectors *Manufacture of chemicals and chemical products* or *Manufacture of basic pharmaceutical products and pharmaceutical preparations*. The sector *Post and telecommunications* can go in *Telecommunications* or *Postal and courier activities* in WIOD and *Research and development* can be assigned to *Scientific research and development* or *Advertising and market research*. Moreover, seven WIOD sectors do not exist in Exiobase (*e.g.*, *Administrative and support service activities*).

[33] Technical details about the aggregation process can be found in Appendix A.5 on page 147.

[34] *Mining of precious metal ores and concentrates*, *Mining of lead, zinc and tin ores and concentrates*, *Mining of other non-ferrous metal ores and concentrates*, *Quarrying of stone*, etc.

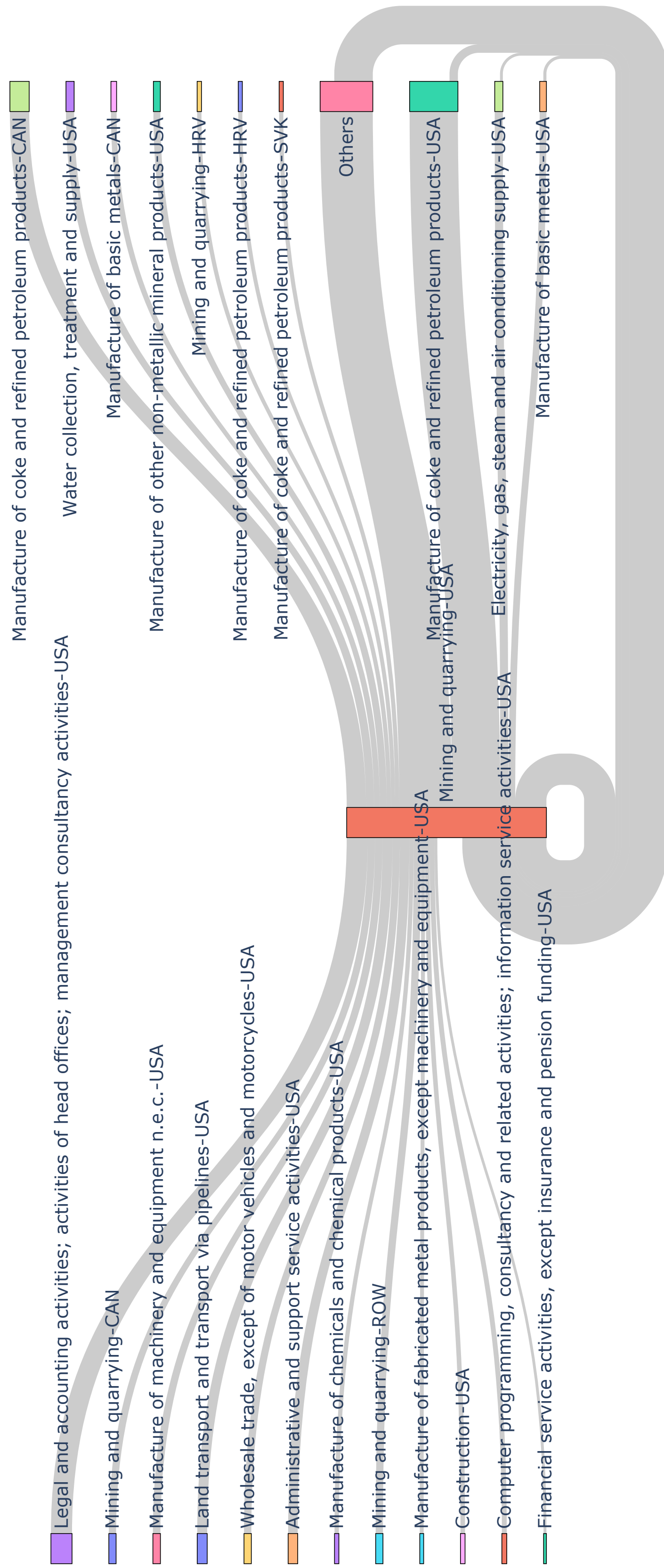

Figure 18: Sankey diagram of *Mining and quarrying* in the USA (WIOD 2014)

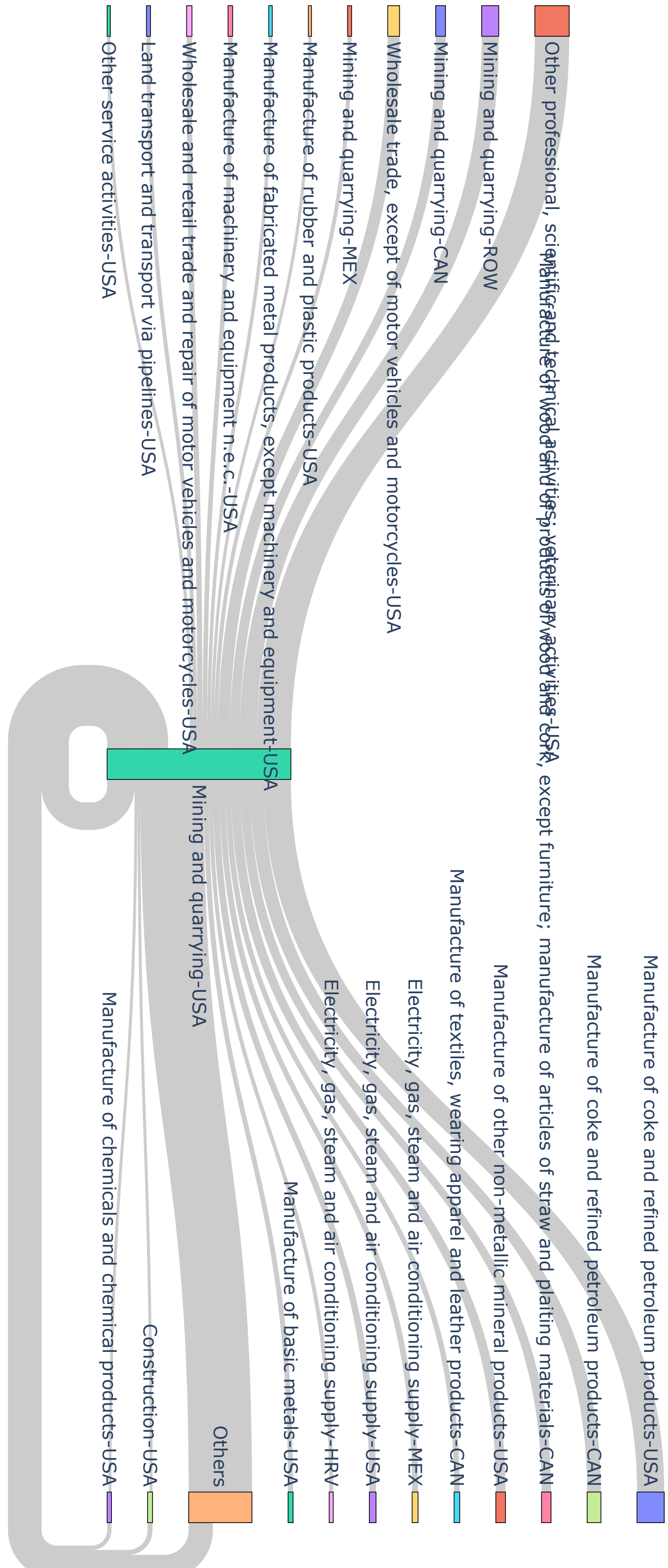

Figure 19: Sankey diagram of *Mining and quarrying* in the USA (Exiobase 2014)

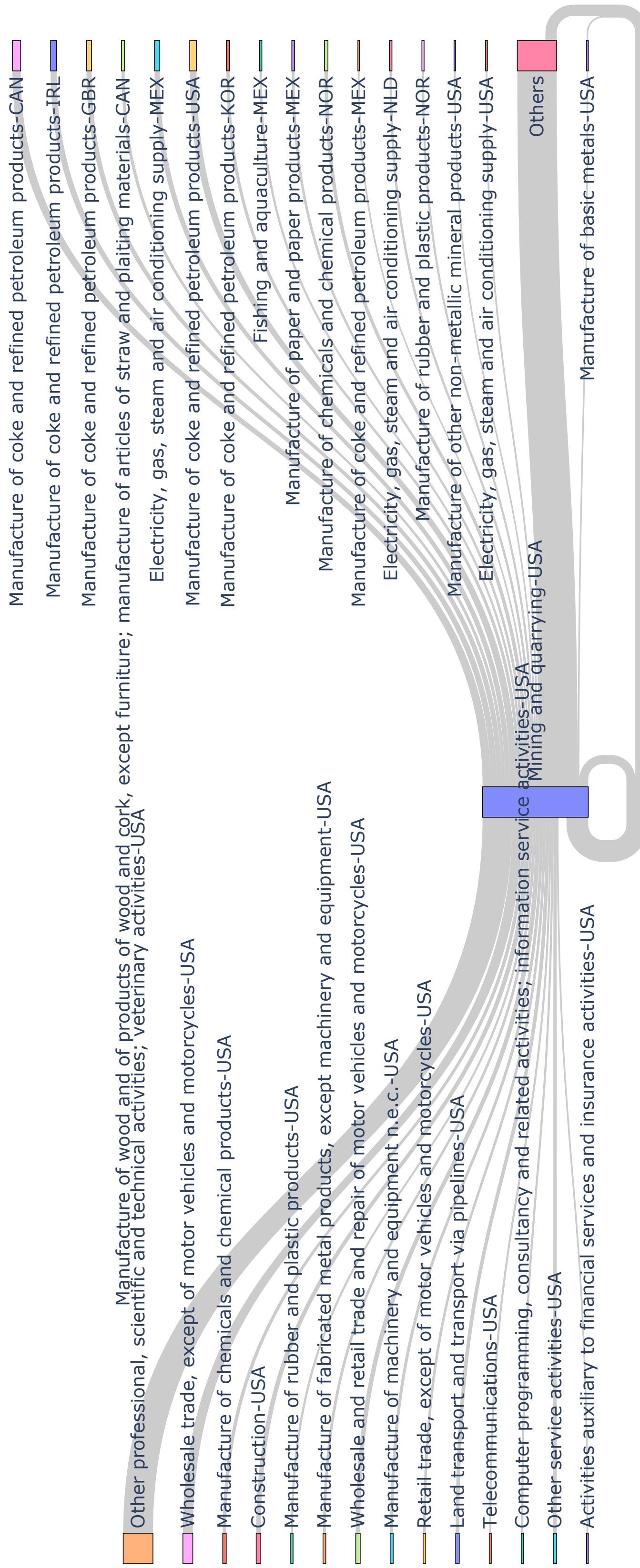

Figure 20: Sankey diagram of *Mining and quarrying* in the USA (Exiobase 2022)

Figures 18 and 19 illustrate the two frames. We center the selected sector, filter the largest technical coefficients[35], and sum the rest to others. On the left of the graph, we can see the main providers and on the right the main client sectors. We notice that the relationships are sensibly similar, since the main upstream sectors are *Services* (mapped differently in WIOD and Exiobase), *Mining and quarrying* in Canada and rest-of-the-world, *Wholesale trade* and *Materials*. The main downstream sectors are *Manufacture of coke and refined petroleum products* in the USA and Canada, *Manufacture of metal and non-metallic minerals*, etc. We note that some differences remain. Interestingly, it appears that the Exiobase 2022 matrix implies a worldwide diversification (more countries are represented). According to Figure 20, we also have less upstream dependencies abroad (the top are in the USA), but the client sector involves more countries (Ireland, Korea, Netherlands, UK, etc.).

Remark 7. *In Appendix B on pages 160–162, we provide another example with Manufacture of computer, electronic and optical products in the USA. We obtain similar conclusions.*

Sparsity of the matrix A In order to analyze the nonnegative matrix A, we compute the sparsity ratio of A defined as the number of elements less than or equal to a threshold ϵ divided by the total number of elements:

$$\text{sparsity}\,(A,\epsilon) = \frac{\#\left\{A_{i,j} \leq \epsilon\right\}}{\text{card}\,A}$$

When ϵ is set to zero, $\#\left\{A_{i,j} \leq 0\right\}$ is equal to the number of zero-valued elements and $\text{sparsity}\,(A,0)$ measures the zero-sparsity of A. Using the previous estimates, we obtain the following ratios for different values of ϵ:

Database	Year	Sparsity ratio			
		$\epsilon = 0$	$\epsilon = 10^{-3}$	$\epsilon = 0.01$	$\epsilon = 0.05$
WIOD	2014	16.76%	98.01%	99.61%	99.94%
Exiobase	2014	32.30%	98.50%	99.69%	99.94%
Exiobase	2022	34.47%	98.44%	99.68%	99.94%

The zero-sparsity of the WIOD matrix is equal to 16.76%, which is not so high. For Exiobase, the figures are higher (32.30% in 2014 and 34.47% in 2018). If we consider the other values of ϵ, the sparsity ratios are very close. This means that many entries in WIOD are very small while they are set to zero in Exiobase.

In Figure 21, we plot the sparsity pattern of the input-output matrix and only the values of $A_{i,j}$ greater than 5% are colored. We notice that the density of the matrix is mainly located within the country submatrices. Outside these intra-country matrices, the input-output table is sparse except for some countries: China, Germany, Russia, USA and the rest-of-the-world region. If we compare with the Exiobase matrices, we obtain very similar profiles (Figures 94 and 95 on pages 157–158). Nevertheless, a deeper analysis shows that the matrices are highly different. For instance, we have reported the sparsity pattern of the matrix $|A_{\text{wiod}} - A_{\text{exiobase}}|$ in Figure 96 on page 158 and we notice that the magnitude of the technical coefficients are not comparable in some cases. Even if the Frobenious norm[36] of $A_{\text{wiod}} - A_{\text{exiobase}}$ is reduced compared to those of A_{wiod} or A_{exiobase}, we observe that some cells of the difference matrix may be greater than 5%.

We introduce several notations. $i \in \mathcal{C}$ (resp. $j \in \mathcal{C}$) means the rows (resp. columns) of matrix A that belong to country $\mathcal{C}$. $A(\mathcal{C}) = \left\{\left(A_{i,j}\right) : i \in \mathcal{C} \wedge j \in \mathcal{C}\right\}$ is the submatrix block

[35] In order to interpret the graph, the threshold has been established at 1.75%.

[36] For year 2014, we have $\|A_{\text{wiod}}\|_2 = 8.12$, $\|A_{\text{exiobase}}\|_2 = 9.05$ and $\|A_{\text{wiod}} - A_{\text{exiobase}}\|_2 = 7.62$.

Figure 21: Sparsity pattern of the input-output matrix A (WIOD 2014)

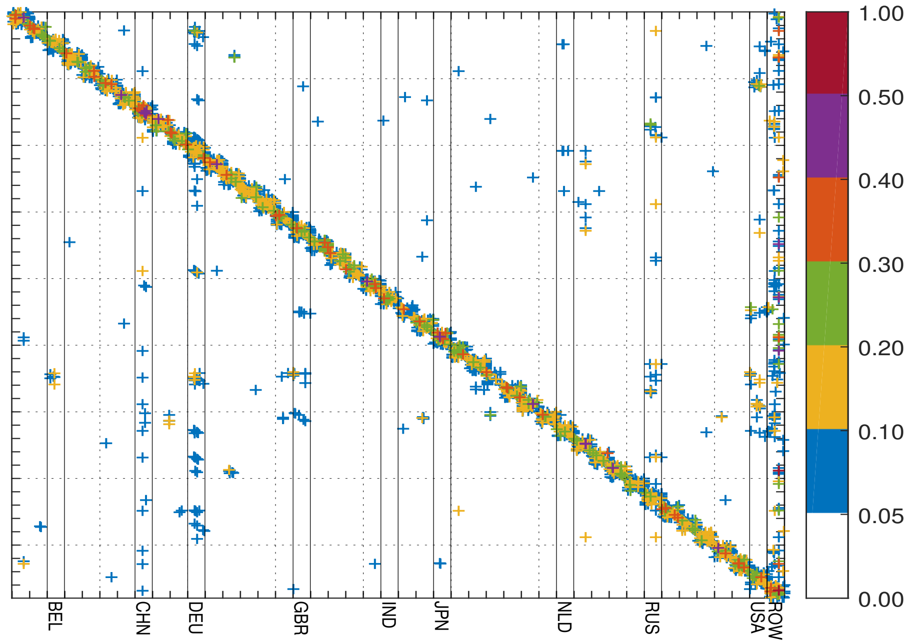

of A corresponding to the country $\mathcal{C}$. The set of diagonal elements is $\mathcal{D}_A(\mathcal{C}) = \{A_{i,i} : i \in \mathcal{C}\}$ while the set of off-diagonal elements correspond to $\mathcal{O}_A(\mathcal{C}) = \{A_{i,j} : i \in \mathcal{C} \wedge j \in \mathcal{C} \wedge i \neq j\}$. The elements whose rows belong to country $\mathcal{C}$ and columns to other countries are denoted by $\mathcal{R}_A(\mathcal{C}) = \{A_{i,j} : i \in \mathcal{C} \wedge j \notin c\}$. In the same way, we define $\mathcal{C}_A(\mathcal{C}) = \{A_{i,j} : i \notin c \wedge j \in \mathcal{C}\}$ as the elements whose columns belong to country $\mathcal{C}$ and rows to other countries. In Table 47 on page 177, we have reported two density metrics with respect to the country. $\max A_{i,j}(\Omega)$ measures the maximum technical coefficient for the set Ω, while $\#\{A_{i,j}(\Omega) \geq 10\%\}$ indicates the number of elements in the set Ω which are greater than 10%. In the case of Australia, $\max A_{i,j}(\Omega)$ is equal to 31% for $\mathcal{D}_A(\mathcal{C})$, 44% for $\mathcal{O}_A(\mathcal{C})$, 11% for $\mathcal{R}_A(\mathcal{C})$, and 22% for $\mathcal{C}_A(\mathcal{C})$, while we obtain the following results for the statistic $\#\{A_{i,j}(\Omega) \geq 10\%\}$: 8 for $\mathcal{D}_A(\mathcal{C})$, 12 for $\mathcal{O}_A(\mathcal{C})$, 1 for $\mathcal{R}_A(\mathcal{C})$, and 2 for $\mathcal{C}_A(\mathcal{C})$. In total, we have 1 241 technical coefficients greater than 10%, which correspond to an average of 30 sectors by country[37]. It is somewhat lower than the figures obtained with the Exiobase matrices[38].

Convergence of the Leontief inverse matrix Let us now analyze the Leontief matrix $\boldsymbol{\mathcal{L}} = (I - A)^{-1}$. In Figure 22, we perform the eigendecomposition $A = V \Lambda V^{-1}$ and plot the spectrum of A. Comparing the magnitude $|\lambda_i|$ of the first five hundred eigenvalues confirms that the WIOD matrix is a little smaller than the Exiobase matrices, even if the difference is not high. Figure 23 reports the Frobenious norm of the power A^k for $k = 0, \ldots, 10$ and the Leontief matrix $\boldsymbol{\mathcal{L}}$. We notice that the differences between the three matrices mainly concern the first and second tiers. Moreover, the convergence of the Leontief matrix is achieved very quickly since the Frobenious norm of A^k is lower than 1 after the third tier and 0.1 after the seventh tier.

[37] 544 are located in the diagonal, 602 are in the off-diagonal country matrices and 95 are intra-country technical coefficients.

[38] The number of technical coefficients greater than 10% is respectively equal to 1 355 and 1 347 (Tables 48 and 49 on pages 178–179).

Figure 22: Spectrum of the matrix A

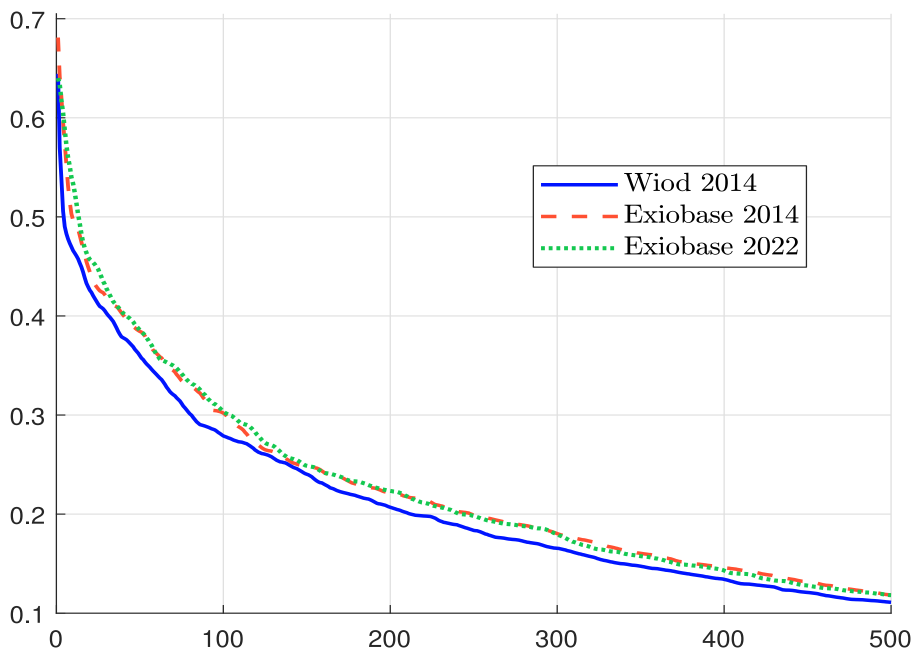

Figure 23: Frobenious norm of the matrix A^k

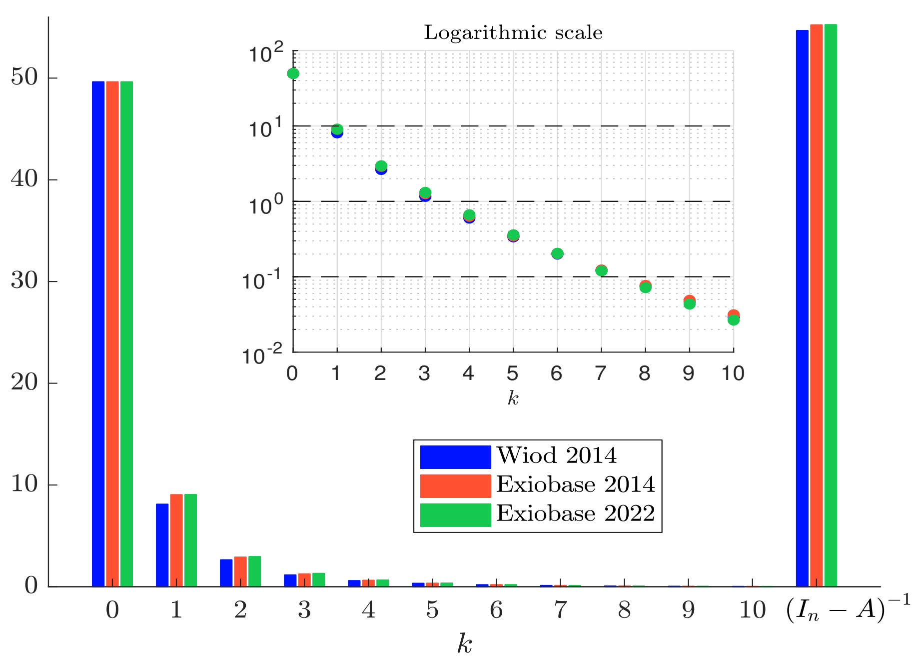

4.3.3 Estimation of the upstream emissions and comparison with the Trucost database

We collect greenhouse gas emissions data from three different sources in order to have the vector of direct emission intensities for the 2 464 sector $\times$ country entries. In the case of WIOD, direct GHG emissions are available in environmental accounts and are computed from the data provided by the Joint Research Centre of the European Commission (Corsatea *et al.*, 2019). For Exiobase, we use the consumption-based account table, which contains the direct GHG emissions (Stadler, 2021). Finally, Trucost provides scope 1 emissions and intensity, but also scope 2, direct emissions, first-tier indirect, upstream scope 3 and downstream scope 3 metrics.

We recall that the vectors of total carbon intensity and emission are equal to $\boldsymbol{\mathcal{CI}}_{\text{total}} = \left(I_n - A^\top\right)^{-1} \boldsymbol{\mathcal{CI}}_1$ and $\boldsymbol{\mathcal{CE}}_{\text{total}} = x \odot \boldsymbol{\mathcal{CI}}_{\text{total}}$. For the k^{th} tier, the formulas become $\boldsymbol{\mathcal{CI}}_{(k)} = \left(A^\top\right)^k \boldsymbol{\mathcal{CI}}_1$ and $\boldsymbol{\mathcal{CE}}_{(k)} = x \odot \boldsymbol{\mathcal{CI}}_{(k)}$. The dimension of all these vectors is $n \times 1$, where n is the number of countries times the number of industries[39]. For Trucost, carbon emissions and intensities are directly available. Direct emissions of input-output models can be compared to scope 1 emissions of Trucost, while the total emissions correspond to scope 1 plus scope 2 plus scope 3 upstream emissions of Trucost. We can also compare the direct plus first-tier indirect emissions of Trucost with the first-tier cumulative emissions $\boldsymbol{\mathcal{CE}}_{(0-1)}$ computed from input-output models.

We can perform a graph analysis similar to the previous Sankey diagrams, but we have now new information about the GHG emissions. The interconnectedness between two nodes depend then on the magnitude of the technical coefficients, but also on the value of the carbon intensities. The upstream analysis of GHG emissions is then different than the upstream analysis of intermediary consumptions. For example, the *Mining and quarrying* sector in the USA has its main upstream dependencies shown in Figure 24, where the size of the nodes is proportional to the intensity of the sectors. We can see that the first-tier emissions (in dark blue) are mostly related to the *Energy* and *Land transport via pipeline* sectors in the USA and to the *Mining and quarrying* sector in Canada. The second-tier (light blue) upstream emissions of this sector mostly come from *Air transport* in both the USA and Canada and *Water transport* in Canada. This representation allows us to quickly visualize the cartography of upstream emissions for a given sector. This approach can also be applied to downstream emissions in a similar way.

Global analysis To perform a global analysis, we aggregate the carbon emissions as follows:

$$\boldsymbol{\mathcal{CE}}_{\text{total}}\left(\boldsymbol{\mathcal{G}}lobal\right) = \sum_{j=1}^{n} \boldsymbol{\mathcal{CE}}_{\text{total},j} = \mathbf{1}_n^\top \boldsymbol{\mathcal{CE}}_{\text{total}}$$

We can then deduce the carbon intensity:

$$\boldsymbol{\mathcal{CI}}_{\text{total}}\left(\boldsymbol{\mathcal{G}}lobal\right) = \frac{\sum_{j=1}^{n} \boldsymbol{\mathcal{CE}}_{\text{total},j}}{\sum_{j=1}^{n} x_j} = \frac{\mathbf{1}_n^\top \boldsymbol{\mathcal{CE}}_{\text{total}}}{\mathbf{1}_n^\top x}$$

In this framework, the global carbon intensity is also equal to the weighted average carbon intensity:

$$\boldsymbol{\mathcal{CI}}_{\text{total}}\left(\boldsymbol{\mathcal{G}}lobal\right) = \frac{\sum_{j=1}^{n} x_j \boldsymbol{\mathcal{CI}}_{\text{total},j}}{\sum_{j=1}^{n} x_j} = \sum_{j=1}^{n} \frac{x_j}{\sum_{i=1}^{n} x_i} \boldsymbol{\mathcal{CI}}_{\text{total},j} = \text{WACI}_{\text{total}}\left(\boldsymbol{\mathcal{G}}lobal\right)$$

[39] In our case, n is equal to 2 464 (44 countries and 56 industries).

Figure 24: Graph analysis of the upstream breakdown (Mining and quarrying, USA)

The total carbon emissions are equal to 32.38 $GtCO_2e$ in WIOD 2014, 40.74 $GtCO_2e$ in Exiobase 2014 and 48.34 $GtCO_2e$ in Exiobase 2022. Therefore, the carbon intensities are respectively equal to 200.92, 341.44 and 282.25 tCO_2e/\$ mn. In Table 15, we report the multiplying coefficients $m_{(k)} = \mathcal{CE}_{(k)}(\mathcal{G}lobal) \Big/ \mathcal{CE}_1(\mathcal{G}lobal)$ and $m_{(0-k)} = \mathcal{CE}_{(0-k)}(\mathcal{G}lobal) \Big/ \mathcal{CE}_1(\mathcal{G}lobal)$, and we also compute the contribution ratio $c_{(0-k)} = \mathcal{CE}_{(0-k)}(\mathcal{G}lobal) \Big/ \mathcal{CE}_{\text{total}}(\mathcal{G}lobal)$. For the WIOD table, the direct plus indirect emissions are 3.14 times the scope 1 emissions, meaning that the indirect emissions are more than two times the direct emissions. In the case of the Exiobase tables, the ratio $m_{(0-\infty)}$ is equal to 2.76 in 2014 and 2.75 in 2022. We notice that the convergence is fast since more than 90% of total emissions are located within the first five tiers. To confirm these results, we compute the upstreamness index $\boldsymbol{\tau}_j^{\text{up}}$ for the 56 sectors and 44 regions. If we consider the median value of $\boldsymbol{\tau}_j^{\text{up}}$, we obtain 2.33, 1.90 and 1.88 while the maximum value of $\boldsymbol{\tau}_j^{\text{up}}$ is 4.30, 4.65 and 4.47. On average, the upstreamness of the WIOD 2014 table is slightly deeper than the upstreamness of the Exiobase tables.

Table 15: Ratio of upstream carbon emissions (global analysis)

Tier	WIOD 2014			Exiobase 2014			Exiobase 2022		
	$m_{(k)}$	$m_{(0-k)}$	$c_{(0-k)}$	$m_{(k)}$	$m_{(0-k)}$	$c_{(0-k)}$	$m_{(k)}$	$m_{(0-k)}$	$c_{(0-k)}$
0	1.00	1.00	31.8%	1.00	1.00	36.2%	1.00	1.00	36.4%
1	0.77	1.76	56.1%	0.72	1.72	62.5%	0.73	1.73	62.9%
2	0.50	2.26	71.9%	0.43	2.15	78.0%	0.42	2.15	78.3%
3	0.32	2.58	82.1%	0.25	2.40	87.0%	0.25	2.40	87.3%
4	0.20	2.78	88.6%	0.15	2.55	92.3%	0.14	2.54	92.5%
5	0.13	2.91	92.7%	0.09	2.63	95.5%	0.08	2.62	95.5%
6	0.08	3.00	95.4%	0.05	2.69	97.3%	0.05	2.67	97.3%
7	0.05	3.05	97.0%	0.03	2.72	98.4%	0.03	2.70	98.4%
8	0.03	3.08	98.1%	0.02	2.73	99.0%	0.02	2.72	99.0%
9	0.02	3.11	98.8%	0.01	2.74	99.4%	0.01	2.73	99.4%
10	0.01	3.12	99.2%	0.01	2.75	99.7%	0.01	2.74	99.7%
∞	0.00	3.14	100.0%	0.00	2.76	100.0%	0.00	2.75	100.0%

In the case of Trucost, we can only compute $m_{(0-1)}$ and $m_{(0-\infty)}$. Results are given in Figure 25. We notice that the multiplying coefficients obtained with Trucost are smaller than those computed with input-output models (1.45–1.54 versus 1.7 for the first tier). Nevertheless, the multiplying coefficient is very high if we integrate scope 3 emissions since we obtain a value of 4.78 in 2019 and 6.75 in 2021. Moreover, a time-series analysis shows that the multiplying coefficients of Trucost tend to increase over time (Table 16).

Table 16: Multiplying coefficient (global analysis, Trucost)

Year	2019	2020	2021
Direct + first-tier indirect	1.45	1.51	1.54
Total (direct + indirect)	1.81	1.89	1.98
$\mathcal{SC}_{1-3}$	4.78	6.42	6.75

Figure 25: Multiplying coefficient $m_{(0-1)}$ and $m_{(0-\infty)}$ (global analysis)

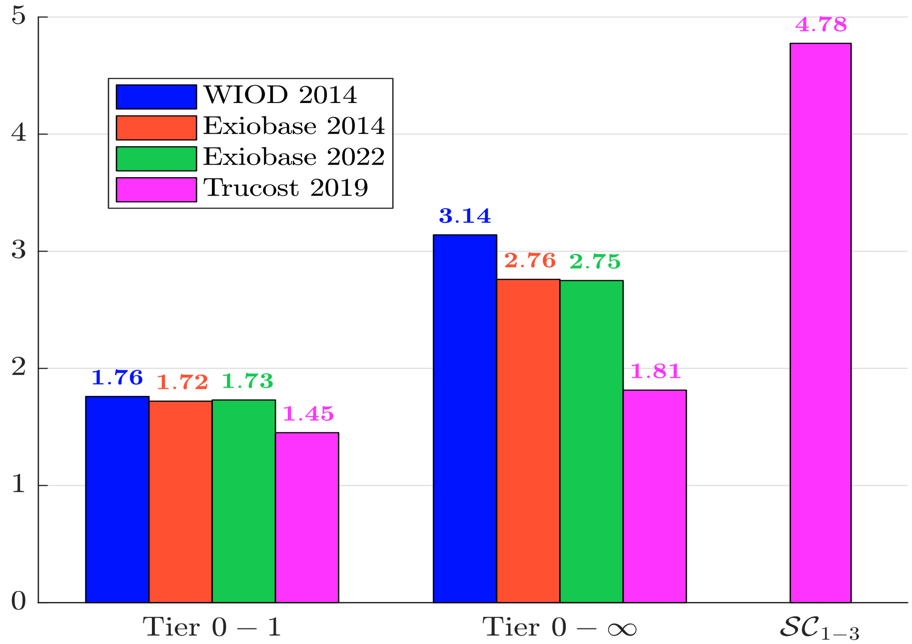

Country analysis Let $j \in \mathcal{C}$ be the set of sectors (or rows) that correspond to country $\mathcal{C}$ and $\mathbf{c}$ the $n \times 1$ vector with $\mathbf{c}_j = 1$ if $j \in \mathcal{C}$ and 0 otherwise. We have:

$$\boldsymbol{\mathcal{CE}}_{\text{total}}(\mathcal{C}) = \sum_{j \in \mathcal{C}} \boldsymbol{\mathcal{CE}}_{\text{total},j} = \mathbf{c}^\top \boldsymbol{\mathcal{CE}}_{\text{total}}$$

and:

$$\boldsymbol{\mathcal{CI}}_{\text{total}}(\mathcal{C}) = \frac{\sum_{j \in \mathcal{C}} \boldsymbol{\mathcal{CE}}_{\text{total},j}}{\sum_{j \in \mathcal{C}} x_j} = \frac{\mathbf{c}^\top \boldsymbol{\mathcal{CE}}_{\text{total}}}{\mathbf{c}^\top x}$$

Again, we can show that the country carbon intensity is also equal to its weighted average carbon intensity: $\boldsymbol{\mathcal{CI}}_{\text{total}}(\mathcal{C}) = \text{WACI}_{\text{total}}(\mathcal{C})$. In Tables 50–52 on pages 180–182, we report the decomposition of total carbon emissions by distinguishing direct, first-tier indirect and indirect emissions. On average, 31.8% and 24.4% of total carbon emissions are explained by direct and first-tier indirect emissions if we consider the WIOD table. We can observe some major differences from one country to another. For instance, Figure 26 shows the multiplying coefficient $m_{(0-\infty)}$ of the different countries. The lowest value is obtained for the USA ($m_{(0-\infty)} = 2.19$), while the largest factor is observed for Switzerland ($m_{(0-\infty)} = 7.21$). On average, we obtain coherent figures between WIOD and Exiobase since the correlation is greater than 70%. This is not the case with the Trucost database. Indeed, we report the multiplying coefficients $m_{(0-1)}$ and multiplying coefficients $m_{(0-\infty)}$ in Table 17 and observe that the Trucost estimates are not correlated with the MRIO estimates[40].

[40] Regardless the correlation analysis (Pearson, Kendall or Spearman analysis), the conclusion is the same at the 90% confidence level.

Figure 26: Multiplying coefficient $m_{(0-\infty)}$ (WIOD 2014)

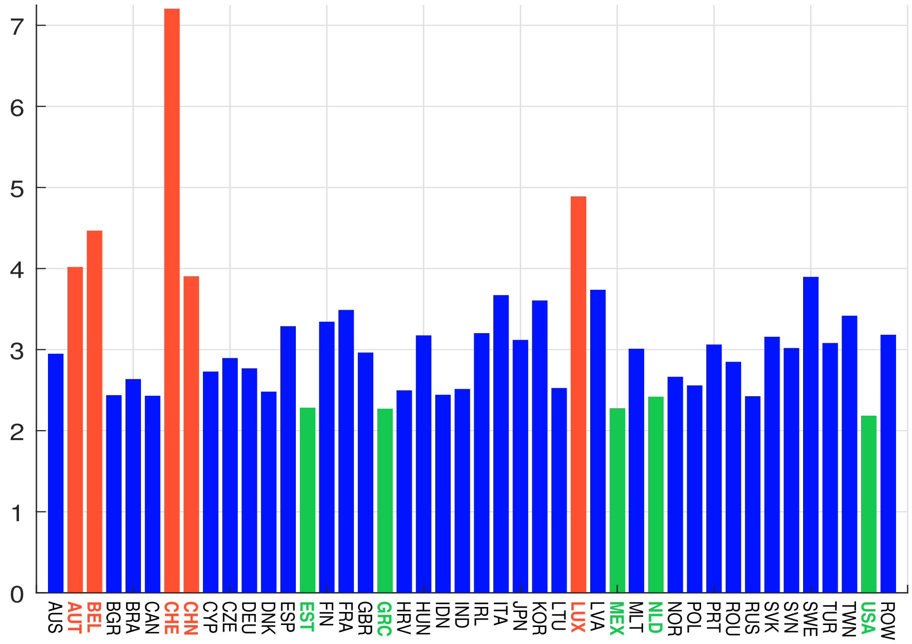

Table 17: Comparison of multiplying coefficients $m_{(0-k)}$ (country analysis)

Data	WIOD		Exiobase		Exiobase		Trucost		Trucost		Trucost	
Year	2014		2014		2022		2019		2020		2021	
k	1	∞	1	∞	1	∞	1	∞	1	∞	1	∞
AUS	1.74	2.95	1.58	2.25	1.55	2.14	1.57	1.87	1.59	1.91	1.69	2.13
BRA	1.69	2.64	1.68	2.30	1.62	2.12	1.64	2.00	1.92	2.31	3.35	3.88
CAN	1.55	2.43	1.61	2.33	1.61	2.29	1.45	1.80	1.44	1.76	1.52	1.90
CHE	2.54	7.21	2.40	5.64	2.46	5.79	1.80	2.47	1.88	2.65	1.91	2.73
CHN	1.91	3.91	1.97	3.89	1.97	3.84	1.24	1.41	1.27	1.48	1.30	1.52
DEU	1.67	2.77	1.68	2.61	1.74	2.89	1.52	2.26	1.59	2.42	1.73	2.65
ESP	1.74	3.29	1.81	3.02	1.81	2.96	1.45	1.81	1.48	1.84	1.70	2.20
FRA	1.73	3.49	1.78	2.99	1.76	2.96	1.82	2.59	1.89	2.63	2.03	2.97
GBR	1.67	2.96	1.66	2.67	1.66	2.67	2.31	3.13	2.18	2.88	2.31	3.05
IDN	1.63	2.44	1.59	2.07	1.64	2.10	1.30	1.50	1.32	1.54	1.37	1.62
IND	1.74	2.51	1.63	2.23	1.65	2.30	1.22	1.36	1.20	1.33	1.21	1.35
ITA	1.83	3.67	2.04	3.61	2.07	3.76	1.35	1.60	1.33	1.61	1.52	1.91
JPN	1.76	3.12	1.87	3.15	1.85	3.09	1.82	2.75	1.96	3.06	2.01	3.20
KOR	1.83	3.61	2.06	4.04	2.16	4.47	1.54	2.06	1.55	2.09	1.65	2.29
RUS	1.71	2.43	1.43	1.77	1.45	1.78	1.23	1.34	1.21	1.30	1.48	1.72
MEX	1.61	2.28	1.60	2.23	1.57	2.15	1.75	2.34	1.80	2.40	1.80	2.48
NLD	1.47	2.42	2.01	3.20	2.02	3.40	2.62	4.02	2.10	3.24	2.80	6.82
TUR	1.82	3.08	1.81	2.70	1.63	2.26	1.24	1.46	1.29	1.50	1.32	1.55
TWN	1.83	3.42	2.13	4.31	2.02	4.04	1.80	2.48	1.83	2.57	1.78	2.54
USA	1.54	2.19	1.60	2.15	1.59	2.15	1.67	2.27	1.69	2.32	1.80	2.57

Table 18: Comparison of multiplying coefficients $m_{(0-k)}$ (sector analysis, GICS level 1 classification)

k	Data Year	WIOD 2014	Exiobase 2014	Exiobase 2022	Trucost 2019	Trucost 2020	Trucost 2021
1	Communication Services	4.44	4.86	5.63	10.85	14.65	26.93
	Consumer Discretionary	2.51	2.87	2.68	3.51	3.98	4.41
	Consumer Staples	2.37	3.38	3.35	3.98	4.63	4.64
	Energy	1.71	2.75	2.93	1.46	1.62	1.59
	Financials	3.64	2.86	2.84	1.88	1.89	1.94
	Health Care	2.58	5.31	5.00	3.65	3.58	3.75
	Industrials	2.66	2.15	2.19	1.52	1.61	1.67
	Information Technology	4.55	4.68	4.47	4.26	4.02	4.55
	Materials	1.78	1.50	1.47	1.42	1.40	1.42
	Real Estate	7.93	6.73	6.91	3.49	4.53	6.25
	Utilities	1.28	1.24	1.23	1.10	1.11	1.14
∞	Communication Services	13.43	12.66	14.02	18.57	24.05	37.79
	Consumer Discretionary	5.63	6.46	5.76	8.20	9.75	11.36
	Consumer Staples	4.90	6.24	6.09	6.91	8.08	8.28
	Energy	2.94	4.09	4.33	1.73	1.84	1.90
	Financials	10.21	7.05	7.33	3.67	3.77	3.85
	Health Care	6.58	13.97	13.74	8.56	8.27	9.08
	Industrials	6.25	4.50	4.52	2.15	2.34	2.49
	Information Technology	14.91	15.04	13.44	8.13	7.63	8.95
	Materials	3.02	2.21	2.09	1.57	1.54	1.60
	Real Estate	13.82	12.80	12.80	5.58	8.38	12.53
	Utilities	1.55	1.39	1.35	1.11	1.13	1.16

Sector analysis We proceed as previously to perform a sector analysis by considering the set of rows $j \in \mathcal{S}$ that correspond to Sector $\mathcal{S}$. Therefore, we replace $\mathbf{c}$ by the $n \times 1$ vector $\mathbf{s}$ with $\mathbf{s}_j = 1$ if $j \in \mathcal{S}$ and 0 otherwise. In Figures 27 and 28, we report the values taken by $m_{(0-1)}$ and $m_{(0-\infty)}$ for the 56 WIOD sectors[41]. For some sectors, the figures are very close, meaning that the multiplying coefficients are similar for the three databases. Nevertheless, there are some sectors for which we observe a high discrepancy. In order to better understand these differences, we compute $m_{(0-1)}$ and $m_{(0-\infty)}$ by considering the GICS level 1 classification (Table 18). In the case of the first-tier emissions, multiplying coefficients are similar between the three databases for Information technology, Materials and Utilities. The highest discrepancy is observed for Communication services. The reason for this is that the sector's direct emissions are very low. If we consider the full upstream supply chain, the multiplying coefficient $m_{(0-\infty)}$ is very different for Financials and Health Care. On the contrary, Utilities is the sector with the highest consistency between the three databases.

Country-sector analysis Finally, we consider the country $\times$ sector level, implying that we compute the multiplying coefficients for the 2 464 rows. Figure 29 shows the histogram of $m_{(0-1)}$ and $m_{(0-\infty)}$. We notice that the distributions are fat-tailed. For instance, we have 16% of rows with a multiplying coefficient $m_{(0-1)}$ greater than 10. In the case of $m_{(0-\infty)}$, this frequency is equal to 40%.

[41] We have the following matching: a dark blue circle for WIOD 2014, a dark orange plus sign for Exiobase 2014, a dark yellow asterisk for Exiobase 2022, a dark purple square for Trucost 2019, a medium green diamond for Trucost 2020, and a light blue five-pointed star for Trucost 2021.

Figure 27: Multiplying coefficient $m_{(0-1)}$ (sector analysis)

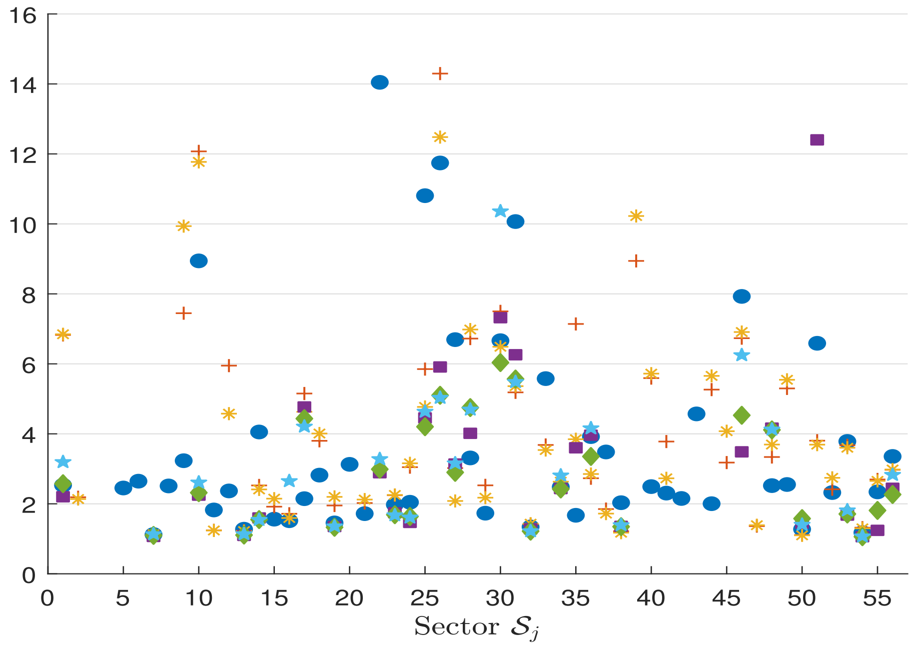

Figure 28: Multiplying coefficient $m_{(0-\infty)}$ (sector analysis)

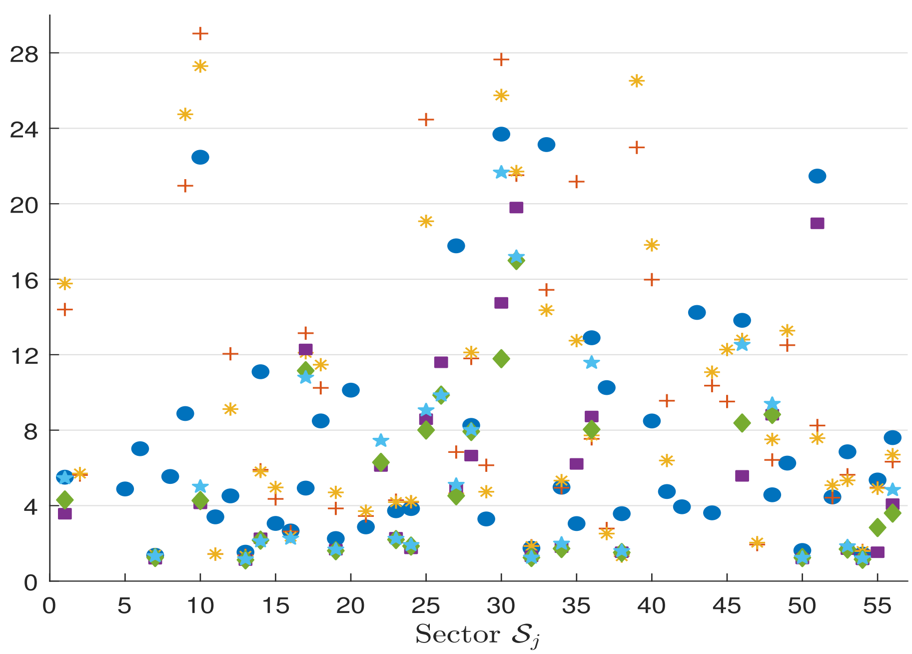

Figure 29: Histogram of multiplying coefficients (country-sector analysis, all databases)

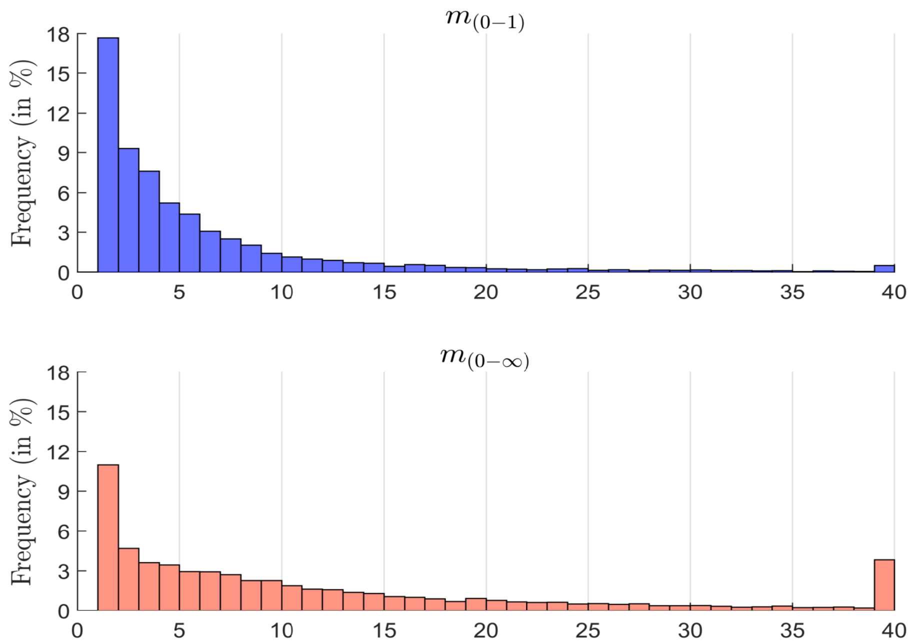

4.3.4 Uncertainty modeling of indirect emissions

Stochastic modeling of multiplying coefficients Following the previous analysis, we can assume that $\mathcal{CE}_{(0-k)} = \tilde{m}_{(0-k)}\mathcal{CE}_1$ where $\tilde{m}_{(0-k)}$ is a random variable which is greater than 1 by construction. We have seen that $\tilde{m}_{(0-k)}$ depends on several factors such as the country or the sector. Therefore, we can write $\tilde{m}_{(0-k)}$ as follows:

$$\tilde{m}_{(0-k)} = 1 + \tilde{\varphi}_{\mathcal{C}}\tilde{\varphi}_{\mathcal{S}}$$

where $\tilde{\varphi}_{\mathcal{C}}$ and $\tilde{\varphi}_{\mathcal{S}}$ are two positive independent random variables that depend on the country $\mathcal{C}$ and the sector $\mathcal{S}$. By assuming that $\tilde{\varphi}_{\mathcal{C}}$ and $\tilde{\varphi}_{\mathcal{S}}$ are two log-normal random variables $\mathcal{LN}\left(\mu_{\mathcal{C}}, \sigma_{\mathcal{C}}^2\right)$ and $\mathcal{LN}\left(\mu_{\mathcal{S}}, \sigma_{\mathcal{S}}^2\right)$, we can show that[42] $\tilde{\varphi}_{\mathcal{C}}\tilde{\varphi}_{\mathcal{S}} \sim \mathcal{LN}\left(\mu_{\mathcal{C}} + \mu_{\mathcal{S}}, \sigma_{\mathcal{C}}^2 + \sigma_{\mathcal{S}}^2\right)$. We deduce that $\tilde{m}_{(0-k)}$ follows a shifted log-normal distribution $\mathcal{SLN}\left(\mu_{\mathcal{C},\mathcal{S}}, \sigma_{\mathcal{C},\mathcal{S}}^2, \xi\right)$, whose mean, standard deviation and shift parameters are equal to $\mu_{\mathcal{C}} + \mu_{\mathcal{S}}$, $\sqrt{\sigma_{\mathcal{C}}^2 + \sigma_{\mathcal{S}}^2}$ and 1.

Sometimes, we would like that the mathematical expectation of $\tilde{m}_{(0-k)}$ matches a given value m_i. For instance, we would like to introduce uncertainty around the estimation of Trucost, but we would like that the mean corresponds to the estimate of Trucost. A first approach is to introduce a scaling factor λ such that $\breve{m}_{(0-k)} = 1 + \lambda\tilde{\varphi}_{\mathcal{C}}\tilde{\varphi}_{\mathcal{S}}$. In this case, the optimal value is equal to $\lambda = (m_i - 1) \bigg/ \left(\mathbb{E}\left[\tilde{m}_{(0-k)}\right] - 1\right)$. We deduce that $\lambda \leq 1$ if $\mathbb{E}\left[\tilde{m}_{(0-k)}\right] \geq m_i$ and, $\lambda > 1$ otherwise. We deduce that the scaling approach does not preserve the variance because $\operatorname{var}\left(\breve{m}_{(0-k)}\right) = \lambda^2 \operatorname{var}\left(\tilde{m}_{(0-k)}\right)$. Therefore, the variance is reduced if $\mathbb{E}\left[\tilde{m}_{(0-k)}\right] \geq m_i$. A second approach consists in introducing a specific random

[42]The proof is given in Appendix A.6 on page 148.

variable $\tilde{\varphi}_i \sim \mathcal{LN}\left(\mu_i, \sigma_i^2\right)$. Therefore, we have $\breve{m}_{(0-k)} = 1 + \tilde{\varphi}_{\mathcal{C}} \tilde{\varphi}_{\mathcal{S}} \tilde{\varphi}_i$. The matching constraint $\mathbb{E}\left[\breve{m}_{(0-k)}\right] = m_i$ and the variance preservation $\operatorname{var}\left(\tilde{m}_{(0-k)}\right) = \operatorname{var}\left(\breve{m}_{(0-k)}\right)$ implies the following optimal values[43]:

$$\sigma_i^2 = \max\left(\ln\left((m_i - 1)^2 + \left(e^{\sigma^2_{\mathcal{C},\mathcal{S}}} - 1\right)\left(\mathbb{E}\left[\tilde{m}_{(0-k)}\right] - 1\right)^2\right) - 2\ln(m_i - 1) - \sigma^2_{\mathcal{C},\mathcal{S}}, 0\right)$$

and:

$$\mu_i = \ln(m_i - 1) - \ln\left(\mathbb{E}\left[\tilde{m}_{(0-k)}\right] - 1\right) - \frac{1}{2}\sigma_i^2$$

Figure 30: Probability density function of the multiplying coefficient

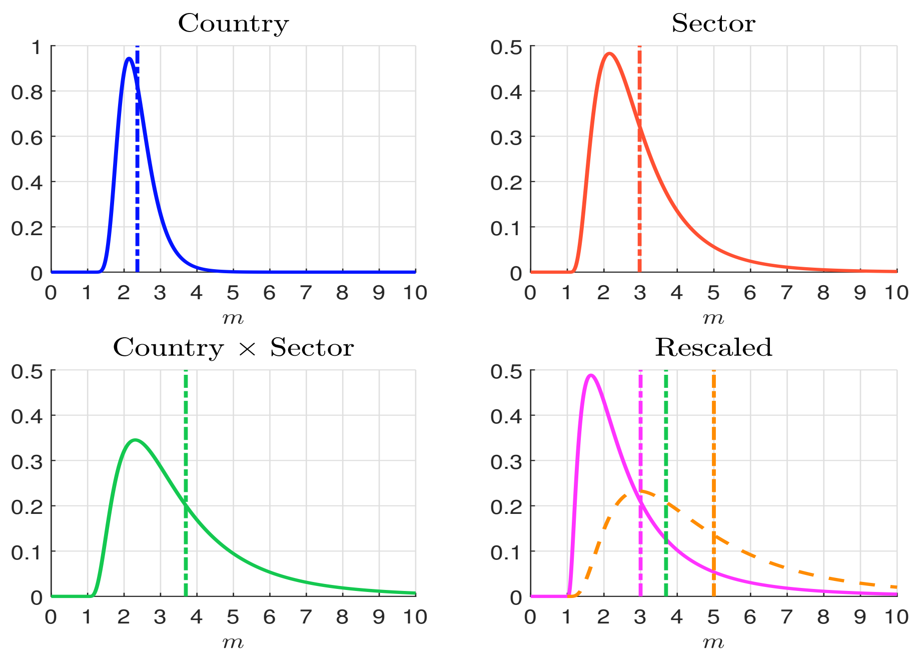

Let us illustrate the calibration problem with an example. We assume that $\mu_{\mathcal{C}} = 0.25$, $\sigma_{\mathcal{C}} = 0.35$, $\mu_{\mathcal{S}} = 0.50$ and $\sigma_{\mathcal{S}} = 0.60$. In Figure 30, we report the probability density function of $\breve{m}_{(0-k)} = 1 + \lambda \tilde{\varphi}_{\mathcal{C}} \tilde{\varphi}_{\mathcal{S}}$ when $\tilde{\varphi}_{\mathcal{S}} = 1$ (top/left panel) and $\tilde{\varphi}_{\mathcal{C}} = 1$ (top/right panel). Therefore, we can see the impact of each factor. We notice that $\breve{m}_{(0-k)}$ takes its value between 1 and 4 when considering the country uncertainty, while it can reach values greater than 6 when capturing the sector effect. The combination of the two factors is given in the bottom/left panel. The mathematical expectation of $\tilde{m}_{(0-k)}$ is 3.69, while its standard deviation is 2.12. If we target $m_i = 3$, the calibration gives $\mu_i = -0.43$ and $\sigma_i = 0.52$. The corresponding probability density function corresponds to the violet line in the bottom/right panel. We verify that $\mathbb{E}\left[\breve{m}_{(0-k)}\right] = 3$ and $\sigma\left(\breve{m}_{(0-k)}\right) = 2.12$. If we target $m_i = 5$, we obtain $\mu_i = 0.40$, $\sigma_i = 0$, $\mathbb{E}\left[\breve{m}_{(0-k)}\right] = 5$ and $\sigma\left(\breve{m}_{(0-k)}\right) = 3.15 > \sigma\left(\tilde{m}_{(0-k)}\right)$. In this case, it is not possible to preserve the variance, but it is the minimum bound for the variance minimization problem.

[43]See Appendix A.7 on page 149.

Maximum likelihood estimation The above framework requires to estimate $2n_{\mathcal{C}} + 2n_{\mathcal{S}}$ parameters, where $n_{\mathcal{C}}$ and $n_{\mathcal{S}}$ are the number of countries and sectors. In practice, this approach is not relevant because it is too granular and we prefer to have a small number of parameters. Therefore, we group countries and sectors in order to obtain $m_{\mathcal{C}}$ country clusters and $m_{\mathcal{S}}$ sector clusters. We denote by C_j (resp. S_k) the j^{th} country (resp. k^{th} sector) cluster. Let $\left\{m_{(0-k),1}, \ldots, m_{(0-k),n}\right\}$ be a sample of n observations. We estimate the parameter vector[44] $\theta = (\mu_{C_1}, \sigma_{C_1}, \mu_{C_2}, \sigma_{C_2}, \ldots, \mu_{S_1}, \sigma_{S_1}, \mu_{S_2}, \sigma_{S_2}, \ldots)$ by the method of maximum likelihood. The expression of the log-likelihood function is:

$$\boldsymbol{\ell}(\theta) = \sum_{i=1}^{n} \sum_{j=1}^{m_{\mathcal{C}}} \sum_{k=1}^{m_{\mathcal{S}}} \mathbb{1}\left\{i \in C_j \wedge i \in S_k\right\} \cdot \boldsymbol{\ell}\left(m_{(0-k),i} - 1, \mu_{C_j}, \sigma_{C_j}, \mu_{S_k}, \sigma_{S_k}\right)$$

where:

$$\boldsymbol{\ell}(x, \mu_{\mathcal{C}}, \sigma_{\mathcal{C}}, \mu_{\mathcal{S}}, \sigma_{\mathcal{S}}) = -\frac{1}{2}\ln(2\pi) - \frac{1}{2}\ln\left(\sigma_{\mathcal{C}}^2 + \sigma_{\mathcal{S}}^2\right) - \ln x - \frac{1}{2}\left(\frac{\ln x - (\mu_{\mathcal{C}} + \mu_{\mathcal{S}})}{\sqrt{\sigma_{\mathcal{C}}^2 + \sigma_{\mathcal{S}}^2}}\right)^2$$

In the case where $2(m_{\mathcal{C}} + m_{\mathcal{S}}) < m_{\mathcal{C}} m_{\mathcal{S}}$, we face an identification issue. Moreover, the model cannot be identified when the $m_{\mathcal{C}} \times m_{\mathcal{S}}$ two-dimensional clustering system is fully separable into two $m_{\mathcal{C}}$ and $m_{\mathcal{S}}$ uni-dimensional clustering systems.

Table 19: Calibration of the multiplying coefficient (no clustering)

	$k=1$				$k=\infty$			
	$\hat{\mu}_{\mathcal{C}}$	$\hat{\sigma}_{\mathcal{C}}$	$\hat{\mu}_{(0-k)}$	$\hat{\sigma}_{(0-k)}$	$\hat{\mu}_{\mathcal{C}}$	$\hat{\sigma}_{\mathcal{C}}$	$\hat{\mu}_{(0-k)}$	$\hat{\sigma}_{(0-k)}$
Country	−0.40	0.61	1.81	0.55	0.32	0.75	2.81	1.57
Sector	0.38	1.09	3.66	4.01	1.25	1.28	8.87	15.93

Table 20: Default parameters of the multiplying coefficient (two-sector clustering)

k	Parameter	Country	Sector #1	Sector #2
1	$\hat{\mu}_{\mathcal{C}_j}$ / $\hat{\mu}_{\mathcal{S}_k}$	−0.40	0.50	1.50
	$\hat{\sigma}_{\mathcal{C}_j}$ / $\hat{\sigma}_{\mathcal{S}_k}$	0.50	1.00	1.00
∞	$\hat{\mu}_{\mathcal{C}_j}$ / $\hat{\mu}_{\mathcal{S}_k}$	0.00	0.75	2.00
	$\hat{\sigma}_{\mathcal{C}_j}$ / $\hat{\sigma}_{\mathcal{S}_k}$	0.50	1.00	1.00

In what follows, we estimate the model by considering the 2 464 observations and merging the six databases (WIOD 2014, Exiobase 2014 and 2022, Trucost 2019, 2020 and 2021). In Table 19, we report the estimated coefficients when we perform no clustering. We also compute $\hat{\mu}_{(0-k)} = \mathbb{E}\left[\tilde{m}_{(0-k)}\right]$ and $\hat{\sigma}_{(0-k)} = \sigma\left(\tilde{m}_{(0-k)}\right)$ using the estimated probability distribution of $\tilde{m}_{(0-k)}$. As expected, the sector dimension is more important than the country dimension. For instance, $\hat{\mu}_{(0-1)}$ takes the value 1.81 if we consider the country dimension, while it is equal to 3.66 for the sector dimension. We now consider the case with two-country and two-sector clusters. For each dimension, we rank the multiplying coefficients, compute the median and split the universe below and above the median. Results are given in Appendix B on page 183. We notice that the differences between the two-country clusters are very small, while there is a high discrepancy between the two-sector clusters.

[44]The dimension of θ is now equal to $2m_{\mathcal{C}} + 2m_{\mathcal{S}} \ll 2n_{\mathcal{C}} + 2n_{\mathcal{S}}$.

This is why we propose to use the default parameters given in Table 20 and not to cluster the countries. Given the high uncertainty of the maximum likelihood estimates, it is better to simplify the analysis and use stylized figures. For the first-tier emissions, the mean of $\tilde{m}_{(0-1)}$ is equal to 3.1 and 3.3 for the first and second clusters. The difference is not significant, but there is more dispersion in the second cluster. Indeed, the standard deviation is equal to 6.6 for the first cluster and 8.9 for the second cluster. Concerning $\tilde{m}_{(0-\infty)}$, the mean and standard deviation are equal to 5.0 and 14.8 for the first cluster, and 6.2 and 21.8 for the second cluster. Finally, the corresponding distribution functions are reported in Figure 31.

Figure 31: Probability density function of $\tilde{m}_{(0-1)}$ and $\tilde{m}_{(0-\infty)}$ (two-sector clustering)

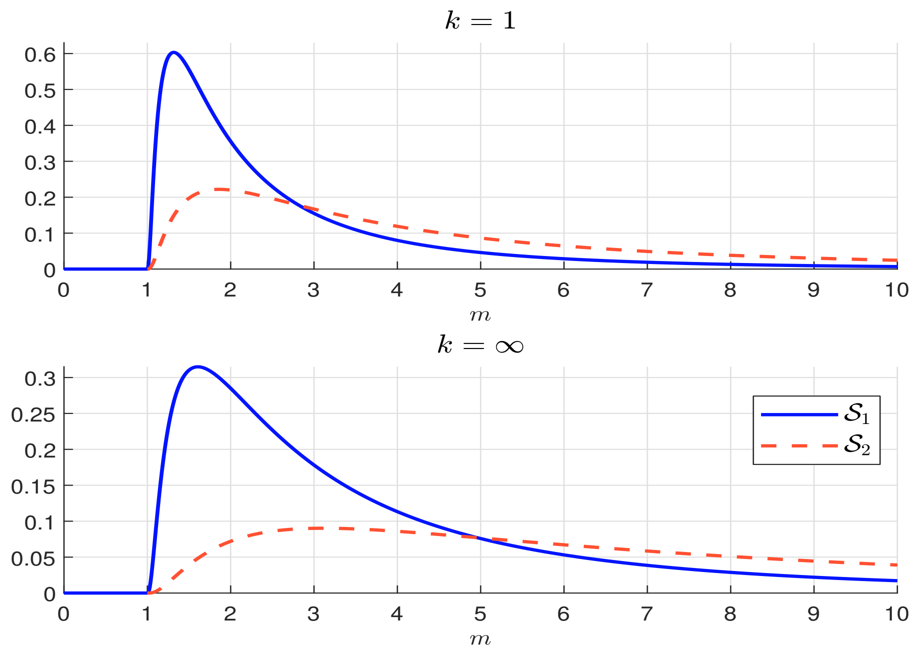

4.4 Application to the MSCI World index

4.4.1 Estimation of upstream intensities

We apply the previous framework to estimate the upstream of the MSCI World index. For that, we first estimate the total carbon intensity for all the issuers of the portfolio:

$$\mathcal{CI}_{\text{total},i} = \mathcal{CI}_{1,i}^{\text{reported}} + \mathcal{CI}_{\text{indirect},i}^{\text{estimated}}$$

where $\mathcal{CI}_{1,i}^{\text{reported}}$ is the scope 1 carbon intensity reported by the issuer i and $\mathcal{CI}_{\text{indirect},i}^{\text{estimated}}$ is the estimated indirect carbon intensity. In the case of Trucost, we use the values estimated by the data provider. For the input-output databases, we use the formula $\mathcal{CI}_{\text{indirect}}^{\text{estimated}} = \left(\left(I_n - A^\top\right)^{-1} - I_n\right)\mathcal{CI}_{\text{direct}}$ and consider the row corresponding to the sector and the country[45] of the issuer i. The scatter plot between Exiobase, Trucost and WIOD estimates is reported in Figure 32. The correlation is 89.6% between Exiobase and Trucost, 95.7% between Exiobase and WIOD, and 91.7% between Trucost and WIOD.

[45] Four countries (HKG, ISR, NZL and SGP) in the MSCI World index are not in the MRIO databases. This is why we map them to the rest-of-the-world region (ROW).

Figure 32: Scatter plot of carbon intensities $\mathcal{CI}_{\text{total}}$ (MSCI World index, May 2023)

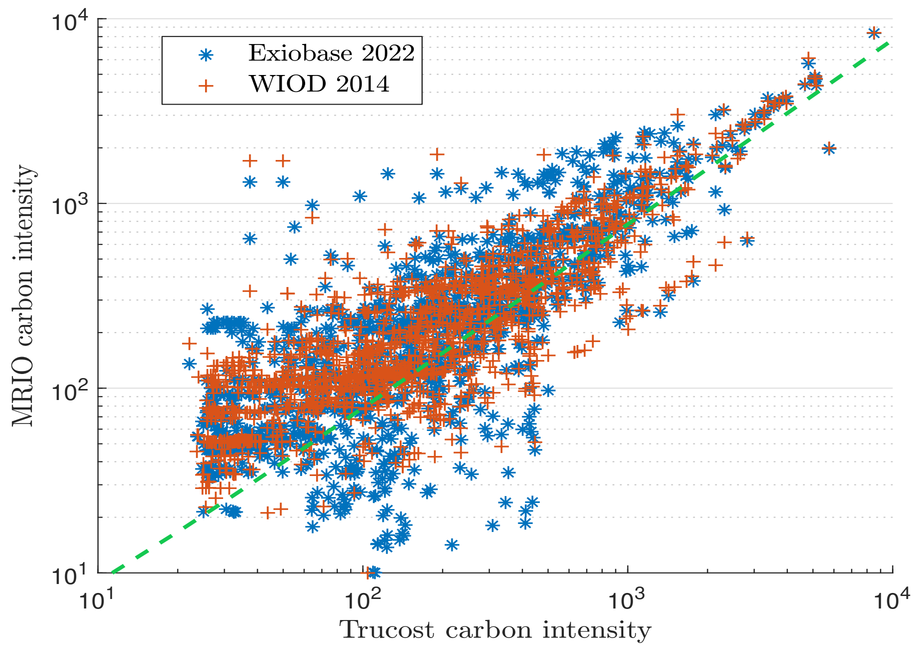

Figure 33: Carbon intensity $\mathcal{CI}_{\text{total}}$ per GICS sector (MSCI World index, May 2023)

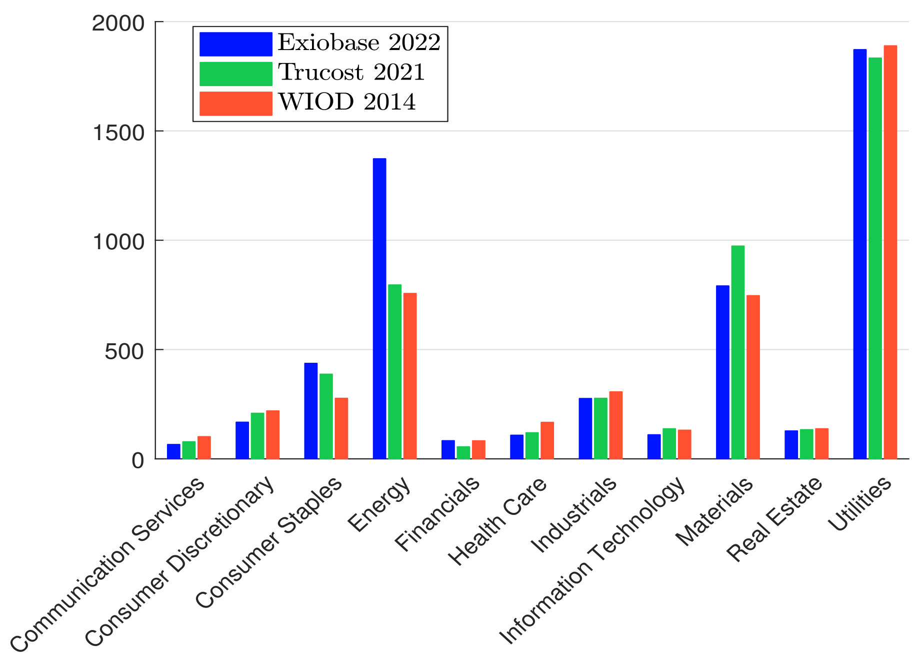

Then, we compute the carbon intensity[46] of the MSCI World index and the GICS level 1 sectors. Results are given in Table 57 on page 183 and Figure 33. The direct plus indirect intensity of the MSCI World index is equal to 299 tCO_2e/\$ mn with Exiobase 2022, 281 tCO_2e/\$ mn with Trucost 2021 and 278 tCO_2e/\$ mn with WIOD 2014. The difference between the lowest and highest values is then equal to 7.5%, which is a low figure. If we consider the GICS sectors, the differences are more important[47], especially for Consumer Staples, Energy and Materials. For instance, the carbon intensity of the Energy sector is equal to 757 tCO_2e/\$ mn with WIOD 2014 and 1 373 tCO_2e/\$ mn with Exiobase 2022. We also compute the contribution of each sector to the carbon intensity of the MSCI World index. We have:

$$c_j(w) = \frac{\sum_{i \in j} w_i \cdot \boldsymbol{\mathcal{CI}}_{\text{total},i}}{\sum_i w_i \cdot \boldsymbol{\mathcal{CI}}_{\text{total},i}}$$

where w is the vector of weights in the MSCI World index and $c_j(w)$ is the contribution of the j^{th} Sector. In Table 21, we notice some significant differences[48]. This concerns the previous mentioned sector (Consumer Staples, Energy and Materials), but also Consumer Discretionary, Health Care and Information Technology.

Table 21: Breakdown of the portfolio intensity per GICS sector (MSCI World index, May 2023)

Sector	Exiobase 2022	Trucost 2021	WIOD 2014
Communication Services	1.5%	1.9%	2.5%
Consumer Discretionary	5.9%	7.8%	8.4%
Consumer Staples	11.6%	10.9%	7.9%
Energy	22.9%	14.1%	13.6%
Financials	4.2%	2.9%	4.5%
Health Care	4.8%	5.7%	8.0%
Industrials	10.2%	10.8%	12.1%
Information Technology	7.5%	10.0%	9.6%
Materials	11.7%	15.3%	11.9%
Real Estate	1.1%	1.2%	1.2%
Utilities	18.6%	19.4%	20.2%

4.4.2 Uncertainty of upstream intensities

Let us assess the uncertainty of the upstream intensity estimation. On average, we have $\overline{\boldsymbol{\mathcal{CI}}}_{\text{total}}(w) = 286$ and $\boldsymbol{\mathcal{CI}}_1(w) = 104$ for the portfolio w of the MSCI World index. Using the framework developed in Section 4.3.4 on page 62, we compute the distribution function of the multiplying coefficient $\tilde{m}_{(0-\infty)}$, estimate the rescaled distribution of $\breve{m}_{(0-\infty)}$ and finally deduce the distribution function of the carbon intensity $\widetilde{\boldsymbol{\mathcal{CI}}}_{\text{total}}(w)$, which is now a random variable and not a single estimated value. Results are reported in Figure 34. We obtain a very asymmetric probability distribution since we have $\Pr\left\{\widetilde{\boldsymbol{\mathcal{CI}}}_{\text{total}}(w) \leq \overline{\boldsymbol{\mathcal{CI}}}_{\text{total}}(w)\right\} \approx 80\%$ and $\Pr\left\{\widetilde{\boldsymbol{\mathcal{CI}}}_{\text{total}}(w) \geq \overline{\boldsymbol{\mathcal{CI}}}_{\text{total}}(w)\right\} \approx 20\%$. This means that there is a high uncertainty on the estimation of the upstream intensity. Indeed, we may consider that there is a significant

[46] We have $\boldsymbol{\mathcal{CI}}_{\text{total}}(w) = \sum_i w_i \cdot \boldsymbol{\mathcal{CI}}_{\text{total},i}$ where w_i is the weight of asset i in the portfolio w.
[47] See Anquetin *et al.* (2022) for a discussion about the disagreement on indirect emissions.
[48] See also Figure 104 on page 164.

probability that the carbon intensity is greater than the computed figure and a high probability that it is significantly smaller than the observation. This uncertainty can be explained by different factors: the estimation of the supply chain (or the matrix A) is not precise, the MRIO supply chain does not accurately reflect the supply chain of issuers, etc.

Figure 34: Distribution function of $\widetilde{\mathcal{CI}}_{\text{total}}(w)$ (MSCI World index, May 2023)

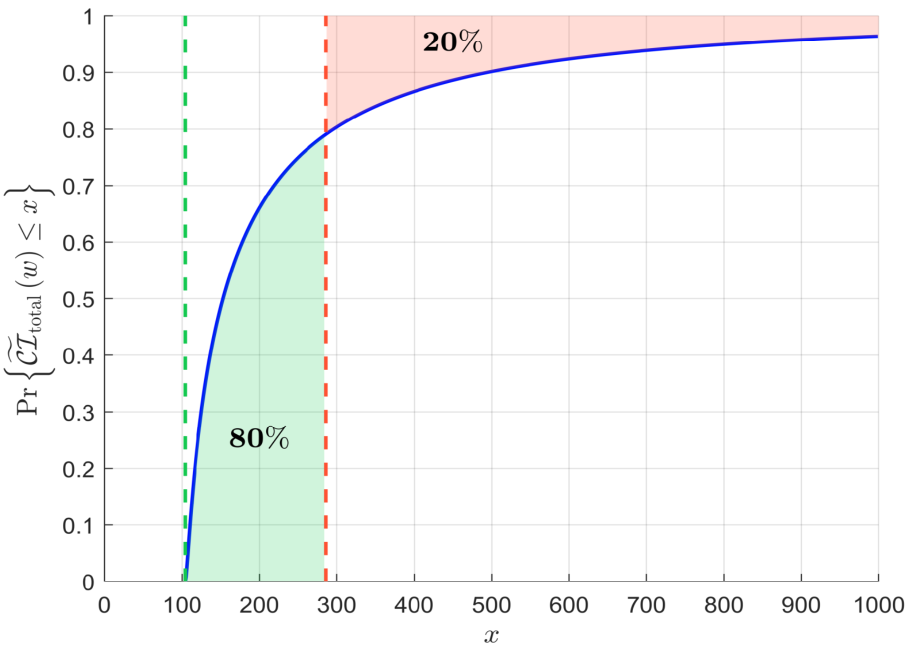

5 Taxation, pass-through and price dynamics

We have seen that a major uncertainty when performing transition stress tests concerns the estimation of supply chain emissions. Moreover, we have limited knowledge about the fraction of regulation costs passed onto the price of products sold by the sector, *i.e.* the pass-through mechanism. In what follows, we will see that this topic is related to the estimation of indirect emissions and can be measured using input-output models.

5.1 Pass-through, tax incidence and downstream diffusion

According to RBB Economics (2014), "*cost pass-through describes what happens when a business changes the price of the production or services it sells following a change in the cost of producing them*". Therefore, a pass-through rate is closely related to the supply and demand elasticity. This concept of price adjustment is extremely common in many fields of economics: exchange rates (Dornbusch, 1987; Campa and Goldberg, 2005), imperfect competition and Cournot-Bertrand equilibria (Dixit and Stiglitz, 1977; Weyl and Fabinger, 2013), product taxation and retail prices (Shrestha and Markowitz, 2016; Seiler *et al.*, 2021), inflation regimes (Richards and Pofahl, 2009; Ha *et al.*, 2020), etc.

We reiterate that the pass-through denotes the capacity of a sector or a company to pass costs through its supply chain. Generally, this parameter ranges from 0% when all the amount is supported by the agent to 100% when the full amount is transferred to the clients[49]. Since this parameter depends on several factors, such as supply and demand elasticity, international trade exposure, market concentration, product homogeneity, etc., its estimation is not easy, implying a large uncertainty on tax incidence in a transition risk framework.

Figure 35: Demand curvature

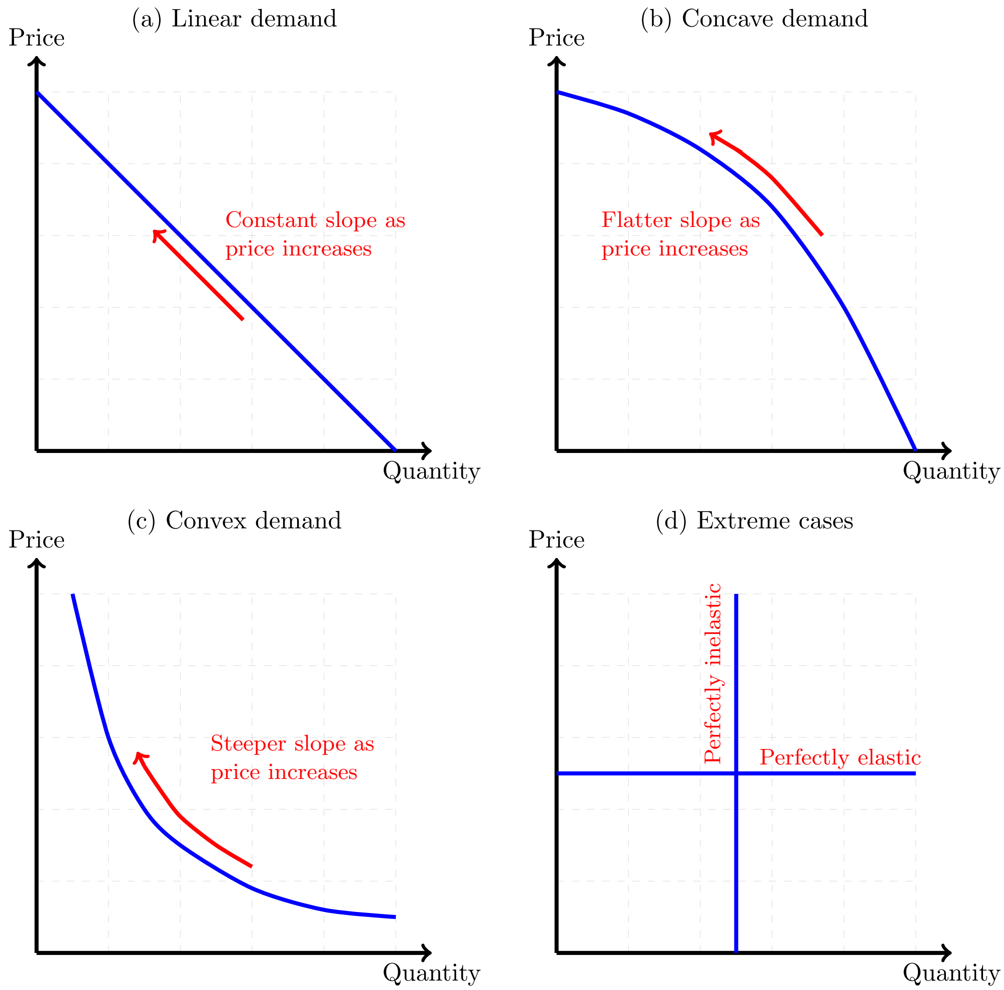

Source: (RBB Economics, 2014, Figure 2, page 16).

5.1.1 Theoretical framework

Following RBB Economics (2014), the pass-through highly depends on the market structure and the supply-demand equilibrium. In Figure 35, we represent different demand curves, whose slope depends on consumer reactions to different price levels. If the curve descends steeply, it suggests that an increase in price would lead to a marginal reduction in sales. This scenario represents inelastic demand, where consumer demand is relatively unchanged when the price moves up or down. Conversely, if the demand curve is flatter, a hike in price will result in a substantial reduction in the quantity demanded. This situation depicts elastic demand, where consumers are highly responsive to price changes. Should a demand

[49] We can occasionally find pass-through rates above 100% when the demand is very convex.

curve be linear, it lacks any curvature, meaning that the rate of decline in demand as the price increases remains constant (top/left panel in Figure 35). In situations where demand decreases more drastically as price elevates, this kind of demand is classified as concave to the origin, as represented in the second panel. As prices ascend in this scenario, the demand curve becomes progressively flatter, signifying an increased price sensitivity or greater elasticity. In this scenario, firms should absorb a portion of the cost, implying a relatively low pass-through rate. Lastly, if the rate of demand reduction decelerates with each price increase, this kind of demand curve is termed convex to the origin. In this case, as prices escalate, the residual demand becomes less sensitive to these price fluctuations (bottom/left panel in Figure 35). Companies can then pass on the costs and set a relatively high pass-through rate.

Perfect competition From an economic viewpoint, the specification of the pass-through depends then on several factors. First, it differs if we consider perfect competition or monopolistic situation. Let $Q_S(p)$ and $Q_D(p)$ be the supply and demand functions with respect to the price p. The market price is the solution of the equation $Q_S(p) = Q_D(p)$. Let us introduce a tax $\boldsymbol{\tau}$, which is paid by the suppliers. The new equilibrium is defined by:

$$Q_S(p - \boldsymbol{\tau}) = Q_D(p)$$

A change in demand induced by a change in the tax implies that:

$$\frac{\mathrm{d}\, Q_S(p - \boldsymbol{\tau})}{\mathrm{d}\, \boldsymbol{\tau}} = \frac{\mathrm{d}\, Q_D(p)}{\mathrm{d}\, \boldsymbol{\tau}}$$

We deduce that:

$$\frac{\mathrm{d}\, Q_S(p - \boldsymbol{\tau})}{\mathrm{d}\, p}\frac{\mathrm{d}\, p}{\mathrm{d}\, \boldsymbol{\tau}} - \frac{\mathrm{d}\, Q_S(p - \boldsymbol{\tau})}{\mathrm{d}\, p} = \frac{\mathrm{d}\, Q_D(p)}{\mathrm{d}\, p}\frac{\mathrm{d}\, p}{\mathrm{d}\, \boldsymbol{\tau}}$$

Since $\dfrac{\mathrm{d}\, Q_S}{\mathrm{d}\, p} \geq 0$ is the price sensitivity of supply and $\dfrac{\mathrm{d}\, Q_D}{\mathrm{d}\, p} \leq 0$ is the price sensitivity of demand, the general formula of the pass-through rate $\boldsymbol{\phi}$ is[50]:

$$\boldsymbol{\phi} = \frac{\mathrm{d}\, p}{\mathrm{d}\, \boldsymbol{\tau}} = \frac{\text{price sensitivity of supply}}{\text{price sensitivity of supply} - \text{price sensitivity of demand}}$$

We deduce that $\boldsymbol{\phi} \in \left[0, 100\%\right]$. In perfect competition, RBB Economics (2014) showed that the industry pass-through rate is given by the following equation:

$$\boldsymbol{\phi}_j = \frac{1}{1 - \dfrac{\text{price-demand elasticity of sector } j}{\text{price-supply elasticity of sector } j}}$$

while the firm-specific pass-through $\boldsymbol{\phi}_i$ should be equal to zero.

Remark 8. *In some specific situations (Giffen effect and Veblen goods), we can have* $\dfrac{\mathrm{d}\, Q_D}{\mathrm{d}\, p} \leq 0$ *and* $\boldsymbol{\phi} > 100\%$.

[50] This formula is different from the one obtained by RBB Economics (2014, page 54), because they assumed that price sensitivity of demand is expressed in absolute value. In this case, we have:

$$\boldsymbol{\phi} = \frac{\text{price sensitivity of supply}}{\text{price sensitivity of supply} + \text{price sensitivity of demand}}$$

Monopoly It is important to note that most intensive sectors, in particular Utilities and Materials, are in situation of quasi-monopoly. In this case, the pass-through is shown to be equal to:

$$\phi = \frac{\text{slope of inverse demand}}{\text{slope of marginal revenue } - \text{ slope of marginal cost}}$$

In the monopolistic context, the pass-through rate depends on the change in demand vs. change in revenue. In the case where the demand is convex, the pass-through may exceed 100%. With constant marginal cost, the monopolistic pass-through rate becomes (Bulow and Pfleiderer, 1983):

$$\phi = \frac{1}{2 + \text{elasticity of slope of inverse demand}}$$

Since the elasticity of slope of inverse demand is negative, we obtain $\phi \geq 1/2$. Contrary to the perfect competition case, the lower bound is not zero in the situation of monopoly and the minimum pass-through rate is 50%.

Oligopoly In the economic theory, we distinguish two main theoretical settings for the modeling of oligopolistic situations. In the Cournot framework, players choose quantities as a strategic variable in non-cooperative competition with the other firms, and the market determines the price of each good. In the Bertrand framework, firms set prices, and the market determines the demand for each good. In a n-firm Cournot competition environment, the industry level pass-through rate follows[51]:

$$\phi_j = \frac{n}{(n+1) + \text{elasticity of slope of inverse demand}}$$

while the firm-specific pass-through rate is $\phi_i = \phi_j / n$. We notice that the lower bound of the Cournot pass-through is $n/(n+1) \geq 50\%$. For example, $\phi_j \geq 75\%$ if there are 3 firms. In the Bertrand setting, Anderson *et al.* (2001) demonstrated that the industry pass-through is:

$$\phi_j = \frac{n}{2 - D + \dfrac{\text{elasticity of slope of inverse demand}}{\text{own price elasticity of demand}}}$$

where D is the aggregate diversion ratio[52]. We notice that the lower bound[53] of the Bertrand pass-through is 50%.

General formula Weyl and Fabinger (2013) derived a general expression for the absolute industry pass-through rate, given a change in marginal costs that can represent perfect competition, monopoly, oligopoly with homogeneous goods (Cournot) and differentiated goods (Bertrand). This expression is based on the curvature of the price/quantity relationship, which determines whether the demand curve is linear, convex or concave. The nested expression is:

$$\phi = \frac{1}{1 - \dfrac{\varepsilon_D + \mathcal{H}}{\varepsilon_S} + \dfrac{\mathcal{H}}{\varepsilon_{\mathcal{H}}} + \dfrac{\mathcal{H}}{\varepsilon_{cs}}} \tag{17}$$

[51] The proof can be found in RBB Economics (2014, page 69).

[52] Following RBB Economics (2014, page 77), the aggregate diversion ratio is "*the proportion of sales lost by one firm as its price is increased that are captured by its rivals*".

[53] Because $D \geq 0$ and the elasticity of slope of inverse demand is negative.

where the parameter $\mathcal{H}$ characterizes whether the setting is perfect competition ($\mathcal{H} = 0$), monopoly ($\mathcal{H} = 1$), symmetric Cournot[54] ($\mathcal{H} = n^{-1}$) or Bertrand differentiated oligopoly[55] ($\mathcal{H} = 1 - D$); $\boldsymbol{\varepsilon}_D$ is the elasticity of demand; $\boldsymbol{\varepsilon}_S$ is the elasticity of competitive supply[56]; $\boldsymbol{\varepsilon}_{\mathcal{H}}$ is the elasticity of the conduct parameter[57] and $\boldsymbol{\varepsilon}_{cs}$ is the elasticity of the inverse consumer surplus[58].

To summarize, the pass-through rate can be lower than 50% only in the perfect competition setting. Otherwise, it is greater than 50% in monopoly and oligopoly settings. It can also be greater than 100% in these settings, in particular when the demand is highly convex.

5.1.2 Calibration of pass-through rates

Literature review Drawing upon an extensive literature review[59], Sautel *et al.* (2022) attributed pass-through rates to sectors. In particular, they gathered them into four categories. For the high-emitting sectors (manufacture of metal, manufacture of non-metallic mineral products, etc.), the pass-through rate ranges from 10% to 100%. The second group corresponds to low-emitting and intermediary demand-oriented sectors, and the pass-through rate is set at 75%. For the sectors that are directed toward the final demand, Sautel *et al.* (2022) distinguished two categories based on elasticity assumptions. When the price elasticity of demand is high (resp. low), pass-through parameters are set at 40% (resp. 100%). Table 22 summarizes the pass-through rates for intensive sectors used by Sautel *et al.* (2022).

Table 22: Pass-through rates (in %) for intensive sectors (Sautel *et al.*, 2022, page 35)

Sector	Rate
Electricity, gas and steam	100%
Petroleum refining	100%
Base metals	78%
Mining	78%
Waste/wastewater	78%
Land transport	78%
Fishery	75%
Non-metallic minerals	60%
Agriculture	50%
Chemicals	40%
Maritime transport	30%
Aviation	30%
Paper	10%

Econometric modeling The main calibration approach of pass-through rates is generally to estimate a cost-price model using standard econometric tools (De Bruyn *et al.*, 2015). The price of a product depends then on the prices of its input components and CO_2

[54] n is the number of competing firms.
[55] D is the aggregate diversion ratio.
[56] The second term $\dfrac{\boldsymbol{\varepsilon}_D + \mathcal{H}}{\boldsymbol{\varepsilon}_S}$ vanishes in the case of constant marginal cost.
[57] It allows for changes of the intensity of competition when quantity or price varies.
[58] We also have:

$$\boldsymbol{\varepsilon}_{cs} = \frac{1}{1 + \text{elasticity of slope of inverse demand}}$$

[59] See Tables 58 and 59 on page 184.

emissions. The linear regression model can then be estimated using ordinary least squares and provides price sensitivities (De Bruyn *et al.*, 2010a). Sometimes, the linear regression model is replaced by a VaR or VECM process. Again, the price sensitivities are estimated by the method of least squares or the method of maximum likelihood (Oberndorfer *et al.*, 2010). We also notice that this framework allows to generate impulse response functions, which measure the effects of a shock on endogenous variables (Alexeeva-Talebi, 2010, 2011). Therefore, we can distinguish short-term and long-term pass-through rates. An alternative approach to the cost-price model is to use a simplified equilibrium model and estimate the demand function using the reduced form or the structural form of the model (Ganapati *et al.*, 2020). These different econometric approaches are suitable to obtain the best estimate given a set of observations. Nevertheless, they are not relevant in our framework when we deal with the uncertainty of pass-through rates.

Stochastic modeling Since the pass-through coefficient is a parameter between 0 and 1, it is common to consider a random variable with a beta distribution $\mathcal{B}(\alpha, \beta)$. When α and β are greater than 1, the distribution has one mode equal to $(\alpha - 1) / (\alpha + \beta - 2)$. This probability distribution is very flexible and allows to obtain various shapes[60]. To calibrate the parameters α and β, we can use the method of maximum likelihood. Let $\{\boldsymbol{\phi}_1, \ldots, \boldsymbol{\phi}_n\}$ be a sample of pass-through rates. According to Roncalli (2020, page 619), the log-likelihood function is:

$$\boldsymbol{\ell}(\alpha, \beta) = (\alpha - 1) \sum_{i=1}^{n} \ln \boldsymbol{\phi}_i + (b - 1) \sum_{i=1}^{n} \ln (1 - \boldsymbol{\phi}_i) - n \ln \mathfrak{B}(\alpha, \beta)$$

An alternative approach is to use the method of moments, whose estimators are[61]:

$$\hat{\alpha} = \frac{\hat{\mu}_{\boldsymbol{\phi}}^2 \left(1 - \hat{\mu}_{\boldsymbol{\phi}}\right)}{\hat{\sigma}_{\boldsymbol{\phi}}^2} - \hat{\mu}_{\boldsymbol{\phi}}$$

and:

$$\hat{\beta} = \frac{\hat{\mu}_{\boldsymbol{\phi}} \left(1 - \hat{\mu}_{\boldsymbol{\phi}}\right)^2}{\hat{\sigma}_{\boldsymbol{\phi}}^2} - \left(1 - \hat{\mu}_{\boldsymbol{\phi}}\right)$$

where $\hat{\mu}_{\boldsymbol{\phi}}$ and and $\hat{\sigma}_{\boldsymbol{\phi}}$ are the empirical mean and standard deviation of the sample.

We consider the case of refineries. We collect the different estimates from the studies listed in Table 59 on page 185. The sample is 36%, 40%, 50%, 50%, 50%, 75%, 90%, 95%, 99%, 99% and 99%. We have $\hat{\mu}_{\boldsymbol{\phi}} = 71.18\%$ and $\hat{\sigma}_{\boldsymbol{\phi}} = 26.10\%$. The ML estimates are $\hat{\alpha} = 1.60$ and $\hat{\beta} = 0.58$, while the MM estimates are $\hat{\alpha} = 1.43$ and $\hat{\beta} = 0.58$. We have reported the probability density function in Figure 36. We notice that the two estimators give very similar results.

The previous approach requires to have a sample for each sector. Unfortunately, data are very sparse. Therefore, we follow Sautel *et al.* (2022) and consider four types of sectors with

[60] We can distinguish three types of shape:

- if $\alpha = 1$ and $\beta = 1$, we obtain the uniform distribution; if $\alpha \to \infty$ and $\beta \to \infty$, we obtain the Dirac distribution at the point $x = 0.5$; if one parameter goes to zero, we obtain a Bernoulli distribution;
- if $\alpha = \beta$, the distribution is symmetric around $x = 0.5$; we have a bell curve when the two parameters α and β are higher than 1, and a U-shape curve when the two parameters α and β are lower than 1;
- if $\alpha > \beta$, the skewness is negative and the distribution is left-skewed, if $\alpha < \beta$, the skewness is positive and the distribution is right-skewed.

[61] The derivation of this result is given in Roncalli (2020, page 193).

Figure 36: Estimated probability density function of the pass-through rate

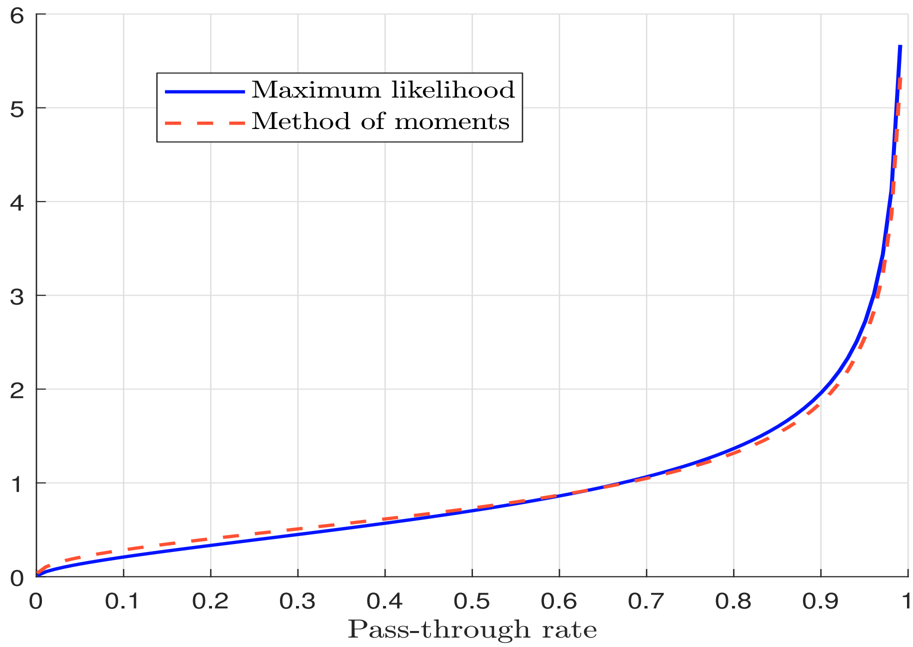

Figure 37: Standard probability distribution of pass-through rates

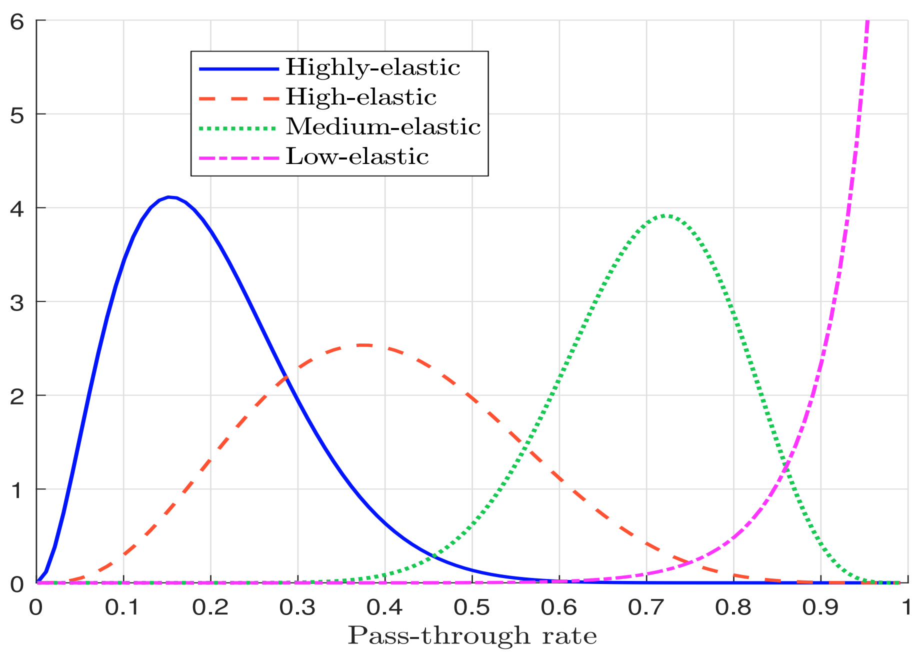

respect to the price-demand elasticity: highly-elastic, high-elastic, medium-elastic and low-elastic. For each type, we define the corresponding beta distribution. The expert-opinion values of the parameters α and β are reported in Table 23. We also give the mean, the standard deviation and the 95% range. Figure 37 shows the associated probability density functions. The first type is right-skewed, while the fourth type is left-skewed. The second and third types are more symmetric. Moreover, we can show that these four distribution functions are ordered since they verify the first-order stochastic dominance principle[62].

Table 23: Probabilistic characterization of the four pass-through types

Statistic		Highly-elastic	High-elastic	Medium-elastic	Low-elastic
Parameters	α	3.0	4.0	14.0	12.0
	β	12.0	6.0	6.0	0.6
Moments	$\mu_{\boldsymbol{\phi}}$	20%	40%	70%	95%
	$\sigma_{\boldsymbol{\phi}}$	10%	15%	10%	6%
Range	$Q_{\boldsymbol{\phi}}(2.5\%)$	5%	14%	49%	79%
	$Q_{\boldsymbol{\phi}}(97.5\%)$	43%	70%	87%	100%

Remark 9. *In Appendix B on page 186, we propose a mapping between the WIOD sectors and the four types. This classification will be used when we will run the Monte Carlo value-at-risk engine.*

5.2 Taxation and price dynamics in input-output models

We now study the impact of taxation on the production costs. For that, we diffuse the carbon tax in the input-output economic model in order to take into account the cascading effects through the value chain. We will see that this topic is related to the computation of the indirect emissions. Nevertheless, the diffusion of the carbon tax depends on the assumption about the reaction function of the suppliers. Several approaches can be considered (sticky price vs. flexible price models), implying that carbon tax costs highly depend on pass-through mechanisms.

5.2.1 Value added approach

By construction, a carbon tax affects the income of producers, that can have different reactions. We first consider a flexible price model and assume that they want to maintain their value added levels.

Remark 10. *In what follows, we note p^{-} the price vector before the introduction of the carbon tax, while p is the price vector that incorporates the taxation effect.*

Impact on production prices We recall that the absolute amount of carbon tax for Sector j is equal to:

$$T_{\text{direct},j} = \boldsymbol{\tau}_j \mathcal{CE}_{1,j}$$

where $\boldsymbol{\tau}_j$ is the nominal carbon tax expressed in $/tCO$_2$e and $\mathcal{CE}_{1,j}$ is the scope 1 emissions of the sector. We deduce that the carbon tax rate is equal to:

$$t_{\text{direct},j} = \frac{T_{\text{direct},j}}{x_j} = \frac{\boldsymbol{\tau}_j \mathcal{CE}_{1,j}}{x_j} = \boldsymbol{\tau}_j \mathcal{CI}_{1,j}$$

[62]See Figure 105 on page 164.

We notice that $t_{\text{direct},j}$ has no unit and is equal to the product of the tax and the scope 1 carbon intensity. The input-output model implies that:

$$p_j x_j = \sum_{i=1}^{n} Z_{i,j} p_i + \sum_{k=1}^{m} V_{k,j} \psi_k + T_{\text{direct},j}$$

We deduce that:

$$p_j = \sum_{i=1}^{n} A_{i,j} p_i + \sum_{k=1}^{m} B_{k,j} \psi_k + t_{\text{direct},j} = \sum_{i=1}^{n} A_{i,j} p_i + \upsilon_j + t_{\text{direct},j}$$

It follows that:

$$p = \left(I_n - A^\top\right)^{-1} \left(\upsilon + t_{\text{direct}}\right)$$

where $t_{\text{direct}} = \left(t_{\text{direct},1}, \ldots, t_{\text{direct},n}\right)$ is the vector of direct tax rates. We retrieve the cost-push price model where the vector υ of value added ratios is replaced by $\upsilon + t_{\text{direct}}$. It follows that the vector of price variations due to the carbon tax is equal to:

$$\Delta p = \left(I_n - A^\top\right)^{-1} t_{\text{direct}} \tag{18}$$

This result is obvious since Equation (3) implies that $\Delta p = \left(I_n - A^\top\right)^{-1} \Delta\upsilon$ and $\Delta\upsilon$ corresponds to the vector t_{direct} of direct tax rates.

Impact on the price index A price index[63] is defined as:

$$\mathcal{PI} = \sum_{i=1}^{n} \alpha_i p_i = \alpha^\top p$$

where $\alpha = (\alpha_1, \ldots, \alpha_n)$ is the weights of the items basket. We deduce that the inflation rate is:

$$\pi = \frac{\Delta \mathcal{PI}}{\mathcal{PI}^-} = \frac{\mathcal{PI} - \mathcal{PI}^-}{\mathcal{PI}^-} = \frac{\alpha^\top \left(I_n - A^\top\right)^{-1} t_{\text{direct}}}{\alpha^\top \left(I_n - A^\top\right)^{-1} \upsilon}$$

We can simplify this formula because $p^- = \left(I_n - A^\top\right)^{-1} \upsilon = \mathbf{1}_n$ and $\mathbf{1}_n^\top \alpha = 1$. Finally, we have:

$$\pi = \alpha^\top \left(I_n - A^\top\right)^{-1} t_{\text{direct}} \tag{19}$$

Computation of the total tax amount The total tax cost is equal to:

$$\begin{aligned} T_{\text{total}} &= x \odot \Delta p \\ &= x \odot \left(I_n - A^\top\right)^{-1} t_{\text{direct}} \end{aligned} \tag{20}$$

while the direct tax cost is $T_{\text{direct}} = x \odot t_{\text{direct}}$. Since we have $x \succeq \mathbf{0}_n$ and $\left(I_n - A^\top\right)^{-1} \succeq I_n$ and using Hadarmard properties[64], we deduce that the total tax cost is greater than the direct tax cost for all the sectors:

$$T_{\text{total},j} \geq T_{\text{direct},j}$$

[63] We adopt here a general definition. In the sequel, we will make the distinction between producer and consumer price indices.

[64] Let A, B and C be three nonnegative matrices. If $B \preceq C$, then $A \odot B \preceq A \odot C$.

Since the total cost for the economy is equal to $\mathcal{C}ost_{\text{total}} = \sum_{j=1}^{n} T_{\text{total},j} = x^\top \left(I_n - A^\top\right)^{-1} t_{\text{direct}}$, the tax incidence is then equal to:

$$\mathcal{TI} = \frac{\mathcal{C}ost_{\text{total}}}{\mathbf{1}_n^\top x} = \frac{x^\top \left(I_n - A^\top\right)^{-1} t_{\text{direct}}}{\mathbf{1}_n^\top x}$$

Some common errors when computing the total tax cost It is tempting to compute T_{total} as follows:

$$\begin{aligned} T_{\text{total}} &= x \odot \left(I_n - A^\top\right)^{-1} t_{\text{direct}} \\ &= \left(I_n - A^\top\right)^{-1} \left(x \odot t_{\text{direct}}\right) \\ &= \left(I_n - A^\top\right)^{-1} T_{\text{direct}} \\ &= \left(I_n - A^\top\right)^{-1} \left(\boldsymbol{\tau} \odot \boldsymbol{\mathcal{CE}}_1\right) \\ &= \boldsymbol{\tau} \odot \left(\left(I_n - A^\top\right)^{-1} \boldsymbol{\mathcal{CE}}_1\right) \\ &= \boldsymbol{\tau} \odot \boldsymbol{\mathcal{CE}}_{\text{total}} \end{aligned}$$

In some research papers, we can find two formulas that seems to be intuitive:

$$T'_{\text{total}} = \left(I_n - A^\top\right)^{-1} T_{\text{direct}} \tag{21}$$

and:

$$T''_{\text{total}} = \boldsymbol{\tau} \odot \boldsymbol{\mathcal{CE}}_{\text{total}} \tag{22}$$

Nevertheless, the two previous equations are generally false because the Hadamard and matrix products are not associative: $A \odot (BC) \neq (A \odot B)\, C$.

Equation (21) is valid only if $t_{\text{direct},j} = t_{\text{direct},j'} = t$ and $T_{\text{direct},j} = T_{\text{direct},j'}$. In this case, we have:

$$\begin{aligned} T_{\text{total}} &= tx \odot \left(I_n - A^\top\right)^{-1} \mathbf{1}_n \\ &= \left(I_n - A^\top\right)^{-1} \mathbf{1}_n \odot tx \\ &= \left(I_n - A^\top\right)^{-1} \mathbf{1}_n \odot T_{\text{direct}} \\ &= \left(I_n - A^\top\right)^{-1} T_{\text{direct}} \end{aligned}$$

Nevertheless, the assumptions are too strong since they imply that $\boldsymbol{\mathcal{CE}}_{1,j} = \boldsymbol{\mathcal{CE}}_{1,j'}$ and $x_j = x_{j'}$. All the sectors must then have the same direct carbon intensities. Concerning Equation (22), it is valid only if the carbon tax is uniform: $\boldsymbol{\tau}_j = \boldsymbol{\tau}_{j'} = \tau$. Indeed, we verify that:

$$\begin{aligned} T_{\text{total}} &= x \odot \left(I_n - A^\top\right)^{-1} t_{\text{direct}} \\ &= x \odot \left(I_n - A^\top\right)^{-1} \tau \boldsymbol{\mathcal{CI}}_1 \\ &= \tau \left(I_n - A^\top\right)^{-1} \boldsymbol{\mathcal{CI}}_1 \odot x \\ &= \tau \boldsymbol{\mathcal{CE}}_{\text{total}} \end{aligned}$$

Mathematical properties Let us denote by $f(\boldsymbol{\tau})$ the function f that depends on the vector $\boldsymbol{\tau} = (\boldsymbol{\tau}_1, \ldots, \boldsymbol{\tau}_n)$ of carbon taxes. Let $\lambda \geq 0$ be a positive scalar. The functions Δp, π, T_{total}, $\mathcal{C}ost_{\text{total}}$ and $\mathcal{TI}$ are homogeneous[65] and additive[66]. For instance, we have:

$$\begin{aligned}\Delta p(\lambda\boldsymbol{\tau}) &= \left(I_n - A^\top\right)^{-1} t_{\text{direct}}(\lambda\boldsymbol{\tau}) \\ &= \lambda\left(I_n - A^\top\right)^{-1} t_{\text{direct}}(\boldsymbol{\tau}) \\ &= \lambda\Delta p(\boldsymbol{\tau})\end{aligned}$$

If the tax is uniform $\boldsymbol{\tau} = \tau\mathbf{1}_n$, the vector of total tax amount is the product of the tax by the total emissions:

$$T_{\text{total}}(\tau\mathbf{1}_n) = \tau\,\boldsymbol{\mathcal{CE}}_{\text{total}}$$

The tax incidence for a given sector is then proportional to the direct + indirect carbon emissions of the sector. At the global level, the tax incidence is equal to the carbon tax times the total carbon intensity of the world:

$$\mathcal{TI}(\tau\mathbf{1}_n) = \frac{\mathbf{1}_n^\top\tau\,\boldsymbol{\mathcal{CE}}_{\text{total}}}{\mathbf{1}_n^\top x} = \tau\,\boldsymbol{\mathcal{CI}}_{\text{total}}(\boldsymbol{\mathcal{G}}lobal)$$

Illustration We consider a variant of Example #2. Table 24 gives the values of $Z_{i,j}$, y_j, x_j and $V_{1,j}$ in \$ mn. The carbon emissions are expressed in ktCO_2e, while the carbon intensities are in tCO_2e/\$ mn. For instance, the intermediary consumption $Z_{1,2}$ is equal to \$800 mn, the final demand y_3 is equal to \$3.3 bn, the output x_4 is equal to \$12.5 bn, the value added $V_{1,2}$ is equal to \$1 800 mn, the carbon emissions $\boldsymbol{\mathcal{CE}}_{1,2}$ are equal to 20 000 tCO_2e and the carbon intensity $\boldsymbol{\mathcal{CI}}_{1,4}$ is equal to 10 tCO_2e/\$ mn.

Table 24: Environmentally extended monetary input-output table (Example #3)

Sector	Z				y	x	$\boldsymbol{\mathcal{CE}}_1$	$\boldsymbol{\mathcal{CI}}_1$
Energy	500	800	1 600	1 250	850	5 000	500	100
Materials	500	400	1 600	625	875	4 000	200	50
Industrials	250	800	2 400	1 250	3 300	8 000	200	25
Services	100	200	800	4 375	7 025	12 500	125	10
Value added	3 650	1 800	1 600	5 000				
Income	5 000	4 000	8 000	12 500				

We have:

$$A = Z\,\text{diag}^{-1}(x) = \begin{pmatrix} 0.10 & 0.20 & 0.20 & 0.10 \\ 0.10 & 0.10 & 0.20 & 0.05 \\ 0.05 & 0.20 & 0.30 & 0.10 \\ 0.02 & 0.05 & 0.10 & 0.35 \end{pmatrix}$$

and:

$$\tilde{\boldsymbol{\mathcal{L}}} = \left(I_4 - A^\top\right)^{-1} = \begin{pmatrix} 1.1881 & 0.1678 & 0.1430 & 0.0715 \\ 0.3894 & 1.2552 & 0.4110 & 0.1718 \\ 0.4919 & 0.4336 & 1.6303 & 0.2993 \\ 0.2884 & 0.1891 & 0.3044 & 1.6087 \end{pmatrix}$$

[65] This means that $f(\lambda\boldsymbol{\tau}) = \lambda f(\boldsymbol{\tau})$.

[66] We have $f(\boldsymbol{\tau} + \boldsymbol{\tau}') = f(\boldsymbol{\tau}) + f(\boldsymbol{\tau}')$.

Then, we compute the vector υ of value added ratios:

$$\upsilon = \begin{pmatrix} 3\,650/5\,000 \\ 1\,800/4\,000 \\ 1\,600/8\,000 \\ 5\,000/12\,500 \end{pmatrix} = \begin{pmatrix} 0.73 \\ 0.45 \\ 0.20 \\ 0.40 \end{pmatrix}$$

We verify that $p^{-} = \tilde{\boldsymbol{\mathcal{L}}}\upsilon = \mathbf{1}_4$. By construction, all the prices are standardized and equal to one in a monetary input-output model. We now introduce a differentiated carbon taxation: $\boldsymbol{\tau}_1 = \$200/\text{tCO}_2\text{e}$ and $\boldsymbol{\tau}_2 = \boldsymbol{\tau}_3 = \boldsymbol{\tau}_4 = \$100/\text{tCO}_2\text{e}$. The direct tax cost is respectively equal to 100, 20, 20 and 12.5 millions of dollars for Energy, Materials, Industrials and Services. We deduce that the vector of carbon tax rates is:

$$t_{\text{direct}} = \begin{pmatrix} 2.00\% \\ 0.50\% \\ 0.25\% \\ 0.10\% \end{pmatrix}$$

It follows that:

$$p = \left(I_n - A^{\top}\right)^{-1} (\upsilon + t_{\text{direct}}) = \begin{pmatrix} 1.0250 \\ 1.0153 \\ 1.0164 \\ 1.0091 \end{pmatrix}$$

If we assume that the basket of goods and services is $\alpha = \left(10\%, 20\%, 30\%, 40\%\right)$, the price index $\mathcal{PI}$ is 1.0141 whereas the inflation rate π is 1.410%. Finally, we compute the total tax cost and obtain the results given in Table 25. The direct tax cost is multiplied by a factor of 2.8 when we consider the diffusion of the carbon tax. We verify that $T_{\text{total}} \neq T'_{\text{total}} \neq T''_{\text{total}}$. Services is the most impacted sector follows by Industrials, Materials and Energy, since the impact ratio $T_{\text{total}}/T_{\text{direct}}$ is respectively equal to 9.1, 6.6, 3.1 and 1.3.

Table 25: Total carbon cost (in \$ mn) (differentiated taxation, Example #3)

Sector	T_{direct}	T_{total}	T'_{total}	T''_{total}	$\mathcal{CE}_{\text{direct}}$	$\mathcal{CE}_{\text{total}}$
Energy	100.00	125.15	125.92	131.49	500.00	657.44
Materials	20.00	61.05	74.41	45.48	200.00	454.76
Industrials	20.00	131.05	94.21	91.70	200.00	916.97
Services	12.50	113.54	58.82	77.49	125.00	774.92
Sum	152.50	430.79	353.36	346.15	1 025.00	2 804.10

Table 26: Total carbon cost (in \$ mn) (uniform taxation, Example #3)

Sector	T_{direct}	T_{total}	T'_{total}	T''_{total}	$\mathcal{CE}_{\text{direct}}$	$\mathcal{CE}_{\text{total}}$
Energy	50.00	65.74	66.51	65.74	500.00	657.44
Materials	20.00	45.48	54.94	45.48	200.00	454.76
Industrials	20.00	91.70	69.62	91.70	200.00	916.97
Services	12.50	77.49	44.40	77.49	125.00	774.92
Sum	102.50	280.41	235.47	280.41	1 025.00	2 804.10

Remark 11. *In Table 26, we consider a uniform tax of* $\$100/\text{tCO}_2\text{e}$. *We verify that* $T_{\text{total}} = T''_{\text{total}}$ *but* $T_{\text{total}} \neq T'_{\text{total}}$.

5.2.2 Mark-up pricing approach

Theoretical framework We now consider a second approach that has been proposed by Gemechu *et al.* (2014) and Mardones and Mena (2020), but the original idea can be found in Llop (2008). Mark-up pricing refers to a commercial strategy where the suppliers determine the selling price by adding a fixed percentage of the production costs. Let p_j^- be the price before the introduction of the carbon tax. We define ξ_j as the price factor induced by the carbon tax[67]: $t_{\text{direct},j} = \xi_j p_j^-$. It follows that $p_j^- = \sum_{i=1}^n A_{i,j} p_i^- + \upsilon_j$ and[68]:

$$\begin{aligned} p_j &= \left(\sum_{i=1}^n A_{i,j} p_i + \upsilon_j\right) + t_{\text{direct},j} \\ &= \left(\sum_{i=1}^n A_{i,j} p_i + \upsilon_j\right) + \xi_j p_j^- \\ &= \left(1+\xi_j\right)\left(\sum_{i=1}^n A_{i,j} p_i + \upsilon_j\right) \end{aligned}$$

We deduce that:

$$\frac{p_j}{1+\xi_j} = \sum_{i=1}^n A_{i,j} p_i + \upsilon_j$$

and:

$$p_j\left(1 - \frac{\xi_j}{1+\xi_j}\right) = \sum_{i=1}^n A_{i,j} p_i + \upsilon_j$$

It follows that:

$$\begin{aligned} p_j &= \sum_{i=1}^n A_{i,j} p_i + \frac{\xi_j}{1+\xi_j} p_j + \upsilon_j \\ &= \sum_{i=1}^n A_{i,j} p_i + p_j\left(1 - \frac{1}{1+\xi_j}\right) + \upsilon_j \end{aligned}$$

In a matrix form, we have:

$$p = A^\top p + \left(I_n - D_\xi\right) p + \upsilon$$

where:

$$D_\xi = \operatorname{diag}\left(\frac{1}{1+\xi_1}, \ldots, \frac{1}{1+\xi_n}\right)$$

Finally, we obtain:

$$p = \left(I_n - A_\xi^\top\right)^{-1} \upsilon$$

where $A_\xi = A + I_n - D_\xi$. Another expression is:

$$p = \tilde{\boldsymbol{\mathcal{L}}}_m \upsilon = \left(D_\xi - A^\top\right)^{-1} \upsilon \tag{23}$$

[67] Since we have $p_j^- = 1$, we obtain $\xi_j = t_{\text{direct},j} / p_j^- = t_{\text{direct},j}$. Nevertheless, we prefer to use the notation ξ_j because it may encompass other indirect costs.

[68] We assume that $p_j \approx p_j^-$.

where $\tilde{\mathcal{L}}_m = \left(D_\xi - A^\top\right)^{-1}$ is the mark-up inverse matrix. The vector of price variations is then:

$$\Delta p = \left(\tilde{\mathcal{L}}_m - \tilde{\mathcal{L}}\right) \upsilon \tag{24}$$

The expression of the price index is $\mathcal{PI} = \alpha^\top \left(D_\xi - A^\top\right)^{-1} \upsilon$ whereas the inflation rate is equal to $\pi = \alpha^\top \left(\tilde{\mathcal{L}}_m - \tilde{\mathcal{L}}\right) \upsilon$. From Equation (24), we also deduce the total tax amount:

$$T_{\text{total}} = x \odot \left(\tilde{\mathcal{L}}_m - \tilde{\mathcal{L}}\right) \upsilon \tag{25}$$

We remark that the mark-up approach implies to replace the identity matrix I_n by the diagonal matrix D_ξ in the cost-push price model. Since we have $D_\xi \preceq I_n$, we deduce that $D_\xi^{-1} \succeq I_n$. In Appendix A.9 on page 151, we show that $\tilde{\mathcal{L}}_m \succeq \tilde{\mathcal{L}}$.

Illustration By considering Example #3, we have:

$$\tilde{\mathcal{L}}_m = \left(D_\xi - A^\top\right)^{-1} = \begin{pmatrix} 1.2170 & 0.1730 & 0.1474 & 0.0735 \\ 0.4017 & 1.2650 & 0.4165 & 0.1740 \\ 0.5067 & 0.4398 & 1.6394 & 0.3021 \\ 0.2965 & 0.1919 & 0.3074 & 1.6121 \end{pmatrix}$$

In the case of the differentiated taxation case, we obtain:

$$p = \tilde{\mathcal{L}}_m \upsilon = \begin{pmatrix} 1.0252 \\ 1.0154 \\ 1.0165 \\ 1.0091 \end{pmatrix}$$

The inflation rate π is equal to 1.421% and the total carbon costs (in \$ mn) are 125.82, 61.53, 132.10 and 114.33. The global cost is then \$433.78 mn vs \$430.79 mn in the value added approach.

5.2.3 Competitive price approach

Theoretical framework In the competitive price model, prices are equal to the average cost of production (Llop, 2008). By assuming that the carbon tax impacts the cost of intermediary consumptions, but not capital and labor costs, the direct cost faced by the j^{th} sector can be allocated as follows:

$$t_{\text{direct},j} = \sum_{i=1}^{n} A_{i,j} p_i^- \zeta_i$$

where ζ_i is the increased cost of sector i expressed as a percentage of the current price p_i^-. We deduce that[69]:

$$\begin{aligned} p_j &= \sum_{i=1}^{n} A_{i,j} p_i + \upsilon_j + t_{\text{direct},j} \\ &= \sum_{i=1}^{n} A_{i,j} p_i + \upsilon_j + \sum_{i=1}^{n} A_{i,j} p_i \zeta_i \\ &= \sum_{i=1}^{n} A_{i,j} p_i \left(1 + \zeta_i\right) + \upsilon_j \end{aligned}$$

[69] Again, we assume that $p_j \approx p_j^-$.

In a matrix form, we have:

$$p = A^\top (I + D_\zeta) p + \upsilon$$

where $D_\zeta = \operatorname{diag}(\zeta_1, \ldots, \zeta_n)$. We deduce that:

$$p = \tilde{\boldsymbol{\mathcal{L}}}_c \upsilon = \left(I_n - A^\top (I + D_\zeta)\right)^{-1} \upsilon \tag{26}$$

where $\tilde{\boldsymbol{\mathcal{L}}}_c = \left(I_n - A^\top (I + D_\zeta)\right)^{-1}$ is the competitive inverse matrix. We also notice that $\tilde{\boldsymbol{\mathcal{L}}}_c = \left(I_n - A_\zeta^\top\right)^{-1}$ where $A_\zeta = (I + D_\zeta) A$. Since $A_\zeta \succeq A$, it is obvious that $\tilde{\boldsymbol{\mathcal{L}}}_c \succeq \tilde{\boldsymbol{\mathcal{L}}}$. Nevertheless, $I_n - A_\zeta^\top$ may be non-invertible and the prices may explode if $(\zeta_1, \ldots, \zeta_n)$ are too high. Finally, we compute the price index $\mathcal{PI}$, the inflation π and the total cost T_{total} as previously by replacing the mark-up inverse matrix $\tilde{\boldsymbol{\mathcal{L}}}_m$ by the competitive inverse matrix $\tilde{\boldsymbol{\mathcal{L}}}_c$.

Illustration By considering Example #3, we have:

$$\tilde{\boldsymbol{\mathcal{L}}}_c = \left(I_4 - A_\zeta^\top\right)^{-1} = \begin{pmatrix} 1.2153 & 0.1948 & 0.1149 & 0.0696 \\ 0.4277 & 1.2817 & 0.3162 & 0.1593 \\ 0.5368 & 0.4803 & 1.4855 & 0.2800 \\ 0.3161 & 0.2082 & 0.2337 & 1.5959 \end{pmatrix}$$

In the case of the differentiated taxation case, we obtain:

$$p = \tilde{\boldsymbol{\mathcal{L}}}_c \upsilon = \begin{pmatrix} 1.0256 \\ 1.0159 \\ 1.0171 \\ 1.0095 \end{pmatrix}$$

The inflation rate π is equal to 1.470% and the total carbon costs (in \$ mn) are 128.18, 63.65, 137.06 and 119.29. The global cost is then \$448.17 mn vs \$430.79 mn in the value added approach.

The previous illustration shows that the competitive model may induce incoherent results, since we obtain a greater global cost than in the two other cases. The reason lies in the computation of the vector ζ. In this example, we have computed them by solving the system of equations $A^\top \zeta = t_{\text{direct}}$. In practice, ζ is set to t_{direct}. In this case, the global cost becomes \$280.19 mn. Nevertheless, this figure is not satisfactory, because the total tax cost of the Energy sector is lower than the direct cost[70]. In fact, the Energy sector has passed 75% of its direct costs on the other sectors.

5.2.4 Pass-through integration

In the sequel, we focus on the value added model, which is the most used approach in the academic literature (Perese, 2010; Zhang *et al.*, 2019; Nakano and Washizu, 2022). Moreover, it is the simplest model to introduce the pass-through mechanism. Indeed, even if the cost-push price framework is a pure flexible price model, we can slightly modify the equations in order to take into account some features of price stickiness. Nevertheless, since the input-output model assumes a linear production function and the final demand is exogenous, the input-output model is too simple to obtain a realistic sticky price model.

[70] We have $T_{\text{total},1} = \$25.32$ mn.

Analytical formula We have:

$$\Delta p = \tilde{\mathcal{L}} \Delta \upsilon = \sum_{k=0}^{\infty} \left(A^{\top}\right)^{k} \Delta \upsilon = \sum_{k=0}^{\infty} \Delta p_{(k)}$$

where $\Delta p_{(k)} = \left(A^{\top}\right)^{k} \Delta \upsilon$ is the price impact at the k^{th} tier. In fact, $\Delta p_{(k)}$ satisfies the following recurrence relation:

$$\left\{ \begin{array}{l} \Delta p_{(k)} = A^{\top} \Delta p_{(k-1)} \\ \Delta p_{(0)} = \Delta \upsilon \end{array} \right.$$

If we consider the price p_j of sector j, we have $\Delta p_{(0),j} = \Delta \upsilon_j$ and:

$$\Delta p_{(k),j} = \sum_{i=1}^{n} A_{i,j} \Delta p_{(k-1),i}$$

This representation helps to better understand the cascading effect of the carbon tax. In the zeroth round, it induces an additional cost $\Delta \upsilon_j$ that is fully passed on the price p_j of the sector. The new price is then $p_j + \Delta p_{(0),j} = p_j + \Delta \upsilon_j$. In the first round, the sector j faces new additional costs due to the price increase of intermediary consumptions. We have $\Delta p_{(1),j} = \sum_{i=1}^{n} A_{i,j} \Delta p_{(0),i} = \sum_{i=1}^{n} A_{i,j} \Delta \upsilon_i$. The iteration process continues and we have $\Delta p_{(2),j} = \sum_{i=1}^{n} A_{i,j} \Delta p_{(1),i} = \sum_{i=1}^{n} \sum_{k=1}^{n} A_{i,j} A_{k,i} \Delta \upsilon_k$ at the second round.

Let us now introduce the pass-through mechanism. By definition, we have $\Delta p_{(0),j} = \boldsymbol{\phi}_j \Delta \upsilon_j$ where $\boldsymbol{\phi}_j$ denotes the pass-through rate of sector j. In the first round, we have:

$$\Delta p_{(1),j} = \sum_{i=1}^{n} A_{i,j} \left(\boldsymbol{\phi}_i \Delta p_{(0),i}\right) = \sum_{i=1}^{n} A_{i,j} \left(\boldsymbol{\phi}_i \Delta \upsilon_i\right)$$

More generally, the recurrence relation becomes:

$$\Delta p_{(k),j} = \sum_{i=1}^{n} A_{i,j} \boldsymbol{\phi}_i \Delta p_{(k-1),i}$$

Let $\boldsymbol{\phi} = (\boldsymbol{\phi}_1, \ldots, \boldsymbol{\phi}_n)$ and $\Phi = \operatorname{diag}(\boldsymbol{\phi})$ be the pass-through vector and matrix. The recurrence matrix form is:

$$\left\{ \begin{array}{l} \Delta p_{(k)} = A^{\top} \Phi \Delta p_{(k-1)} \\ \Delta p_{(0)} = \Phi \Delta \upsilon \end{array} \right.$$

We deduce that:

$$\begin{aligned} \Delta p &= \sum_{k=0}^{\infty} \left(A^{\top} \Phi\right)^{k} \Phi \Delta \upsilon \\ &= \left(I_n - A^{\top} \Phi\right)^{-1} \Phi \Delta \upsilon \\ &= \tilde{\mathcal{L}}(\boldsymbol{\phi}) \Delta \upsilon \end{aligned} \tag{27}$$

where $\tilde{\mathcal{L}}(\boldsymbol{\phi}) = \left(I_n - A^{\top} \Phi\right)^{-1} \Phi$.

Mathematical properties Because A is a substochastic matrix and Φ is a positive diagonal matrix, we verify that $\boldsymbol{\phi}' \succeq \boldsymbol{\phi} \Rightarrow \tilde{\mathcal{L}}\left(\boldsymbol{\phi}'\right) \succeq \tilde{\mathcal{L}}(\boldsymbol{\phi})$. The lower bound is then obtained when $\boldsymbol{\phi} = \mathbf{0}_n$ while the upper bound is reached when $\boldsymbol{\phi} = \mathbf{1}_n$.

Application to the carbon tax By applying the previous analysis to the carbon tax, we have $\Delta v = t_{\text{direct}}$. In this case, the concept of the total tax cost must be redefined because one part of the costs is paid by the producers and another part by the consumers. By consumer, we must understand the downstream of the value chain. We have:

$$\begin{aligned} T_{\text{producer}} &= x \odot (I_n - \Phi)\, t_{\text{direct}} \\ &= x \odot (\mathbf{1}_n - \boldsymbol{\phi}) \odot t_{\text{direct}} \\ &= (\mathbf{1}_n - \boldsymbol{\phi}) \odot T_{\text{direct}} \end{aligned}$$

and:

$$T_{\text{consumer}} = T_{\text{downstream}} = x \odot \tilde{\boldsymbol{\mathcal{L}}} (\boldsymbol{\phi})\, t_{\text{direct}}$$

We deduce that:

$$\begin{aligned} T_{\text{total}} &= T_{\text{producer}} + T_{\text{consumer}} \\ &= x \odot \left(I_n - \Phi + \tilde{\boldsymbol{\mathcal{L}}} (\boldsymbol{\phi}) \right) t_{\text{direct}} \end{aligned}$$

If $\boldsymbol{\phi}_j = 100\%$, we have $\tilde{\boldsymbol{\mathcal{L}}} (\mathbf{1}_n) = \tilde{\boldsymbol{\mathcal{L}}}$ and $\Delta p = \tilde{\boldsymbol{\mathcal{L}}}\, t_{\text{direct}}$. This corresponds to the initial approach. If $\boldsymbol{\phi}_j = 0\%$, we have $\tilde{\boldsymbol{\mathcal{L}}} (\mathbf{0}_n) = \mathbf{0}_{n,n}$, $\Delta p = \mathbf{0}_n$, $T_{\text{producer}} = T_{\text{direct}}$ but $T_{\text{consumer}} = \mathbf{0}_n$. The costs passed on the consumers (or the downstream of the value chain) are equal to zero because the direct costs are initially absorbed by the producers.

Remark 12. *The functions Δp, π, T_{total}, $\mathcal{C}ost_{\text{total}}$ and $\mathcal{TI}$ remain homogeneous and additive with respect to $\boldsymbol{\tau}$. We can also show that*[71]*:*

$$\boldsymbol{\phi}' \succeq \boldsymbol{\phi} \Rightarrow T_{\text{total}} \left(\boldsymbol{\tau}, \boldsymbol{\phi}' \right) \succeq T_{\text{total}} \left(\boldsymbol{\tau}, \boldsymbol{\phi} \right)$$

The impact of the tax is maximum when $\boldsymbol{\phi} = \mathbf{1}_n$ and minimum when $\boldsymbol{\phi} = \mathbf{0}_n$. If we consider a uniform pass-through, the total cost of the carbon tax is an increasing function of the pass-through rate.

Illustration We consider again Example #3 and the differentiated taxation. We assume that the pass-through rates are uniform ($\boldsymbol{\phi}_1 = \boldsymbol{\phi}_2 = \boldsymbol{\phi}_3 = \boldsymbol{\phi}_4$). The evolution of the total cost is shown in Figure 38. When $\boldsymbol{\phi}_j = 0\%$, T_{total} is equal to \$152.50 mn and is the lower bound. The upper bound is reached when $\boldsymbol{\phi}_j = 100\%$ and we obtain $T_{\text{total}} = \$430.79$ mn. We have also indicated the contribution of each sector by distinguishing the direct and indirect costs. Figure 39 corresponds to the case where only Energy passes the direct cost on the other sectors. Finally, we report the inflation rate in Figure 40 by assuming that $\boldsymbol{\phi}_2 = \boldsymbol{\phi}_3 = \boldsymbol{\phi}_4 = 100\%$. The pass-through rate $\boldsymbol{\phi}_1$ depends on the carbon tax. It is low for small carbon taxes, but it increases with the level of the carbon tax[72].

[71] We have:

$$\begin{aligned} (*) &= I_n - \Phi + \tilde{\boldsymbol{\mathcal{L}}} (\boldsymbol{\phi}) \\ &= I_n - \Phi + \sum_{k=0}^{\infty} \left(A^\top \Phi \right)^k \Phi \\ &= I_n + \sum_{k=1}^{\infty} \left(A^\top \Phi \right)^k \Phi \end{aligned}$$

The proof is straightforward once we apply Properties NN1-NN4 (Appendix A.8 on page 150.).

[72] We assume that $\boldsymbol{\phi}_1 = 1 - e^{-\lambda \boldsymbol{\tau}_1^\eta}$ with $\lambda = 7.5 \times 10^{-4}$ and $\eta = 1.5$.

Figure 38: Producer and consumer cost contributions (uniform pass-through rate, Example #3)

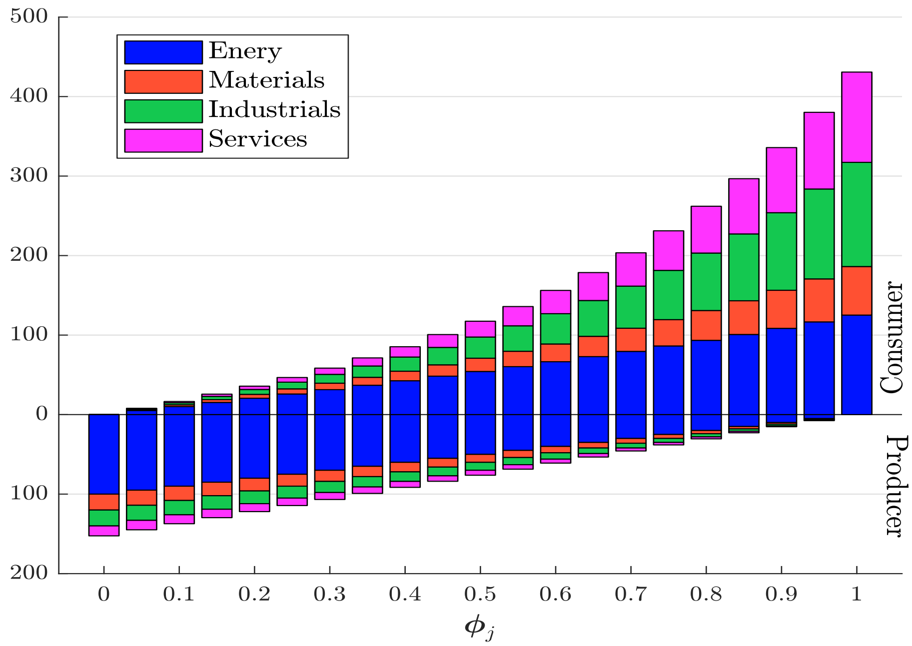

Figure 39: Producer and consumer cost contributions ($\phi_2 = \phi_3 = \phi_4 = 0\%$)

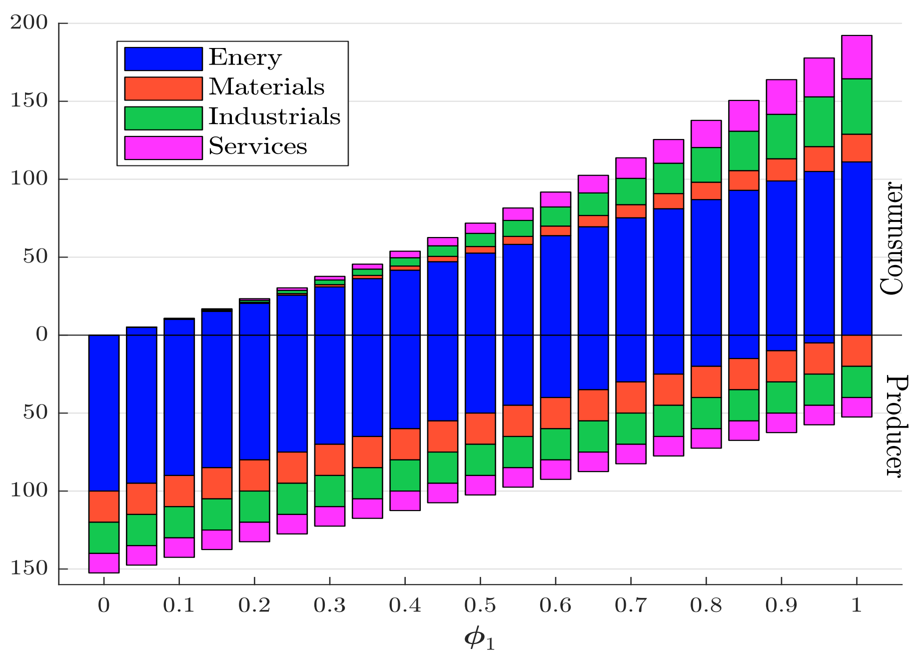

Figure 40: Relationship between the carbon tax and the inflation rate)

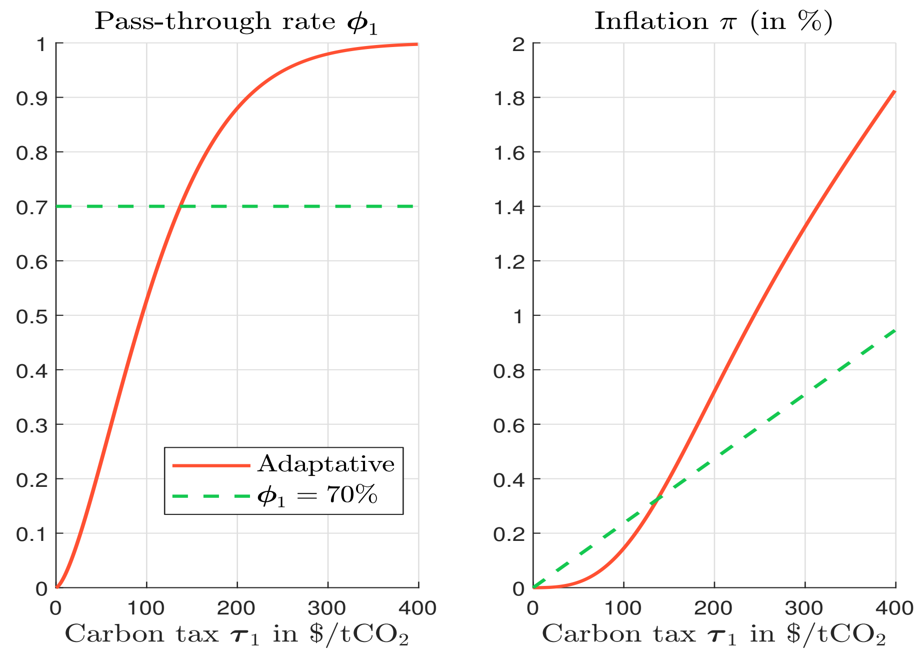

5.3 Empirical results

We apply the taxation framework to the Exiobase and WIOD tables. We reiterate that the figures for carbon emissions are the last available data, but not the input-output tables. Therefore, we can face some issues when comparing the results obtained with the 2014 input-output tables (Exiobase 2014 and WIOD 2014) and the 2022 table (Exiobase 2022). This is particularly true when we compute the inflation rate, the total cost for the economy and the tax incidence. Therefore, we focus on the Exiobase 2022 in this section and report some additional figures about WIOD 2014 and Exiobase 2014 for information.

5.3.1 The case of a global carbon tax

Uniform taxation We first consider a uniform tax $\boldsymbol{\tau}$ across all the countries and a uniform pass-through rate $\boldsymbol{\phi}$ across all the sectors. We compute the direct cost $\mathcal{C}ost_{\text{direct}} = \sum_{j=1}^{n} T_{\text{direct}}$ and the total cost $\mathcal{C}ost_{\text{total}} = \sum_{j=1}^{n} T_{\text{total}}$, which depends on the pass-through rate. Results are reported in Figures 41 and 42, and Table 27. For instance, if the carbon tax is set to \$100/tCO$_2$e, the direct cost is equal to \$4.8 tn while the total cost is \$6.1 tn if $\boldsymbol{\phi} = 50\%$ and \$13.3 tn if $\boldsymbol{\phi} = 100\%$. This represents 2.8%, 3.6% and 7.8% of the world GDP. In the case where we apply a carbon tax of \$500/tCO$_2$e, these costs become respectively \$24.2, \$30.4 and \$66.4 tn.

In Figure 43, we compute the cost multiplier $\mathcal{C}ost_{\text{total}}/\mathcal{C}ost_{\text{direct}}$ with respect to the pass-through rate $\boldsymbol{\phi}$. First, we verify that it does not depend on the level of the carbon tax because we apply a uniform taxation. Second, the cost multiplier is equal to the multiplicative factor of carbon emissions when the pass-through rate is equal to 100%:

$$\frac{\mathcal{C}ost_{\text{total}}\left(\boldsymbol{\tau}, \mathbf{1}_n\right)}{\mathcal{C}ost_{\text{direct}}\left(\boldsymbol{\tau}, \mathbf{1}_n\right)} = m_{(0-\infty)}$$

Figure 41: World economic cost in $ tn (global analysis, uniform taxation, Exiobase 2022)

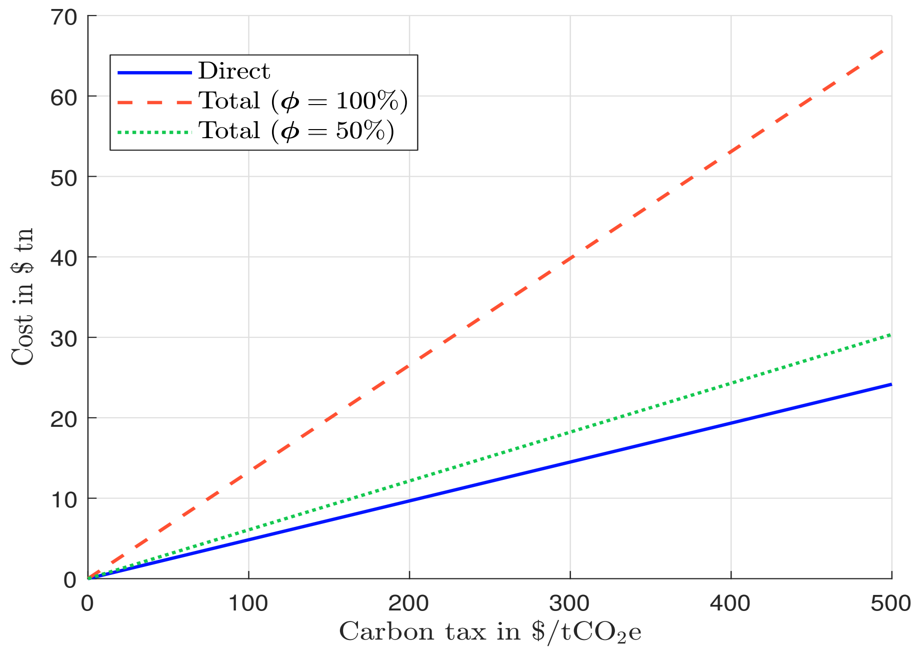

Figure 42: World economic cost in % of GDP (global analysis, uniform taxation, Exiobase 2022)

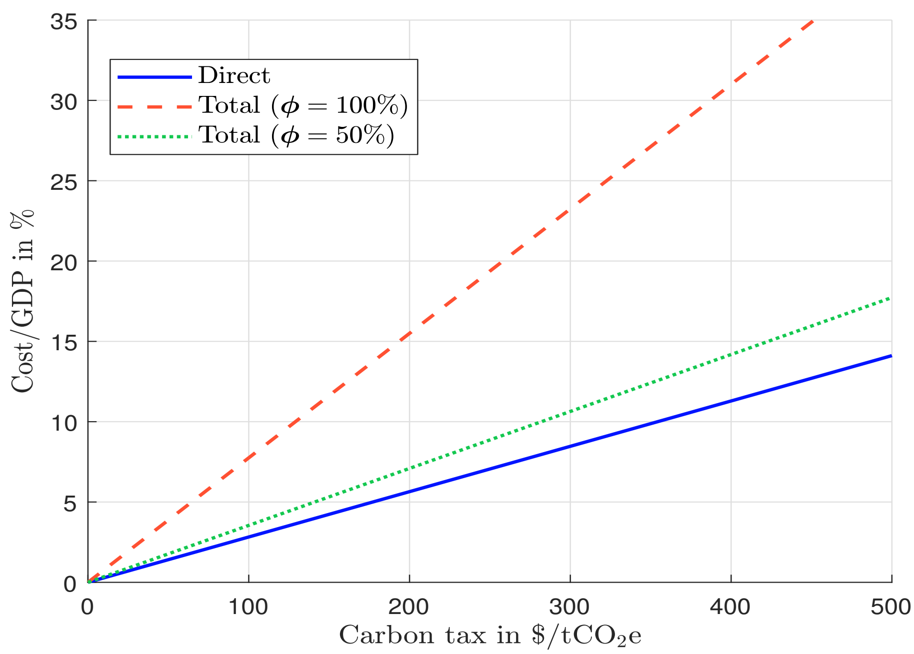

Table 27: World economic cost (global analysis, uniform taxation)

τ	Database	Year	Direct		Total					
					$\phi = 10\%$		$\phi = 50\%$		$\phi = 100\%$	
			\$ tn	in %	\$ tn	in %	\$ tn	in %	\$ tn	in %
50	WIOD	2014	1.62	1.01	1.63	1.01	2.08	1.29	5.09	3.16
	Exiobase	2014	2.04	1.71	2.05	1.72	2.56	2.15	5.62	4.71
	Exiobase	2022	2.42	1.41	2.44	1.42	3.04	1.77	6.64	3.87
100	WIOD	2014	3.24	2.01	3.26	2.03	4.15	2.58	10.18	6.32
	Exiobase	2014	4.07	3.41	4.11	3.44	5.12	4.29	11.24	9.42
	Exiobase	2022	4.83	2.82	4.87	2.84	6.07	3.55	13.27	7.75
250	WIOD	2014	8.09	5.03	8.15	5.06	10.38	6.44	25.44	15.80
	Exiobase	2014	10.19	8.54	10.26	8.60	12.80	10.73	28.11	23.56
	Exiobase	2022	12.09	7.06	12.18	7.11	15.18	8.86	33.18	19.37
500	WIOD	2014	16.19	10.06	16.31	10.13	20.75	12.89	50.88	31.60
	Exiobase	2014	20.37	17.07	20.53	17.20	25.60	21.45	56.22	47.12
	Exiobase	2022	24.17	14.11	24.36	14.22	30.37	17.73	66.37	38.75

Third, we notice the high convexity of the relationship between the pass-through rate and the multiplier. Indeed, we can approximate the cost multiplier by this function[73]:

$$\frac{\mathcal{C}ost_{\text{total}}\left(\boldsymbol{\tau}, \phi \mathbf{1}_n\right)}{\mathcal{C}ost_{\text{direct}}\left(\boldsymbol{\tau}, \phi \mathbf{1}_n\right)} \approx 1 + m_{(1-\infty)} \phi^3$$

Contrary to the common idea, the impact of the pass-through rate is not quadratic, but cubic! Therefore, a small error in the estimation of the pass-through rate may induce a high error in the estimation of the costs.

Figure 43: Cost multiplier (global analysis, uniform taxation, Exiobase 2022)

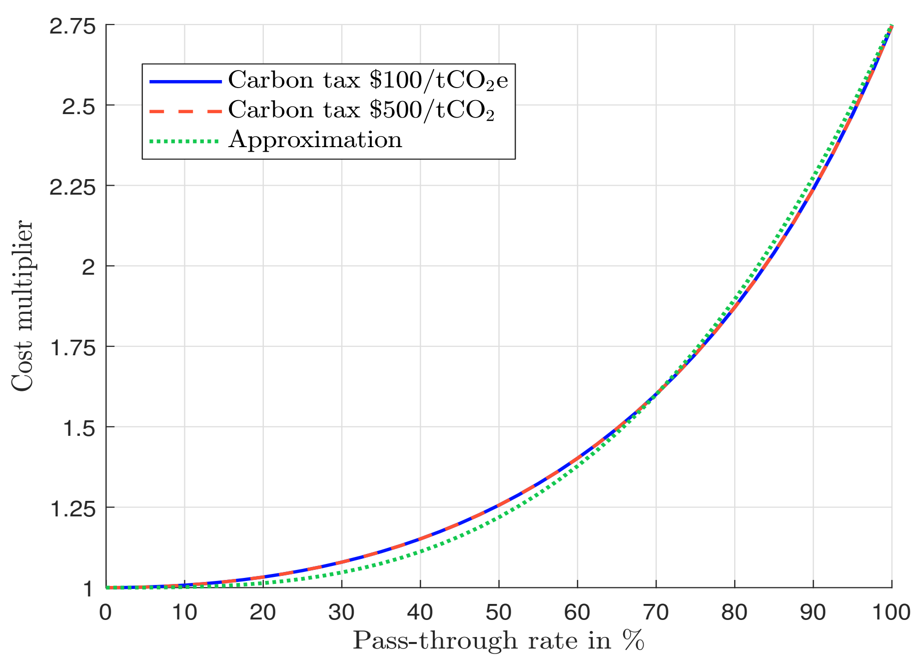

[73]This approximation also holds for the WIOD table (see Figure 106 on page 165)

Remark 13. *The cubic power of the approximation $1 + m_{(1-\infty)}\phi^3$ depends on the connectivity of the graph associated to the matrix A. Higher the upstreamness/downstreamness index, higher the power of the approximation.*

We now analyze the impact of the carbon tax on the inflation. For that, we define two price indices: the producer price index (PPI) wherein the basket weights are proportional to the output ($\alpha_j \propto x_j$) and the consumer price index (CPI) wherein the basket weights are proportional to the final demand ($\alpha_j \propto y_j$). Results are given in Figure 44. Again, the inflation rate depends on the pass-through rate. In the case of a carbon tax of \$500/tCO_2e and a pass-through rate of 100%, the PPI inflation rate is close to 40%, while the CPI inflation rate reaches 30%. These global figures are the results of a high discrepancy between country inflation rates. For instance, we report the 95% confidence interval of the PPI inflation rate in Figure 107 on page 165. We also indicate the inflation rate for seven countries. We notice that the inflation rate is above the median for Russia, China and Turkey and below the median for Germany, Japan, United Kingdom and USA. In order to have a global view, Figure 45 show the world map of the country inflation rates for a uniform tax of \$100/tCO_2e. There are three factors (composition of the items basket, impact of the value chain and direct carbon emissions of the country) that explain the dispersion of the inflation rates:

$$\pi = \underbrace{\alpha^\top}_{\text{Basket}} \cdot \underbrace{\tilde{\boldsymbol{\mathcal{L}}}(\boldsymbol{\phi})}_{\text{Value chain}} \cdot \underbrace{t_{\text{direct}}}_{\text{Scope 1}}$$

The direct costs are the main contributor, followed by the impact of the downstream diffusion of the carbon tax. In Figure 46, we report the contribution of the second factor (see page 166 for the first factor). The low inflation rate in Europe is explained by the low direct emissions, but Europe is highly penalized by its value chain. China is both impacted by the two factors, while the high inflation in Russia is mainly due to its indirect emissions because the impact of its value chain is one of the lowest in the world.

Figure 44: World inflation rate in % (global analysis, uniform taxation, Exiobase 2022)

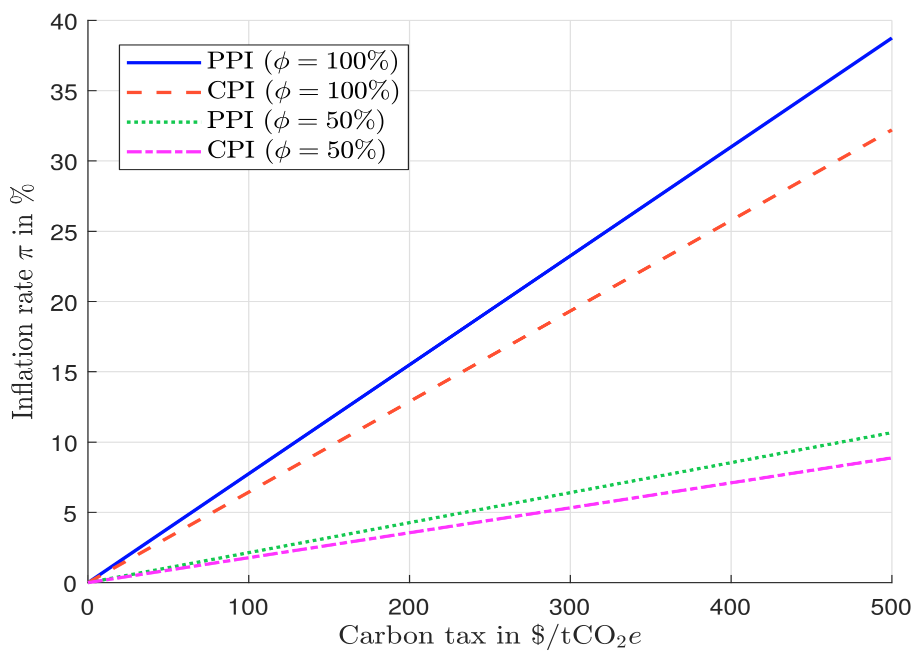

Figure 45: Production inflation rate in % (global analysis, uniform taxation, $\boldsymbol{\tau} = \$100/tCO_2e$, $\boldsymbol{\phi} = 100\%$, Exiobase 2022)

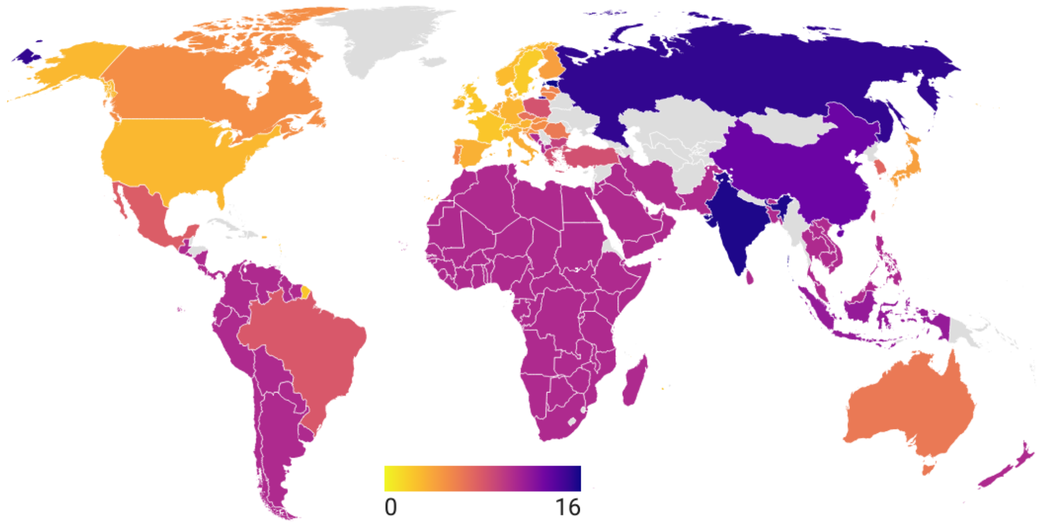

Source: Author's calculations (created by Datawrapper).

Figure 46: Contribution of the global value chain in % (global analysis, uniform taxation, $\boldsymbol{\tau} = \$100/tCO_2e$, $\boldsymbol{\phi} = 100\%$, Exiobase 2022)

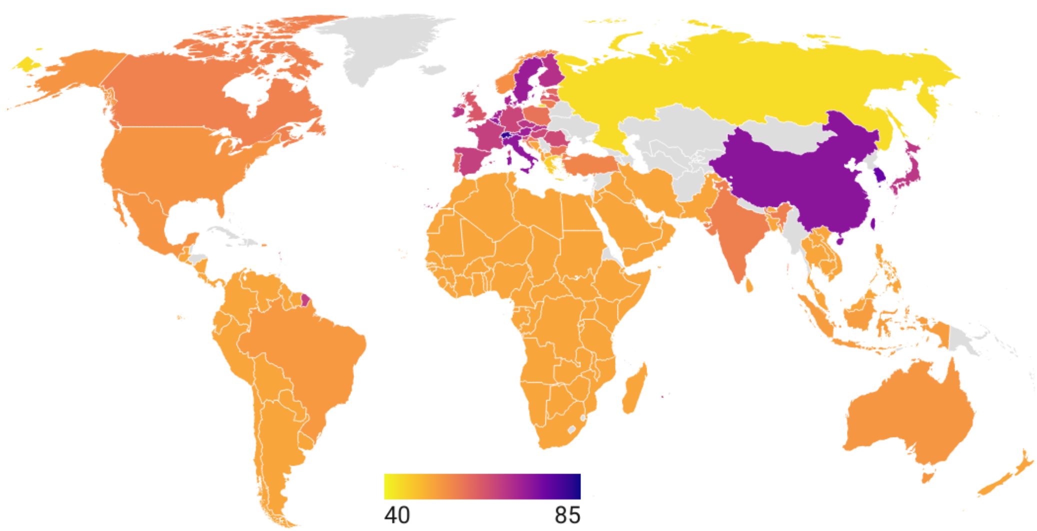

Source: Author's calculations (created by Datawrapper).

Differentiated taxation We now consider a carbon tax applied only to the energy sectors: *Electricity, gas, steam and air conditioning supply* ($\mathcal{S}_{13}$), *Land transport and transport via pipelines* ($\mathcal{S}_{19}$), *Manufacture of coke and refined petroleum products* ($\mathcal{S}_{24}$) and *Mining and quarrying* ($\mathcal{S}_{39}$). These sectors represent about 10% of the world output, but they are responsible of 50% of the scope 1 carbon emissions. Results are given in Table 28. On average, the total cost is divided by a factor of two with respect to the uniform taxation.

Table 28: World economic cost (global analysis, differentiated taxation)

τ	Database	Year	Direct		Total					
					$\phi = 10\%$		$\phi = 50\%$		$\phi = 100\%$	
			\$ tn	in %	\$ tn	in %	\$ tn	in %	\$ tn	in %
50	WIOD	2014	0.89	0.55	0.90	0.56	1.16	0.72	3.05	1.90
	Exiobase	2014	0.98	0.82	0.99	0.83	1.26	1.05	3.03	2.54
	Exiobase	2022	1.09	0.64	1.10	0.64	1.40	0.82	3.35	1.96
100	WIOD	2014	1.77	1.10	1.79	1.11	2.32	1.44	6.11	3.79
	Exiobase	2014	1.96	1.64	1.97	1.65	2.52	2.11	6.06	5.08
	Exiobase	2022	2.18	1.28	2.20	1.29	2.81	1.64	6.70	3.91
250	WIOD	2014	4.44	2.76	4.48	2.78	5.79	3.60	15.27	9.48
	Exiobase	2014	4.89	4.10	4.93	4.13	6.29	5.27	15.16	12.70
	Exiobase	2022	5.46	3.19	5.51	3.22	7.02	4.10	16.75	9.78
500	WIOD	2014	8.87	5.51	8.95	5.56	11.58	7.19	30.53	18.96
	Exiobase	2014	9.78	8.20	9.86	8.27	12.58	10.55	30.31	25.40
	Exiobase	2022	10.92	6.38	11.01	6.43	14.04	8.19	33.51	19.56

5.3.2 Regional taxation

Following Chen *et al.* (2023), we are now conducting an analysis of a regional taxation scenario wherein carbon tax is singularly imposed within a specific region of the world. This situation is likely to occur due to the lack of uniformity in carbon pricing, as shown in Figure 6 on page 19.

The case of a European tax We first consider a uniform taxation on EU member countries, which is certainly the most likely scenario. Figure 47 shows the total cost in trillions of dollars and the total cost over GDP (in %) for a carbon price ranging from zero to \$500/tCO_2e and a pass-through parameter of 50% and 100%. In this scenario, a \$500/tCO_2e carbon tax with a 100% pass-through would result in a worldwide cost of \$4.5 tn, with a \$4 tn cost supported by EU countries and a \$0.5 tn cost for non-EU ones. When EU sectors absorb their increasing costs by passing only 50% through the value chain, non-EU countries are less affected by carbon tax diffusion, and their cost decreases from \$521 bn to \$54 bn. Moreover, the cost over GDP for EU sectors decreases as long as they absorb the carbon tax, going from 14% when they fully pass the carbon tax to 8% when direct emitters bear half of the costs incurred by carbon taxation.

Table 29 displays the results for the fifteen largest EU countries with a \$100/tCO_2e carbon tax. In the case where pass-through is fixed at 50%, Germany will have a Cost/GDP ratio of 1.14% with WIOD 2014, 1.74% with Exiobase 2014, and 1.31% with Exiobase 2022. Sweden and Poland are respectively the less and most impacted countries. More generally, we observe three groups of countries with low, medium and high severity[74]. Furthermore,

[74]The first group (low severity) is made up of France, Sweden and Ireland. In the third group (high

Figure 47: Economic cost of the carbon tax (EU, uniform taxation, Exiobase 2022)

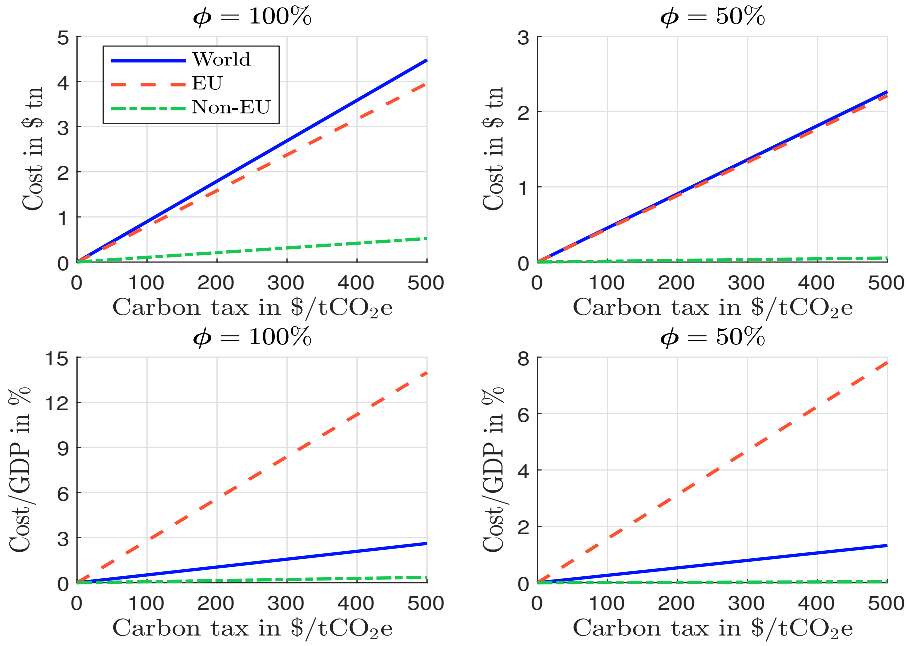

Figure 48: Cost breakdown with respect to the pass-through rate (EU, uniform taxation, Exiobase 2022)

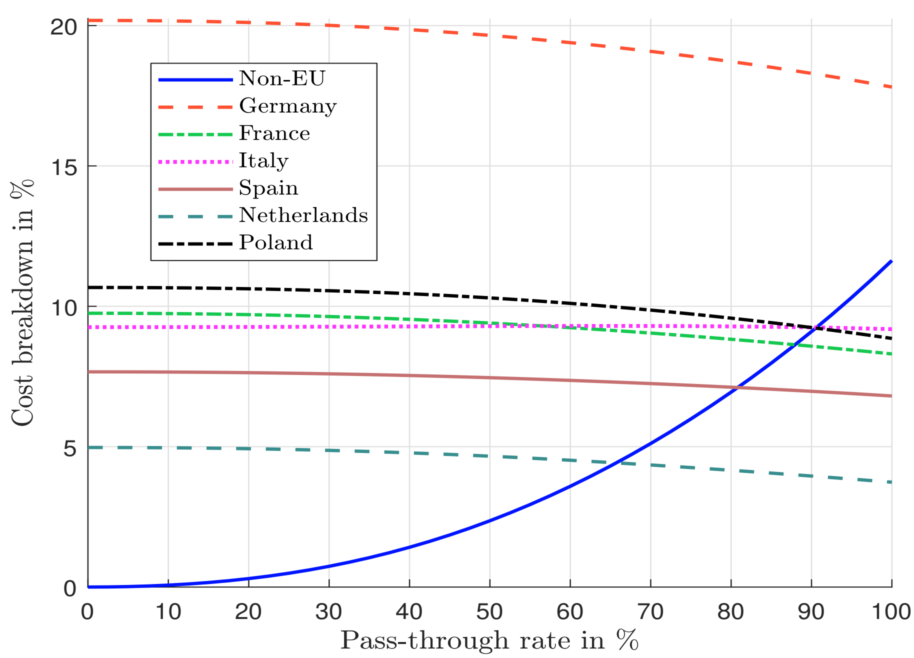

Figure 49: Cost breakdown (EU, uniform taxation, $\phi = 50\%$, Exiobase 2022)

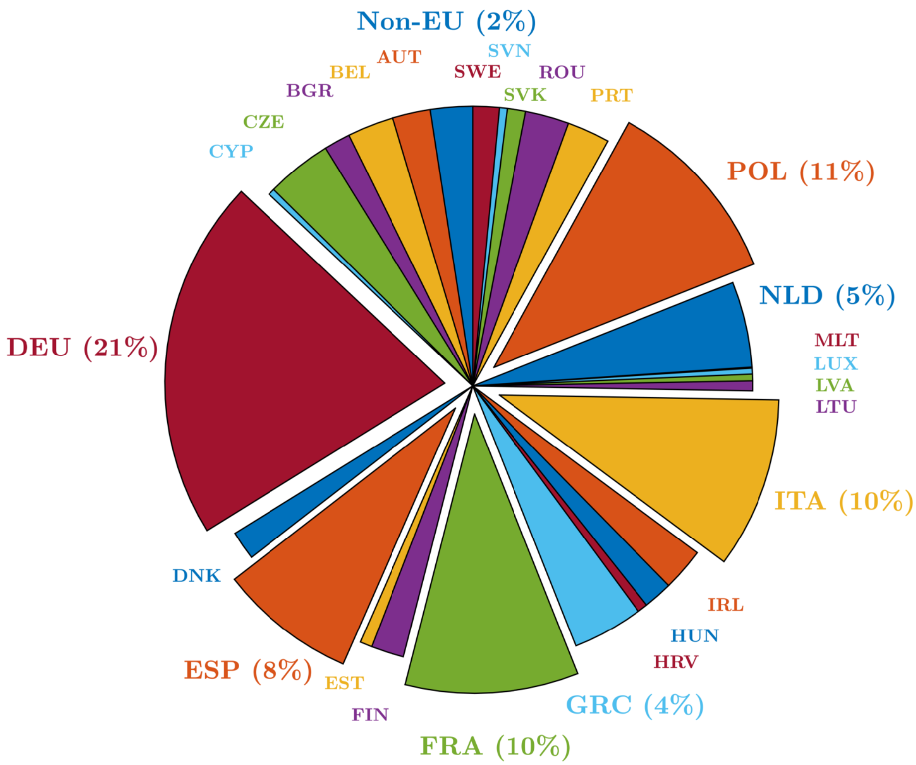

Figure 50: Cost breakdown (EU, uniform taxation, $\phi = 100\%$, Exiobase 2022)

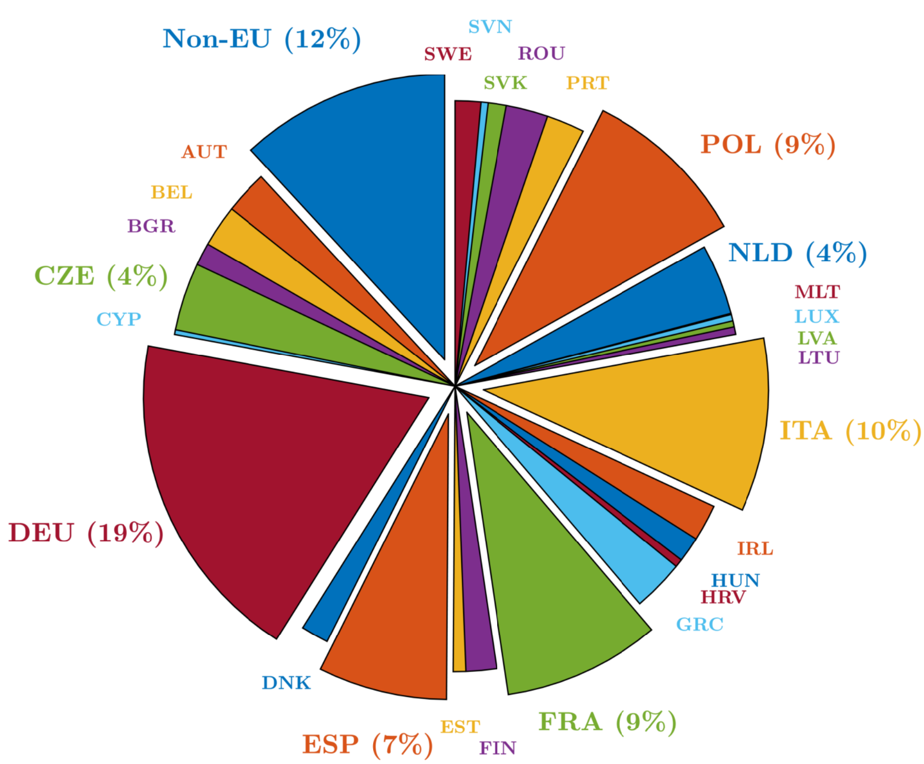

if we examine the cost breakdown with respect to the pass-through rate in Figure 48, the higher the pass-through for EU countries, the higher the cost breakdown for non-EU countries. However, surprisingly, it does not change significantly for EU countries. For instance, Germany has the highest cost breakdown, ranging from 20% with a 50% pass-through rate (compared to 2% for non-EU countries) to 18% with a 100% pass-through rate (compared to 12% for non-EU counties). More details of this breakdown can be found in Figures 49 and 50. With a uniform taxation and a 50% pass-through rate, Germany would support 21% of the overall cost, while Poland would support 11%. Results are comparable[75] with those obtained with the WIOD 2014 database[76].

Table 29: Cost/GDP in % of the fifteen largest EU countries (EU, uniform taxation, $\boldsymbol{\tau} = \$100/tCO_2e$)

Database	WIOD 2014		Exiobase 2014		Exiobase 2022	
Pass-through rate	50%	100%	50%	100%	50%	100%
Germany	1.14	2.05	1.74	3.00	1.31	2.35
France	0.55	1.06	1.04	1.83	0.93	1.62
Italy	0.79	1.68	1.26	2.37	1.14	2.23
Spain	0.99	1.96	1.70	3.11	1.37	2.47
Netherlands	1.50	2.25	1.72	2.81	1.30	2.07
Poland	2.94	5.30	5.04	8.44	4.06	6.91
Sweden	0.51	1.02	0.78	1.44	0.72	1.42
Belgium	0.79	1.53	1.26	2.20	1.11	1.94
Ireland	0.72	1.11	1.75	2.74	1.10	1.81
Austria	0.68	1.50	1.41	3.00	1.14	2.52
Denmark	1.15	1.76	1.62	3.16	1.19	2.23
Finland	1.08	2.08	1.98	3.51	1.66	3.18
Romania	2.01	3.78	3.73	6.91	2.70	4.98
Czech Republic	2.00	3.76	3.40	6.77	2.64	5.26
Portugal	1.20	2.32	2.53	4.56	2.50	4.29

The case of an American or Chinese tax We consider a scenario where carbon tax is only applied to the USA. Results are given in Figure 51. Here again, decreasing pass-through parameter (and absorbing the tax) leads to a smaller impact for both American and non-American sectors. For instance, with a $\$500/tCO_2e$ carbon tax, costs for the USA sectors would range from \$4.4 tn with a 100% pass-through rate to only \$2.9 tn with a 50% pass-through rate. Similarly as in the first scenario, impact of cost on GDP would also decrease, going from almost 12% to less than 8% for American sectors. To a certain extent, we conclude that the American tax has the same impact than a European tax at the global level.

Eventually, we consider a scenario where only China sets up a carbon tax. Results are provided in Figure 52. A $\$500/tCO_2e$ carbon tax on Chinese sectors would represent a \$25 tn worldwide cost, where almost \$24 tn would be supported by Chinese sectors. Surprisingly, sectors outside of China appear to be less affected, as total cost would represent only \$1.3 tn. This may seem counter intuitive, when knowing the high dependency of the world to

severity), we find Poland, Finland, Romania, Czech Republic and Portugal.

[75] We have corrected the carbon emissions for Estonia sectors, because the original Exiobase 2022 database contains some numerical errors for this country. Otherwise, Estonia would have a contribution of 6%, which is impossible.

[76] See Figures 113 and 114 on page 169.

Figure 51: Economic cost of the carbon tax (USA, uniform taxation, Exiobase 2022)

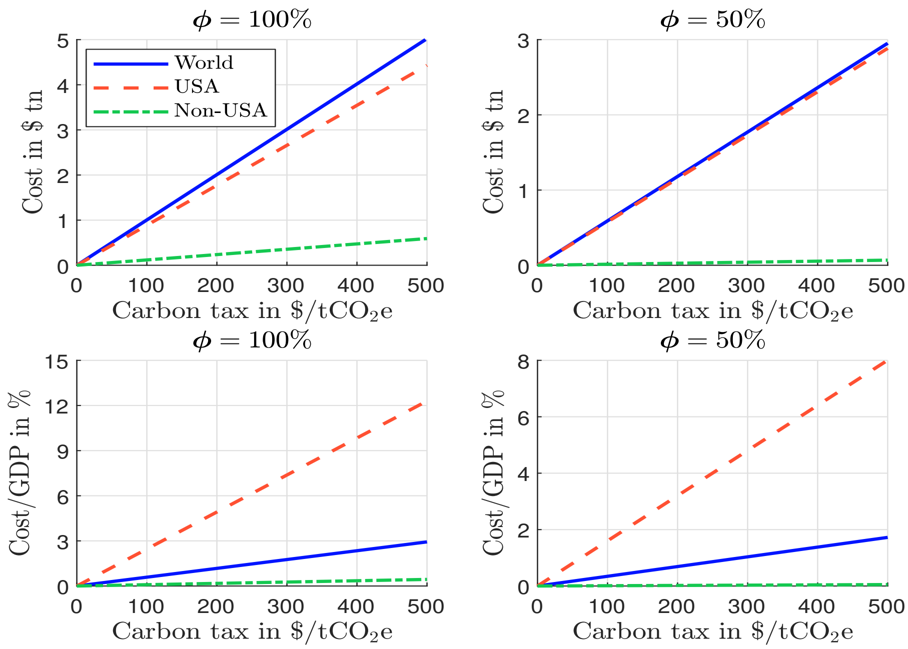

Figure 52: Economic cost of the carbon tax (China, uniform taxation, Exiobase 2022)

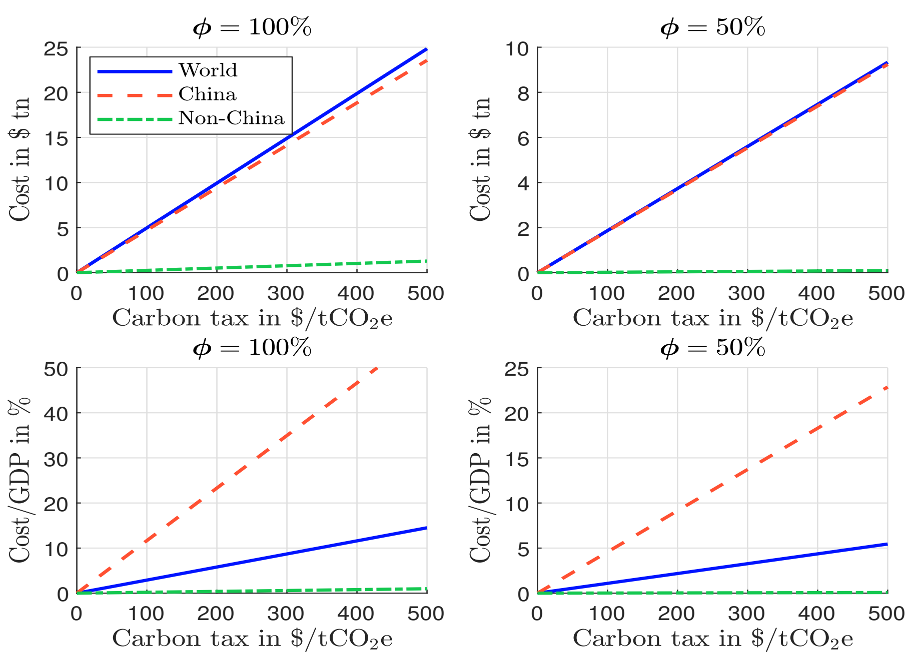

Chinese industries. Nevertheless, same conclusions can be drawn, as passing less monetary amount through the value chain will lead to a decrease in Cost/GDP ratio, going from more than 50% with a 100% pass-through rate to less than 25% with a 50% pass-through rate for Chinese sectors.

Table 30: Domestic and foreign impacts (in \$ bn) of a regional tax (uniform taxation, $\phi = 100\%$, Exiobase 2022)

Carbon tax	Domestic impact			Foreign impact		
	EU	USA	China	EU	USA	China
$100/tCO$_2$e	792	886	4 710	104	118	257
$250/tCO$_2$e	1 979	2 215	11 774	261	296	643
$500/tCO$_2$e	3 959	4 430	23 549	521	592	1 287

Table 31: Fifteen largest impacted foreign countries (uniform taxation, $\tau = \$100/tCO_2e$, $\phi = 100\%$, Exiobase 2022)

Rank	EU tax		US tax		Chinese tax	
1	ROW	25.25%	CHN	24.74%	ROW	36.89%
2	CHN	23.62%	ROW	18.60%	USA	12.95%
3	USA	11.45%	CAN	9.35%	KOR	8.87%
4	GBR	8.77%	MEX	8.51%	IND	6.91%
5	CHE	4.32%	KOR	6.89%	JPN	6.44%
6	KOR	4.05%	JPN	5.05%	DEU	3.61%
7	IND	3.67%	IND	4.28%	MEX	2.19%
8	JPN	3.31%	DEU	2.80%	FRA	1.88%
9	TUR	2.62%	BRA	2.51%	GBR	1.83%
10	TWN	2.08%	GBR	2.34%	BRA	1.75%
11	CAN	2.06%	FRA	1.63%	IDN	1.74%
12	RUS	1.96%	TWN	1.59%	CAN	1.62%
13	BRA	1.90%	IRL	1.47%	ITA	1.59%
14	MEX	1.70%	ITA	1.43%	AUS	1.31%
15	NOR	1.46%	NLD	1.23%	TUR	1.11%

Table 30 shows the global foreign impact in the case of a EU, US and Chinese tax for threes value of the carbon price. China always has the highest impact on foreign countries, with a cost of \$1 287 bn for a \$500/tCO$_2$e carbon price, while EU foreign impact is only \$521 bn. In order to better understand the winners and the losers, we report the fifteen largest countries impacted by a carbon tax in Table 31. In this scenario, taxation is set to \$100/tCO$_2$e and pass-through parameter is set to 100%. When the tax is applied in the European union, the rest-of-the-world region is the most impacted, representing 25.25% of the overall cost supported by foreign countries. It is followed by China (23.62%), United States (11.45%) and Great Britain (8.77%). It would also be the case with a Chinese tax, but it now represents more than 36% of the foreign costs. It is then followed by United States (12.95%), South Korea (8.87%) and India (6.91%). In the case of a US tax, China would be the most impacted country, by representing 24.74% of the overall impact, followed by the rest-of-the-world region (18.60%), Canada (9.35%) and Mexico (8.51%). It is important to notice that the USA has strong commercial relations with China, but also with other American countries (Canada, Mexico, Brazil). These results emphasize the commercial links between countries, and as a result, a potential exposure to a carbon tax. For instance, if we focus on Turkey, it is highly connected with EU, as it would be the 9^{th} most impacted country by a EU carbon tax. It would also be impacted in the case of a Chinese tax, as it would be the 15^{th} most impacted country. The impact would be smaller in the case of a carbon tax in the USA. In a similar way, we notice the importance of Germany (DEU) in China and USA supply chain.

Markov chain interpretation of tax transmission channels between countries In order to understand the previous results, we consider the Markov representation of the tax diffusion:

$$\begin{cases} \Delta p_{(k)} = A^\top \Phi \Delta p_{(k-1)} \\ \Delta p_{(0)} = \Phi t_{\text{direct}} \end{cases}$$

We consider the following block decomposition of the matrix A:

$$A = \left(\begin{array}{c|c} a_c & a_{c,\text{row}} \\ \hline a_{\text{row},c} & a_{\text{row}} \end{array}\right)$$

where c and row indicate the indices of the given country and the rest-of-the-world region. We apply the same partition to the vectors $t_{\text{direct}} := t = (t_c, t_{\text{row}})$, $T_{\text{total}} := T = (T_c, T_{\text{row}})$, $x = (x_c, x_{\text{row}})$ and $\boldsymbol{\phi} = (\boldsymbol{\phi}_c, \boldsymbol{\phi}_{\text{row}})$. We first consider the case with one sector. We have:

$$A^\top \Phi = \begin{pmatrix} \boldsymbol{\phi}_c a_c & \boldsymbol{\phi}_{\text{row}} a_{\text{row},c} \\ \boldsymbol{\phi}_c a_{c,\text{row}} & \boldsymbol{\phi}_{\text{row}} a_{\text{row}} \end{pmatrix}$$

and:

$$\left(A^\top \Phi\right)^2 = \begin{pmatrix} \boldsymbol{\phi}_c^2 a_c^2 + \boldsymbol{\phi}_c \boldsymbol{\phi}_{\text{row}} a_{c,\text{row}} a_{\text{row},c} & \boldsymbol{\phi}_c \boldsymbol{\phi}_{\text{row}} a_c a_{\text{row},c} + \boldsymbol{\phi}_{\text{row}}^2 a_{\text{row},c} a_{\text{row}} \\ \boldsymbol{\phi}_c^2 a_c a_{c,\text{row}} + \boldsymbol{\phi}_c \boldsymbol{\phi}_{\text{row}} a_{c,\text{row}} a_{\text{row}} & \boldsymbol{\phi}_c \boldsymbol{\phi}_{\text{row}} a_{c,\text{row}} a_{\text{row},c} + \boldsymbol{\phi}_{\text{row}}^2 a_{\text{row}}^2 \end{pmatrix}$$

We assume that the country applies a carbon tax. Since we have $t = (t_c, 0)$, it follows that $\Delta p_{(0)} = (\boldsymbol{\phi}_c t_c, 0)$. At the zeroth tier, the producer cost is $\left(x_c \left(1 - \boldsymbol{\phi}_c\right) t_c, 0\right)$ while the consumer cost is $(x_c \boldsymbol{\phi}_c t_c, 0)$. We deduce that:

$$T_{(0)} = \begin{pmatrix} x_c t_c \\ 0 \end{pmatrix}$$

At the first tier, we have $\Delta p_{(1)} = A^\top \Phi \Delta p_{(0)}$ or:

$$\Delta p_{(1)} = \begin{pmatrix} \boldsymbol{\phi}_c^2 a_c \\ \boldsymbol{\phi}_c^2 a_{c,\text{row}} \end{pmatrix} t_c$$

The part of the tax that has been passed by the country on the rest-of-the-world region depends on the technical coefficient $a_{c,\text{row}}$. If $a_{c,\text{row}} > 0$, the rest-of-the-world region needs buying some goods to the country. The country exports then inflation to the rest-of-the-world region. At the first tier, the total cost is then:

$$T_{(1)} = \begin{pmatrix} x_c a_c \\ x_{\text{row}} a_{c,\text{row}} \end{pmatrix} \boldsymbol{\phi}_c^2 t_c$$

In particular, $T_{(1),\text{row}} = 0$ if $a_{c,\text{row}} = 0$ and there is no exported inflation. At the second tier, we have $\Delta p_{(2)} = A^\top \Phi \Delta p_{(1)}$ or:

$$\Delta p_{(2)} = \begin{pmatrix} \boldsymbol{\phi}_c^3 a_c^2 + \boldsymbol{\phi}_c^2 \boldsymbol{\phi}_{\text{row}} a_{c,\text{row}} a_{\text{row},c} \\ \boldsymbol{\phi}_c^3 a_c a_{c,\text{row}} + \boldsymbol{\phi}_c^2 \boldsymbol{\phi}_{\text{row}} a_{c,\text{row}} a_{\text{row}} \end{pmatrix} t_c$$

We deduce that:

$$T_{(2)} = \begin{pmatrix} x_c \phi_c a_c^2 + x_c \phi_{\mathrm{row}} a_{c,\mathrm{row}} a_{\mathrm{row},c} \\ x_{\mathrm{row}} \phi_c a_c a_{c,\mathrm{row}} + x_{\mathrm{row}} \phi_{\mathrm{row}} a_{c,\mathrm{row}} a_{\mathrm{row}} \end{pmatrix} \phi_c^2 t_c$$

Therefore, the country may face an imported inflation from the rest-of-the-world region. We distinguish three cases:

1. If $a_{c,\mathrm{row}} = 0$, the imported inflation is equal to zero, because the exported inflation for the rest-of-the-world was equal to zero at the first tier;
2. If $a_{c,\mathrm{row}} > 0$, the imported inflation may be positive or null;
   (a) It is positive if $a_{\mathrm{row},c} > 0$; this means that the country buy goods to the rest-of-the world region;
   (b) It is equal to zero if $a_{\mathrm{row},c} = 0$.

The relative magnitude of the exported inflation depends on the following ratio:

$$R_{\mathrm{row} \longrightarrow c} = \frac{\phi_{\mathrm{row}} a_{c,\mathrm{row}} a_{\mathrm{row},c}}{\phi_c a_c^2}$$

If $R_{\mathrm{row} \longrightarrow c} \gg 1$, the contribution of the exported inflation is high, otherwise it is low. We observe this situation when $\phi_{\mathrm{row}} \gg \phi_c$ and $a_{c,\mathrm{row}} a_{\mathrm{row},c} \gg a_c^2$. In a similar way, the imported inflation continues to be significant in the second tier if $a_{c,\mathrm{row}} \gg 0$ and $\phi_c a_c + \phi_{\mathrm{row}} a_{\mathrm{row}} \gg 0$. In this case, the rest-of-the-world region faces two types of inflation: the internal inflation if $\phi_{\mathrm{row}} > 0$ and the exported inflation.

Let us consider an example to illustrate the previous analytical framework. We assume that $A_c = 0.7$, $A_{c,\mathrm{row}} = 0.3$, $A_{\mathrm{row},c} = 0.2$, $A_{\mathrm{row}} = 0.3$ and $\phi_c = \phi_{\mathrm{row}} = 0.9$. In Figure 53, we plot the directed graph associated to the adjacency matrix of the Markov chain. The color map indicates the magnitude of the edges. Figure 54 shows the evolution of the matrix $(\Phi A)^k$ with respect to the k^{th} tier. We notice that the directed graph becomes more and more red, indicating that the transmission becomes weaker. In Figures 115–118 on pages 170–171, we consider two other examples. In the case of matrix #2, we have $A_c = 0.2$, $A_{c,\mathrm{row}} = 0.2$, $A_{\mathrm{row},c} = 0.5$, $A_{\mathrm{row}} = 0.4$. We notice that the largest edge of the directed graph is from the rest-of-the-world region to the country, but very quickly this transmission channel vanishes because the magnitude of the other edges is low. This is less the case with the matrix #3, which is defined by $A_c = 0.4$, $A_{c,\mathrm{row}} = 0.4$, $A_{\mathrm{row},c} = 0.5$, $A_{\mathrm{row}} = 0.5$. The previous analysis can be extend to many sectors and countries. For instance, matrix #4 corresponds to the following example:

$$A = \begin{pmatrix} 0.5 & 0.2 & 0.1 \\ 0.3 & 0.5 & 0.2 \\ 0.1 & 0.3 & 0.4 \end{pmatrix}$$

with a uniform pass-through rate of 90%. Results are given in Figures 55 and 56.

In Figure 57, we plot the directed graph of the global value chain using the Exiobase 2022 input-output table. Let $\mathcal{C}_1$ and $\mathcal{C}_2$ be two countries. We compute the average value[77] $\bar{A}(\mathcal{C}_1, \mathcal{C}_2)$ of the technical coefficients $A_{i,j}$ such that $i \in \mathcal{C}_1 \wedge j \in \mathcal{C}_2$. In order to obtain a better visualization, we have limited the analysis to 12 countries: Canada, China, Germany, France, United Kingdom, India, Japan, Republic of Korea, Mexico, Turkey, Taiwan and

[77] The coefficients are weighted using the following rules $w_{i,j} \propto x_i x_j$.

Figure 53: Directed graph (matrix #1)

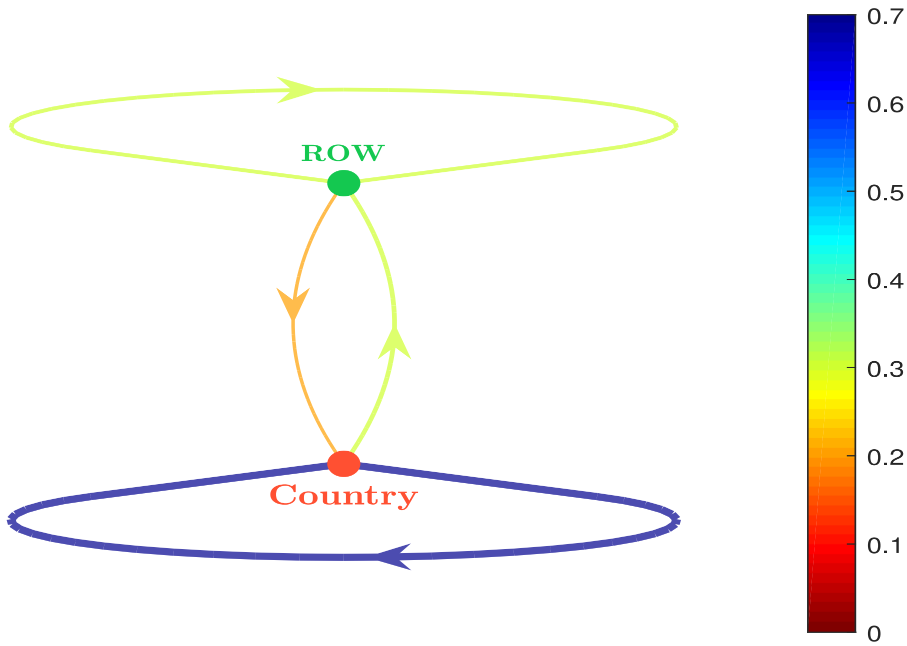

Figure 54: Impact of the k^{th} tier on the directed graph (matrix #1)

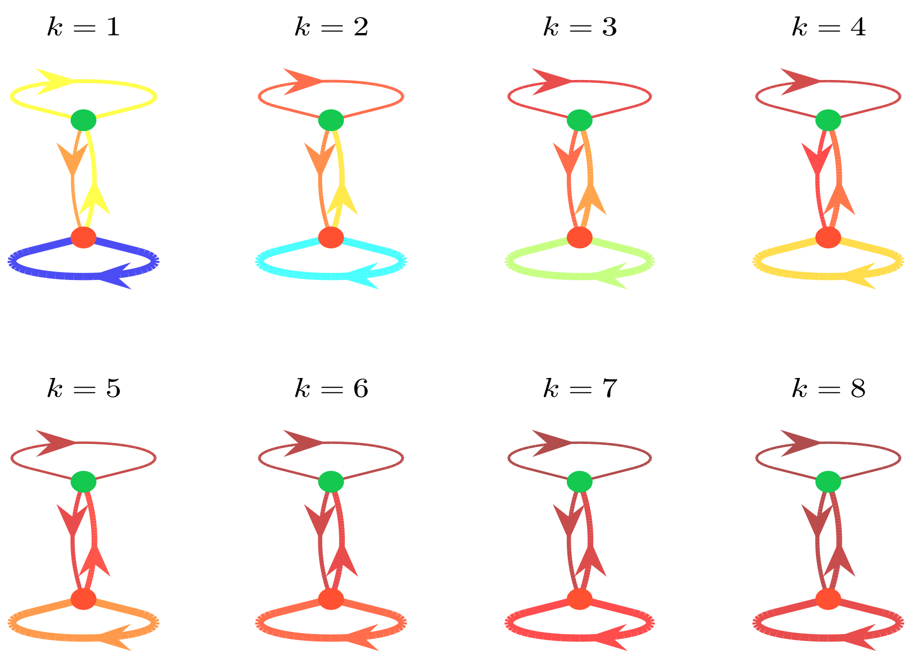

Figure 55: Directed graph (matrix #4)

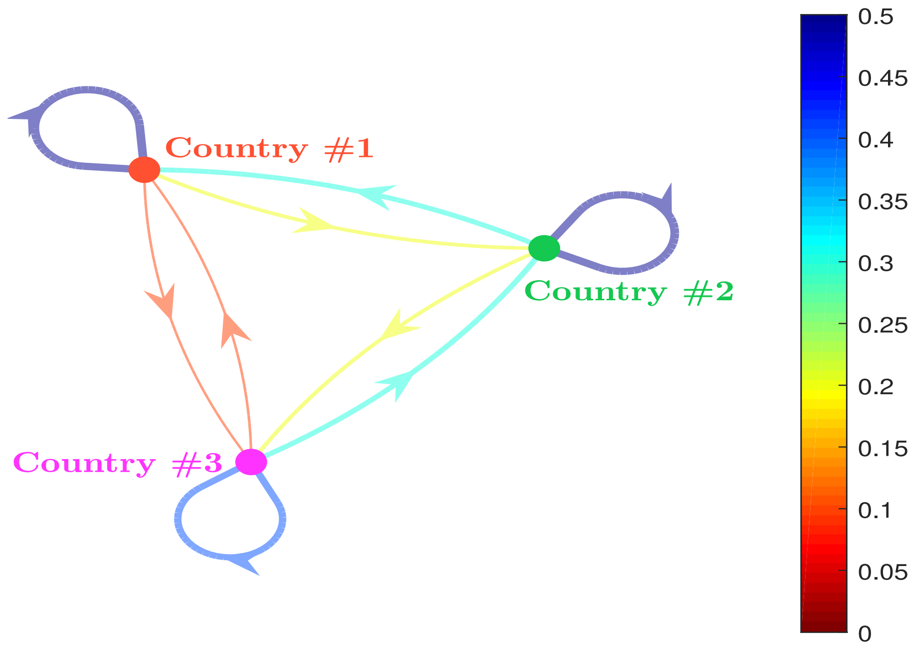

Figure 56: Impact of the k^{th} tier on the directed graph (matrix #4)

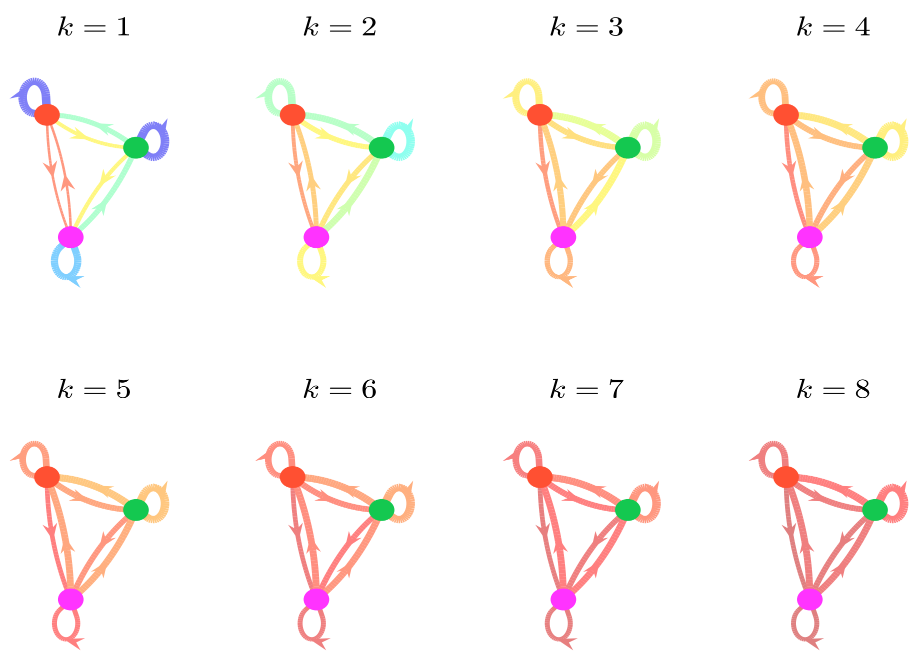

Figure 57: Directed graph of the global value chain (Exiobase 2022)

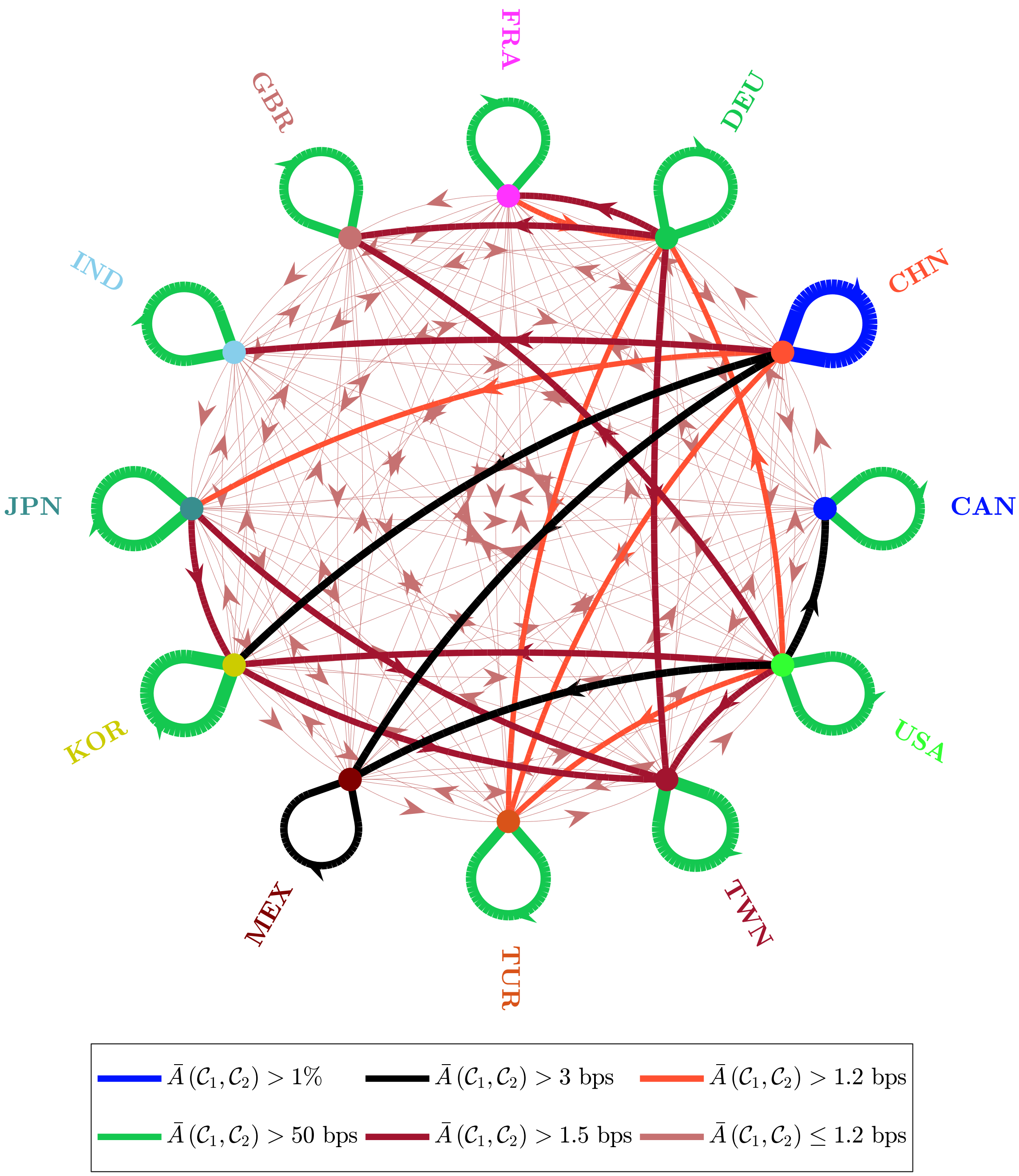

the United States. The width and color of the edge $\mathcal{E}(\mathcal{C}_1, \mathcal{C}_2)$ depend on the magnitude of $\bar{A}(\mathcal{C}_1, \mathcal{C}_2)$. Bigger the value of $\bar{A}(\mathcal{C}_1, \mathcal{C}_2)$, larger the width of $\mathcal{E}(\mathcal{C}_1, \mathcal{C}_2)$. We notice that the largest edges are located within countries. China, followed by Korea and Taiwan, is the country with the highest density of inter-sector flows. Besides this intra-country dominance, we find four main inter-country relationships: CHN/KOR, CHN/MEX, USA/CAN and USA/MEX. Then, we have two blocks of regional relationships. The first block concerns the Asian supply chain (CHN/JPN/KOR/TWN), while the second block is the European value chain (DEU/FRA/GBR). We also find some bilateral relationships: CHN/IND, DEU/TWN, USA/GBR and USA/KOR. Finally, the fourth level mainly concerns the interconnectedness between Turkey on the one hand, and China, Germany and the United States on the other hand.

Remark 14. *Since $\bar{A}(\mathcal{C}, \mathcal{C}) \gg \bar{A}(\mathcal{C}, \mathcal{C}')$, this is normal that the carbon tax affects mainly the country $\mathcal{C}$ and far less the other countries $\mathcal{C}'$.*

5.3.3 Stochastic pass-through rates

We now consider a more realistic framework since we assume that the pass-through rates are stochastic and follow a beta distribution. We consider the mapping classification between the sectors and the four types given in Table 60 on page 186.

The case of independent pass-through rates We first assume that pass-through rates are independent and test four levels of carbon tax: 50, 100, 250 and 500. Since $\boldsymbol{\phi}$ is a random vector, the economic cost is stochastic. We use the Monte Carlo method with 3 000 simulations to estimate the distribution function of the economic cost. Results are reported on pages 172–173. In fact, we notice that the statistics are proportional to the carbon tax. Therefore, we focus on the \$100/tCO_2e level in Figure 58. We notice that the confidence level is relatively small. The total cost for the economy is between 8 and 9 trillions of dollars, or between 4.7% and 5.3% of the world GDP. The cost multiplier takes a value around 1.8, meaning that the diffusion of the carbon tax induces a supplementary cost of 80% in top of the direct costs. Finally, the tax generates a significant inflation between 3% and 4.5%.

Remark 15. *The previous figures correspond to a uniform non-stochastic pass-through rate between* 70% *and* 80%.

The cost faced by each sector depends on its direct emissions and its interconnectedness with the supply chain. We report the statistics for the fifteen largest impacted sectors[78] in Table 32 and Figures 59 and 60. The most intensive sector is naturally highly penalized. Indeed, *Electricity, gas, steam and air conditioning supply* has a contribution of 20% and its cost is greater than 50% of its current output. Then, we find a group of eight sectors, whose contribution is greater than 4%. They concern crop and animal production, manufacture of goods and construction. We also notice that one half of these fifteen sectors face a cost, which represents at least 10% of the sector output. Nevertheless, about 70% and 45% of the sectors have a cost lower than 5% and 2% of their output. These results clearly show that the risk is located in a few number of sectors.

[78]They are *Electricity, gas, steam and air conditioning supply* ($\mathcal{S}_{13}$), *Crop and animal production, hunting and related service activities* ($\mathcal{S}_{11}$), *Mining and quarrying* ($\mathcal{S}_{38}$), *Manufacture of basic metals* ($\mathcal{S}_{21}$), *Manufacture of other non-metallic mineral products* ($\mathcal{S}_{32}$), *Manufacture of coke and refined petroleum products* ($\mathcal{S}_{24}$), *Manufacture of chemicals and chemical products* ($\mathcal{S}_{23}$), *Sewerage; waste collection, treatment and disposal activities; materials recovery; remediation activities and other waste management services* ($\mathcal{S}_{50}$), *Construction* ($\mathcal{S}_{10}$), *Manufacture of fabricated metal products, except machinery and equipment* ($\mathcal{S}_{27}$) *Manufacture of food products, beverages and tobacco products* ($\mathcal{S}_{28}$), *Manufacture of machinery and equipment n.e.c.* ($\mathcal{S}_{30}$), *Land transport and transport via pipelines* ($\mathcal{S}_{19}$), *Public administration and defence; compulsory social security* ($\mathcal{S}_{44}$), and *Air transport* ($\mathcal{S}_{7}$).

Figure 58: Economic impact (global analysis, τ = \$100/tCO$_2$e, stochastic pass-through, Exiobase 2022)

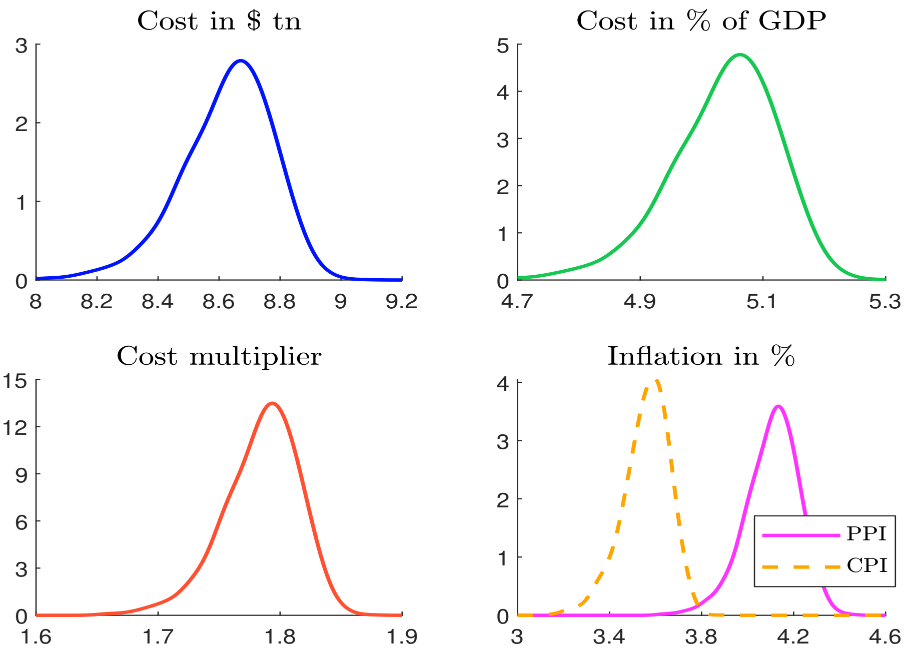

Table 32: Fifteen largest impacted sectors (global analysis, τ = \$100/tCO$_2$e, stochastic pass-through, Exiobase 2022)

	Cost in \$ tn			Contribution in %			Cost in %		
Quantile	5%	50%	95%	5%	50%	95%	5%	50%	95%
$\mathcal{S}_{13}$	1.72	1.77	1.79	20.1	20.4	20.8	52.9	54.6	55.2
$\mathcal{S}_{11}$	0.89	0.90	0.91	10.2	10.4	10.7	16.8	17.0	17.2
$\mathcal{S}_{38}$	0.75	0.77	0.78	8.8	8.9	9.1	20.5	20.9	21.1
$\mathcal{S}_{21}$	0.59	0.63	0.65	7.0	7.3	7.4	13.3	14.2	14.8
$\mathcal{S}_{32}$	0.58	0.60	0.62	6.8	7.0	7.1	25.0	26.2	26.8
$\mathcal{S}_{24}$	0.44	0.48	0.49	5.2	5.5	5.7	13.8	14.9	15.4
$\mathcal{S}_{23}$	0.36	0.39	0.41	4.4	4.5	4.6	7.0	7.5	7.8
$\mathcal{S}_{50}$	0.34	0.35	0.35	3.9	4.0	4.1	28.4	28.6	28.7
$\mathcal{S}_{10}$	0.31	0.34	0.39	3.7	4.0	4.4	2.4	2.7	3.0
$\mathcal{S}_{27}$	0.17	0.19	0.19	2.0	2.1	2.2	5.6	6.0	6.2
$\mathcal{S}_{28}$	0.14	0.15	0.17	1.7	1.8	1.9	2.1	2.2	2.4
$\mathcal{S}_{30}$	0.14	0.15	0.17	1.6	1.8	1.9	2.9	3.4	3.6
$\mathcal{S}_{19}$	0.13	0.14	0.15	1.6	1.6	1.7	3.2	3.3	3.4
$\mathcal{S}_{44}$	0.13	0.14	0.14	1.5	1.6	1.6	1.2	1.3	1.3
$\mathcal{S}_{7}$	0.11	0.12	0.12	1.3	1.3	1.4	10.9	11.1	11.2

Figure 59: Sector contribution in % (global analysis, $\boldsymbol{\tau}$ = \$100/tCO$_2$e, stochastic pass-through, Exiobase 2022)

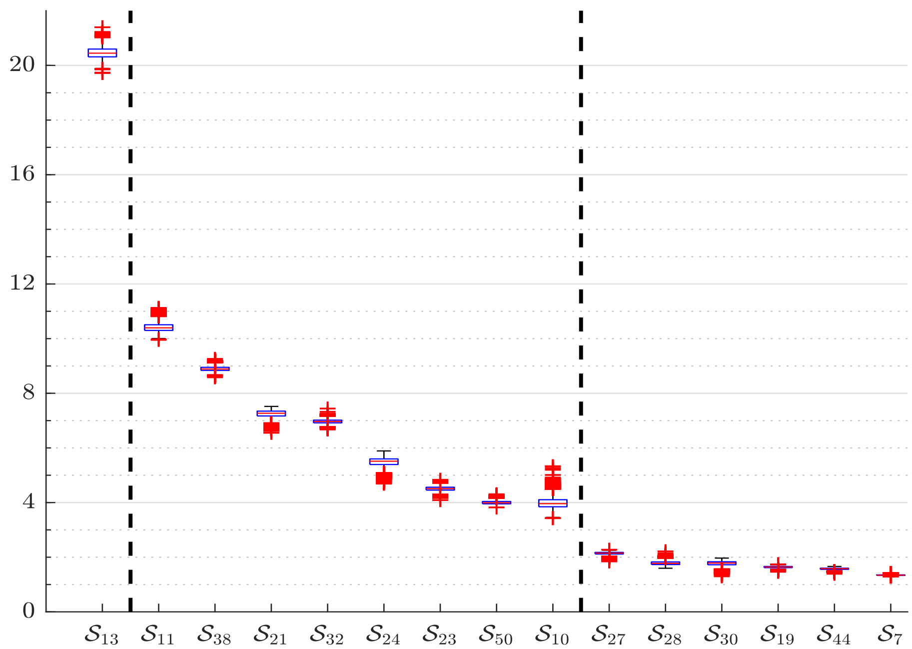

Figure 60: Sector cost in % (global analysis, $\boldsymbol{\tau}$ = \$100/tCO$_2$e, stochastic pass-through, Exiobase 2022)

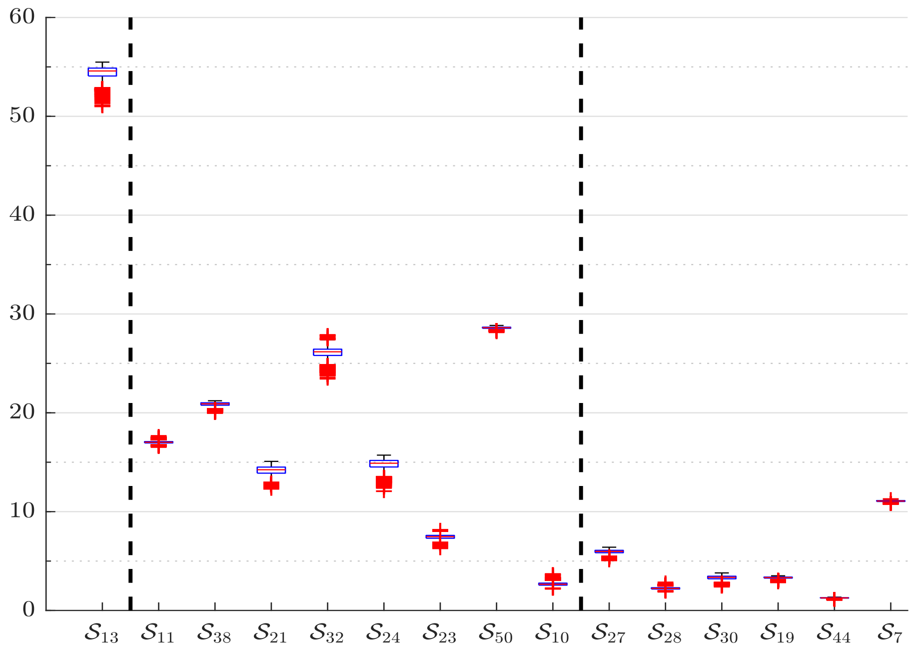

The case of correlated pass-through rates We consider that the pass-through rates are correlated[79] and we use the copula representation of the random vector $\boldsymbol{\phi} = (\boldsymbol{\phi}_1, \ldots, \boldsymbol{\phi}_n)$:

$$\begin{aligned} \mathbf{F}(p_1, \ldots, p_n) &= \Pr(\boldsymbol{\phi}_1 \leq p_1, \ldots, \boldsymbol{\phi}_n \leq p_n) \\ &= \mathbf{C}\left(\mathbf{F}_1(p_1), \ldots, \mathbf{F}_n(p_n)\right) \end{aligned}$$

where $\mathbf{C}$ is the copula function and $\mathbf{F}_j$ is the margin of $\boldsymbol{\phi}_j \sim \mathfrak{B}\left(\alpha_j, \beta_j\right)$. In particular, we assume that the copula function is Gaussian with a uniform correlation matrix $C_n(\rho)$. The simulation step of the random vector $\boldsymbol{\phi}$ consists in generating uniform random variates[80] $(u_1, \ldots, u_n) \sim \mathbf{C}$ and applying the inverse of the Beta function:

$$\boldsymbol{\phi}_j = \mathcal{B}^{-1}\left(p_j; \alpha_j, \beta_j\right)$$

In Figure 61, we report the probability density function of the economic cost in % of the GDP. Since $\mathbb{E}[\boldsymbol{\phi}]$ does not depend on the copula function, we verify that the average economic cost does not depend on the correlation parameter ρ. Nevertheless, we observe that it has a big impact on the shape of the distribution function. The case $\rho = 0$ corresponds to the minimum standard deviation while increasing the parameter ρ flattens the probability distribution. This implies that the risk increases with ρ. For instance, we report the 99% worst-case scenario with respect to ρ in Figure 62. We confirm that the minimum and maximum risk is reached when $\rho = 0$ and $\rho = 1$.

Figure 61: Distribution function of the economic cost (global analysis, $\boldsymbol{\tau}$ = \$100/tCO_2e, stochastic pass-through, Gaussian copula, Exiobase 2022)

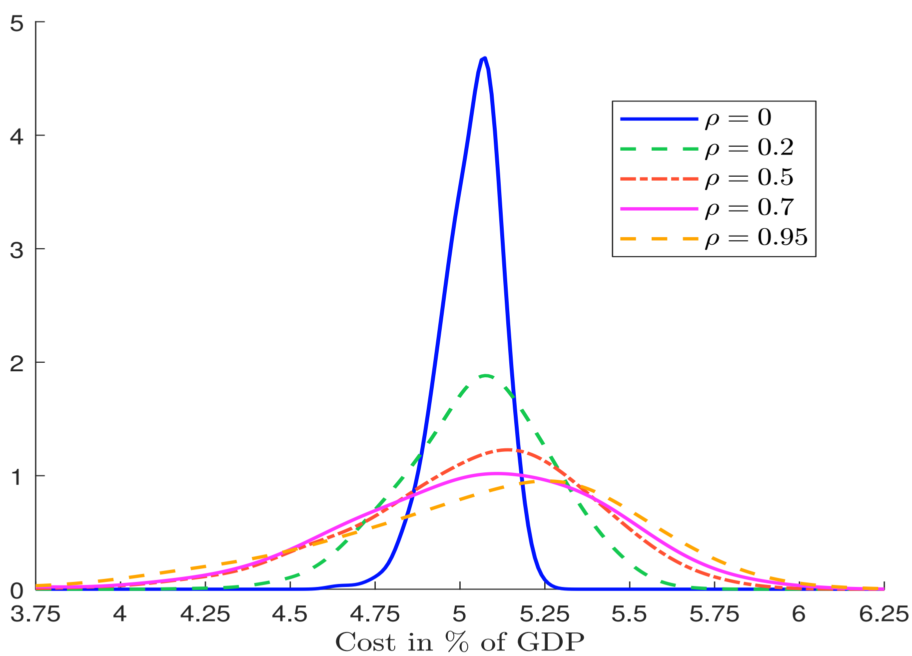

[79] In practice, the companies tend to align not only their prices but also their operating parameters such as pass-through. Therefore, it makes more sense to introduce a high degree of correlation in the context of competitive markets.

[80] Following Roncalli (2020, Chapters 11 and 13), we use the transformation method to simulate the Gaussian copula: $u = \Phi\left(\sqrt{\rho}\mathcal{N}(0,1) + \sqrt{1-\rho}\mathcal{N}(\mathbf{0}_n, I_n)\right)$.

Figure 62: 99% worst-case scenario of the economic cost (global analysis, $\boldsymbol{\tau} = \$100/\text{tCO}_2\text{e}$, stochastic pass-through, Gaussian copula, Exiobase 2022)

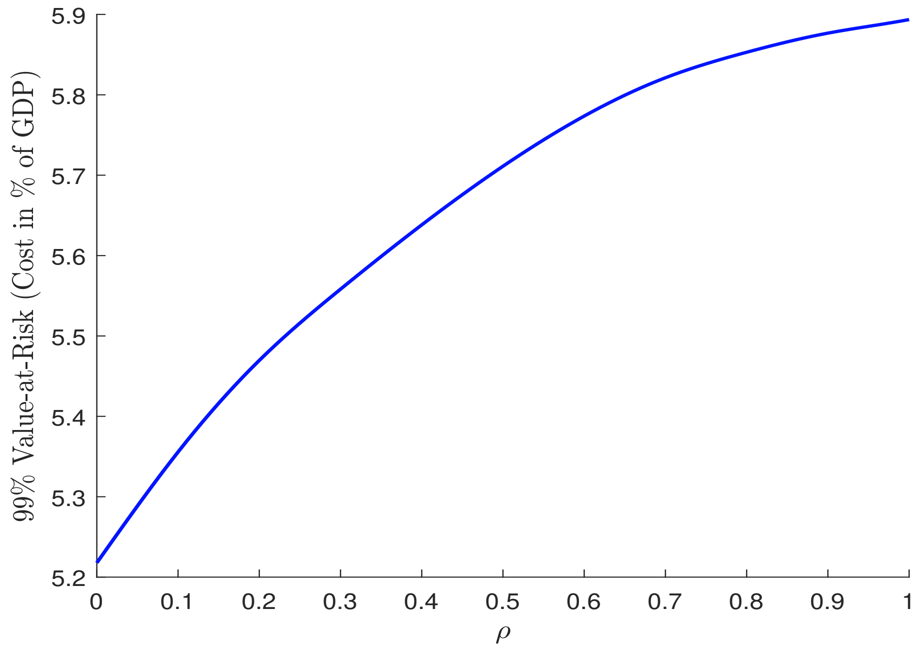

5.3.4 Upper and lower bounds of the total economic cost

We have previously seen that the lower and upper bounds of $\tilde{\boldsymbol{\mathcal{L}}}(\boldsymbol{\phi})$ are reached when $\boldsymbol{\phi} = \mathbf{0}_n$ and $\boldsymbol{\phi} = \mathbf{1}_n$. We have also deduced that the functions Δp, π, T_{total}, $\mathcal{C}ost_{\text{total}}$ and $\mathcal{TI}$ share the same bounds. Since $\mathcal{C}ost_{\text{total}} = x^\top \tilde{\boldsymbol{\mathcal{L}}}(\boldsymbol{\phi})\, t_{\text{direct}}$, it follows that[81]:

$$\begin{aligned}
(*) \quad \Leftrightarrow \quad & x^\top \tilde{\boldsymbol{\mathcal{L}}}(\mathbf{0}_n)\, t_{\text{direct}} \leq \mathcal{C}ost_{\text{total}} \leq x^\top \tilde{\boldsymbol{\mathcal{L}}}(\mathbf{1}_n)\, t_{\text{direct}} \\
\Leftrightarrow \quad & x^\top t_{\text{direct}} \leq \mathcal{C}ost_{\text{total}} \leq x^\top \left(I_n - A^\top\right)^{-1} t_{\text{direct}} \\
\Leftrightarrow \quad & x^\top (\boldsymbol{\tau} \odot \boldsymbol{\mathcal{CI}}_1) \leq \mathcal{C}ost_{\text{total}} \leq x^\top \left(I_n - A^\top\right)^{-1} (\boldsymbol{\tau} \odot \boldsymbol{\mathcal{CI}}_1) \\
\Leftrightarrow \quad & \boldsymbol{\tau}^\top \boldsymbol{\mathcal{CE}}_1 \leq \mathcal{C}ost_{\text{total}} \leq x^\top \left(I_n - A^\top\right)^{-1} (\boldsymbol{\tau} \odot \boldsymbol{\mathcal{CI}}_1)
\end{aligned}$$

It is not possible to simplify the expression of the upper bound. If we assume a uniform tax $\boldsymbol{\tau}_i = \boldsymbol{\tau}_j = \tau$, we obtain:

$$\tau\, \boldsymbol{\mathcal{CE}}_{\text{direct}}(\boldsymbol{\mathcal{G}}lobal) \leq \mathcal{C}ost_{\text{total}} \leq \tau\, \boldsymbol{\mathcal{CE}}_{\text{total}}(\boldsymbol{\mathcal{G}}lobal)$$

The lower bound is the product of the tax and the direct carbon emissions, while the upper bound is the product of the tax and the total carbon emissions. Using the relationship $\boldsymbol{\mathcal{CE}}_{\text{total}}(\boldsymbol{\mathcal{G}}lobal) = m_{(0-\infty)} \boldsymbol{\mathcal{CE}}_{\text{direct}}(\boldsymbol{\mathcal{G}}lobal)$, the previous equation becomes $\mathcal{C}ost_{\text{direct}} \leq \mathcal{C}ost_{\text{total}} \leq m_{(0-\infty)} \mathcal{C}ost_{\text{direct}}$. By assuming that the multiplying coefficient is random, we finally obtain:

$$\mathcal{C}ost_{\text{direct}} \leq \mathcal{C}ost_{\text{total}} \leq \tilde{m}_{(0-\infty)} \mathcal{C}ost_{\text{direct}}$$

where $\tilde{m}_{(0-\infty)}$ follows a shifted log-normal distribution $\mathcal{SLN}\left(\mu_m, \sigma_m^2, 1\right)$. The lower bound $\mathcal{C}ost^-_{\text{total}}$ is then constant and certain, while the upper bound $\mathcal{C}ost^+_{\text{total}}$ is stochastic. We

[81] We have $x^\top (\boldsymbol{\tau} \odot \boldsymbol{\mathcal{CI}}_1) = \sum_{j=1}^n x_j \boldsymbol{\tau}_j \boldsymbol{\mathcal{CI}}_{1,j} = \boldsymbol{\tau}^\top \boldsymbol{\mathcal{CE}}_1$.

propose to choose the α-quantile value:

$$\mathcal{C}ost_{\text{total}}^{+} = \left(1 + e^{\mu_m + \Phi^{-1}(\alpha)\sigma_m}\right) \mathcal{C}ost_{\text{direct}}$$

For instance, Figure 63 shows the upper and lower bounds of the world economic cost when we implement a uniform tax of \$100/tCO_2e and use the following country values: $\mu_m = 0.32$ and $\sigma_m = 0.75$. We have also indicated the value of the total cost we previously found in Figure 41 and Table 27.

Figure 63: Lower and upper bounds of the world economic cost (global analysis, $\boldsymbol{\tau}$ = \$100/tCO_2e, Exiobase 2022)

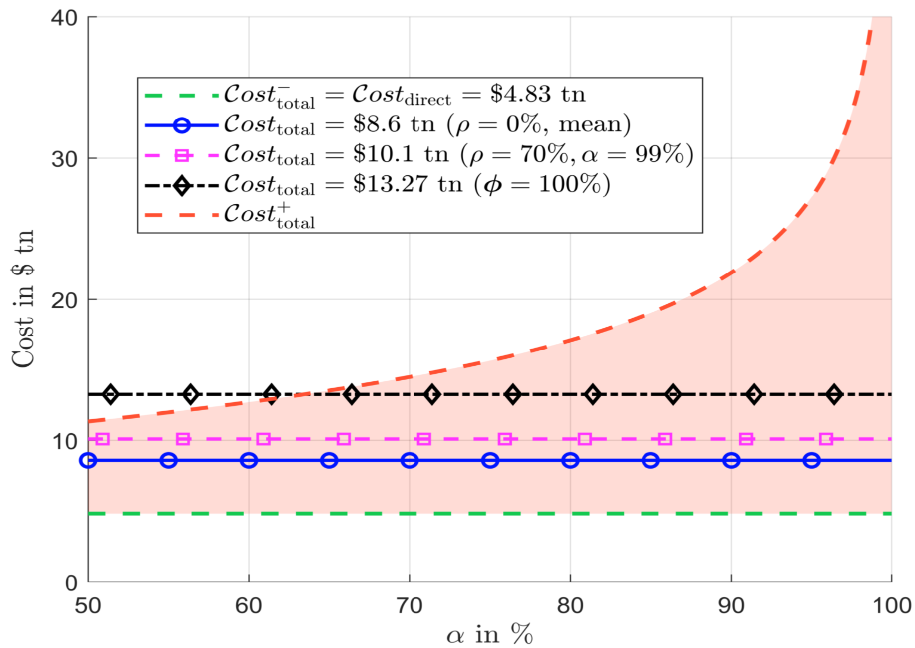

6 Climate value-at-risk

In this last section, we use the different tools developed above to define the climate value-at-risk of investment portfolios. First, we propose a model of earnings-at-risk based on the input-output framework. Then, we implement a Monte Carlo value-at-risk where pass-through rates are stochastic and the scenario for the carbon tax is given. We complement this conditional value-at-risk by an unconditional value-at-risk by considering that the carbon tax is also stochastic. Finally, we estimate the impact of carbon tax on the market portfolio. These different analyses are illustrated with the MSCI World index portfolio.

6.1 Earnings-at-risk modeling

We use the value added model to define an issuer's earnings-at-risk. To do this, we need to define the accounting identities to measure the impact of the carbon tax on earnings. We use a simple model where we do not split value added between labor, capital and other taxes. We also assume a proportionality rule between income and value added. We can then derive a formula for the impact ratio at the sector level. Using a substitution trick, we can then estimate the earnings-at-risk at the issuer level.

6.1.1 Derivation of the value added variation

Before the implementation of the tax, we have:

$$\left\{ \begin{array}{l} x^- = (I_n - A)^{-1} y^- \\ p^- = \left(I_n - A^\top\right)^{-1} \upsilon^- \end{array} \right.$$

The accounting identity formula for the income of Sector j is:

$$x_j^- p_j^- = x_j^- \sum_{i=1}^n A_{i,j} p_i^- + x_j^- \upsilon_j^-$$

We deduce that the value added amount V_j^- is equal to:

$$V_j^- := x_j^- \upsilon_j^- = x_j^- p_j^- - x_j^- \sum_{i=1}^n A_{i,j} p_i^- \tag{28}$$

After the introduction of the carbon tax, the accounting identity becomes:

$$x_j p_j = x_j \sum_{i=1}^n A_{i,j} p_i + V_j + \left(1 - \phi_j\right) T_{\mathrm{direct},j}$$

where $\left(1 - \phi_j\right) T_{\mathrm{direct},j}$ is the direct cost of the carbon tax that reduces the value added[82]. We deduce that the value added V_j is equal to:

$$V_j = x_j p_j - x_j \sum_{i=1}^n A_{i,j} p_i - \left(1 - \phi_j\right) T_{\mathrm{direct},j} \tag{29}$$

From Equations (28) and (29), we deduce that:

$$\begin{array}{rcl} \Delta V_j & = & V_j - V_j^- \\ & = & \left(x_j p_j - x_j^- p_j^-\right) + \left(x_j^- \sum_{i=1}^n A_{i,j} p_i^- - x_j \sum_{i=1}^n A_{i,j} p_i\right) - \left(1 - \phi_j\right) T_{\mathrm{direct},j} \\ & = & \left(x_j \left(p_j^- + \Delta p_j\right) - x_j^- p_j^-\right) + \left(x_j^- \sum_{i=1}^n A_{i,j} p_i^- - x_j \sum_{i=1}^n A_{i,j} \left(p_i^- + \Delta p_i\right)\right) - \\ & & \left(1 - \phi_j\right) T_{\mathrm{direct},j} \end{array}$$

Finally, we obtain the following formula for the value added variation:

$$\begin{array}{rcl} \Delta V_j & = & \underbrace{x_j \Delta p_j}_{\text{Price impact}} + \underbrace{\left(x_j - x_j^-\right) p_j^-}_{\text{Final demand impact}} - \underbrace{\left(x_j - x_j^-\right) \sum_{i=1}^n A_{i,j} p_i^-}_{\text{Intermediary demand impact}} - \underbrace{x_j \sum_{i=1}^n A_{i,j} \Delta p_i}_{\text{Production cost impact}} - \\ & & \underbrace{\left(1 - \phi_j\right) T_{\mathrm{direct},j}}_{\text{Direct impact}} \end{array} \tag{30}$$

[82] We recall that $\phi_j T_{\mathrm{direct},j}$ is passed on the value chain and impacts the price of goods.

The variation of the value added has five components. The first component $x_j \Delta p_j$ is the price impact, which is generally a positive factor. The second and third components $\left(x_j - x_j^-\right) p_j^-$ and $\left(x_j - x_j^-\right) \sum_{i=1}^n A_{i,j} p_i^-$ measure the impact of the final and intermediary demands. These two terms are generally negative because $x_j \leq x_j^-$. The fourth component is the increase in the production cost $x_j \sum_{i=1}^n A_{i,j} \Delta p_i$, whereas the last term is the direct impact on the producers. Using the previous formula, we can define the value added shock as follows:

$$\mathbb{S}_j = \frac{\Delta V_j}{V_j^-}$$

where $\mathbb{S}_j$ is the relative variation of the value added.

Remark 16. *The matrix form of the value added variation is:*

$$\Delta V = x \odot \Delta p + \left(x - x^-\right) \odot p^- - \left(x - x^-\right) \odot A^\top p^- - x \odot A^\top \Delta p - \left(I_n - \Phi\right) T_{\text{direct}} \quad (31)$$

The inelastic case Let us assume that the final demand remains constant: $y_j = y_j^-$. This implies that $x_j = x_j^-$. The second and third components vanish and Equation (30) becomes:

$$\begin{aligned} \Delta V_j &= x_j \Delta p_j - x_j \sum_{i=1}^n A_{i,j} \Delta p_i - \left(1 - \boldsymbol{\phi}_j\right) T_{\text{direct},j} \\ &= x_j \left(\Delta p_j - \sum_{i=1}^n A_{i,j} \Delta p_i\right) - \left(1 - \boldsymbol{\phi}_j\right) T_{\text{direct},j} \end{aligned}$$

Let $\Delta v_j = \dfrac{\Delta V_j}{x_j}$ be the value added variation per output. We deduce that:

$$\Delta v = \left(I_n - A^\top\right) \Delta p - \left(I_n - \Phi\right) t_{\text{direct}}$$

Since we have $\Delta p = \left(I_n - A^\top \Phi\right)^{-1} \Phi \, t_{\text{direct}}$, we finally obtain:

$$\Delta v = \left(\Phi + \left(I_n - A^\top\right) \tilde{\boldsymbol{\mathcal{L}}}\left(\boldsymbol{\phi}\right) - I_n\right) t_{\text{direct}} \quad (32)$$

We consider two special cases:

- If $\boldsymbol{\phi} = \mathbf{0}_n$, we have $\Delta v = -t_{\text{direct}}$ and $\Delta V = -T_{\text{direct}}$;
- If $\boldsymbol{\phi} = \mathbf{1}_n$, we have $\Delta v = t_{\text{direct}}$ and $\Delta V = T_{\text{direct}}$.

We retrieve two extreme situations when we study the theory of optimal taxation (Farhi and Gabaix, 2020). In the first case, the tax is perfectly efficient because the entire burden of the tax falls on producers, we observe a transfer from producers to governments and the tax reduces producer surplus (Bergstrom, 1982). In the second case, the entire burden of the tax falls on consumers and there is a transfer from consumers to the government. Moreover, we observe a negative effect of the carbon tax since the producer surplus has increased because selling prices have increased and the demand has not decreased. Therefore, we face a curious situation where producers capture a surplus, which is exactly equal to the carbon tax revenues. This case obviously contradicts the double dividend assumption (Goulder, 2002).

We consider Example #3 described on page 78 and the differentiated carbon taxation: $\boldsymbol{\tau}_1 = \$200/\text{tCO}_2\text{e}$ and $\boldsymbol{\tau}_2 = \boldsymbol{\tau}_3 = \boldsymbol{\tau}_4 = \$100/\text{tCO}_2\text{e}$. By assuming that $\boldsymbol{\phi}_j = 0.5$, we obtain $\Delta p = \left(1.08\%, 0.42\%, 0.33\%, 0.16\%\right)$ and $\Delta V = (-425, -666.5, -1\,664.7, -1\,364.7)$. The value added shocks are then respectively equal to -0.12%, -0.37%, -1.04% and -0.27%. In Figure 64, we report the relative variation of the value added in % when we consider a uniform pass-through. We notice that some shocks are almost linear (*e.g.*, energy) and others are convex (*e.g.*, industrials).

Figure 64: Relative variation of value added (uniform pass-through, inelastic case, differentiated taxation, Example #3)

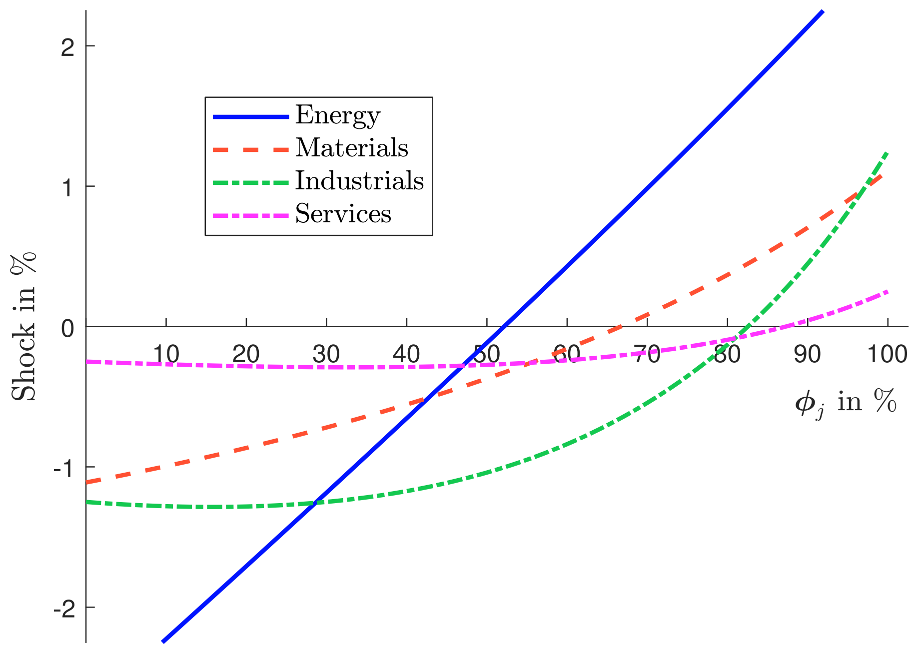

The elastic case We now assume that the final demand depends on the price: $y_j = f_j(p_j)$. We denote by $y = f(p) = \left(f_1(p_1), \ldots, f_n(p_n)\right)$ the vector-valued function of the price-demand relation. We have:

$$x = (I_n - A)^{-1} f(p) = \boldsymbol{\mathcal{L}} f(p)$$

We deduce that:

$$\begin{aligned}\Delta V &= \boldsymbol{\mathcal{L}} f(p) \odot \Delta p + \left(\boldsymbol{\mathcal{L}} f(p) - x^-\right) \odot p^- - \left(\boldsymbol{\mathcal{L}} f(p) - x^-\right) \odot A^\top p^- - \\ &\quad \boldsymbol{\mathcal{L}} f(p) \odot A^\top \Delta p - (I_n - \Phi) T_{\text{direct}} \end{aligned} \qquad (33)$$

where $\Delta p = \tilde{\boldsymbol{\mathcal{L}}}(\boldsymbol{\phi}) t_{\text{direct}}$ and $p = p^- + \Delta p$. Equation (33) is the general formula to compute the value added variation. It encompasses different special cases. If the demand function is inelastic, $f(p) = y^-$ and $x = (I_n - A)^{-1} y^- = x^-$ and we retrieve the inelastic case. If the demand function is linear ($y_j = a_j - b_j p_j$), we deduce that[83] $\Delta y_j = y_j - y_j^- = -b_j \Delta p_j$ and:

$$x - x^- = -(I_n - A)^{-1}(b \odot \Delta p)$$

[83] Because we have $y_j^- = a_j - b_j p_j^-$.

Since $b \succeq \mathbf{0}_n$ and $\Delta p \succeq \mathbf{0}_n$, we deduce that $x \preceq x^-$. All the outputs are reduced. We can then decompose ΔV as the sum of positive impacts $\Delta V_{(+)}$ and negative impacts $\Delta V_{(-)}$:

$$\begin{cases} \Delta V = \Delta V_{(+)} - \Delta V_{(-)} \\ \Delta V_{(+)} = x^- \odot \Delta p + (I_n - A)^{-1} (b \odot \Delta p) \odot A^\top p \\ \Delta V_{(-)} = x^- \odot A^\top \Delta p + (I_n - A)^{-1} (b \odot \Delta p) \odot p + (I_n - \Phi) T_{\text{direct}} \end{cases} \tag{34}$$

To use the previous model, we need to calibrate the slope b_j of the demand function. We reiterate that the price elasticity of demand is defined as:

$$\boldsymbol{\varepsilon}_j = \frac{\Delta y_j / y_j^-}{\Delta p_j / p_j^-}$$

It follows that:

$$\frac{\Delta y_j}{\Delta p_j} = \boldsymbol{\varepsilon}_j \frac{y_j^-}{p_j^-}$$

Since we have $\Delta y_j = -b_j \Delta p_j$, we deduce that:

$$b_j = -\frac{\Delta y_j}{\Delta p_j} = -\boldsymbol{\varepsilon}_j \frac{y_j^-}{p_j^-} = -\boldsymbol{\varepsilon}_j y_j^-$$

because $p_j^- = 1$.

We consider again Example #3. By assuming that $\boldsymbol{\varepsilon} = (-0.20, -0.40, -0.50, -1.00)$ and $\boldsymbol{\phi}_j = 0.5$, we obtain $\Delta p = \left(1.08\%, 0.42\%, 0.33\%, 0.16\%\right)$, $\Delta x = (-8.69, -6.64, -13.23, -20.02)$ and $\Delta V = (-1\,067.2, -965.7, -1\,928.1, -2\,164.2)$. The value added shocks are then respectively equal to -0.29%, -0.54%, -1.21% and -0.43%. In Figure 65, we report the relative variation of value added in % when we consider a uniform pass-through rate and a price elasticity of demand equal to -1. Compared to Figure 64, the shocks are more negative because the outputs are reduced. Moreover, we observe a negative relationship between the pass-through rate and the shock for the sector of services. In Figure 66, we draw the relationship between the price elasticity of demand and the value added shock when the pass-through rate is set to 100%. If the elasticity is sufficiently high, the value added decreases even if the pass-though rate is high.

6.1.2 Earnings-at-risk definition

At the sector level We assume that the earnings' shock is proportional to the value added variation:

$$\frac{\text{Ebitda}_j - \text{Ebitda}_j^-}{\text{Ebitda}_j^-} = \frac{\Delta V_j}{V_j^-} = \mathbb{S}_j$$

If $\Delta V_j \leq 0$, the shock is negative and the earnings are decreasing. This is the expected effect of a linear commodity tax.

In Figures 67 and 68, we compute the earnings' shocks for the 2 464 sectors[84] by using the Exiobase 2022 table and draw the corresponding histogram[85]. The range of the shocks is between -15% and $+15\%$. In the inelastic case, we verify that a pass-through of 0% induces a systematic negative earnings-at-risk whereas a pass-through of 100% leads to a positive earnings-at-risk. In the elastic case, the distribution of $\mathbb{S}_j$ highly depends on the values taken by the price elasticity of demand.

Figure 65: Relative variation of value added (uniform pass-through, elastic case, $\varepsilon_j = -1$, differentiated taxation, Example #3)

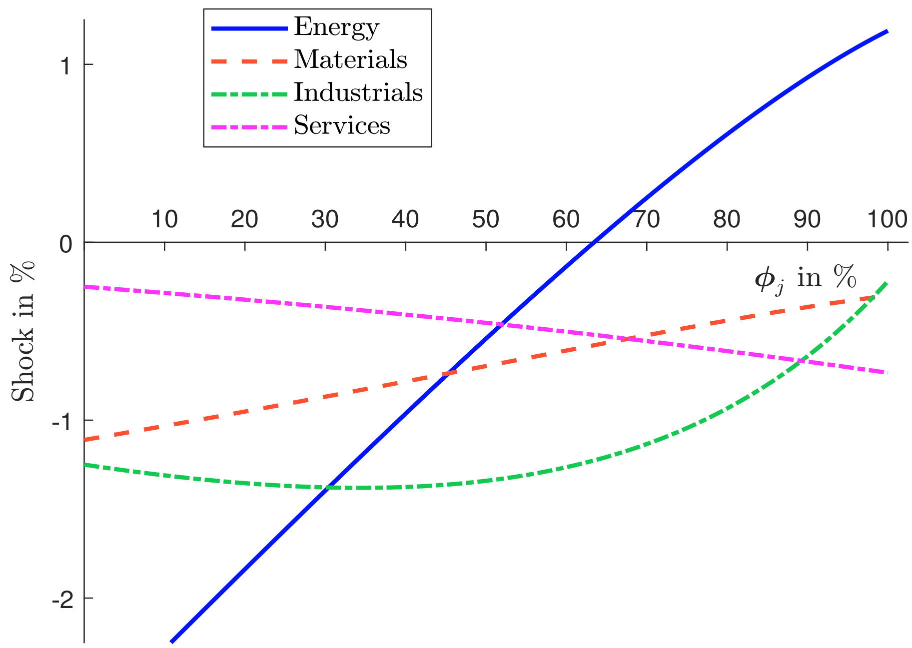

Figure 66: Relationship between the price elasticity of demand and the value added shock ($\phi_j = 100\%$, differentiated taxation, Example #3)

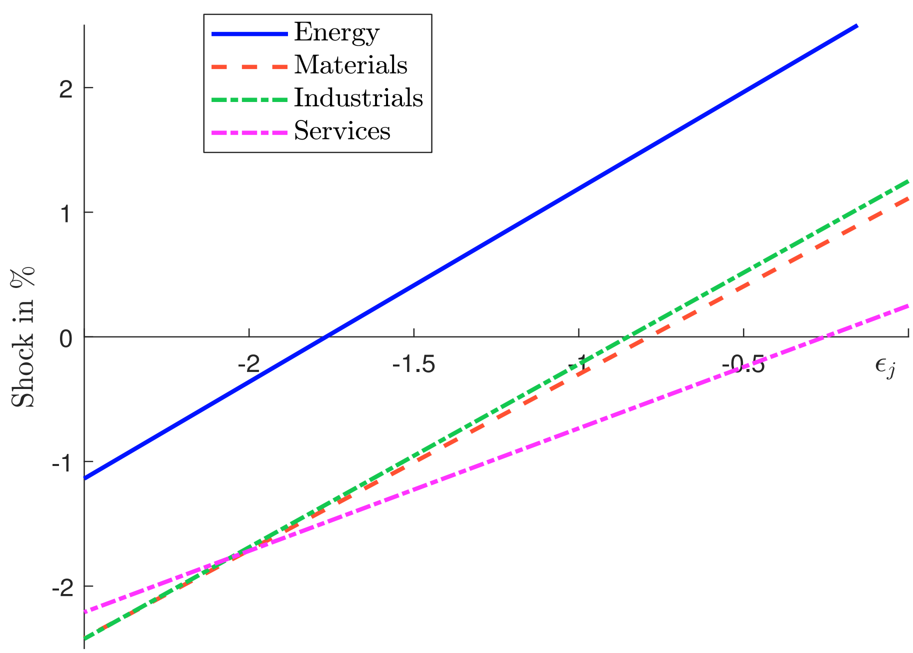

Figure 67: Histogram of earnings' shocks in % (global analysis, $\boldsymbol{\tau} = \$100/\text{tCO}_2\text{e}$, inelastic case, Exiobase 2022)

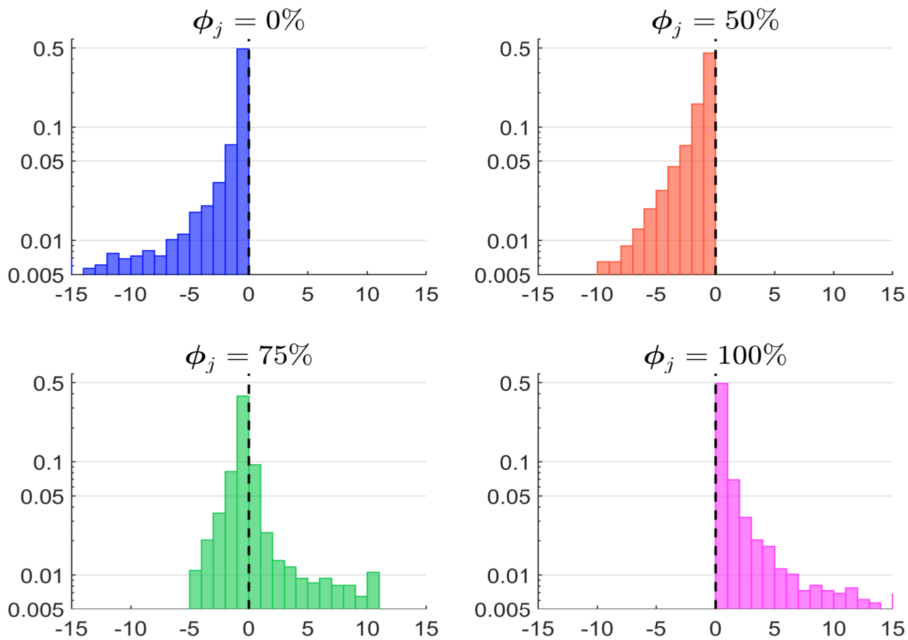

Figure 68: Histogram of earnings' shocks in % (global analysis, $\boldsymbol{\tau} = \$100/\text{tCO}_2\text{e}$, elastic case, Exiobase 2022)

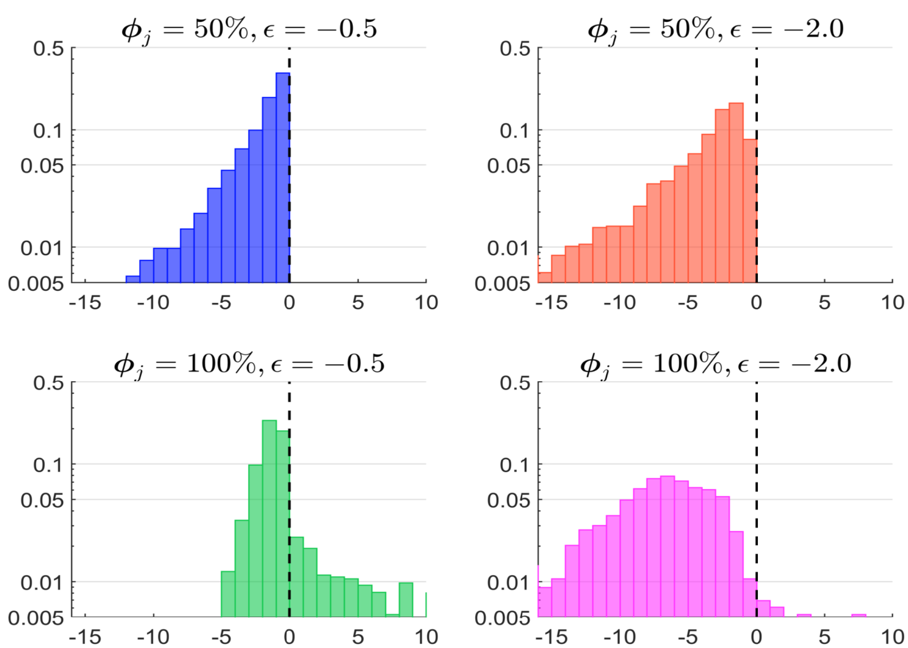

Figure 69: Relationship between ϕ_j, ε_j and b_j

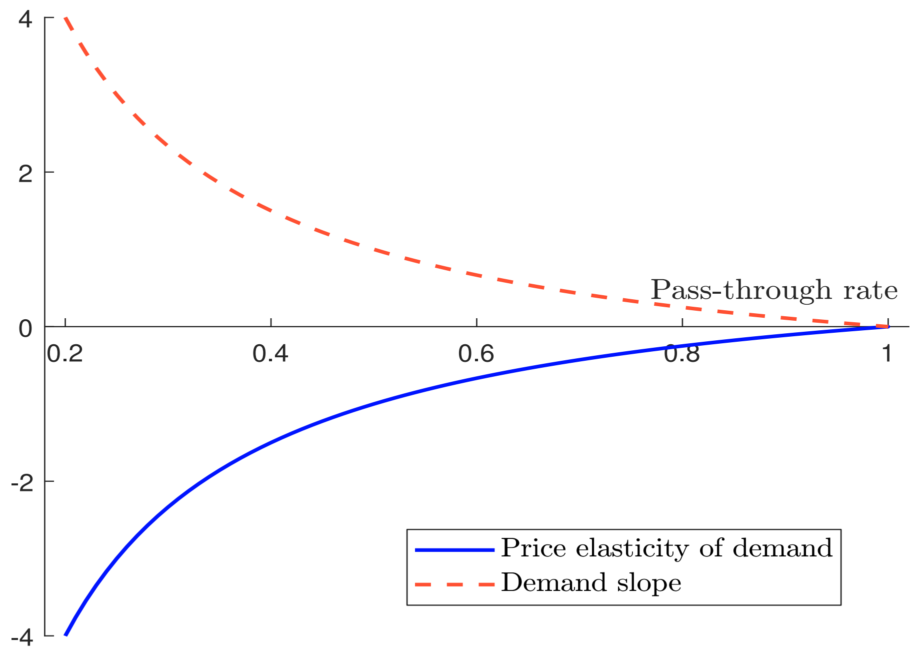

We have previously seen that:

$$\phi \approx \frac{1}{1 - \frac{\varepsilon}{\varepsilon'}}$$

where ε and ε' are the price elasticities of demand and supply. By assuming that $\varepsilon' = 1$, we deduce that:

$$\varepsilon_j = 1 - \frac{1}{\phi_j} \tag{35}$$

We use this formula to calibrate the slope of the demand function. Therefore, we have:

$$b_j = -\left(1 - \frac{1}{\phi_j}\right) y_j^- = \frac{1 - \phi_j}{\phi_j} y_j^- \tag{36}$$

In Figure 69, we draw the relationship between pass-through rate, price-demand elasticity and slope. In order to be more realistic, we use the mapping between the sectors and the four types given in Table 60 on page 186 and assume that ϕ is stochastic. Since we have $\widetilde{\phi}_j \sim \mathcal{B}\left(\alpha_j, \beta_j\right)$, we deduce that $\tilde{\varepsilon}_j$ is stochastic and follows the negative beta prime distribution: $-\tilde{\varepsilon}_j \sim \mathcal{B}'\left(\beta_j, \alpha_j\right)$. In Appendix A.10 on page 151, we show that:

$$\mathbb{E}\left[\tilde{\varepsilon}_j\right] = -\frac{\beta_j}{\alpha_j}$$

Therefore, we can link the demand slope to the pass-through rate by assuming that $\tilde{\varepsilon}_j$ is stochastic or by replacing $\tilde{\varepsilon}_j$ by its mathematical expectation (see Table 33 below). In Figure 70, we estimate the probability density function of the earnings' shock when we consider that the pass-through rates are stochastic and independent, and the elasticity is

[84] We recall that we have 44 countries and 56 sectors.

[85] In order to better read them, the y-axis is in logarithmic scale.

given by Equation (35). For that, we use 3 000 Monte Carlo simulations and we pool the shocks of the 2 464 sectors. We notice that the distribution has a negative skewness and 80% of the sectors face a negative shock. We also report the probability density function when we replace the elasticities by their mathematical expectation. We deduce that the two approaches give similar results. This statement holds even if we consider dependent pass-through rates generated with a Gaussian copula[86].

Table 33: Probabilistic characterization of the four pass-through types

	Highly-elastic	High-elastic	Medium-elastic	Low-elastic
α_j	3.00	4.00	14.00	12.00
β_j	12.00	6.00	6.00	0.60
$\mathbb{E}\left[\widetilde{\phi}_j\right]$	0.20	0.40	0.70	0.95
$\mathbb{E}\left[\tilde{\varepsilon}_j\right]$	−4.20	−1.50	−0.43	−0.05

Figure 70: Probability density function of earnings' shocks (global analysis, $\boldsymbol{\tau} = \$100/tCO_2e$, stochastic pass-through and elasticity, Exiobase 2022)

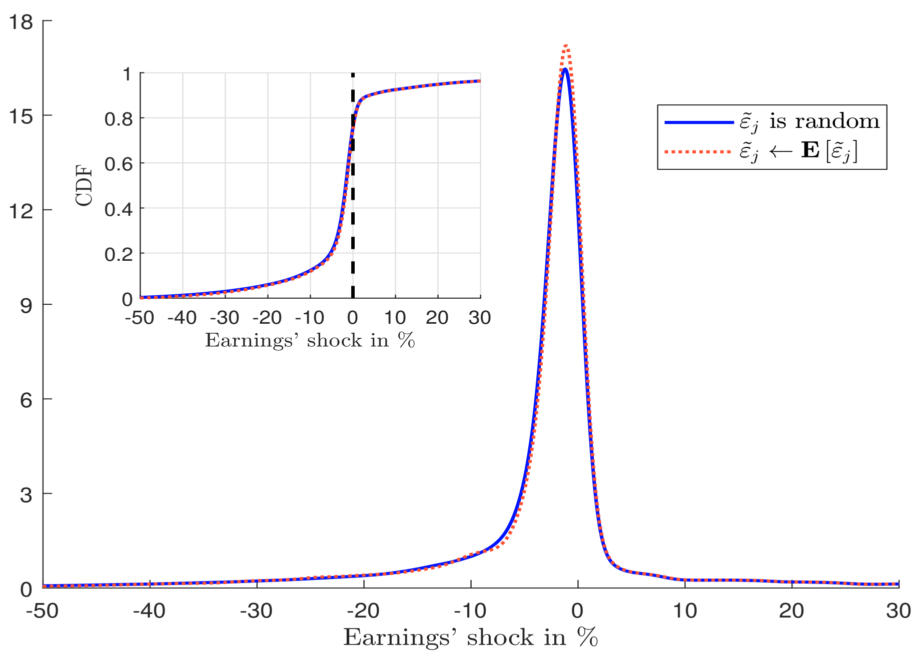

At the issuer level We can decompose the sector earnings-at-risk as follows:

$$\mathbb{S}_j = \mathbb{S}_j^{(\mathrm{gvc})} + \mathbb{S}_j^{(\mathrm{direct})}$$

where $\mathbb{S}_j^{(\mathrm{gvc})}$ is the earnings' shock due to the global value chain (GVC) and $\mathbb{S}_j^{(\mathrm{direct})}$ is the specific and direct impact of the carbon tax. We have:

$$\mathbb{S}_j^{(\mathrm{gvc})} = \frac{x_j \Delta p_j + \left(x_j - x_j^-\right) p_j^- - \left(x_j - x_j^-\right) \sum_{i=1}^n A_{i,j} p_i^- - x_j \sum_{i=1}^n A_{i,j} \Delta p_i}{V_j^-}$$

[86] See Figure 123 on page 174.

and:

$$\mathbb{S}_j^{(\text{direct})} = -\frac{\left(1-\phi_j\right) T_{\text{direct},j}}{V_j^-}$$

We define the earnings' shock for issuer i in a similar manner:

$$\mathbb{S}_i = \mathbb{S}_i^{(\text{gvc})} + \mathbb{S}_i^{(\text{direct})}$$

We assume that $\mathbb{S}_i^{(\text{gvc})} \approx \mathbb{S}_j^{(\text{gvc})}$ with $i \in j$. Therefore, we use the shock of the sector due to the global value chain as a proxy of the shock of the issuer. For the direct and specific shock, we use the substitution trick by replacing the sector figures by the issuer figures:

$$\begin{aligned}
\mathbb{S}_i^{(\text{direct})} &= -\frac{(1-\boldsymbol{\phi}_i)\, T_{\text{direct},i}}{V_i^-} \\
&= -\frac{(1-\boldsymbol{\phi}_i)\, \boldsymbol{\tau}_i\, \boldsymbol{\mathcal{CE}}_{1,i}}{V_i^-} \\
&= -\frac{1}{\upsilon_i^-}\,(1-\boldsymbol{\phi}_i)\, \boldsymbol{\tau}_i\, \boldsymbol{\mathcal{CI}}_{1,i}
\end{aligned}$$

where υ_i^- is the value added ratio[87] of issuer i.

Remark 17. *In the case where υ_i^- is not available, we can use the value added ratio υ_j^- of the corresponding sector. Using the Exiobase 2022 database, the* 10% *and* 90% *quantiles of υ_j^- are equal to* 22.4% *and* 78.0%*. At the global level, the value added ratio is equal to* 49.6%*.*

In Table 34, we report the statistics of υ_i^- per GICS sector[88]. Utilities and Industrials have the lowest value added ratio (25.1% and 27.6%), while Financials and Health Care have the highest value added ratio (66.3% and 56.5%). We find similar results as Exiobase 2022 when looking at the $Q_{10\%}$ and $Q_{90\%}$ figures. Nevertheless, there is a difference in the average value added ratio (39.7% vs. 49.6%).

Table 34: Mean and quantiles of the value added ratio in % (MSCI World, May 2023)

Sector	Mean	$Q_{10\%}$	$Q_{25\%}$	$Q_{75\%}$	$Q_{90\%}$
Communication Services	38.9	16.6	24.1	47.5	70.5
Consumer Discretionary	33.8	13.9	19.6	43.4	60.4
Consumer Staples	36.4	13.9	23.8	49.1	61.6
Energy	33.4	9.4	16.3	47.0	61.0
Financials	66.3	30.1	52.3	85.4	94.0
Health Care	56.5	27.3	44.7	69.7	78.5
Industrials	27.6	11.2	17.1	36.3	46.8
Information Technology	52.5	27.0	37.3	69.5	78.4
Materials	29.0	13.8	19.9	36.8	48.0
Real Estate	48.0	22.6	33.1	67.2	75.5
Utilities	25.1	6.0	16.3	33.1	47.6
MSCI World index	39.7	14.0	22.4	55.5	72.3

Source: Factset (2023) & Authors' calculations.

[87] We reiterate that it is defined as the ratio of net value added V_i^- to the total value of production x_i^-.

[88] The value added ratio is computed using the gross margin rate provided by Factset (2023).

In Tables 35, 36 and 37, we compute the earnings' shocks for the MSCI World index portfolio. Using the Exiobase 2022 database, we calculate the GVC shocks $\mathbb{S}_j^{(\mathrm{gvc})}$ when the pass-through rate is uniform and equal to $\boldsymbol{\phi}$. The price-demand elasticity is given by $\boldsymbol{\varepsilon}_j = 1 - \boldsymbol{\phi}_j^{-1}$. We use the same assumptions to calculate the direct shocks $\mathbb{S}_i^{(\mathrm{direct})}$ for each issuer of the portfolio. Let $j = \mathcal{M}ap\left(i\right)$ be the mapping function that returns the WIOD country $\times$ sector of the issuer i. Then, we sum the two shocks in order to obtain the total shock $\mathbb{S}_i = \mathbb{S}_{\mathcal{M}ap(i)}^{(\mathrm{gvc})} + \mathbb{S}_i^{(\mathrm{direct})}$ of the issuer. For each GICS sector, we report the quantiles 1%, 5% and 10%, and its average shock[89]:

$$\begin{aligned}
\mathbb{S}_j\left(w\right) &= \frac{\sum_{i\in j} w_i \left(\mathbb{S}_{\mathcal{M}ap(i)}^{(\mathrm{gvc})} + \mathbb{S}_i^{(\mathrm{direct})}\right)}{\sum_{i\in j} w_i} \\
&= \frac{\sum_{i\in j} w_i \, \mathbb{S}_{\mathcal{M}ap(i)}^{(\mathrm{gvc})}}{\sum_{i\in j} w_i} + \frac{\sum_{i\in j} w_i \, \mathbb{S}_i^{(\mathrm{direct})}}{\sum_{i\in j} w_i} \\
&= \mathbb{S}_j^{(\mathrm{gvc})}\left(w\right) + \mathbb{S}_j^{(\mathrm{direct})}\left(w\right)
\end{aligned}$$

In the case of a global uniform taxation with a carbon tax of \$100/tCO_2e, we notice the high impact of the pass-through rate on the earnings' shocks at the issuer level and the aggregated GICS sector level. With a 25% pass-through rate, the earnings' shock of the MSCI World index is negative and is equal to −4.41%. The global value chain is responsible for −1.18% of this shock, while the direct earnings' shock is responsible for −3.23%. Each sector faces a negative shock, in particular Utilities, Energy and Materials (−57.82%, −20.35% and −12.79%). Nevertheless, the impact is very low for two sectors: Communication Services (−0.41%) and Information Technology (−0.58%). The situation changes as the pass-through rate increases. Indeed, with a 75% pass-through parameter, the earnings' shock of the MSCI World index is close to 0, and high emitting sectors like Utilities, Materials or Industrials face a positive shock (+9.02%, +6.20% and +0.71%). When the pass-through rate gets closer to 1, this phenomenon of positive earnings' shock is spreading to more and more sectors. With a 95% pass-through rate, the earnings' shock of the MSCI World index is positive (+4.69%) because of the major contribution of the global value chain (+4.91%). Moreover, Energy, Utilities and Materials faces very high positive earnings' shock (+52.95%, +38.44% and +15.92%). This means that they earn money after taxation, since they pass their direct costs through the value chain, and they do not face global value chain costs from other sectors as they are on top of the value chain. Figure 71 displays the relationship between the pass-through rate and the earnings' shock for the MSCI World index. We observe a quasi linear relation between direct earnings' shock and pass-through rate, and a convex relation between total earnings' shock and pass-through rate. At GICS sector level, the relation highly differs from one sector to another (Figure 72). Indeed, both Consumer Staples and Energy sectors face a positive earnings's shock with a pass-through rate around 80%, but the high convexity of the relation for the Energy sector leads its earnings' shock to increase very rapidly and to reach high levels. The relation is more linear for Materials and Utilities.

[89] We must not confuse the index j of the WIOD sector with the index j of the GICS sector. We reiterate that we have 2 464 country $\times$ sector rows in the WIOD database. $\mathbb{S}_j^{(\mathrm{gvc})} = \mathbb{S}_{\mathcal{M}ap(i)}^{(\mathrm{gvc})}$ refers then to the GVC component of the earnings' shock corresponding to the WIOD sector j of the issuer i, whereas $\mathbb{S}_j\left(w\right)$, $\mathbb{S}_j^{(\mathrm{gvc})}\left(w\right)$ and $\mathbb{S}_j^{(\mathrm{direct})}\left(w\right)$ refer to the earnings' shocks corresponding to the GICS sector j. In the first case, we have 2 464 values of $\mathbb{S}_j^{(\mathrm{gvc})}$ and 1 485 values of $\mathbb{S}_{\mathcal{M}ap(i)}^{(\mathrm{gvc})}$ because there were 1 485 issuers in the MSCI World index at the end of May 2023. In the second case, we have 11 values of $\mathbb{S}_j\left(w\right)$, $\mathbb{S}_j^{(\mathrm{gvc})}\left(w\right)$ and $\mathbb{S}_j^{(\mathrm{direct})}\left(w\right)$, because we have 11 GICS level 1 sectors.

Table 35: Earnings' shock in % (global uniform taxation, $\boldsymbol{\tau} = \$100/tCO_2e$, $\boldsymbol{\phi} = 25\%$, Exiobase 2022, MSCI World index, May 2023)

Sector	$\mathbb{S}_j$	$\mathbb{S}_j^{(gvc)}$	$\mathbb{S}_j^{(direct)}$	$Q_{1\%}(\mathbb{S}_i)$	$Q_{5\%}(\mathbb{S}_i)$	$Q_{10\%}(\mathbb{S}_i)$
Communication Services	−0.41	−0.37	−0.04	−2.20	−1.68	−0.93
Consumer Discretionary	−2.23	−1.01	−1.22	−121.56	−4.76	−2.59
Consumer Staples	−3.37	−2.62	−0.74	−18.17	−10.52	−6.63
Energy	−20.35	−9.37	−10.98	−59.49	−44.40	−31.90
Financials	−1.24	−0.64	−0.60	−3.09	−1.64	−1.49
Health Care	−0.76	−0.63	−0.13	−3.11	−1.77	−1.49
Industrials	−3.49	−0.59	−2.89	−52.49	−26.57	−8.75
Information Technology	−0.58	−0.48	−0.10	−8.92	−1.95	−1.52
Materials	−12.79	1.01	−13.80	−97.73	−70.38	−43.20
Real Estate	−0.96	−0.51	−0.45	−5.68	−1.88	−1.63
Utilities	−57.82	−3.76	−54.06	−319.59	−156.31	−129.59
MSCI World index	−4.41	−1.18	−3.23	−111.52	−31.84	−14.46

Table 36: Earnings' shock in % (global uniform taxation, $\boldsymbol{\tau} = \$100/tCO_2e$, $\boldsymbol{\phi} = 75\%$, Exiobase 2022, MSCI World index, May 2023)

Sector	$\mathbb{S}_j$	$\mathbb{S}_j^{(gvc)}$	$\mathbb{S}_j^{(direct)}$	$Q_{1\%}(\mathbb{S}_i)$	$Q_{5\%}(\mathbb{S}_i)$	$Q_{10\%}(\mathbb{S}_i)$
Communication Services	−0.29	−0.28	−0.01	−2.48	−1.27	−0.74
Consumer Discretionary	−1.23	−0.82	−0.41	−40.68	−2.10	−1.89
Consumer Staples	−1.73	−1.49	−0.25	−7.80	−5.92	−4.00
Energy	−1.93	1.74	−3.66	−40.19	−22.31	−11.58
Financials	−0.59	−0.39	−0.20	−1.22	−0.76	−0.58
Health Care	−0.71	−0.66	−0.04	−2.12	−1.68	−1.62
Industrials	0.71	1.67	−0.96	−9.36	−3.61	−2.33
Information Technology	−0.40	−0.36	−0.03	−3.26	−1.94	−1.83
Materials	6.20	10.80	−4.60	−25.14	−15.82	−12.37
Real Estate	−0.55	−0.40	−0.15	−2.07	−0.95	−0.91
Utilities	9.02	27.04	−18.02	−64.81	−19.71	−13.02
MSCI World index	−0.06	1.01	−1.08	−16.59	−5.34	−2.74

Table 37: Earnings' shock in % (global uniform taxation, $\boldsymbol{\tau} = \$100/tCO_2e$, $\boldsymbol{\phi} = 95\%$, Exiobase 2022, MSCI World index, May 2023)

Sector	$\mathbb{S}_j$	$\mathbb{S}_j^{(gvc)}$	$\mathbb{S}_j^{(direct)}$	$Q_{1\%}(\mathbb{S}_i)$	$Q_{5\%}(\mathbb{S}_i)$	$Q_{10\%}(\mathbb{S}_i)$
Communication Services	−0.00	−0.00	−0.00	−0.34	−0.22	−0.17
Consumer Discretionary	0.13	0.21	−0.08	−8.06	−0.52	−0.43
Consumer Staples	1.75	1.80	−0.05	−0.96	−0.45	−0.26
Energy	52.95	53.68	−0.73	−1.26	−0.39	3.73
Financials	−0.00	0.04	−0.04	−0.37	−0.13	−0.10
Health Care	−0.08	−0.07	−0.01	−0.46	−0.24	−0.19
Industrials	3.44	3.64	−0.19	−1.28	−0.51	−0.45
Information Technology	0.07	0.08	−0.01	−0.49	−0.43	−0.42
Materials	15.92	16.84	−0.92	−2.51	−0.22	0.25
Real Estate	−0.01	0.02	−0.03	−0.38	−0.13	−0.12
Utilities	38.44	42.04	−3.60	−0.44	−0.13	11.31
MSCI World index	4.69	4.91	−0.22	−0.89	−0.43	−0.27

Figure 71: Relationship between the pass-through rate and the earnings' shock of the MSCI World index (global uniform taxation, $\tau = \$100/tCO_2e$, Exiobase 2022, MSCI World index, May 2023)

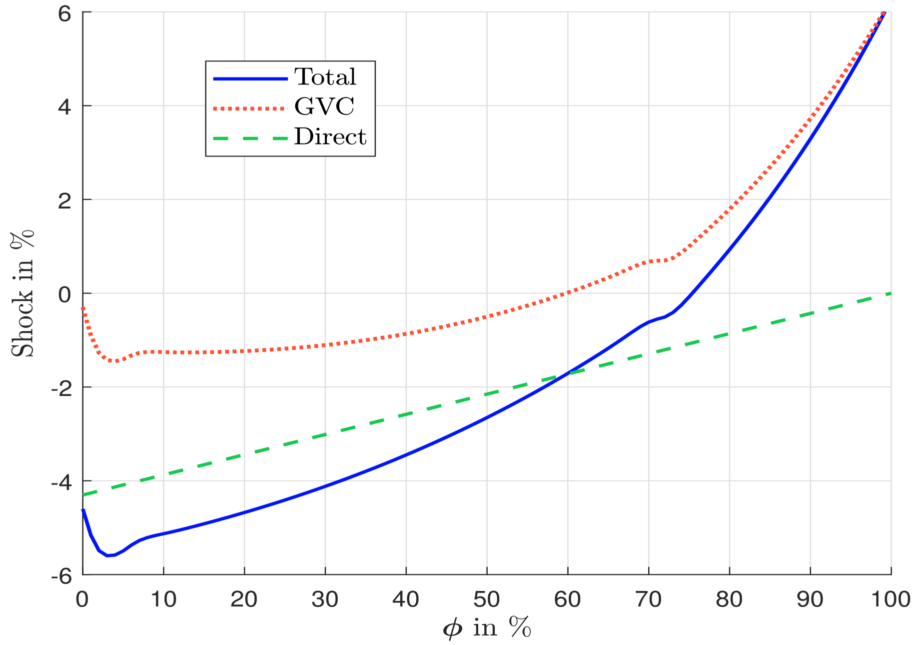

Figure 72: Relationship between the pass-through rate and the earnings' shock of GICS sectors (global uniform taxation, $\tau = \$100/tCO_2e$, Exiobase 2022, MSCI World index, May 2023)

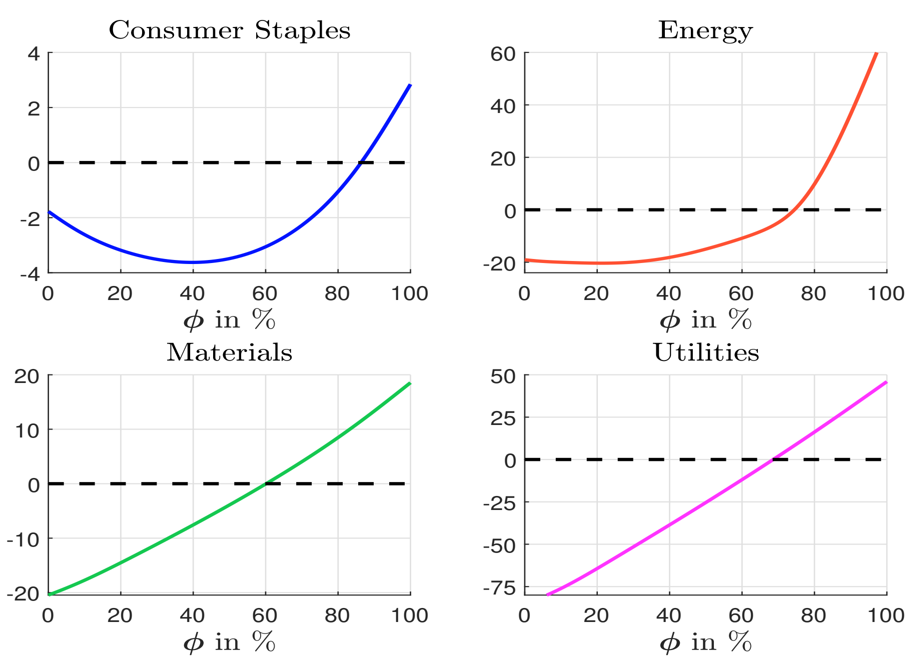

In order to obtain more realistic values of earnings' shocks, we consider the classification of sectors into the four pass-through types: highly-elastic, high-elastic, medium-elastic and low-elastic. We use the average pass-through rate[90] of the beta distribution $\mathcal{B}\left(\alpha_j, \beta_j\right)$:

$$\mathbb{E}\left[\widetilde{\phi}_j\right] = \mathbb{E}\left[\mathcal{B}\left(\alpha_j, \beta_j\right)\right] = \frac{\alpha_j}{\alpha_j + \beta_j}$$

For the price-demand elasticity, we reiterate that $\mathbb{E}\left[\tilde{\varepsilon}_j\right] = -\alpha_j^{-1}\beta_j$. Results are reported in Table 38. In this case, we find that there are two winning sectors: Energy and Utilities. Indeed, they face highly positive earnings' shock (51.41% and 37.98%) with a high contribution of the global value chain. With a figure of −3.97%, Consumer Staples is clearly the most loser sector. Taking into account the different contributions, the impact on the MSCI World index is then positive. Figures 73 and 74 show the boxplot of earnings' shocks for each GICS sector. We observe a high heterogeneity both between and within sectors. Nevertheless, it seems that most of winner issuers are located in high emitting sectors. This result calls into question the effectiveness of a carbon tax, as the tax burden is not necessarily borne by those for whom it was intended.

Table 38: Earnings' shock in % (global uniform taxation, $\boldsymbol{\tau} = \$100/\text{tCO}_2\text{e}$, average pass-through rate, Exiobase 2022, MSCI World index, May 2023)

Sector	$\mathbb{S}_j$	$\mathbb{S}_j^{(\text{gvc})}$	$\mathbb{S}_j^{(\text{direct})}$	$Q_{1\%}(\mathbb{S}_i)$	$Q_{5\%}(\mathbb{S}_i)$	$Q_{10\%}(\mathbb{S}_i)$
Communication Services	−0.33	−0.31	−0.02	−2.76	−1.45	−0.87
Consumer Discretionary	−2.21	−1.33	−0.87	−96.99	−4.10	−2.98
Consumer Staples	−3.97	−3.34	−0.62	−15.33	−9.21	−6.75
Energy	51.41	52.11	−0.70	−1.56	−0.74	2.76
Financials	−0.74	−0.50	−0.24	−1.63	−0.87	−0.77
Health Care	−0.49	−0.44	−0.05	−1.93	−1.21	−1.00
Industrials	−0.17	0.93	−1.10	−59.97	−11.37	−4.55
Information Technology	−0.52	−0.48	−0.04	−4.09	−2.45	−2.32
Materials	−0.51	10.03	−10.54	−91.46	−58.51	−43.95
Real Estate	−0.19	−0.16	−0.03	−0.81	−0.80	−0.79
Utilities	37.98	41.44	−3.46	−2.58	−0.80	10.82
MSCI World index	2.58	3.44	−0.86	−53.09	−7.78	−4.32

Remark 18. *The figures presented in Tables 37 and 38 illustrate the complexity and potential unintended consequences of introducing a global uniform carbon tax. The earnings shocks underscore the importance of considering the heterogeneous impacts of climate policies across sectors. For instance, Energy and Utilities show the largest negative shocks under a limited pass-through rate scenario, whereas they might experience positive earning variations when considering average pass-through rates as per their elasticity group category. However, Energy and Utilities are traditionally the most impacted sectors in classical stress testing exercises. This implies that certain sectors could pass on the costs of the carbon tax to their consumers and the downstream value chain, thereby lessening their financial strain. At the same time, other sectors with lower emission intensities could face increased input costs without being able to pass on a significant portion of the carbon price, thus experiencing negative shocks. This raises a concern about the fairness of the mechanism since the tax burden might be indirectly shifted towards sectors or entities with lower emission profiles.*

[90] The values are given in Table 23 on page 75.

Figure 73: Boxplot of earnings' shock in % (global uniform taxation, $\boldsymbol{\tau}$ = \$100/tCO_2e, average pass-through rate, Exiobase 2022, MSCI World, May 2023)

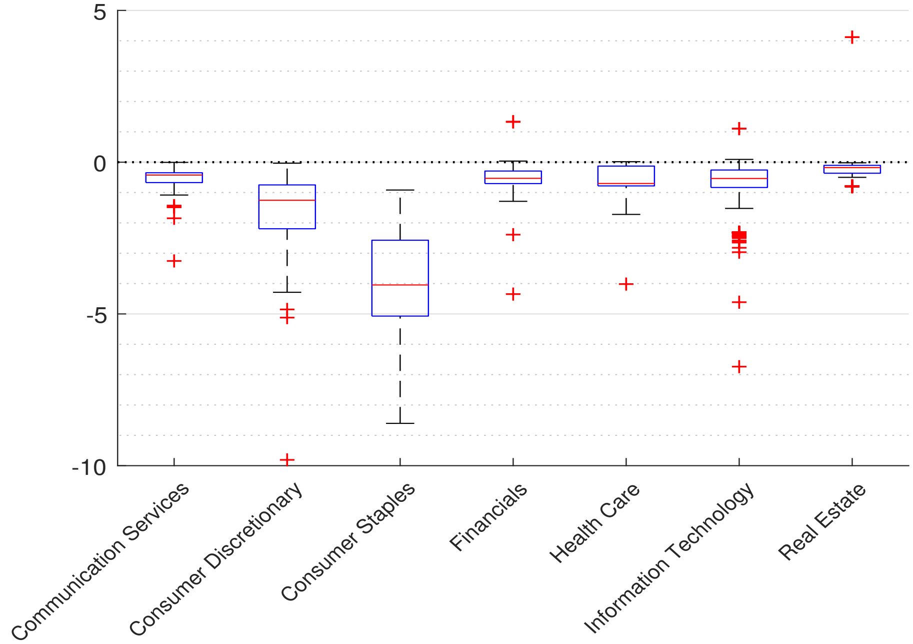

Figure 74: Boxplot of earnings' shock in % (global uniform taxation, $\boldsymbol{\tau}$ = \$100/tCO_2e, average pass-through rate, Exiobase 2022, MSCI World, May 2023)

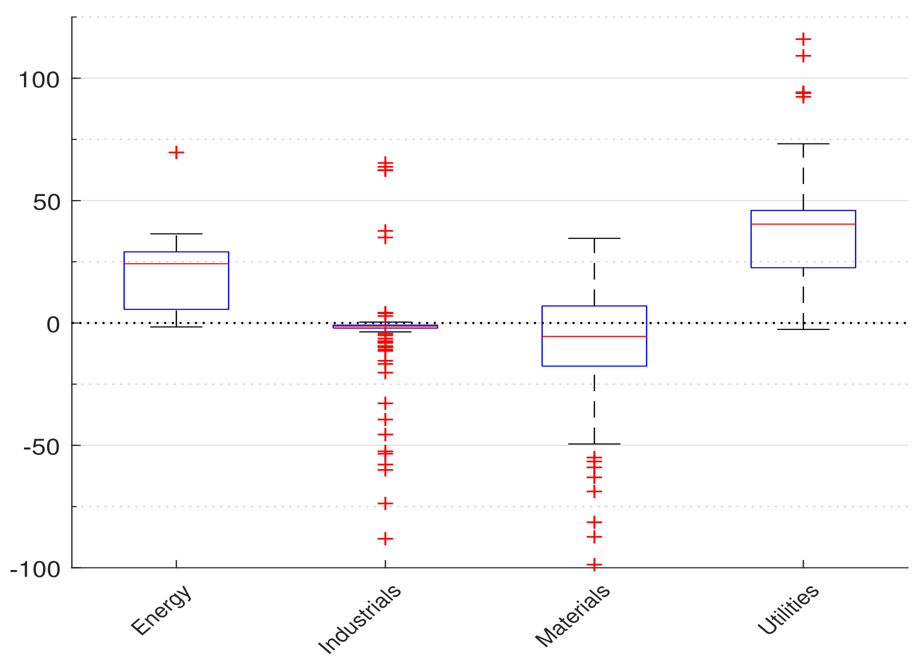

The implications of these findings are multifaceted. Policymakers must strike a delicate balance to mitigate potential systemic effects. Optimizing the pass-through parameters could help limit these effects, yet regulators have little direct control over these parameters. Hence, the effectiveness of a carbon tax as a tool for carbon reduction comes into question. While the carbon tax has its merits, it also has inherent risks. It might cascade through the supply chain, affecting even those entities with less direct pollution. Furthermore, its regressive nature could exacerbate income inequality, as it impacts households unequally (Semet, 2023). This concern becomes more pronounced when the concept of a 'fair transition' *is introduced, implying an equitable shift to a low-carbon economy. In conclusion, a comprehensive understanding of these findings could lead to improved climate policies. While it is clear that sectoral differences are key to effective policy design, it is equally important to assess the potential cascading effects and equity implications of such policies. Addressing these challenges is critical for a successful transition to a sustainable low-carbon future.*

6.2 From climate earnings-at-risk to portfolio value-at-risk

6.2.1 Asset return modeling

Following Bouchet and Le Guenedal (2020), we define the valuation ratio of the firm i as the ratio between the enterprise value $\mathcal{EV}_i$ and the earnings Ebitda_i:

$$\mathbb{R}_i = \frac{\mathcal{EV}_i}{\mathrm{Ebitda}_i}$$

$\mathbb{R}_i$ is called the EV to EBIDTA ratio or valuation multiple. If we assume that $\mathbb{R}_i$ is constant[91], we have:

$$\frac{\mathcal{EV}_i - \mathcal{EV}_i^-}{\mathcal{EV}_i^-} = \frac{\mathbb{R}_i \cdot \mathrm{Ebitda}_i - \mathbb{R}_i^- \cdot \mathrm{Ebitda}_i^-}{\mathbb{R}_i^- \cdot \mathrm{Ebitda}_i^-} = \frac{\mathrm{Ebitda}_i - \mathrm{Ebitda}_i^-}{\mathrm{Ebitda}_i^-} = \mathbb{S}_i$$

The variation of the enterprise value is then equal to the earnings' shock. Since the enterprise value represents the total assets $\mathcal{EV}_i = \mathcal{MC}_i + D_i$, where $\mathcal{MC}_i$ is the market capitalization (equity) and D_i is the total net debt, we deduce that $\Delta\mathcal{MC}_i = \Delta\mathcal{EV}_i$ by assuming that the debt remains constant. Therefore, the earning shock is fully passed on the equity price:

$$\Delta\mathcal{MC}_i = \mathbb{S}_i \cdot \mathcal{EV}_i^-$$

We deduce that the value of the market capitalization after the carbon tax is equal to:

$$\mathcal{MC}_i = \mathcal{MC}_i^- + \mathbb{S}_i \cdot \mathcal{EV}_i^-$$

The equity return is then equal to:

$$R_i = \frac{\mathcal{MC}_i - \mathcal{MC}_i^-}{\mathcal{MC}_i^-} = \mathbb{S}_i \cdot \frac{\mathcal{EV}_i^-}{\mathcal{MC}_i^-} = \mathbb{S}_i \cdot \mathbb{L}_i^- \tag{37}$$

The equity return is then the product of the earnings' shock and the leverage (or EV to MC) ratio. Since this ratio is greater than 1, we have $|R_i| \geq |\mathbb{S}_i|$. The earnings's shock is then amplified by the leverage ratio[92]. In Figure 75, we compute the portfolio return $R(w) = \sum_i w_i R_i$ of the MSCI World index. We verify that the relationship between $\boldsymbol{\phi}$ and $R(w)$ is a leveraged version of the total earnings' shock given in Figure 71 on page 119. While we had $\mathbb{S}(w) \in [-6\%, 6\%]$, we obtain $R(w) \in [-9\%, 9\%]$, implying a global leverage of 150% for the MSCI World index.

[91] In practice, this ratio can be subject to significant variations when considering long time periods.

[92] For instance, if $\mathbb{S}_i = -10\%$ and $\mathbb{L}_i^- = 2$, we obtain $R_i = -20\%$.

Figure 75: Relationship between the pass-through rate and the portfolio return of the MSCI World index (global uniform taxation, $\boldsymbol{\tau} = \$100/\text{tCO}_2\text{e}$, Exiobase 2022, MSCI World index, May 2023)

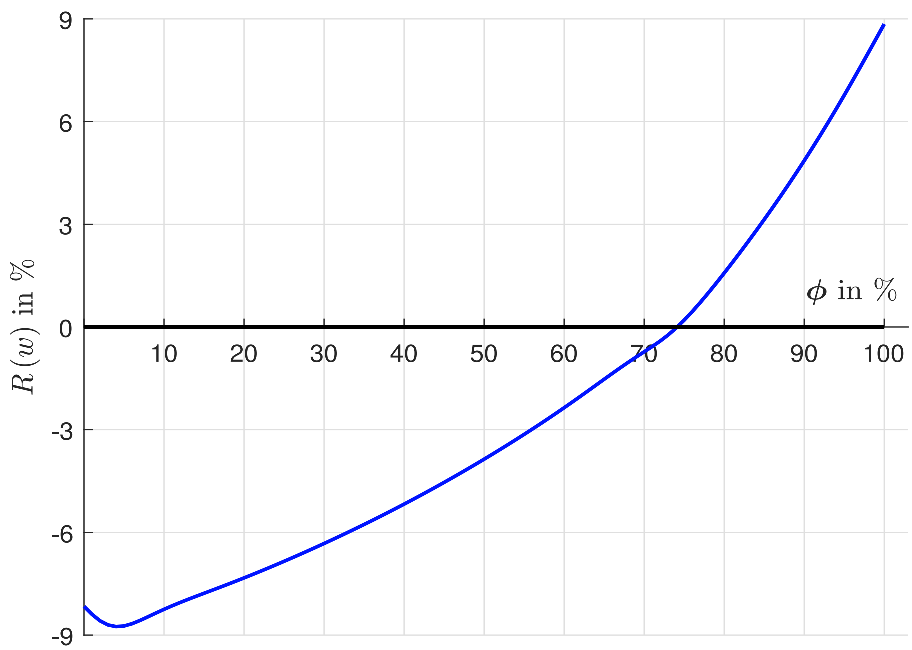

Remark 19. *Another approach to price the equity is to consider the discounted cash flow approach:*

$$\mathcal{MC}_i \sim DCF_i = \sum_{t=1}^{\infty} \frac{\mathcal{CF}_i(t)}{(1 + \mathcal{WACC}_i)^t}$$

where $\mathcal{CF}_i(t)$ are the cash-flows (or the earnings) and $\mathcal{WACC}_i$ is the cost of capital of the company:

$$\mathcal{WACC}_i = \frac{\mathcal{MC}_i}{\mathcal{MC}_i + D_i} \times \mathcal{C}_E + \frac{D_i}{\mathcal{MC}_i + D_i} \times \mathcal{C}_D$$

where $\mathcal{C}_E$ and $\mathcal{C}_D$ are the cost of equity and the cost of debt. We can see that the impact on equity depends on many factors. The main drivers of the equity valuation remain the future cash flows, the cost of capital and the capital structure. If there is an earnings' shock, we obtain:

$$DCF_i(\mathbb{S}_i) = \sum_{t=1}^{\infty} \frac{\mathcal{CF}_i(t)(1 + \mathbb{S}_i)}{\left(1 + \mathcal{WACC}_i(\mathbb{S}_i)\right)^t}$$

If we assume that $\mathcal{WACC}_i(\mathbb{S}_i)$ does not depend on the earnings' shock, we have:

$$DCF_i(\mathbb{S}_i) = \sum_{t=1}^{\infty} \frac{\mathcal{CF}_i(t)(1 + \mathbb{S}_i)}{(1 + \mathcal{WACC}_i)^t} = (1 + \mathbb{S}_i) DCF_i(0)$$

In this case, we have $R_i = \mathbb{S}_i$. If the cash flows are constant ($\mathcal{CF}_i(t) = \mathcal{CF}_i$), it follows *that:*

$$\begin{aligned} DCF_i(\mathbb{S}_i) &= \sum_{t=1}^{\infty} \frac{\mathcal{CF}_i(1+\mathbb{S}_i)}{(1+\mathcal{WACC}_i(\mathbb{S}_i))^t} \\ &= \frac{\mathcal{CF}_i(1+\mathbb{S}_i)}{\mathcal{WACC}_i(\mathbb{S}_i)} \\ &= (1+\mathbb{S}_i)\frac{\mathcal{WACC}_i(0)}{\mathcal{WACC}_i(\mathbb{S}_i)} DCF_i(0) \end{aligned}$$

Therefore, we obtain:

$$R_i = (1+\mathbb{S}_i)\frac{\mathcal{WACC}_i(0)}{\mathcal{WACC}_i(\mathbb{S}_i)} - 1$$

We usually observe a high convexity of $\mathcal{WACC}_i(\mathbb{S}_i)$, implying that $|R_i| > |\mathbb{S}_i|$. This convexity effect will exacerbate even further the current results. More generally, the future cash flows, the cost of capital and the capital structure are fully interconnected. For instance, the capital structure also influences the WACC. The companies with high level of debt suffer from higher cost of capital everything else being equal. However, some specific activities might require refining the equity return model given in Equation (37). In particular, perpetual annuity activities, such as telecommunication or heath care (which require a lot of initial investment and then lower operating costs), could be considered independently. Indeed, the impact on their equity value should be less sensitive to their leverage level (which is naturally high). In this reserach paper, we assume that the shock are fully transmitted to the equity valuation and amplified by corporate leverage ratio and leave business specific consideration for further research.

6.2.2 Description of the Monte carlo algorithm

We can now describe the algorithm to compute the value-at-risk of the portfolio w. In what follows, n and m are respectively the number of sectors of the MRIO database and the number of issuers of the portfolio w. The index j refers to the j^{th} sector, while the index i corresponds to the i^{th} issuer[93]. The inputs of the VaR algorithm are:

- The matrices x, A and y of the MRIO database that describe the relationships between the sectors;
- The carbon intensity $\mathcal{CI}_{1,j}$ of the sectors;
- The carbon intensity $\mathcal{CI}_{1,i}^{\text{issuer}}$, the value added ratio v_i^{issuer} and the leverage ratio $\mathbb{L}_i^{\text{issuer}}$ of the issuers;
- The mapping function $j = \mathcal{M}ap(i)$ between the issuers and the sectors;
- The portfolio weights $w = (w_1, \ldots, w_m)$.

Algorithm 1 describes the computation of the conditional value-at-risk (and the expected shortfall) of the portfolio w at the confidence level α. The parameters of the algorithm are:

- The coefficients α_j and β_j of the beta distribution $\mathcal{B}(\alpha_j, \beta_j)$ for the different sectors to simulate the stochastic pass-through rates;
- The correlation ρ of the Gaussian copula;

[93] Moreover, we use the superscript "issuer" when the variable concerns the issuers and not the sectors.

Algorithm 1 Compute the conditional value-at-risk at the confidence level α

Initialize $t_{\text{direct}} \leftarrow \mathbf{0}_n$, $V \leftarrow \mathbf{0}_n$, $\boldsymbol{\tau}^{\text{issuer}} \leftarrow \mathbf{0}_m$, $t_{\text{direct}}^{\text{issuer}} \leftarrow \mathbf{0}_m$, $\boldsymbol{\phi} \leftarrow \mathbf{0}_n$, $b \leftarrow \mathbf{0}_n$, $\Phi \leftarrow \mathbf{0}_{n,n}$, $p \leftarrow \mathbf{0}_n$, $\Delta y \leftarrow \mathbf{0}_n$, $\Delta V^{(\text{gvc})} \leftarrow \mathbf{0}_n$, $\mathbb{S}^{(\text{gvc})} \leftarrow \mathbf{0}_n$, $\mathbb{S}^{(\text{gvc,issuer})} \leftarrow \mathbf{0}_m$, $\mathbb{S}^{(\text{direct,issuer})} \leftarrow \mathbf{0}_m$, $\mathbb{S}^{\text{issuer}} \leftarrow \mathbf{0}_m$, $R^{\text{issuer}} \leftarrow \mathbf{0}_m$ and $L(w) \leftarrow \mathbf{0}_{n_S}$
Compute $\boldsymbol{\mathcal{L}} \leftarrow (I_n - A)^{-1}$
for $j = 1 : n$ **do**
    $t_{\text{direct},j} \leftarrow \boldsymbol{\tau}_j \, \boldsymbol{\mathcal{CI}}_{1,j}$
    $V_j \leftarrow x_j \left(1 - \sum_{i=1}^{n} A_{i,j}\right)$
end for
for $i = 1 : m$ **do**
    $j \leftarrow \mathcal{M}ap\,(i)$
    $\boldsymbol{\tau}_i^{\text{issuer}} \leftarrow \boldsymbol{\tau}_j$
    $t_{\text{direct},i}^{\text{issuer}} \leftarrow \boldsymbol{\tau}_i \, \boldsymbol{\mathcal{CI}}_{1,i}^{\text{issuer}}$
end for
for $s = 1 : n_S$ **do**
    $u_1 \leftarrow \mathcal{N}(0,1)$
    for $j = 1 : n$ **do**
        $u_2 \leftarrow \mathcal{N}(0,1)$
        $\boldsymbol{\phi}_j \leftarrow \mathcal{B}^{-1}\left(\Phi\left(\sqrt{\rho}\,u_1 + \sqrt{1-\rho}\,u_2\right); \alpha_j, \beta_j\right)$
        $b_j \leftarrow -\left(1 - \boldsymbol{\phi}_j^{-1}\right) y_j$
        $\boldsymbol{\phi}_j \leftarrow \min\left(\boldsymbol{\phi}_j, \boldsymbol{\phi}^+\right)$
        $\Phi_{j,j} \leftarrow \boldsymbol{\phi}_j$
    end for
    $\Delta p \leftarrow \left(I_n - A^\top \Phi\right)^{-1} \Phi \, t_{\text{direct}}$
    for $j = 1 : n$ **do**
        $p_j \leftarrow 1 + \Delta p_j$
        $\Delta y_j \leftarrow -b_j \Delta p_j$
    end for
    $x \leftarrow \boldsymbol{\mathcal{L}}\left(y + \Delta_y\right)$
    for $j = 1 : n$ **do**
        $\Delta V_j^{(\text{gvc})} \leftarrow x_j \left(p_j - \sum_{i=1}^{n} A_{i,j} p_i\right) - V_j$
        $\mathbb{S}_j^{(\text{gvc})} \leftarrow \Delta V_j^{(\text{gvc})} / V_j$
    end for
    for $i = 1 : m$ **do**
        $j \leftarrow \mathcal{M}ap\,(i)$
        $\mathbb{S}_i^{(\text{gvc,issuer})} \leftarrow \mathbb{S}_j^{(\text{gvc})}$
        $\boldsymbol{\phi}_i^{\text{issuer}} \leftarrow \boldsymbol{\phi}_j$
        $\mathbb{S}_i^{(\text{direct,issuer})} \leftarrow -\left(1 - \boldsymbol{\phi}_i^{\text{issuer}}\right) t_{\text{direct},i}^{\text{issuer}} / \upsilon_i^{\text{issuer}}$
        $\mathbb{S}_i^{\text{issuer}} \leftarrow \mathbb{S}_i^{(\text{gvc,issuer})} + \mathbb{S}_i^{(\text{direct,issuer})}$
        $R_i^{\text{issuer}} \leftarrow \mathbb{S}_i^{\text{issuer}} \cdot \mathbb{L}_i^{\text{issuer}}$
    end for
    $L_s(w) \leftarrow -\sum_{i=1}^{m} w_i R_i^{\text{issuer}}$
end for
$\text{VaR}_\alpha(w) \leftarrow Q_\alpha\left(L(w)\right)$
$\text{ES}_\alpha(w) \leftarrow \left(\sum_{s=1}^{n_S} \mathbb{1}\left\{L_s(w) \geq \text{VaR}_\alpha(w)\right\} \cdot L_s(w)\right) \Big/ \left(\sum_{s=1}^{n_S} \mathbb{1}\left\{L_s(w) \geq \text{VaR}_\alpha(w)\right\}\right)$
return $\text{VaR}_\alpha(w)$ and $\text{ES}_\alpha(w)$

Algorithm 2 Compute the unconditional value-at-risk at the confidence level α

Initialize $t_{\text{direct}} \leftarrow \mathbf{0}_n$, $V \leftarrow \mathbf{0}_n$, $\boldsymbol{\tau}^{\text{issuer}} \leftarrow \mathbf{0}_m$, $t^{\text{issuer}}_{\text{direct}} \leftarrow \mathbf{0}_m$, $\boldsymbol{\phi} \leftarrow \mathbf{0}_n$, $b \leftarrow \mathbf{0}_n$, $\Phi \leftarrow \mathbf{0}_{n,n}$, $p \leftarrow \mathbf{0}_n$, $\Delta y \leftarrow \mathbf{0}_n$, $\Delta V^{(\text{gvc})} \leftarrow \mathbf{0}_n$, $\mathbb{S}^{(\text{gvc})} \leftarrow \mathbf{0}_n$, $\mathbb{S}^{(\text{gvc,issuer})} \leftarrow \mathbf{0}_m$, $\mathbb{S}^{(\text{direct,issuer})} \leftarrow \mathbf{0}_m$, $\mathbb{S}^{\text{issuer}} \leftarrow \mathbf{0}_m$, $R^{\text{issuer}} \leftarrow \mathbf{0}_m$ and $L(w) \leftarrow \mathbf{0}_{n_S}$

Compute $\boldsymbol{\mathcal{L}} \leftarrow (I_n - A)^{-1}$

for $j = 1 : n$ **do**
- $V_j \leftarrow x_j \left(1 - \sum_{i=1}^{n} A_{i,j}\right)$

end for

for $s = 1 : n_S$ **do**
- $\tau \leftarrow \exp\left(\mu + \sigma \mathcal{N}(0,1)\right)$
- $u_1 \leftarrow \mathcal{N}(0,1)$
- **for** $j = 1 : n$ **do**
  - $\boldsymbol{\tau}_j \leftarrow \tau$
  - $t_{\text{direct},j} \leftarrow \boldsymbol{\tau}\, \boldsymbol{\mathcal{CI}}_{1,j}$
  - $u_2 \leftarrow \mathcal{N}(0,1)$
  - $\boldsymbol{\phi}_j \leftarrow \mathcal{B}^{-1}\left(\Phi\left(\sqrt{\rho}\, u_1 + \sqrt{1-\rho}\, u_2\right); \alpha_j, \beta_j\right)$
  - $b_j \leftarrow -\left(1 - \boldsymbol{\phi}_j^{-1}\right) y_j$
  - $\boldsymbol{\phi}_j \leftarrow \min\left(\boldsymbol{\phi}_j, \boldsymbol{\phi}^{+}\right)$
  - $\Phi_{j,j} \leftarrow \boldsymbol{\phi}_j$
- **end for**
- $\Delta p \leftarrow \left(I_n - A^{\top}\Phi\right)^{-1} \Phi\, t_{\text{direct}}$
- **for** $j = 1 : n$ **do**
  - $p_j \leftarrow 1 + \Delta p_j$
  - $\Delta y_j \leftarrow -b_j \Delta p_j$
- **end for**
- $x \leftarrow \boldsymbol{\mathcal{L}}\left(y + \Delta_y\right)$
- **for** $j = 1 : n$ **do**
  - $\Delta V_j^{(\text{gvc})} \leftarrow x_j \left(p_j - \sum_{i=1}^{n} A_{i,j} p_i\right) - V_j$
  - $\mathbb{S}_j^{(\text{gvc})} \leftarrow \Delta V_j^{(\text{gvc})} / V_j$
- **end for**
- **for** $i = 1 : m$ **do**
  - $j \leftarrow \mathcal{M}ap(i)$
  - $\boldsymbol{\tau}_i^{\text{issuer}} \leftarrow \boldsymbol{\tau}_j$
  - $t^{\text{issuer}}_{\text{direct},i} \leftarrow \boldsymbol{\tau}_i\, \boldsymbol{\mathcal{CI}}^{\text{issuer}}_{1,i}$
  - $\mathbb{S}_i^{(\text{gvc,issuer})} \leftarrow \mathbb{S}_j^{(\text{gvc})}$
  - $\boldsymbol{\phi}_i^{\text{issuer}} \leftarrow \boldsymbol{\phi}_j$
  - $\mathbb{S}_i^{(\text{direct,issuer})} \leftarrow -\left(1 - \boldsymbol{\phi}_i^{\text{issuer}}\right) t^{\text{issuer}}_{\text{direct},i} / \upsilon_i^{\text{issuer}}$
  - $\mathbb{S}_i^{\text{issuer}} \leftarrow \mathbb{S}_i^{(\text{gvc,issuer})} + \mathbb{S}_i^{(\text{direct,issuer})}$
  - $R_i^{\text{issuer}} \leftarrow \mathbb{S}_i^{\text{issuer}} \cdot \mathbb{L}_i^{\text{issuer}}$
- **end for**
- $L_s(w) \leftarrow -\sum_{i=1}^{m} w_i R_i^{\text{issuer}}$

end for

$\text{VaR}_\alpha(w) \leftarrow Q_\alpha\left(L(w)\right)$

$\text{ES}_\alpha(w) \leftarrow \left(\sum_{s=1}^{n_S} \mathbb{1}\left\{L_s(w) \geq \text{VaR}_\alpha(w)\right\} \cdot L_s(w)\right) \Big/ \left(\sum_{s=1}^{n_S} \mathbb{1}\left\{L_s(w) \geq \text{VaR}_\alpha(w)\right\}\right)$

return $\text{VaR}_\alpha(w)$ and $\text{ES}_\alpha(w)$

- The values $\boldsymbol{\tau}_j$ of the carbon tax for the different sectors;
- The number n_S of simulations.

There are different steps in the algorithm. Lines 3–6 compute the direct tax rate and the value added of the sectors, while Lines 7–10 compute the direct tax rate of issuers. Lines 13–20 simulate the random vector of pass-though rates and define the demand slope of the sectors. The GVC shock at the sector level and the total shock at the issuer level are respectively calculated in Lines 21–30 and Lines 31–38. We can then deduce the loss of the portfolio for the s^{th} simulation:

$$L_s(w) = -\sum_{i=1}^{m} w_i R_i^{\text{issuer}}$$

Finally, we compute the value-at-risk and the expected shortfall in Lines 41 and 42. Since the carbon tax may be different from one sector to another, Algorithm 1 can be used to simulate the impact of a differentiated tax, and not only a uniform tax. For the unconditional value-at-risk, the carbon tax is stochastic. By assuming that $\boldsymbol{\tau}$ follows a log-normal distribution $\mathcal{LN}\left(\mu, \sigma^2\right)$, we obtain Algorithm 2. We only describe the case of the uniform tax, but implementing a differentiated taxation is straightforward. Indeed, we have to change Lines 7 and 10 of the algorithm. Line 7 simulates the uniform tax, while Line 10 assigns the simulated tax to all the sectors. If we would like to apply the tax to a subset Ω of sectors (or a region), we have to replace $\boldsymbol{\tau}_j \leftarrow \tau$ by **if** $j \in \Omega$ **then** $\boldsymbol{\tau}_j \leftarrow \tau$ **else** $\boldsymbol{\tau}_j \leftarrow 0$ **end if**.

Remark 20. *We introduce a cap $\boldsymbol{\phi}^+$, which indicates the maximum value taken by the pass-through rates. This allows to consider a binding policy that could control the pass-through mechanisms, especially the price increase. An example is the so-called tariff shield imposed in France in 2022.*

6.2.3 Application to the MSCI World index portfolio

The term climate value-at-risk has been coined by Dietz *et al.* (2016). Nevertheless, there are very few studies that have estimated the value-at-risk of investment portfolios. Generally, they focus on the loss distribution of an asset class at the global level without making reference to the returns of individual securities. Our approach is different and closer to market practices of risk management (Roncalli, 2020) when we manage the risk of an equity portfolio. Therefore, we can use the traditional tools associated to risk measures, especially those of risk allocation.

To estimate the value-at-risk, we consider 3 000 Monte Carlo simulations. Figure 76 shows the results with respect to the parameter ρ of the Gaussian copula[94]. We notice that the value-at-risk is negative if the correlation between the pass-through rates is low. This case is not realistic, because the pass-through decisions of firms are not independent of each other. This is why we generally consider that the correlation between pass-through rates is between 70% and 100%. We deduce that the 99% value-at-risk is about 2% and 4% if $\boldsymbol{\phi}^+$ is respectively equal to 100% and 50%. These figures are not so high for a \$100/tCO$_2$e carbon tax.

We also estimate the unconditional value-at-risk by assuming that the carbon tax follows a log-normal distribution. Using an initial price of \$100/tCO$_2$e, a drift of 20% and a volatility of 50%, the parameters of the probability distribution are $\mu = 4.68$ and $\sigma = 0.50$. This corresponds to an average carbon tax of \$122/tCO$_2$e and a standard deviation of \$65/tCO$_2$e.

[94]See Figure 124 on page 174 for the expected shortfall risk measure.

Figure 76: Value-at-risk at the 99% confidence level (global uniform taxation, $\boldsymbol{\tau} = \$100/\text{tCO}_2\text{e}$, stochastic pass-through rate, Gaussian copula, Exiobase 2022, MSCI World, May 2023)

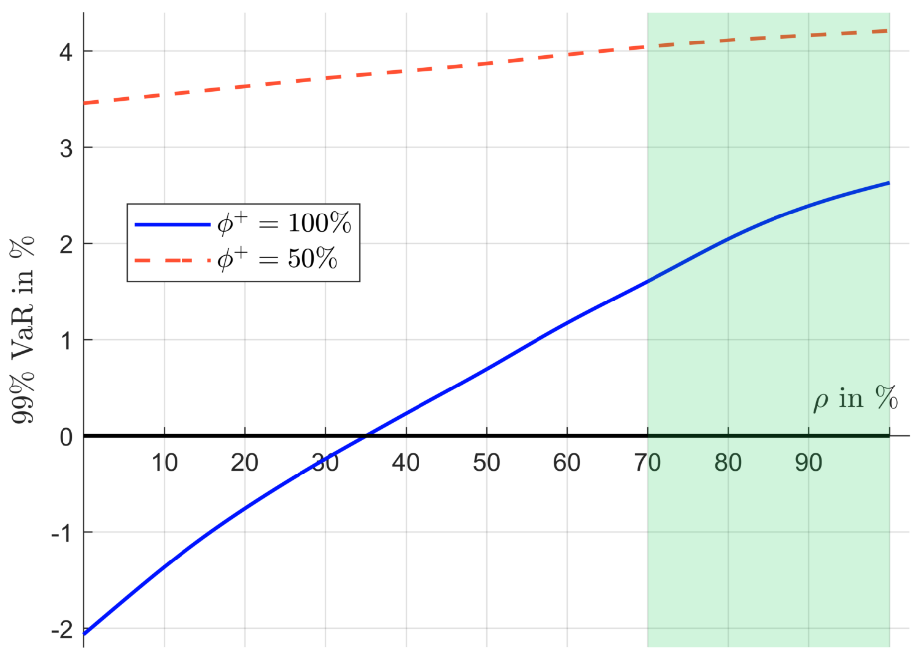

Since we have two sources of uncertainty (pass-though rates and the carbon tax), the number of Monte Carlo simulations is increased and equal to 10 000. Results are given in Table 39. We only report the estimates when the parameter of the Gaussian copula is between 70% and 100%. Again, the unconditional value-at-risk is relatively low when $\boldsymbol{\phi}^+$ is equal to 100%. It begins to be significant when $\boldsymbol{\phi}^+$ is set to 50% since $\text{VaR}_{99\%}(w)$ is around 11%.

Table 39: Unconditional Value-at-risk at the 99% confidence level (global uniform taxation, stochastic pass-through rate, Gaussian copula, Exiobase 2022, MSCI World, May 2023)

ρ		70%	80%	90%	100%
$\boldsymbol{\phi}^+ = 100\%$	$\text{VaR}_\alpha(w)$	2.02	2.07	2.91	3.59
	$\text{ES}_\alpha(w)$	3.86	3.95	4.23	4.31
$\boldsymbol{\phi}^+ = 50\%$	$\text{VaR}_\alpha(w)$	10.38	10.77	11.25	11.33
	$\text{ES}_\alpha(w)$	13.31	13.34	13.32	13.39

As said previously, we can use the traditional tools to manage the risk of the portfolio. In particular, we can perform a risk decomposition of the Monte Carlo value-at-risk. Following Roncalli (2020, Section 2.3, pages 104-116), we apply the Euler allocation principle to estimate the risk contribution of each issuer (or asset). We recall that the portfolio loss is defined as:

$$L = \sum_{i=1}^{m} L_i = -\sum_{i=1}^{m} w_i R_i$$

By assuming that asset returns are elliptically distributed, the risk contribution of asset i is equal to:

$$\begin{aligned}\mathcal{RC}_i &= \mathbb{E}\left[L_i \mid L = \mathrm{VaR}_\alpha(L)\right] \\ &= \mathbb{E}[L_i] + \frac{\operatorname{cov}(L, L_i)}{\sigma^2(L)}\left(\mathrm{VaR}_\alpha(L) - \mathbb{E}[L]\right)\end{aligned}$$

Estimating the risk contributions with simulated Monte Carlo scenarios is then straightforward. It suffices to replace the statistical moments by their sample statistics:

$$\mathcal{RC}_i = \bar{L}_i + \frac{\sum_{s=1}^{n_S}\left(L_s - \bar{L}\right)\left(L_{i,s} - \bar{L}_i\right)}{\sum_{s=1}^{n_S}\left(L_s - \bar{L}\right)^2}\left(\mathrm{VaR}_\alpha(L) - \bar{L}\right)$$

where $L_{i,s} = -w_i R_{i,s}$ and $L_s = \sum_{i=1}^m L_{i,s}$ are the losses of asset i and portfolio w for the s^{th} simulated scenario, and $\bar{L}_i = n_S^{-1}\sum_{s=1}^{n_S} L_{i,s}$ and $\bar{L} = n_S^{-1}\sum_{s=1}^{n_S} L_s$ is the average losses of asset i and portfolio w by considering all the Monte Carlo scenarios. By definition of the Euler allocation principle, we have $\sum_{i=1}^m \mathcal{RC}_i = \mathrm{VaR}_\alpha(L)$ and we can compute the risk contribution of any sub-portfolio ϖ by using the additivity property: $\mathcal{RC}(\varpi) = \sum_{i\in\varpi}\mathcal{RC}_i$.

Table 40: Risk decomposition of the unconditional Value-at-risk at the 99% confidence level (global uniform taxation, stochastic pass-through rate, Gaussian copula, $\rho = 80\%$, Exiobase 2022, MSCI World, May 2023)

Sector	w_j	$\phi^+ = 100\%$		$\phi^+ = 50\%$	
		$\mathcal{RC}_j$	$\mathcal{RC}_j^\star$	$\mathcal{RC}_j$	$\mathcal{RC}_j^\star$
Communication Services	7.3	0.03	1.7	0.08	0.8
Consumer Discretionary	10.7	0.31	14.8	1.11	10.3
Consumer Staples	7.3	0.24	11.4	0.89	8.2
Energy	4.6	0.53	25.4	2.32	21.6
Financials	12.7	0.14	6.9	0.50	4.6
Health Care	13.2	0.07	3.3	0.33	3.0
Industrials	10.4	0.25	12.2	0.99	9.2
Information Technology	24.4	0.13	6.4	0.28	2.6
Materials	4.1	0.29	14.1	1.22	11.4
Real Estate	2.4	0.02	0.8	0.08	0.7
Utilities	2.9	0.06	3.0	2.98	27.6
Sum	100.0	2.07	100.0	10.77	100.0

In Table 40 and Figure 77, we report the risk allocation when we allocate the value-at-risk between the GICS level 1 sectors, assuming that a maximum pass-through rate level of 100% and 50% is imposed. w_j is the weight of sector j, $\mathcal{RC}_j$ is its absolute risk contribution while $\mathcal{RC}_j^\star = \mathcal{RC}_j / \mathrm{VaR}_\alpha(L)$ corresponds to its relative risk contribution. Each sector carries a different risk profile, which fluctuates based on the pass-through rate. For instance, Information Technology constitutes a significant portion of the total market capitalization with a weight of 24.4%. However, its risk contribution is relatively low at 6.4% when ϕ^+ is set to 100% and 2.6% when ϕ^+ set to 50%. Energy, despite its lower weight of 4.6% in the MSCI World index, demonstrates a notably higher risk contribution. When $\phi^+ = 100\%$, its risk contribution is equal to 25.4%. This suggests that the Energy sector carries a substantial amount of risk relative to its weight. More intriguingly, although the relative value slightly decreases due to the steep increase in the risk contribution of Utilities, the risk contribution share of Energy does not significantly depend on ϕ^+. It remains above 20% whether the pass-through is capped at 50% or 100%. Utilities exhibits the highest risk contribution at a 50% pass-through cap, accounting for 27.6% of the total risk. If the parameter ϕ^+ is set to 100%, the risk contribution would steeply decrease to 3%, reflecting the low input costs of this sector. This indicates that Utilities might be a highly volatile sector, possibly subject to more significant equity price fluctuations. In summary, the risk contributions across sectors vary widely, and the pass-through rate significantly influences these contributions. Therefore, when creating a balanced portfolio, it is essential to carefully consider the potential returns from each sector and the associated risks.

Figure 77: Risk allocation (global uniform taxation, stochastic pass-through rate, Gaussian copula, $\rho = 80\%$, Exiobase 2022, MSCI World, May 2023)

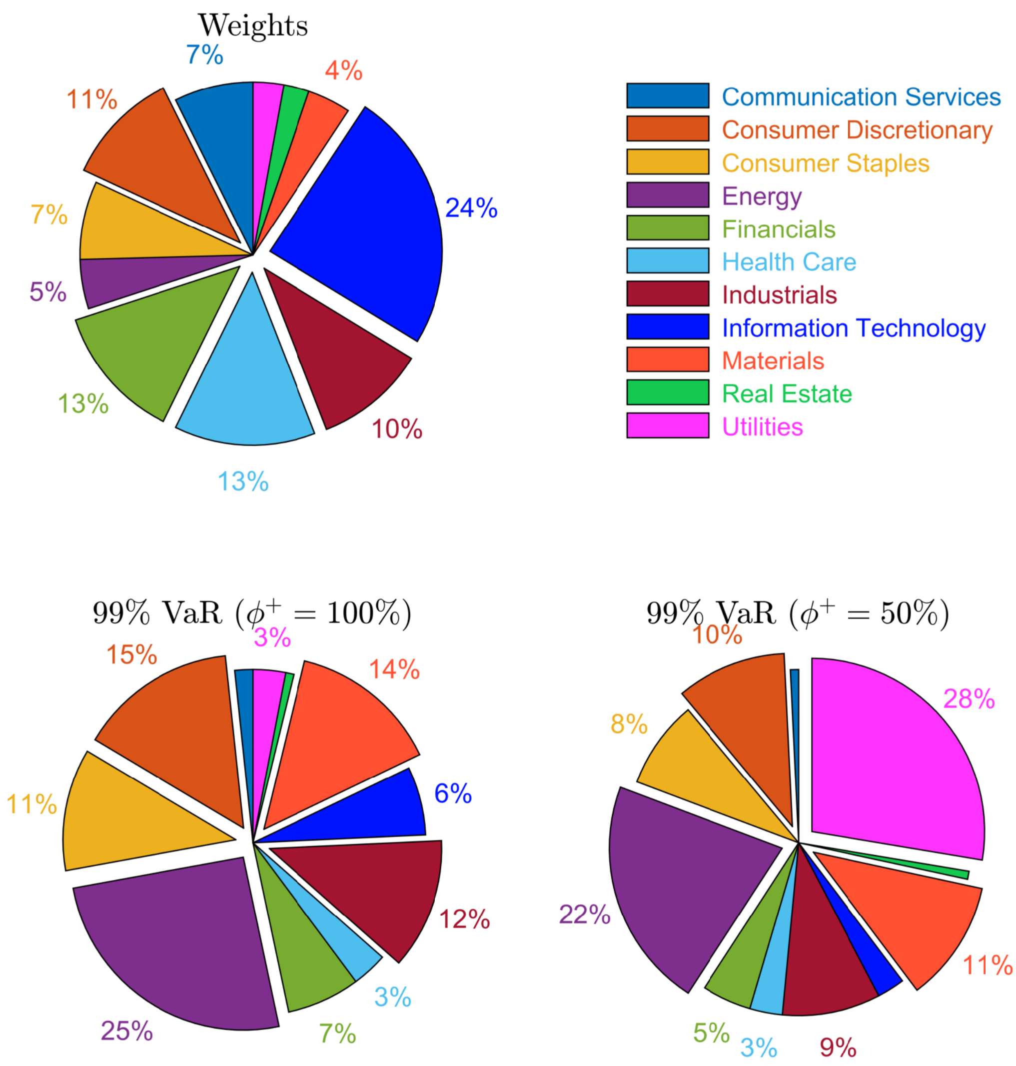

Remark 21. *Another popular approach to perform the risk allocation of the value-at-risk is based on the Kernel method. In this case, we use the Nadaraya-Watson estimator to compute the conditional expectation* $\mathbb{E}\left[L_i \mid L = \mathrm{VaR}_\alpha(L)\right]$. *We can also extend the two approaches when the risk measure is the expected shortfall (Roncalli, 2023).*

6.3 Impact on the market portfolio

The previous framework can be used to analyze the allocation distortion of the market portfolio. Let w_i^- be the current weight of asset i. The weight after the implementation of the carbon tax is equal to[95]:

$$w_i = \frac{\mathcal{MC}_i}{\sum_{k=1}^m \mathcal{MC}_k} = \left(\frac{1 + R_i}{1 + \sum_{k=1}^m w_k^- R_k} \right) w_i^- \tag{38}$$

In Figure 78, we report the sectoral evolution of the MSCI World index. We use the same color code and ordering as those applied in Figure 77 on page 130. We notice the big impact of the carbon tax and the pass-though on the market portfolio composition. Again, we notice that the most impacted sectors are Utilities and Energy (see also Table 61 on page 187).

In the case where we use stochastic pass-through rates and a random carbon tax, Equation (38) becomes:

$$\tilde{w}_i = \left(\frac{1 + \tilde{R}_i}{1 + \sum_{k=1}^m w_k^- \tilde{R}_k} \right) w_i^-$$

The weights are random and can be simulated using our framework. Then, we can estimate the probability distribution of $\tilde{w}_i$. To illustrate, we plot the probability density function of the portfolio weights using the simulated returns of the unconditional value-at-risk in Figure 79. Again, we notice the big impact of the pass-through cap $\boldsymbol{\phi}^+$. Depending of its value, sectors are winners or losers.

Remark 22. *In this section, we have illustrated the methodology using a uniform carbon tax. However, we can also consider a regional carbon tax and analyze the impact on country allocations.*

Remark 23. *This type of analysis is important in the context of net zero investing (Barahhou et al., 2022; Ben Slimane et al., 2023) or climate hedging Roncalli et al. (2020, 2021). In the first case, a carbon tax has an impact on market risk premia, which is an important element in the strategic asset allocation of the core/satellite portfolio. In the second case, it complements the carbon beta estimation by introducing forward-looking features.*

Remark 24. *All the results that have been obtained in this section are based on the assumption:* $\boldsymbol{\varepsilon}' = 1$. *This means that the price elasticity of the supply is equal to one. When* $\boldsymbol{\varepsilon}' \neq 1$, *the relationship between* $\boldsymbol{\varepsilon}$ *and* $\boldsymbol{\phi}$ *is* $\boldsymbol{\varepsilon} = \left(1 - \boldsymbol{\phi}^{-1}\right) \boldsymbol{\varepsilon}'$. *For some sectors, we know that* $\boldsymbol{\varepsilon}' \approx 0$, *which means that the slope of the demand in our study may be overestimated. Furthermore, we do not take into account the substitution effects between products within a given sector. This is a drawback of our analysis, especially in the Utilties sector. Indeed, the previous results may change if consumers have the choice between green and brown electricity. Nevertheless, the present study shows that the carbon tax may not be efficient if the supply of green electricity is not sufficiently elastic.*

[95] Because we have:

$$w_i = \frac{\mathcal{MC}_i^- + \mathbb{S}_i \cdot \mathcal{EV}_i^-}{\sum_{k=1}^m \left(\mathcal{MC}_k^- + \mathbb{S}_k \cdot \mathcal{EV}_k^- \right)}$$

and:

$$\frac{1 + \dfrac{\mathbb{S}_i \cdot \mathcal{EV}_i^-}{\mathcal{MC}_i^-}}{1 + \dfrac{\sum_{k=1}^m \mathbb{S}_k \cdot \mathcal{EV}_k^-}{\sum_{k=1}^m \mathcal{MC}_k^-}} = \frac{1 + R_i}{1 + \dfrac{\sum_{k=1}^m \mathcal{MC}_k^- R_k}{\sum_{k=1}^m \mathcal{MC}_k^-}} = \frac{1 + R_i}{1 + \sum_{k=1}^m w_k^- R_k}$$

Figure 78: Sector allocation in % of the market portfolio (global uniform taxation, Exiobase 2022, MSCI World, May 2023)

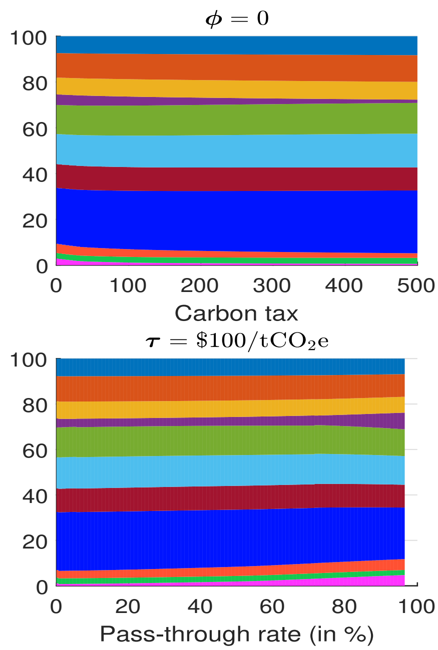

Figure 79: Probability density function of sector allocation (global uniform taxation, stochastic pass-through rate, Gaussian copula, $\rho = 80\%$, Exiobase 2022, MSCI World, May 2023)

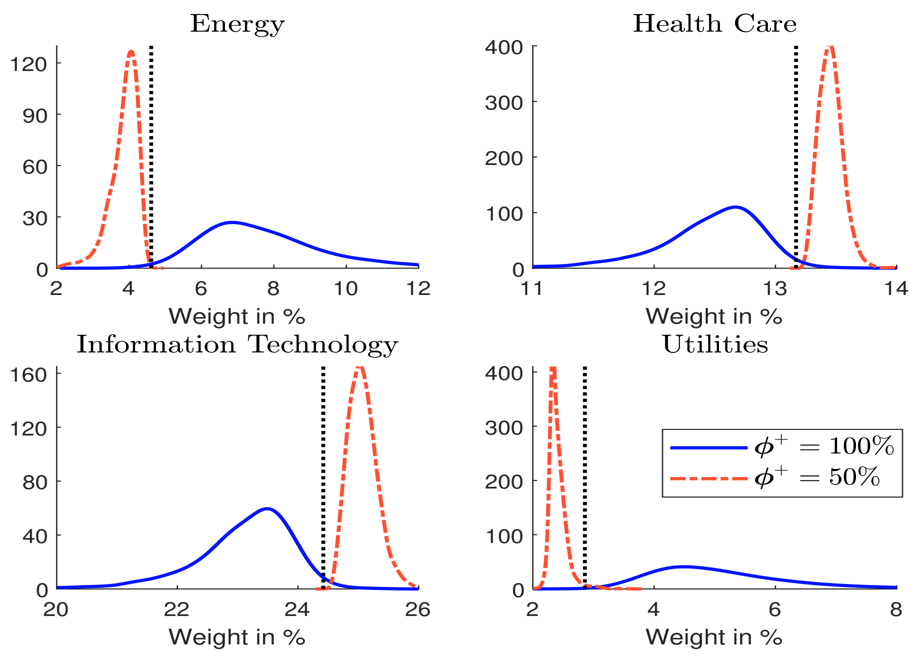

7 Conclusion

This paper aims to identify uncertainties in climate stress testing, estimate an issuer's total carbon emissions and consider the cascading effects of carbon pricing throughout the supply chain. It recognises that each sector will pass some of its rising costs through the supply chain, known as the *pass-through* effect. To achieve this, we propose a methodology that incorporates uncertainty at each stage of the stress test, from the carbon pricing scenario to the diffusion of the carbon tax through the economy at the issuer, sector and country level. This highlights the complexity of the supply chain and the interconnectedness of global economic actors.

The severity of NGFS scenarios is a critical factor in the uncertainty of climate scenarios, as it varies and has different implications for transition and physical risks, ultimately affecting both assets and carbon pricing. In practice, carbon pricing mechanisms are a critical tool for implementing public policy and reducing emissions. This can be through external carbon pricing (such as ETS or carbon taxes) or internal methods (such as shadow pricing or internal carbon fees). At present, there is a lack of homogeneity and global coordination in carbon pricing around the world. In terms of carbon taxes, there is considerable variation at the country level, with rates ranging from 0 to \$130/tCO_2e. The impact of a carbon tax on the MSCI World index in terms of cost over dividend or cost over profit also varies widely across sectors. For a carbon tax of \$100/tCO_2e, the cost over dividend for Utilities is more than 200, while for Communication Services it is less than 1. In the NGFS scenarios, the carbon tax is an implicit price and is determined endogenously by the integrated assessment model. This is both a strength and a weakness of the NGFS scenarios. An implicit carbon price has some advantages because it is an optimal solution. From a public policy perspective, it indicates the level at which governments need to set the carbon tax. It also has some drawbacks because we do not know whether the optimal policy response function will be effectively implemented by governments. In addition, the NGFS scenarios have been designed primarily for climate stress testing and are presented as inputs for "*central banks considering how best to integrate climate scenarios into stress testing exercises*". Nevertheless, we may wonder whether the NGFS scenarios are stress scenarios or a macroeconomic forecasting exercise that depends on six alternative climate change pathways. In the latter case, only the divergent net-zero and delayed transition scenarios can claim to be transition risk scenarios for stress testing programs. These two ambiguities (implicit carbon tax and stress severity) do not help investors to stress test their investment portfolios. Therefore, instead of using shadow carbon prices, which are implicit and endogenous outputs, we think it is easier to consider flat carbon taxes, which are explicit and exogenous inputs. This solution also has the great advantage of resolving the second ambiguity. Indeed, the severity of the stress is measured by the absolute level of the carbon tax. In this approach, a stress scenario is then fully described by the amount of the carbon tax. The higher the carbon tax, the higher the severity of the stress scenario. This approach is equivalent to a conditional stress test. We propose to complement this approach by considering an unconditional stress test exercise. This is possible because we show that both explicit and implicit carbon prices can be fitted by a log-normal probability distribution. This implies fat-tail risk, which is an important statistical property of climate change and global warming.

In this paper we show that the total economic cost of carbon taxation is bounded. The lower bound is the sum of carbon taxes times direct emissions, while the upper bound is the sum of carbon taxes times direct plus indirect emissions. Although the measurement of carbon footprints can be improved, we believe that current Scope 1 measures are good estimates of direct emissions. Unfortunately, the estimation of indirect emissions is not standardised and the confidence level of upstream and downstream Scope 3 emissions provided by data providers is poor. Therefore, the next level of uncertainty is the estimation of indirect carbon emissions from the supply chain. With this in mind, we are developing a formula based on environmentally extended input-output models to estimate indirect and total carbon intensities, as well as indirect and total carbon emissions. This methodology takes into account each level of the supply chain. We then test this approach using three different databases: WIOD 2014, Exiobase 2014 and Exiobase 2022. Our research provides a transparent measure of carbon intensity that can be compared with carbon footprints calculated by data providers. In addition, we have derived the multiplier between total and direct emissions and provided a stochastic modelling of the multiplier. Using the three MRIO databases, we find that for each tonne of CO_2 emitted, we can expect a multiplier of between 2.75 and 3.14 to cover all induced upstream emissions. We have also estimated the total carbon intensity of the MSCI World index. We compare these figures with Trucost 2021 data and find similar results. For example, in the utilities sector, the estimated carbon intensity is 1 872tCO_2e/\$ mn for Exiobase 2022, 1 833tCO_2e/\$ mn for Trucost 2021 and 1 889tCO_2e/\$ mn for WIOD 2014. As for the carbon tax, we propose a stochastic modelling of the multiplying coefficient. We assume that it depends on country and sector factors and that each factor is log-normally distributed. By exploiting the mathematical properties of this probability distribution, we obtain that the multiplying coefficient follows a shifted log-normal distribution. We can then estimate the probability distribution of the upper bound of the total economic cost. For example, a \$100/tCO_2e global carbon tax implies a cost between \$4.83 and \$21.80 tn at the 90% confidence interval.

The final level of uncertainty is the estimation of the cost passed through the supply chain following a carbon tax. We therefore calibrate the pass-through rate using stochastic modelling based on sector elasticity. We distinguish four classes of sectors: highly-elastic, high-elastic, medium-elastic and low-elastic sectors. For each class, we calibrate a beta distribution. We then analyse the impact of carbon taxation on price dynamics. We have a choice of three pricing approaches: value added protection, mark-up pricing and competitive equilibrium. We find that the value added method is the most appropriate approach to incorporate pass-through mechanisms. Under this assumption, producers want to maintain their level of value added by changing their prices. This is equivalent to the cost-push price model, where the dual inverse matrix is replaced by a Leontief multiplier matrix, which depends on both the input-output matrix A of technical coefficients and the diagonal matrix Φ of pass-through rates. We then derive a formula to calculate the total cost and the inflation rate. We propose a decomposition of costs into two elements: a producer-based cost and a consumer-based (or downstream) cost. By testing the sensitivity of total costs to the pass-through parameter, we find a high convexity of the relationship. In particular, the function between the pass-through rate and the multiplier coefficient is cubic, which implies that small errors in the pass-through estimate can lead to large errors in the cost estimate. We also explore the effect of carbon taxation by playing with two key elements: the aforementioned pass-through parameter and the level of coordination (playing with regional taxes only). We propose different scenarios: a global tax (uniform and differentiated) and a regional tax applied in the EU, the US or China. In the case of a global tax, we find that each \$100/tCO_2e incremental tax induces a total cost of 5% of GDP and a CPI inflation rate of 3.5%. In the case of a regional tax, we observe rising inflation and significant costs within the region, but moderate inflation and low costs outside the region. On average, 90% of the total cost is borne by the countries implementing the tax, while the impact on the rest of the world is only 10%. These breakdown figures raise the issue of distortions of competitiveness when taxation is not coordinated across countries. For example, in the case of an EU tax system with a carbon tax of \$500/tCO_2e and a pass-through rate of 100%, EU countries would have to bear a cost of \$4 tn, while non-EU countries would have to bear only 521 bn. Moreover, the cost as a percentage of GDP would be almost 15% for EU countries and less than 0.5% for non-EU countries. These results depend on the pass-through rate. For example, if EU sectors pass on only half of their direct costs, the costs for non-EU countries fall from \$521 to \$54 bn. Another result is that the economic costs do not depend only on the level of the carbon tax and the pass-through rate. They also depend on the structure of the value chain within the country and between the country and the rest of the world. For example, we find that a Chinese tax is five times more costly than a European or American tax. Part of the explanation is the highest carbon intensity of Chinese sectors, but the main explanation is that the density of the supply chain within the Chinese economy is higher than the density of the European or American value chain. In addition, we confirm that the collateral risks of foreign countries are strongly related to the upstream supply chain. We explain this asymmetry between upstream and downstream effects by the fact that we observe higher concentration in the upstream than in the downstream. In other words, the upstream network is generally undiversified, while the downstream network is well diversified. This explains why Canada, Mexico and Korea will be the three most affected foreign countries if a carbon tax is implemented in the US. To better understand the mechanisms behind the diffusion of the carbon tax across countries, we propose a visual representation of the value chain thanks to graph theory.

Using the value added model, we also define the earnings-at-risk due to a carbon tax. We provide a general formula of the value added shock and notice that it again depends on the pass-through rate and the price elasticity of the demand. In the inelastic case, the tax can be perfectly efficient if the pass-though rate is equal to zero. Nevertheless, it becomes less efficient when we include pass-through mechanism. In particular, in the case of perfect pass-through, the carbon tax is inefficient and is captured by producers, which increase their earnings. If we turn to the elastic case, the earnings' shocks depend on the price-demand function. For instance, we show that if we calibrate the price elasticity of demand with respect to the pass-through rate, 20% of sectors face a positive shock of their earnings and not a negative shock. These results question the efficiency of the carbon tax. Moreover, this means there are losers, but also winners.

A global uniform carbon tax of \$100/tCO_2e has various impacts on earnings' shocks, significantly influenced by the pass-through rate. When this latter is set at 25%, sectors such as Utilities, Energy, and Materials face considerable negative shocks, while Information Technology and Communication Services are only slightly affected. However, as the pass-through rate increases, high emitting sectors like Utilities and Materials start to experience positive shocks, essentially earning money post-taxation by passing direct costs along the value chain. This phenomenon becomes even more pronounced with a 95% pass-through rate, leading to a positive earnings' shock for the MSCI World index. These findings suggest a nuanced interaction between the pass-through rate and the effectiveness of the carbon tax as a tool for carbon reduction. While a high pass-through rate might result in financial gains for traditionally high emitting sectors, it also raises questions about the equity and systemic effects of such a policy. Specifically, lower emitting sectors or entities may bear a larger burden as they face increased costs without the ability to pass on a significant portion of the carbon price. Moreover, the regressive nature of the carbon tax could potentially exacerbate income inequality, affecting households unequally. It is therefore crucial for policymakers to consider these potential cascading effects and the differential impacts across sectors when designing climate policies. A comprehensive understanding of these dynamics is essential for ensuring a successful and equitable transition to a sustainable low-carbon future.

In our model, we calculate the earnings shock by taking into account changes in input prices and direct costs. This approach highlights the dual contribution of risk related to the pass-through rate. In the Monte Carlo exercise, we observe minimal, or even positive, average shocks, indicating an increase in earnings when a carbon tax is introduced in scenarios where pass-through rates are high or calibrated based on literature and empirical observations. By introducing correlation into the pass-through mechanism, we derive a 99% value-at-risk of 4% for the MSCI World index. This value represents the expected baseline loss in a scenario with a global carbon price of \$100/tCO_2e. Using an unconditional framework, we estimate that the 99% value-at-risk for the MSCI World index can be as high as 11%. The main contributing sectors are "*the usual suspects*' (Utilities, Energy, Industrials and materials), but also Consumer Discretionary and Consumer Staples.

The results of this study need to be interpreted with caution. This research focuses primarily on examining a single transmission channel: the resulting changes in prices and trading volumes in response to carbon regulation, and their impact on equity distortions and hence portfolio value-at-risk. However, it is important to recognise a number of mechanisms that potentially generate financial losses in the context of the transition to a greener economy. These mechanisms include technological risk, where companies fail to innovate and maintain their competitive edge, and market or reputational risk, where capital may not flow to companies perceived as too risky. Taken together, these mechanisms could exacerbate the results. The role of pass-through is also crucial. Our value-at-risk results are substantially attenuated by the pass-through effect (eliminating it could result in a value-at-risk three times as high). In the context of this paper, which is primarily concerned with the impact of a carbon price shock, we show that the impact on investment indices may not depend exclusively on carbon intensity and leverage. A comprehensive consideration of demand elasticity across all sectors is essential. Finally, we suggest that the more intensive sectors positioned at the top of the supply chain could benefit by shifting costs to other activities. These empirical results are interesting, but this research is first and foremost a methodological paper. It lays the groundwork for performing bottom-up stress testing at the issuer level with a carbon tax and calculating a climate value-at-risk of an investment portfolio. Future work could include alternative transition mechanisms to study their direct and indirect effects and assess their impact on financial assets.

Uncertainty is at the heart of our stress test model. Uncertainty relates to pass-through rates, price-demand elasticities, carbon prices, indirect emissions, etc. However, the concept of uncertainty is not homogeneous and falls into two categories. Using the risk management terminology (Roncalli, 2020), we need to distinguish between model variables (or inputs) and model parameters. Model variables are risk factors. For example, the carbon tax and direct emissions are two risk factors in our model, while the pass-through rate and price-demand elasticity are two model parameters. In this framework, the conditional value-at-risk exercise that we have performed can be related to model risk, while the unconditional value-at-risk exercise mixes both model risk and risk factor valuation. We note that our assessment of model risk is partial because we assume that the structure of the supply chain is known. In practice, it is estimated and is subject to large uncertainties, especially when we perform the bottom-up approach at the issuer level. An extension of this research is then to consider that the matrix of technical coefficients is estimated with errors. This is equivalent to assuming that the adjacency matrix of the graph associated with the value chain is stochastic. We can then use graph theory to incorporate the model risk of the supply chain into our stress testing framework. This is a topic for future research.

References

Acharya, V. V., Berner, R., Engle, R., Jung, H., Stroebel, J., Zeng, X., and Zhao, Y. (2023). Climate Stress Testing. *Annual Review of Financial Economics*, forthcoming.

ACPR (2021). A First Assessment of Financial Risks Stemming from Climate Change: The Main Results of the 2020 Climate Pilot Exercise. *Analyses et Synthèses*, 122.

Adenot, T., Brière, M., Counathe, P., Jouanneau, M., Le Berthe, T., and Le Guenedal, T. (2022). Cascading Effects of Carbon Price Through the Value Chain: Impact on Firm's Valuation. *SSRN*, 4043923.

Ahluwalia, M. B. (2017). The Business of Pricing Carbon: How Companies are Pricing Carbon to Mitigate Risks and Prepare for a Low-Carbon Future. *C2ES Brief*, *Center for Climate and Energy Solutions*, September.

Alexeeva-Talebi, V. (2010). Cost Pass-through in Strategic Oligopoly: Sectoral Evidence for the EU ETS. *ZEW Discussion Paper*, 10-056.

Alexeeva-Talebi, V. (2011). Cost Pass-through of the EU Emissions Allowances: Examining the European Petroleum Markets. *Energy Economics*, 33(S1), pp. 75-83.

Allen, T., Dees, S., Caicedo Graciano, C. M., ..., and Vernet, L. (2020). Climate-related Scenarios for Financial Stability Assessment: An Application to France. *Banque de France Working Paper*, 774.

Alogoskoufis, S., Dunz, N., Emambakhsh, T., ..., and Salleo, C. (2021). ECB Economy-wide Climate Stress Test: Methodology and Results. *ECB Occasional Paper*, 281.

Anderson, S. P., De Palma, A., and Kreider, B. (2001). Tax Incidence in Differentiated Product Oligopoly. *Journal of Public Economics*, 81(2), pp. 173-192.

Anquetin, T., Coqueret, G., Tavin, B., and Welgryn, L. (2022). Scopes of Carbon Emissions and their Impact on Green Portfolios. *Economic Modelling*, 115, 105651.

Antràs, P., Chor, D., Fally, T., and Hillberry, R. (2012). Measuring the Upstreamness of Production and Trade Flows. *American Economic Review*, 102(3), pp. 412-416.

Antràs, P., and Chor, D. (2018). On the Measurement of Upstreamness and Downstreamness in Global Value Chains. In Ing, L. Y., and Yu, M. (Eds), *World Trade Evolution: Growth, Productivity and Employment*, Routledge-ERIA Studies in Development Economics, pp. 126-194.

Barahhou, I., Ben Slimane, M., Oulid Azouz, N., and Roncalli, T. (2022). Net Zero Investment Portfolios — Part 1. The Comprehensive Integrated Approach. *SSRN*, 4283998.

Bartolucci, S., Caccioli, F., Caravelli, F., and Vivo, P. (2023). Correlation between Upstreamness and Downstreamness in Random Global Value Chains. *arXiv*, 2303.06603.

Battiston, S., Mandel, A., Monasterolo, I., Schütze, F., and Visentin, G. (2017). A Climate Stress-test of the Financial System. *Nature Climate Change*, 7(4), pp. 283-288.

Ben Slimane, M., Lucius, D., Roncalli, T., and Xu, J. (2023). Net Zero Investment Portfolios — Part 2. The Core-Satellite Approach. *forthcoming*.

Bennani, L., Le Guenedal, T., Lepetit, F., Ly, L., Mortier, V., Roncalli, T., and Sekine, T. (2018). How ESG Investing Has Impacted the Asset Pricing in the Equity Market. *SSRN*, 3316862.

Bergstrom, T. C. (1982). On Capturing Oil Rents with a National Excise Tax. *American Economic Review*, 72(1), pp. 194-201.

Bouchet, V., and Le Guenedal, T. (2020). Credit Risk Sensitivity to Carbon Price. *SSRN*, 3574486.

Bulow, J. I., and Pfleiderer, P. (1983). A Note on the Effect of Cost Changes on Prices. *Journal of Political Economy*, 91(1), pp. 182-185.

Cahen-Fourot, L., Campiglio, E., Godin, A., Kemp-Benedict, E., and Trsek, S. (2021). Capital Stranding Cascades: The Impact of Decarbonisation on Productive Asset Utilisation. *Energy Economics*, 103, 105581.

Campa, J. M., and Goldberg, L. S. (2005). Exchange Rate Pass-Through into Import Prices. *Review of Economics and Statistics*, 87(4), pp. 679-690.

Cartellier, F. (2022). Climate Stress Testing, an Answer to the Challenge of Assessing Climate-related Risks to the Financial System?. *SSRN*, 4179311.

Chen, H., Jebeli, H., Johnston, C., Paltsev, S., and Tremblay, M-C. (2023). An Investigation into the Effects of Border Carbon Adjustments on the Canadian Economy. *Bank of Canada Staff Working paper*, 2023-27.

Clarkson, R., and Deyes, K. (2002). Estimating the Social Cost of Carbon Emissions. *Government Economic Service Working Paper*, 140.

Cludius, J., De Bruyn, S., Schumacher, K., and Vergeer, R. (2020). Ex-post Investigation of Cost Pass-through in the EU ETS — An Analysis for Six Industry Sectors. *Energy Economics*, 91, 104883.

Corsatea, T. D., Lindner, S., Arto, I., ..., and Neuwahl, F. (2019). World Input-output Database Environmental Accounts — Update 2000-2016. *JRC Technical Report*, 29727.

Daly, H. E. (1968). On Economics as a Life Science. *Journal of Political Economy*, 76(3), pp. 392-406.

De Bruyn, S., Markowska, A., De Jong, F., and Bles, M. (2010a). Does the Energy Intensive Industry Obtain Windfall Profits through the EU ETS? An Econometric Analysis for Products from the Refineries, Iron and Steel and Chemical Sectors. *CE Delft Report*, April.

De Bruyn, S., Markowska, A., and Nelissen, D. (2010b). Will the Energy-intensive Industry Profit from EU ETS under Phase 3?. *CE Delft Report*, October.

De Bruyn, S. M., Vergeer, R., Schep, E., ..., and Healy, S. (2015). Ex-post Investigation of Cost Pass-through in the EU ETS — An Analysis for Six Sectors. *CE Delft Report*, November.

Demailly, D., and Quirion, P. (2006). CO_2 Abatement, Competitiveness and Leakage in the European Cement Industry under the EU ETS: Grandfathering versus Output-based Allocation. *Climate Policy*, 6(1), pp. 93-113.

Dietz, S., Bowen, A., Dixon, C., and Gradwell, P. (2016). Climate Value at Risk of Global Financial Assets. *Nature Climate Change,* 6(7), pp. 676-679.

Dietzenbacher, E., Los, B., Stehrer, R., Timmer, M., and De Vries, G. (2013). The Construction of World Input-output Tables in the WIOD Project. *Economic Systems Research*, 25(1), pp. 71-98.

Dixit, A. K., and Stiglitz, J. E. (1977). Monopolistic Competition and Optimum Product Diversity. *American Economic Review*, 67(3), pp. 297-308.

Dornbusch, R. (1987). Exchange Rates and Prices. *American Economic Review*, 77(1), pp. 93-106.

Drei, A., Le Guenedal, T., Lepetit, F., Mortier, V., Roncalli, T., and Sekine, T. (2019). ESG Investing in Recent Years: New Insights from Old Challenges. *SSRN*, 3683469.

Dunz, N., Emambakhsh, T., Hennig, T., ..., and Salleo, C. (2021). ECB's Economy-Wide Climate Stress Test. *ECB Occasional Paper*, 281.

Environmental Protection Agency (2022). *Report on the Social Cost of Greenhouse Gases: Estimates Incorporating Recent Scientific Advances*. United States Government, September 2022.

ESMA (2022). Sustainable Finance Roadmap (2022-2024). *Report*, 30-379-1051, 10 February 2022.

Fama, E. F. and Stern, J. M. (2016). A Look Back at Modern Finance: Accomplishments and Limitations. *Journal of Applied Corporate Finance*, 28(4), pp. 10-16.

Farhi, E., and Gabaix, X. (2020). Optimal Taxation with Behavioral Agents. *American Economic Review*, 110(1), pp. 298-336.

Financial Stability Board (2009). *Guidance to Assess the Systemic Importance of Financial Institutions, Markets and Instruments: Initial Considerations*. Report to the G-20 Finance Ministers and Central Bank Governors, October 2009.

Ganapati, S., Shapiro, J. S., and Walker, R. (2020). Energy Cost Pass-through in US Manufacturing: Estimates and Implications for Carbon Taxes. *American Economic Journal: Applied Economics*, 12(2), pp. 303-42.

Gemechu, E. D., Butnar, I., Llop, M., and Castells, F. (2014). Economic and Environmental effects of CO_2 Taxation: An Input-output Analysis for Spain. *Journal of Environmental Planning and Management*, 57(5), pp. 751-768.

Goulder, L. H. (2002). Environmental Taxation and the Double Dividend: A Reader's Guide. In Gouler, L. (Ed), *Environmental Policy Making in Economies with Prior Tax Distortions*, Edward Elgar Publishing, pp. 46-72.

Gourdel, R., and Sydow, M. (2021). Non-banks Contagion and the Uneven Mitigation of Climate Risk. *ECB Working Paper*, 2757.

Grippa, P., and Mann, S. (2018). Climate-Related Stress Testing: Transition Risks in Norway. *IMF Working Paper*, 232.

Gutierrez, M. S. (2008). *Economic Activity and Atmospheric Pollution in Spain: An Input-output Approach.* PhD Thesis, Universitat de Barcelona.

Ha, J., Stocker, M. M., and Yilmazkuday, H. (2020). Inflation and Exchange Rate Pass-through. *Journal of International Money and Finance*, 105, 102187.

Han, J., Tan, Z., Chen, M., Zhao, L., Yang, L., and Chen, S. (2022). Carbon Footprint Research Based on Input-Output Model — A Global Scientometric Visualization Analysis. *International Journal of Environmental Research and Public Health*, 19(18), 11343.

Harpankar, K. (2019). Internal Carbon Pricing: Rationale, Promise and Limitations. *Carbon Management*, 10(2), pp. 219-225.

Interagency Working Group on Social Cost of Greenhouse Gases (2015). *Technical Support Document: Technical Update of the Social Cost of Carbon for Regulatory Impact Analysis Under Executive Order 12866*. United States Government, July 2015.

Interagency Working Group on Social Cost of Greenhouse Gases (2021). *Technical Support Document: Social Cost of Carbon, Methane, and Nitrous Oxide, Interim Estimates under Executive Order 13990*. United States Government, February 2021.

Intergovernmental Panel on Climate Change (2018). Global Warming of 1.5°C. *Special Report*.

Intergovernmental Panel on Climate Change (2022). Climate Change 2022: Mitigation of Climate Change — Contribution of Working Group III to the Sixth Assessment Report of the IPCC. *Report*.

Jackson, R. W., Schwarm, W. R., Okuyama, Y., and Islam, S. (2006). A Method for Constructing Commodity by Industry Flow Matrices. *Annals of Regional Science*, 40, pp. 909-920.

Jourde, T., and Moreau, Q. (2022). Systemic Climate Risk. *SSRN*, 4300469.

Kitzes, J. (2013). An Introduction to Environmentally-extended Input-output Analysis. *Resources*, 2(4), pp. 489-503.

Le Guenedal, T. (2022). *Financial Modeling of Climate-related Risks*. PhD thesis, Institut Polytechnique de Paris.

Leontief, W. W. (1936). Quantitative Input and Output Relations in the Economic Systems of the United States. *Review of Economics and Statistics*, 18(3), pp. 105-125.

Leontief, W. W. (1941). *Structure of American Economy, 1919-1929: An Empirical Application of Equilibrium Analysis*. Harvard University Press.

Leontief, W. (1970). Environmental Repercussions and the Economic Structure: An Input-output Approach. *Review of Economics and Statistics*, 52(3), pp. 262-271.

Llop, M. (2008). Economic Impact of Alternative Water Policy Scenarios in the Spanish Production System: An Input-output Analysis. *Ecological Economics*, 68(1-2), pp. 288-294.

McKinsey & Company, and Ecofys (2006). *EU ETS Review: Report on International Competitiveness*. European Commission Directorate General for Environment, December.

Mardones, C., and Mena, C. (2020). Economic, Environmental and Distributive Analysis of the Taxes to Global and Local Air Pollutants in Chile. *Journal of Cleaner Production*, 259, 120893.

MILLER, R. E., and BLAIR, P. D. (2009). *Input-output Analysis: Foundations and Extensions*. Second edition, Cambridge University Press.

MINX, J. C., WIEDMANN, T., WOOD, R., ..., and ACKERMAN, F. (2009). Input-output Analysis and Carbon Footprinting: An Overview of Applications. *Economic Systems Research*, 21(3), pp. 187-216.

NAKANO, S., and WASHIZU, A. (2022). A Study on Energy Tax Reform for Carbon Pricing Using an Input-Output Table for the Analysis of a Next-Generation Energy System. *Energies*, 15(6), 2162.

NAQVI, A., and MONASTEROLO, I. (2021). Assessing the Cascading Impacts of Natural Disasters in a Multi-layer Behavioral Network Framework. *Scientific Reports*, 11, 20146.

NGFS (2020). Guide to Climate Scenario Analysis for Central Banks and Supervisors. *Report*, June.

NGFS (2022). NGFS Scenarios for Central Banks and Supervisors. *Report*, September.

NGUYEN, Q., DIAZ-RAINEY, I., and KURUPPUARACHCHI, D. (2021). Predicting Corporate Carbon Footprints for Climate Finance Risk Analyses: A Machine Learning Approach. *Energy Economics*, 95, 105129.

NORDHAUS, W. D. (1991). To Slow or Not to Slow: The Economics of the Greenhouse Effect. *Economic Journal*, 101(407), pp. 920-937.

NORDHAUS, W. D. (2017). Revisiting the Social Cost of Carbon. *Proceedings of the National Academy of Sciences*, 114(7), pp. 1518-1523.

OBERNDORFER, U., ALEXEEVA-TALEBI, V., and LÖSCHEL, A. (2010). Understanding the Competitiveness Implications of Future Phases of EU ETS on the Industrial Sectors. *ZEW Discussion Paper*, 10-044.

PERESE, K. (2010). Input-Output Model Analysis: Pricing Carbon Dioxide Emissions. *Tax Analysis Division, Congressional Budget Office Working Paper Series*, Washington, DC.

PONSSARD, J. P., and WALKER, N. (2008). EU Emissions Trading and the Cement Sector: A Spatial Competition Analysis. *Climate Policy*, 8(5), pp. 467-493.

POUPARD, A., FETET, M., and POSTIC, S. (2022). Global Carbon Accounts in 2022. *Climate Brief*, *Institute for Climate Economics*, September, 11 pages.

RAYMOND, C., HORTON, R. M., ZSCHEISCHLER, J., ..., and WHITE, K. (2020). Understanding and Managing Connected Extreme Events. *Nature climate change*, 10(7), pp. 611-621.

RBB Economics (2014). Cost Pass-through: Theory, Measurement, and Potential Policy Implications. *A Report prepared for the Office of Fair Trading*, February.

REINDERS, H. J., SCHOENMAKER, D., and VAN DIJK, M. (2023). A Finance Approach to Climate Stress Testing. *Journal of International Money and Finance*, 131, 102797.

RENNERT, K., PREST, B. C., PIZER, W. A., ..., and ERRICKSON, F. (2022). The Social Cost of Carbon: Advances in Long-term Probabilistic Projections of Population, GDP, Emissions, and Discount Rates. *Brookings Papers on Economic Activity*, Fall, pp. 223-305.

Richards, T. J., and Pofahl, G. M. (2009). Commodity Prices and Food Inflation. *American Journal of Agricultural Economics*, 91(5), pp. 1450-1455.

Richters, O., Bertram, C., Kriegler, E., ..., and Zwerling, M. (2022). NGFS Climate Scenario Database. *Technical Documentation*, V3.1, November.

Roncalli, T. (2020). *Handbook of Financial Risk Management*. Chapman and Hall/CRC Financial Mathematics Series.

Roncalli, T. (2023). *Handbook of Sustainable Finance*. *SSRN*, 4277875.

Roncalli, T., Le Guenedal, T., Lepetit, F., Roncalli, T., and Sekine, T. (2020). Measuring and Managing Carbon Risk in Investment Portfolios. *SSRN*, 3681266.

Roncalli, T., Le Guenedal, T., Lepetit, F., Roncalli, T., and Sekine, T. (2021). The Market Measure of Carbon Risk and its Impact on the Minimum Variance Portfolio. *Journal of Portfolio Management*, 47(9), pp. 54-68.

Roncoroni, A., Battiston, S., Escobar-Farfán, L. O., and Martinez-Jaramillo, S. (2021). Climate Risk and Financial Stability in the Network of Banks and Investment Funds. *Journal of Financial Stability*, 54, 100870.

Rose, S. K., Diaz, D. B., and Blanford, G. J. (2017). Understanding the Social Cost of Carbon: A Model Diagnostic and Inter-comparison Study. *Climate Change Economics*, 8(02), 1750009.

Sautel, O., Mini, C., Bailly, H., and Dieye, R. (2022). *La tarification du carbone et ses répercussions. Exposition sectorielle au surcoût carbone.* Les Notes de La Fabrique, Presses des Mines.

Schechter, E. (1996). *Handbook of Analysis and its Foundations*. Academic Press.

Schweimayer, G., and Stoyanova, N. (2022). Incorporating ESG Risk In Fundamental Market Risk Models. *Amundi Working paper*, 134.

Seiler, S., Tuchman, A., and Yao, S. (2021). The Impact of Soda Taxes: Pass-through, Tax Avoidance, and Nutritional Effects. *Journal of Marketing Research*, 58(1), pp. 22-49.

Semet, R. (2023). The Impact of Climate Risks on Social Inequality. *SSRN*, 4322639.

Shrestha, V., and Markowitz, S. (2016). The Pass-through of Beer Taxes to Prices: Evidence from State and Federal Tax Changes. *Economic Inquiry*, 54(4), pp. 1946-1962.

Shrimali, G. (2022). Scope 3 Emissions: Measurement and Management. *Journal of Impact and ESG Investing*, 3(1), pp. 31-54.

Sijm, J., Neuhoff, K., and Chen, Y. (2006). CO_2 Cost Pass-through and Windfall Profits in the Power Sector. *Climate Policy*, 6(1), pp. 49-72.

Stadler, K. (2021). Pymrio: A Python Based Multi-regional Input-Output Analysis Toolbox. *Journal of Open Research Software*, 9(1), pp. 1-8.

Stadler, K., Wood, R., Bulavskaya, T., ..., and Tukker, A. (2018). EXIOBASE 3: Developing a Time Series of Detailed Environmentally Extended Multi-Regional Input-Output Tables. *Journal of Industrial Ecology*, 22(3), pp. 502-515.

TIMMER, M. P., DIETZENBACHER, E., LOS, B., STEHRER, R., and DE VRIES, G. J. (2015). An Illustrated User Guide to the World Input-Output Database: The Case of Global Automotive Production. *Review of International Economics*, 23(3), pp. 575-605.

TUKKER, A., DE KONING, A., WOOD, R., ..., and KUENEN, J. (2013). EXIOPOL — Development and Illustrative Analyses of a Detailed Global MR EE SUT/IOT. *Economic Systems Research*, 25(1), pp. 50-70.

Vivid Economics (2014). Case Studies: Report Prepared for DECC. *Final Report*, June.

VERMEULEN, R., SCHETS, E., LOHUIS, M., KÖLBL, B., JANSEN, D.-J., and HEERINGA, W. (2018). An Energy Transition Risk Stress Test for the Financial System of the Netherlands. *DNB Occasional Studies*, 16(7).

WAGNER, G. (2021). Recalculate the Social Cost of Carbon. *Nature Climate Change*, 11(4), pp. 293-294.

WAGNER, G., ANTHOFF, D., CROPPER, M., ..., and STOCK, J. H. (2021). Eight Priorities for Calculating the Social Cost of Carbon. *Nature*, 590(7847), pp. 548-550.

WANG, P., DENG, X., ZHOU, H., and YU, S. (2019). Estimates of the Social Cost of Carbon: A Review Based on Meta-Analysis. *Journal of Cleaner Production*, 209, pp. 1494-1507.

WEYL, E. G., and FABINGER, M. (2013). Pass-through as An Economic Tool: Principles of Incidence under Imperfect Competition. *Journal of Political Economy*, 121(3), pp. 528-583.

WIEDMANN, T. (2009). A Review of Recent Multi-region Input-output Models used for Consumption-based Emission and Resource Accounting. *Ecological Economics*, 69(2), pp. 211-222.

World Bank (2021). State and Trends of Carbon Pricing 2021. *Report*.

ZHANG, H., HEWINGS, G. J., and ZHENG, X. (2019). The Effects of Carbon Taxation in China: An Analysis based on Energy Input-output Model in Hybrid Units. *Energy Policy*, 128, pp. 223-234.

A Technical appendix

A.1 Notations

Table 41: Notations

	Symbol	Description
Carbon footprint (GHG Protocol)	$\boldsymbol{\mathcal{CE}}$	Carbon emissions
	$\boldsymbol{\mathcal{CI}}$	Carbon intensity
	$\boldsymbol{\mathcal{SC}}_1$	Scope 1
	$\boldsymbol{\mathcal{SC}}_2$	Scope 2
	$\boldsymbol{\mathcal{SC}}_3^{\mathrm{up}}$	Upstream scope 3
	$\boldsymbol{\mathcal{SC}}_3^{\mathrm{down}}$	Downstream scope 3
	$\boldsymbol{\mathcal{SC}}_3$	Scope 3 ($= \boldsymbol{\mathcal{SC}}_3^{\mathrm{up}} + \boldsymbol{\mathcal{SC}}_3^{\mathrm{down}}$)
	$\boldsymbol{\mathcal{SC}}_{1-2}$	Scope $1 + 2$
	$\boldsymbol{\mathcal{SC}}_{1-3}^{\mathrm{up}}$	Upstream scope $1 + 2 + 3$ ($= \boldsymbol{\mathcal{SC}}_1 + \boldsymbol{\mathcal{SC}}_2 + \boldsymbol{\mathcal{SC}}_3^{\mathrm{up}}$)
	$\boldsymbol{\mathcal{SC}}_{1-3}$	Scope $1 + 2 + 3$
Leontief analysis	x_i	Sector i production
	$Z_{i,j}$	Sector i to sector j transaction
	y_i	Sector i final demand
	A	Direct output matrix
	$\breve{A}$	Direct input matrix
	$\boldsymbol{\mathcal{L}}$	Leontief inverse matrix
	$\tilde{\boldsymbol{\mathcal{L}}}$	Dual inverse (or upstream) matrix
	$\breve{\boldsymbol{\mathcal{L}}}$	Downstream multiplier matrix
	Φ	Pass-through matrix
Carbon footprint (EEIO analysis)	$\boldsymbol{\mathcal{CI}}_{\mathrm{total}}^{\mathrm{up}}$	Total upstream intensity
	$\boldsymbol{\mathcal{CI}}_{\mathrm{total}}^{\mathrm{down}}$	Total downstream intensity
	$\boldsymbol{\mathcal{CI}}_{\mathrm{indirect}}^{\mathrm{up}}$	Indirect upstream intensity
	$\boldsymbol{\mathcal{CI}}_{\mathrm{indirect}}^{\mathrm{down}}$	Indirect downstream intensity
	$\boldsymbol{\mathcal{CI}}_{(k)}^{\mathrm{up}}$	k^{th}-tier upstream intensity
	$\boldsymbol{\mathcal{CI}}_{(1-k)}^{\mathrm{up}}$	First k tier upstream intensity
	$\boldsymbol{\mathcal{CI}}_{(k)}^{\mathrm{down}}$	k^{th}-tier downstream intensity
	$\boldsymbol{\mathcal{CI}}_{(1-k)}^{\mathrm{down}}$	First k tier downstream intensity

A.2 Calibration of the log-normal distribution (social cost of carbon)

We assume that $\mathrm{SCC} \sim \mathcal{LN}\left(\mu, \sigma^2\right)$ and $\mathrm{SCC}(\alpha) = k_\alpha \mathbb{E}[\mathrm{SCC}]$. Moreover, we consider that $m_{\mathrm{SCC}} = \mathbb{E}[\mathrm{SCC}]$ and k_α are given. We deduce that μ and σ satisfy the following system of non-linear equations:

$$\left\{ \begin{array}{l} \mathbb{E}[\mathrm{SCC}] = \exp\left(\mu + \dfrac{1}{2}\sigma^2\right) = m_{\mathrm{SCC}} \\ \mathrm{SCC}(\alpha) = \exp\left(\mu + \Phi^{-1}(\alpha)\,\sigma\right) = k_\alpha m_{\mathrm{SCC}} \end{array} \right.$$

It follows that $\ln m_{\mathrm{SCC}} = \mu + \frac{1}{2}\sigma^2$ and $\ln k_\alpha + \ln m_{\mathrm{SCC}} = \mu + \Phi^{-1}(\alpha)\,\sigma$. We obtain a second-order polynomial equation:

$$\frac{1}{2}\sigma^2 - \Phi^{-1}(\alpha)\,\sigma + \ln k_\alpha = 0$$

Since the discriminant is equal to $\Delta = \Phi^{-1}(\alpha)^2 - 2\ln k_\alpha$, we obtain a solution if and only if $k_\alpha \leq k_\alpha^\star = \exp\left(\frac{1}{2}\Phi^{-1}(\alpha)^2\right)$. Below, we give the value of the threshold $k_\alpha^\star$ for typical values of α:

α	0.75	0.85	0.90	0.95	0.99
$k_\alpha^\star$	1.26	1.71	2.27	3.87	14.97

We notice that we have two positive roots σ' and σ''. One solution produces a bell-shape distribution, while the other solution exhibits a high kurtosis and corresponds to a L-shape distribution with a near-zero mode. Therefore, it is better to select the solution with the lowest value of σ. Finally, the solution are:

$$\mu' = \ln k_\alpha + \ln m_{\mathrm{SCC}} - \Phi^{-1}(\alpha)^2 + \Phi^{-1}(\alpha)\sqrt{\Phi^{-1}(\alpha)^2 - 2\ln k_\alpha}$$

and:

$$\sigma' = \Phi^{-1}(\alpha) - \sqrt{\Phi^{-1}(\alpha)^2 - 2\ln k_\alpha}$$

To illustrate the previous calibration approach, we assume that $m_{\mathrm{SCC}} = \$50/\mathrm{tCO}_2$ and $k_{95\%} = 3$. The solution is then $\mu' = 3.48$ and $\sigma' = 0.93$, and we report the corresponding probability density function in Figure 80. We notice that the second solution $(\mu' = 1.13, \sigma' = 2.36)$ produces a L-shape distribution.

Figure 80: Calibrated probability distribution of the SCC ($m_{\mathrm{SCC}} = \$50/\mathrm{tCO}_2$ and $k_{95\%} = 3$)

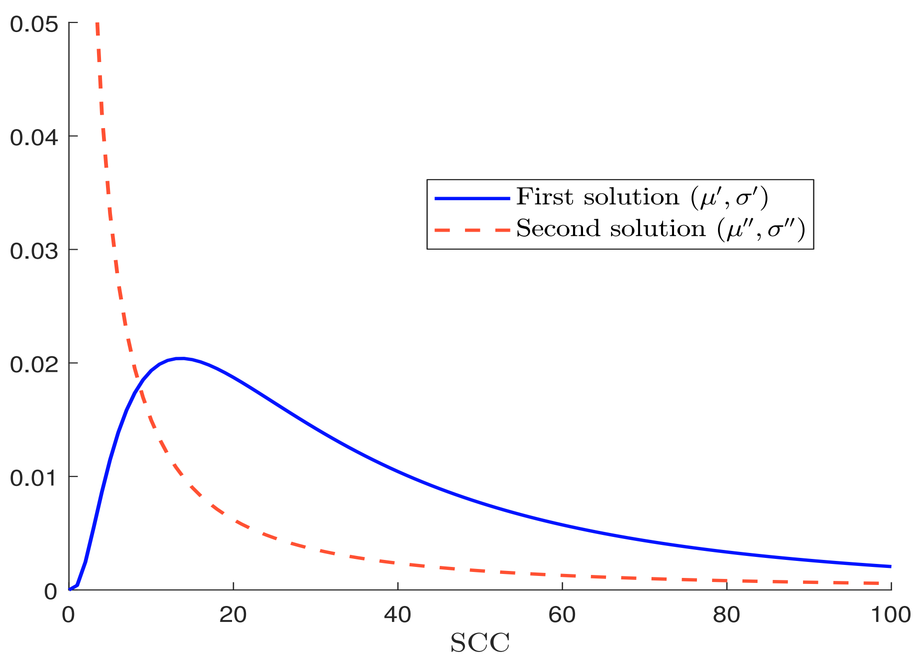

A.3 Downstream analysis of Example #2

Using the data given in Table 10 on page 39, we compute the downstream matrix $\breve{A}$:

$$\begin{aligned}\breve{A} &= \operatorname{diag}(x)^{-1} Z \\ &= \operatorname{diag}(x)^{-1} A \operatorname{diag}(x) \\ &= \begin{pmatrix} 0.10000 & 0.16000 & 0.32000 & 0.25000 \\ 0.12500 & 0.10000 & 0.40000 & 0.15625 \\ 0.03125 & 0.10000 & 0.30000 & 0.15625 \\ 0.00800 & 0.01600 & 0.06400 & 0.35000 \end{pmatrix}\end{aligned}$$

where the output vector x is equal to the ratio between scope 1 carbon emissions and intensities. We deduce the downstream multiplier matrix:

$$\breve{\mathcal{L}} = \begin{pmatrix} 1.18811 & 0.31149 & 0.78705 & 0.72104 \\ 0.20970 & 1.25525 & 0.86717 & 0.59085 \\ 0.08938 & 0.20550 & 1.63035 & 0.47568 \\ 0.02859 & 0.05497 & 0.19156 & 1.60872 \end{pmatrix}$$

In Tables 42, 43 and 44, we report the downstream carbon intensities and emissions. These figures can be compared to those obtained in the case of the upstream analysis (Tables 11, 12 and 13 on pages 39–42).

Table 42: Direct and indirect downstream carbon intensities (Example #2)

Sector	$\mathcal{CI}_1$	$\mathcal{CI}_{\text{total}}^{\text{down}}$	$\mathcal{CI}_{\text{direct}}^{\text{down}}$	$\mathcal{CI}_{\text{indirect}}^{\text{down}}$	$\mathcal{CI}_{\text{direct}}^{\text{down}}$	$\mathcal{CI}_{\text{indirect}}^{\text{down}}$	$\frac{\mathcal{CI}_{\text{total}}^{\text{down}}}{\mathcal{CI}_1}$
	(in tCO_2e/\$ mn)				(in %)		
Energy	100.00	161.27	100.00	61.27	62.01%	37.99%	1.61
Materials	50.00	111.32	50.00	61.32	44.92%	55.08%	2.23
Industrials	25.00	64.73	25.00	39.73	38.62%	61.38%	2.59
Services	10.00	26.48	10.00	16.48	37.76%	62.24%	2.65

Table 43: Tier decomposition of downstream carbon intensities (Example #2)

	Sector	1	2	3	4	5	10	15	∞
$\mathcal{CI}_{(k)}^{\text{down}}$	Energy	28.50	14.68	8.00	4.45	2.48	0.14	0.00	0.00
	Materials	29.06	14.39	7.92	4.39	2.45	0.13	0.01	0.00
	Industrials	17.19	10.00	5.54	3.09	1.72	0.09	0.01	0.00
	Services	6.70	4.14	2.44	1.40	0.79	0.04	0.00	0.00
$\mathcal{CI}_{(1-k)}^{\text{down}}$	Energy	28.50	43.17	51.18	55.63	58.11	61.10	61.26	61.27
	Materials	29.06	43.45	51.37	55.76	58.21	61.15	61.31	61.32
	Industrials	17.19	27.19	32.73	35.82	37.54	39.61	39.72	39.73
	Services	6.70	10.84	13.27	14.67	15.46	16.43	16.48	16.48

We notice that the results of the downstream analysis are different. While the energy and materials sectors have the lowest upstream indirect emissions, they have the highest downstream emissions. The reason lies in the structure of the supply chain. Most of output from energy and materials sectors are destined to be used by the value chain to produce goods and services. On the contrary, industrials and services sectors requires a lot of output from the value chain to directly produce goods and services. In this context, carbon emissions generally move down for energy and materials sectors, while they move up for industrials and services sectors.

Table 44: Breakdown of downstream carbon emissions (Example #2)

Sector	$\mathcal{CE}^{\text{down}}_{\text{direct}}$	$\mathcal{CE}^{\text{down}}_{\text{indirect}}$ (in ktCO_2e)	$\mathcal{CE}^{\text{down}}_{\text{total}}$	$\mathcal{CE}^{\text{down}}_{\text{direct}}$	$\mathcal{CE}^{\text{down}}_{\text{indirect}}$ (in %)	$\mathcal{CE}^{\text{down}}_{\text{total}}$
Energy	500	267.30	767.30	48.78	21.70	34.00
Materials	200	169.08	369.08	19.51	13.72	16.35
Industrials	200	429.23	629.23	19.51	34.84	27.88
Services	125	366.31	491.31	12.20	29.73	21.77
Total	1 025	1 231.91	2 256.91	100.00	100.00	100.00

A.4 Derivation of the upstreamness index

We notice that:

$$\frac{\partial \left(I_n - A^\top\right)^{-1}}{\partial A^\top} = \left(I_n - A^\top\right)^{-1}\left(I_n - A^\top\right)^{-1}$$

and:

$$\frac{\partial \sum_{k=0}^{\infty}\left(A^\top\right)^k}{\partial A^\top} = \sum_{k=0}^{\infty} k\left(A^\top\right)^{k-1}$$

It follows that:

$$\begin{aligned}
\sum_{k=0}^{\infty} k\left(A^\top\right)^k &= A^\top \sum_{k=0}^{\infty} k\left(A^\top\right)^{k-1} \\
&= A^\top \frac{\partial \sum_{k=0}^{\infty}\left(A^\top\right)^k}{\partial A^\top} \\
&= A^\top \frac{\partial \left(I_n - A^\top\right)^{-1}}{\partial A^\top} \\
&= A^\top \left(I_n - A^\top\right)^{-1}\left(I_n - A^\top\right)^{-1}
\end{aligned}$$

Finally, we deduce that:

$$\begin{aligned}
\sum_{k=0}^{\infty} k \cdot \mathcal{CI}^{\text{up}}_{(k)} &= \left(\sum_{k=0}^{\infty} k\left(A^\top\right)^k\right)\mathcal{CI}_1 \\
&= A^\top \left(I_n - A^\top\right)^{-1}\left(I_n - A^\top\right)^{-1}\mathcal{CI}_1
\end{aligned}$$

and:

$$\tau^{\text{up}}_j = \frac{\left(A^\top\left(I_n - A^\top\right)^{-1}\left(I_n - A^\top\right)^{-1}\mathcal{CI}_1\right)_j}{\left(\left(I_n - A^\top\right)^{-1}\mathcal{CI}_1\right)_j}$$

A.5 Sector and region aggregation/mapping in input-output matrices

We consider a multi-regional input-output table (Z, x) with $n_{\mathcal{S}}$ sectors (or industries) and $n_{\mathcal{C}}$ countries (or regions) defined by $Z = \left(Z_{i,j}\right)$ and $x = (x_i)$. We note $Z(\mathcal{C}_1, \mathcal{C}_2) = \left\{\left(Z_{i,j}\right) : i \in \mathcal{C}_1 \wedge j \in \mathcal{C}_2\right\}$ the submatrix of Z, whose rows belong to country $\mathcal{C}_1$ and columns belong to country $\mathcal{C}_2$. In a similar way, we define $x(\mathcal{C}) = \{(x_i) : i \in \mathcal{C}\}$ the country subvector of x corresponding to country $\mathcal{C}$. We assume that the sectors are arranged in the same order whatever the given country. Let $\mathbb{S}$ be the original sector classification. We would like to map $\mathbb{S}$ to a new sector classification $\mathbb{S}^*$ with $n_{\mathcal{S}^*}$ sectors. This is equivalent to apply the $n_{\mathcal{S}} \times n_{\mathcal{S}^*}$ mapping matrix $M = (M_{i,j})$ with $M_{i,j} = \mathcal{M}ap(i,j)$, where the mapping function is defined as:

$$\mathcal{M}ap(i,j) = \begin{cases} 1 & \text{if } \{i \in \mathbb{S}\} \in \{j \in \mathbb{S}^\star\} \\ 0 & \text{otherwise} \end{cases}$$

We have:

$$Z^*(\mathcal{C}_1, \mathcal{C}_2) = M^\top Z(\mathcal{C}_1, \mathcal{C}_2) M$$

and:

$$x^*(\mathcal{C}) = M^\top x(\mathcal{C})$$

We can collect the different matrices $Z^*(\mathcal{C}_1, \mathcal{C}_2)$ and $x^*(\mathcal{C})$ in order to form the new multi-regional input-output table (Z^*, x^*). Another solution is to apply the augmented mapping matrix $I_{n_\mathcal{C}} \otimes M$. We obtain $Z^* = (I_{n_\mathcal{C}} \otimes M^\top) Z (I_{n_\mathcal{C}} \otimes M)$ and $x^* = (I_{n_\mathcal{C}} \otimes M^\top) x$. We can then compute the matrix $A^* = \left(A^*_{i,j}\right)$ for the new sector classification since the technical coefficients are equal to $A^*_{i,j} = Z^*_{i,j}/x_j$.

To perform an aggregating by region, we use the same technique. Let (Z, x) be the original input-output table. We would like to map the region classification $\mathbb{C}$ to a new region classification $\mathbb{C}^*$ with $n_{\mathcal{C}^*}$ sectors. The dimension of the mapping matrix M becomes $n_\mathcal{C} \times n_{\mathcal{C}^*}$ while the mapping function is defined as $\mathcal{M}ap(i,j) = 1$ if $\{i \in \mathbb{C}\} \in \{j \in \mathbb{C}^\star\}$ and $\mathcal{M}ap(i,j) = 0$ otherwise. Finally, we have $Z^* = (M^\top \otimes I_{n_\mathcal{S}}) Z (M \otimes I_{n_\mathcal{S}})$ and $x^* = (M^\top \otimes I_{n_\mathcal{S}}) x$.

A.6 Product of log-normal random variables

Let $X = (X_1, \ldots, X_n) \sim \mathcal{LN}(\mu, \Sigma)$ be a log-normal random vector. We consider the following transformation: $X_i = e^{Z_i}$ where $Z = (Z_1, \ldots, Z_n) \sim \mathcal{N}(\mu, \Sigma)$ is a Gaussian random vector. It follows that $\mu = (\mu_1, \ldots, \mu_n)$ is the mean vector of Z, $\Sigma = (\Sigma_{i,j})$ is the covariance matrix of Z and $\Sigma_{i,j} = \rho_{i,j}\sigma_i\sigma_j$ is the covariance between Z_i and Z_j. We denote by $Y = \prod_{i=1}^n X_i$ the product of X_i's. We deduce that:

$$Y = \prod_{i=1}^n X_i = \prod_{i=1}^n e^{Z_i} = e^{\sum_{i=1}^n Z_i} = e^{Z^\star}$$

where $Z^\star \sim \mathcal{N}(\mu_z, \sigma_z^2)$, $\mu_z = \mathbb{E}[Z^\star] = \sum_{i=1}^n \mu_i = \mathbf{1}_n^\top \mu$ and $\sigma_z^2 = \operatorname{var}(Z^\star) = \sum_{i=1}^n \sigma_i^2 + 2\sum_{i>j} \rho_{i,j}\sigma_i\sigma_j = \mathbf{1}_n^\top \Sigma \mathbf{1}_n$. Finally, we conclude that Y is a log-normal random variable:

$$Y = \prod_{i=1}^n X_i \sim \mathcal{LN}\left(\mathbf{1}_n^\top \mu, \mathbf{1}_n^\top \Sigma \mathbf{1}_n\right)$$

In the case of two independent log-normal random variables, we have:

$$X_1 X_2 \sim \mathcal{LN}\left(\mu_1 + \mu_2, \sigma_1^2 + \sigma_2^2\right)$$

A.7 Calibration of the multiplying coefficient (upstream emissions)

A.7.1 The mean-decreasing case

We assume that $\tilde{m}_{(0-k)} \sim \mathcal{SLN}\left(\mu_{\mathcal{C},\mathcal{S}}, \sigma_{\mathcal{C},\mathcal{S}}, \xi\right)$ and $\breve{m}_{(0-k)} - \xi = \left(\tilde{m}_{(0-k)} - \xi\right) \tilde{\varphi}_i$ where $\tilde{\varphi}_i \sim \mathcal{LN}\left(\mu_i, \sigma_i^2\right)$. We deduce that:

$$\mathbb{E}\left[\breve{m}_{(0-k)} - \xi\right] = \mathbb{E}\left[\tilde{m}_{(0-k)} - \xi\right] e^{\mu_i + 0.5\sigma_i^2}$$

If we assume that $\mathbb{E}\left[\tilde{m}_{(0-k)}\right] = m_i$, it follows that:

$$\mu_i + \frac{1}{2}\sigma_i^2 = \ln \frac{m_i - \xi}{\mathbb{E}\left[\tilde{m}_{(0-k)}\right] - \xi} = \ln R_i \tag{39}$$

where R_i is the ratio between $m_i - \xi$ and $\mathbb{E}\left[\tilde{m}_{(0-k)}\right] - \xi$. The variance of $\breve{m}_{(0-k)}$ has the following expression:

$$\operatorname{var}\left(\breve{m}_{(0-k)}\right) = \left(e^{\sigma_{\mathcal{C},\mathcal{S}}^2 + \sigma_i^2} - 1\right) e^{2\left(\mu_{\mathcal{C},\mathcal{S}} + \mu_i\right) + \left(\sigma_{\mathcal{C},\mathcal{S}}^2 + \sigma_i^2\right)}$$

The equation $\operatorname{var}\left(\breve{m}_{(0-k)}\right) = \operatorname{var}\left(\tilde{m}_{(0-k)}\right)$ implies that:

$$\begin{aligned}(*) \quad &\Leftrightarrow \quad \left(e^{\sigma_{\mathcal{C},\mathcal{S}}^2 + \sigma_i^2} - 1\right) e^{2\left(\mu_{\mathcal{C},\mathcal{S}} + \mu_i\right) + \left(\sigma_{\mathcal{C},\mathcal{S}}^2 + \sigma_i^2\right)} = \left(e^{\sigma_{\mathcal{C},\mathcal{S}}^2} - 1\right) e^{2\mu_{\mathcal{C},\mathcal{S}} + \sigma_{\mathcal{C},\mathcal{S}}^2} \\ &\Leftrightarrow \quad \left(e^{\sigma_{\mathcal{C},\mathcal{S}}^2 + \sigma_i^2} - 1\right) e^{2\mu_i + \sigma_i^2} = \left(e^{\sigma_{\mathcal{C},\mathcal{S}}^2} - 1\right)\end{aligned}$$

Using Equation (39), it comes that:

$$\left(e^{\sigma_{\mathcal{C},\mathcal{S}}^2 + \sigma_i^2} - 1\right) = \frac{\left(e^{\sigma_{\mathcal{C},\mathcal{S}}^2} - 1\right)}{R_i^2}$$

If the solution exists, it is equal to:

$$\sigma_i^2 = \ln\left(1 + \frac{\left(e^{\sigma_{\mathcal{C},\mathcal{S}}^2} - 1\right)}{R_i^2}\right) - \sigma_{\mathcal{C},\mathcal{S}}^2$$

and:

$$\mu_i = \ln \frac{m_i - \xi}{\mathbb{E}\left[\tilde{m}_{(0-k)}\right] - \xi} - \frac{1}{2}\sigma_i^2$$

The solution exists if and only if the following condition is satisfied:

$$\begin{aligned}(*) \quad &\Leftrightarrow \quad 1 + \frac{e^{\sigma_{\mathcal{C},\mathcal{S}}^2} - 1}{R_i^2} \geq e^{\sigma_{\mathcal{C},\mathcal{S}}^2} \\ &\Leftrightarrow \quad e^{\sigma_{\mathcal{C},\mathcal{S}}^2} - 1 \geq R_i^2\left(e^{\sigma_{\mathcal{C},\mathcal{S}}^2} - 1\right) \\ &\Leftrightarrow \quad R_i^2 \leq 1\end{aligned}$$

We deduce that the condition is $R_i \in [0, 1]$ because $\mathbb{E}\left[\tilde{m}_{(0-k)}\right] > \xi$ and $m_i > \xi$. This means that we can decrease the mean by preserving the variance, but not the contrary. The reason is the following. The variance of a log-normal random variable $\mathcal{LN}\left(\mu, \sigma^2\right)$ is an increasing function of the mean parameter μ. Since $R_i > 1$ increases μ, it also increases the variance.

A.7.2 The mean-increasing case

In the case $R_i > 1$, we would like to find the optimal values of (μ_i, σ_i) such that we minimize the variance of $\breve{m}_{(0-k)}$ subject to the constraints $\mathbb{E}\left[\tilde{m}_{(0-k)}\right] = m_i$ and $\sigma_i^2 \geq 0$. The Lagrange function associated to this problem is:

$$\begin{aligned} f\left(\mu_i, \sigma_i^2, \lambda_m, \lambda_\sigma\right) &= \left(e^{\sigma^2_{\mathcal{C},\mathcal{S}}+\sigma_i^2} - 1\right) e^{2\left(\mu_{\mathcal{C},\mathcal{S}}+\mu_i\right)+\left(\sigma^2_{\mathcal{C},\mathcal{S}}+\sigma_i^2\right)} - \\ & \quad \lambda_m \left(\xi + e^{\left(\mu_{\mathcal{C},\mathcal{S}}+\mu_i\right)+0.5\left(\sigma^2_{\mathcal{C},\mathcal{S}}+\sigma_i^2\right)} - m_i\right) - \lambda_\sigma \sigma_i^2 \end{aligned}$$

Since we have $e^{\left(\mu_{\mathcal{C},\mathcal{S}}+\mu_i\right)+0.5\left(\sigma^2_{\mathcal{C},\mathcal{S}}+\sigma_i^2\right)} = m_i - \xi$, the first-order conditions are:

$$\frac{\partial\, f\left(\mu_i, \sigma_i^2, \lambda_m, \lambda_\sigma\right)}{\partial\, \mu_i} = 2\left(e^{\sigma^2_{\mathcal{C},\mathcal{S}}+\sigma_i^2} - 1\right)\left(m_i - \xi\right)^2 - \lambda_m\left(m_i - \xi\right) = 0$$

and:

$$\frac{\partial\, f\left(\mu_i, \sigma_i^2, \lambda_m, \lambda_\sigma\right)}{\partial\, \sigma_i^2} = \left(2e^{\sigma^2_{\mathcal{C},\mathcal{S}}+\sigma_i^2} - 1\right)\left(m_i - \xi\right)^2 - \frac{\lambda_m}{2}\left(m_i - \xi\right) - \lambda_\sigma = 0$$

while the Kuhn-Tucker condition is $\min\left(\lambda_\sigma, \sigma_i^2\right) = 0$. We deduce that:

$$2e^{\sigma^2_{\mathcal{C},\mathcal{S}}+\sigma_i^2}\left(m_i - \xi\right)^2 - 2\lambda_\sigma = 0$$

Let us assume that $\lambda_\sigma = 0$. The Kuhn–Tucker condition implies that $\sigma_i^2 > 0$. The previous equation becomes then $2e^{\sigma^2_{\mathcal{C},\mathcal{S}}+\sigma_i^2}\left(m_i - \xi\right)^2 = 0$, but it has no solution since $m_i - \xi > 0$. Therefore, the only solution is reached when $\lambda_\sigma > 0$ and $\sigma_i^2 = 0$. We deduce that the optimal values are:

$$\left\{\begin{array}{rcl} \mu_i &=& \ln\left(m_i - \xi\right) - \left(\mu_{\mathcal{C},\mathcal{S}} + \frac{1}{2}\sigma^2_{\mathcal{C},\mathcal{S}}\right) \\ \sigma_i &=& 0 \\ \lambda_m &=& 2\left(e^{\sigma^2_{\mathcal{C},\mathcal{S}}} - 1\right)\left(m_i - \xi\right) \\ \lambda_\sigma &=& e^{\sigma^2_{\mathcal{C},\mathcal{S}}}\left(m_i - \xi\right)^2 \end{array}\right.$$

This solution is equivalent to using the scaling factor:

$$\begin{aligned} \lambda &= \exp\left(\ln\left(m_i - \xi\right) - \left(\mu_{\mathcal{C},\mathcal{S}} + \frac{1}{2}\sigma^2_{\mathcal{C},\mathcal{S}}\right)\right) \\ &= \frac{m_i - \xi}{e^{\mu_{\mathcal{C},\mathcal{S}}+\frac{1}{2}\sigma^2_{\mathcal{C},\mathcal{S}}}} \\ &= \frac{m_i - \xi}{\mathbb{E}\left[\tilde{m}_{(0-k)}\right] - \xi} \end{aligned}$$

The minimum standard deviation of $\breve{m}_{(0-k)}$ is then equal to $\lambda\sigma\left(\tilde{m}_{(0-k)}\right)$.

A.8 Ordering properties of nonnegative matrices

Let A, B, C and D be nonnegative square matrices. We can show that:

(NN1) $A \succeq B \Rightarrow AC \succeq BC$;

(NN2) $A \succeq B \wedge C \succeq D \Rightarrow AC \succeq BD$;

(NN3) $A \succeq B \wedge C \succeq D \Rightarrow A + C \succeq B + D$;

(NN4) $A \succeq B \wedge k \geq 1 \Rightarrow A^k \succeq B^k$;

The proof of the first property NN1 is the following. We have $(AC)_{i,j} = \sum_{k=1}^n A_{i,k}C_{k,j}$ and $(BC)_{i,j} = \sum_{k=1}^n B_{i,k}C_{k,j}$. Since we have $A_{i,k} \geq B_{i,k}$ and $C_{k,j} \geq 0$, we deduce that $A_{i,k}C_{k,j} \geq B_{i,k}C_{k,j}$ and $(AC)_{i,j} \geq (BC)_{i,j}$. This implies that $AC \succeq BC$. For the second property NN2, we have $(AC)_{i,j} = \sum_{k=1}^n A_{i,k}C_{k,j}$, $(BD)_{i,j} = \sum_{k=1}^n B_{i,k}D_{k,j}$, $A_{i,k}C_{k,j} \geq B_{i,k}D_{k,j}$, $(AC)_{i,j} \geq (BD)_{i,j}$ and $AC \succeq BD$. Property NN3 holds because $A_{i,j} \geq B_{i,j}$ and $C_{i,j} \geq D_{i,j}$ implies $A_{i,j} + C_{i,j} \geq B_{i,j} + D_{i,j}$. The fourth property NN4 is a consequence of the second property. Let us assume that $A \succeq B \Rightarrow A^k \succeq B^k$. We deduce that $A \succeq B \wedge A^k \succeq B^k \Rightarrow AA^k \succeq BB^k$ or $A \succeq B \wedge A^k \succeq B^k \Rightarrow A^{k+1} \succeq B^{k+1}$. Moreover, we have $A \succeq B \wedge A \succeq B \Rightarrow AA \succeq BB$ or $A \succeq B \Rightarrow A^2 \succeq B^2$. The induction hypothesis is then proved for $k = 1, 2, \ldots, \infty$.

A.9 Proof of the inequality $\tilde{\mathcal{L}}_m \succeq \tilde{\mathcal{L}}$

We have: $\tilde{\mathcal{L}}_m = \left(D_\xi - A^\top\right)^{-1} = \left(D_\xi I_n - D_\xi D_\xi^{-1} A^\top\right)^{-1} = \left(I_n - D_\xi^{-1} A^\top\right)^{-1} D_\xi^{-1}$. Since A is a nonnegative matrix and $D_\xi^{-1} \succeq I_n$, $D_\xi^{-1} A^\top$ is also a nonnegative matrix. Let us assume that $D_\xi^{-1} A^\top$ remains substochastic. We have $\tilde{\mathcal{L}}_m = \sum_{k=0}^\infty \left(D_\xi^{-1} A^\top\right)^k D_\xi^{-1}$. Using Properties NN2 and NN4 of Appendix A.8, we have $D_\xi^{-1} A^\top \succeq A^\top$, $\left(D_\xi^{-1} A^\top\right)^k \succeq \left(A^\top\right)^k$ and $\left(D_\xi^{-1} A^\top\right)^k D_\xi^{-1} \succeq \left(A^\top\right)^k$. Finally, we apply Property NN3 and deduce that $\sum_{k=0}^\infty \left(D_\xi^{-1} A^\top\right)^k D_\xi^{-1} \succeq \sum_{k=0}^\infty \left(A^\top\right)^k$ and $\tilde{\mathcal{L}}_m \succeq \tilde{\mathcal{L}}$.

This proof highlights the fact that $D_\xi - A^\top$ may be non-invertible. A sufficient (but not necessary) condition is that $D_\xi^{-1} A^\top$ is a substochastic matrix. This implies that $\sum_{j=1}^n \left(1 + \xi_j\right) A_{i,j} \leq 1$ or $\sum_{j=1}^n \xi_j A_{i,j} \leq 1 - \sum_{j=1}^n A_{i,j}$. This means that if the tax is too high, we can observe exploding prices.

A.10 Mathematical expectation of the price elasticity of demand

We assume that $\tilde{\phi} \sim \mathcal{B}(\alpha, \beta)$. Since we have $\tilde{\varepsilon} = 1 - \tilde{\phi}^{-1}$, we deduce that:

$$
\begin{aligned}
\mathbb{E}\left[\tilde{\varepsilon}\right] &= 1 - \mathbb{E}\left[\frac{1}{\tilde{\phi}}\right] \\
&= 1 - \int_0^1 \frac{1}{x} \frac{x^{\alpha-1}(1-x)^{\beta-1}}{\mathfrak{B}(\alpha,\beta)} \,\mathrm{d}x \\
&= 1 - \int_0^1 \frac{x^{\alpha-2}(1-x)^{\beta-1}}{\mathfrak{B}(\alpha,\beta)} \,\mathrm{d}x \\
&= 1 - \frac{\mathfrak{B}(\alpha-1,\beta)}{\mathfrak{B}(\alpha,\beta)} \int_0^1 \frac{x^{\alpha-2}(1-x)^{\beta-1}}{\mathfrak{B}(\alpha-1,\beta)} \,\mathrm{d}x \\
&= 1 - \frac{\mathfrak{B}(\alpha-1,\beta)}{\mathfrak{B}(\alpha,\beta)}
\end{aligned}
$$

Using the relationship between the beta and gamma functions, we obtain:

$$\begin{aligned}
\mathbb{E}\left[\tilde{\varepsilon}\right] &= 1-\frac{\Gamma\left(\alpha-1\right)\Gamma\left(\beta\right)\Gamma\left(\alpha+\beta\right)}{\Gamma\left(\alpha+\beta-1\right)\Gamma\left(\alpha\right)\Gamma\left(\beta\right)} \\
&= 1-\frac{\Gamma\left(\alpha-1\right)\Gamma\left(\alpha+\beta\right)}{\Gamma\left(\alpha+\beta-1\right)\Gamma\left(\alpha\right)} \\
&= 1-\frac{\alpha+\beta}{\alpha} \\
&= -\frac{\beta}{\alpha}
\end{aligned}$$

B Additional results

B.1 Figures

Figure 81: GDP impact by 2030 (% change from baseline) — B2D scenario

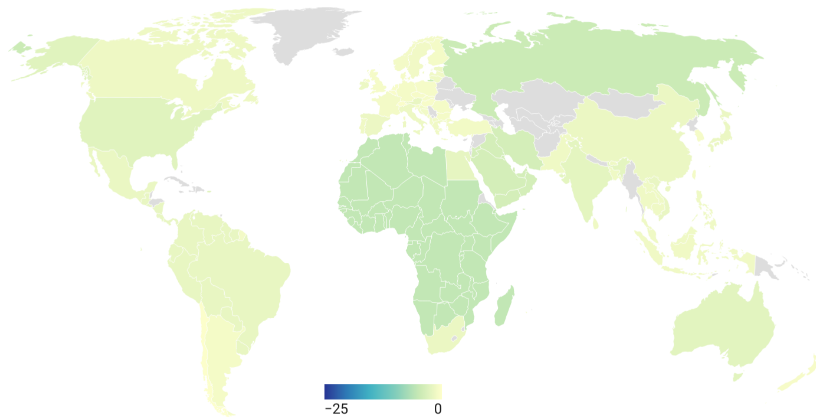

Source: https://data.ene.iiasa.ac.at/ngfs & Author's calculations (created by Datawrapper).

Figure 82: GDP impact by 2030 (% change from baseline) — CP scenario

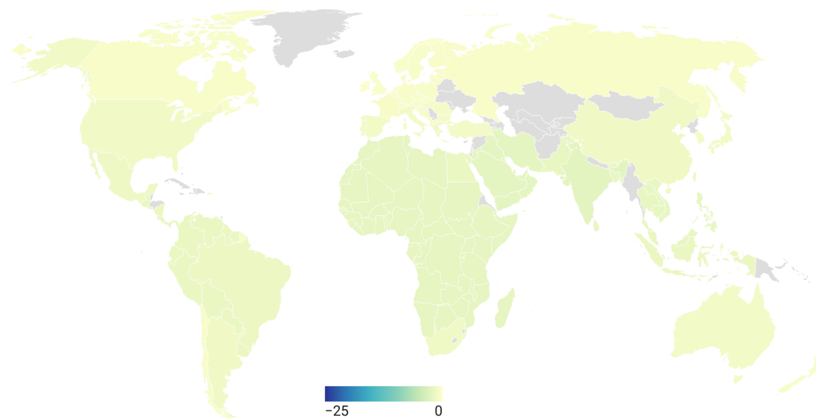

Source: https://data.ene.iiasa.ac.at/ngfs & Author's calculations (created by Datawrapper).

Figure 83: GDP impact by 2030 (% change from baseline) — DNZ scenario

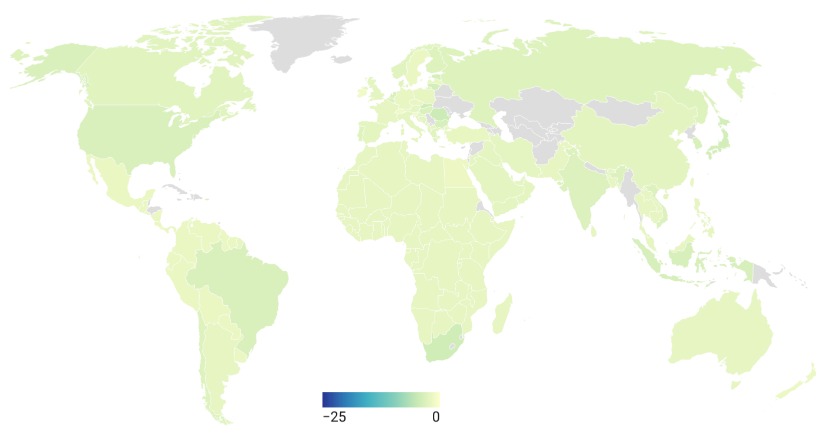

Source: https://data.ene.iiasa.ac.at/ngfs & Author's calculations (created by Datawrapper).

Figure 84: GDP impact by 2030 (% change from baseline) — DT scenario

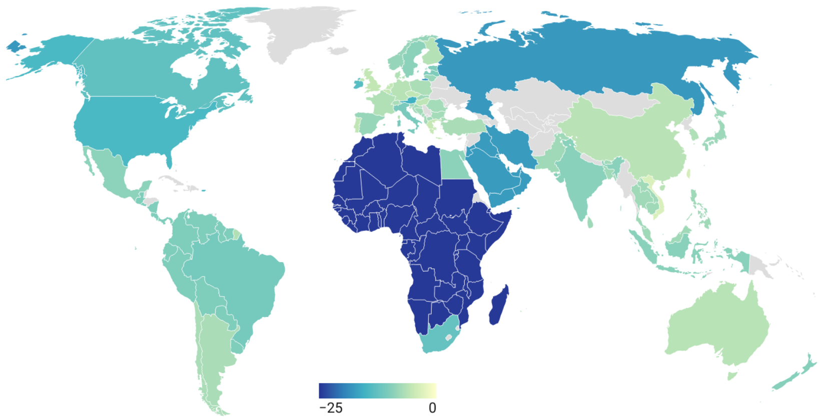

Source: https://data.ene.iiasa.ac.at/ngfs & Author's calculations (created by Datawrapper).

Figure 85: GDP impact by 2030 (% change from baseline) — NDC scenario

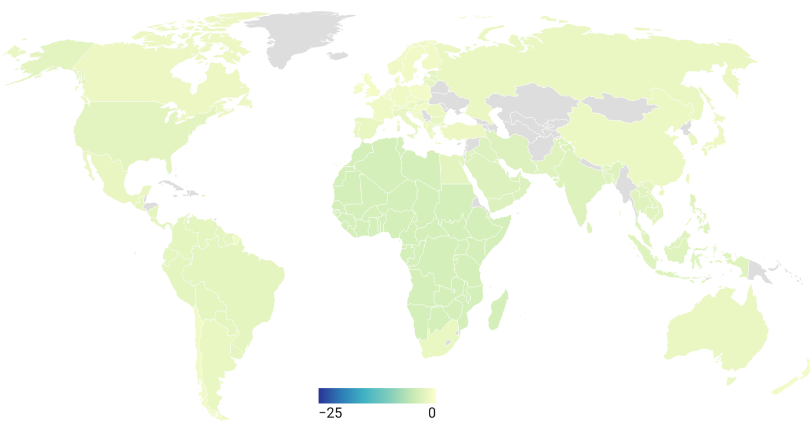

Source: https://data.ene.iiasa.ac.at/ngfs & Author's calculations (created by Datawrapper).

Figure 86: GDP impact by 2030 (% change from baseline) — NZ scenario

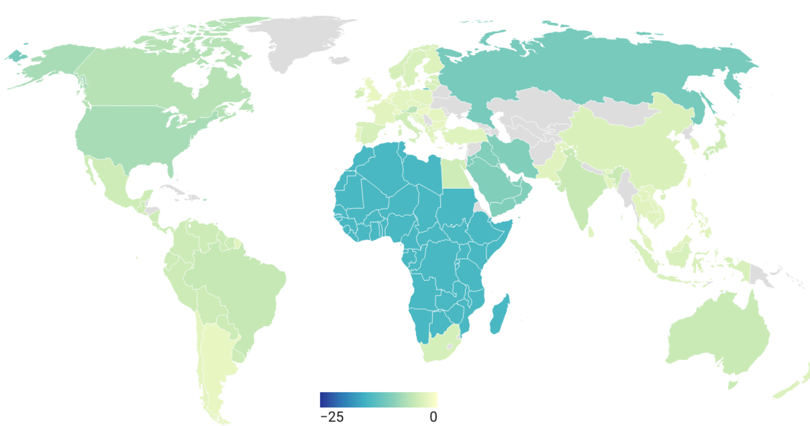

Source: https://data.ene.iiasa.ac.at/ngfs & Author's calculations (created by Datawrapper).

Figure 87: GDP impact by 2050 (% change from baseline) — B2D scenario

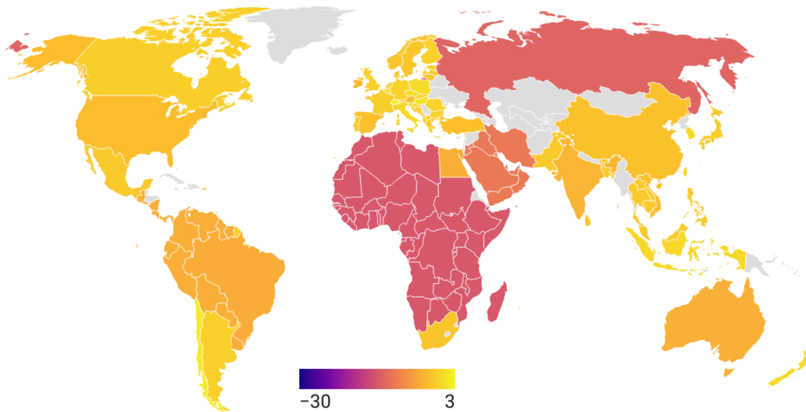

Source: https://data.ene.iiasa.ac.at/ngfs & Author's calculations (created by Datawrapper).

Figure 88: GDP impact by 2050 (% change from baseline) — CP scenario

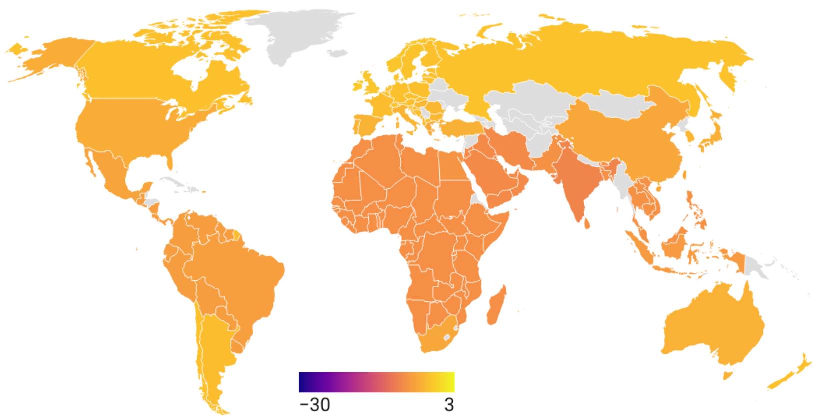

Source: https://data.ene.iiasa.ac.at/ngfs & Author's calculations (created by Datawrapper).

Figure 89: GDP impact by 2050 (% change from baseline) — DNZ scenario

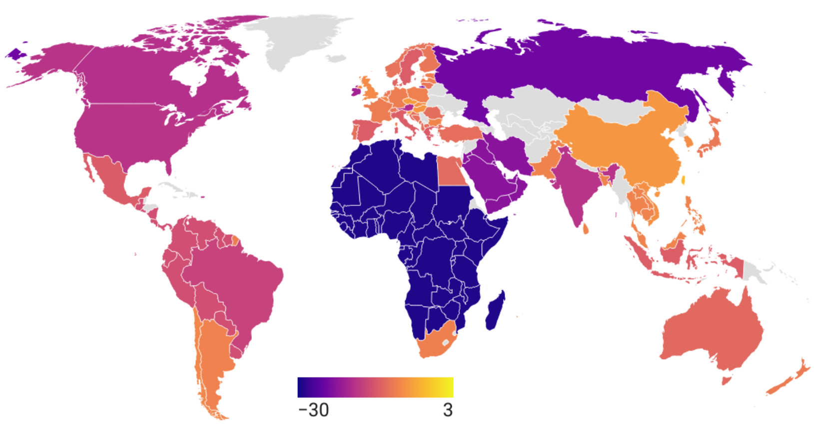

Source: https://data.ene.iiasa.ac.at/ngfs & Author's calculations (created by Datawrapper).

Figure 90: GDP impact by 2050 (% change from baseline) — DT scenario

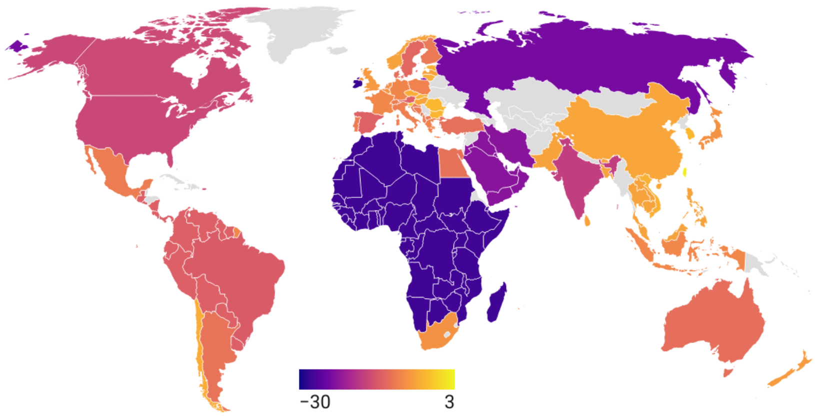

Source: https://data.ene.iiasa.ac.at/ngfs & Author's calculations (created by Datawrapper).

Figure 91: GDP impact by 2050 (% change from baseline) — NDC scenario

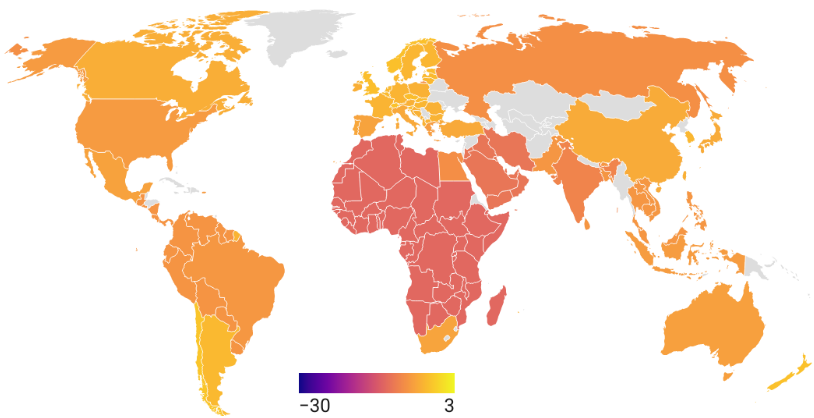

Source: https://data.ene.iiasa.ac.at/ngfs & Author's calculations (created by Datawrapper).

Figure 92: GDP impact by 2050 (% change from baseline) — NZ scenario

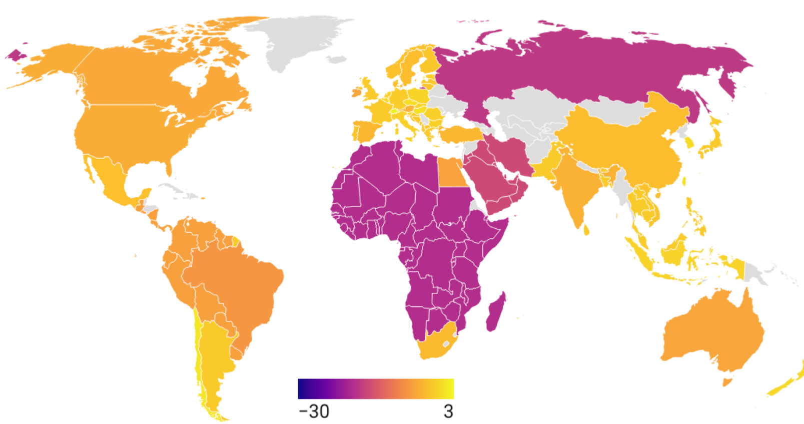

Source: https://data.ene.iiasa.ac.at/ngfs & Author's calculations (created by Datawrapper).

Figure 93: Comparison of EU and UK ETS carbon prices

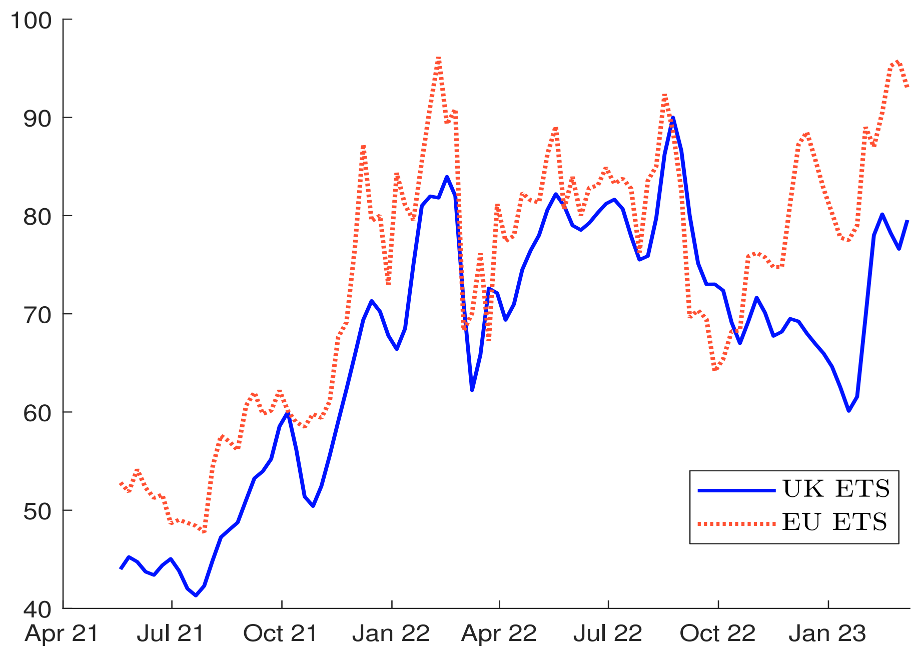

Source: Bloomberg (2023), Factset (2023).

Figure 94: Sparsity pattern of the input-output matrix A (Exiobase 2014)

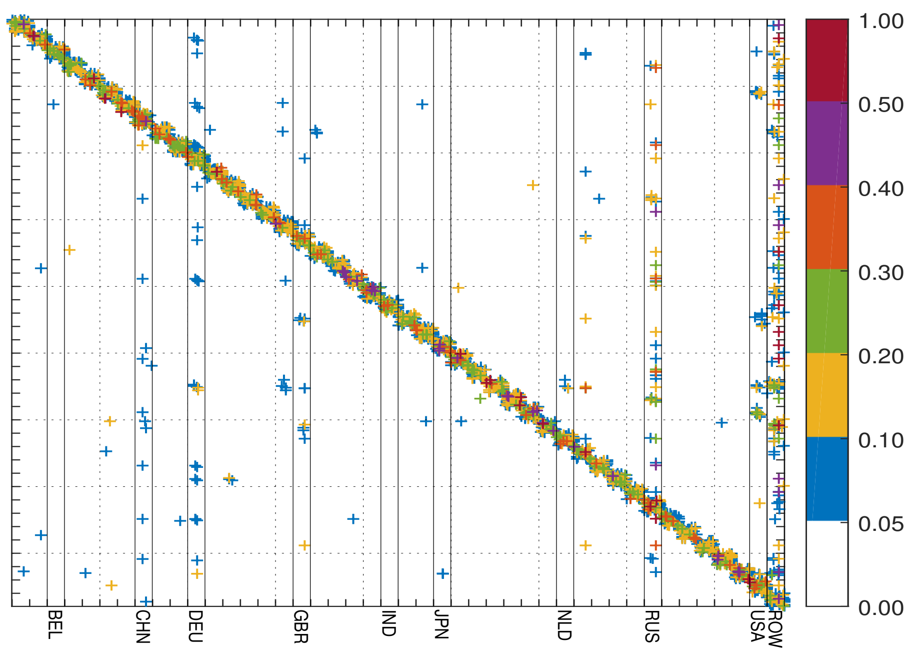

Figure 95: Sparsity pattern of the input-output matrix A (Exiobase 2022)

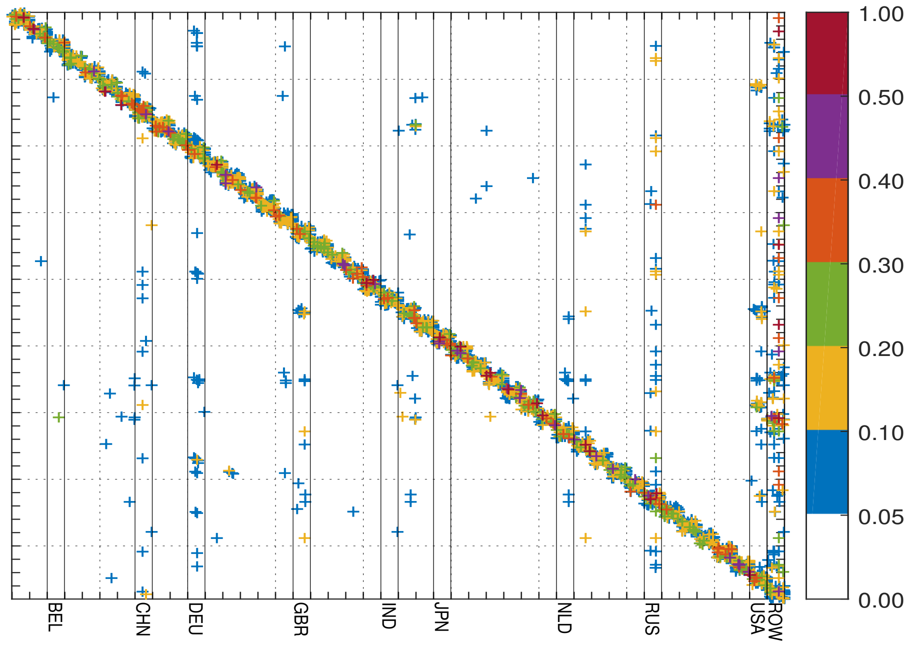

Figure 96: Sparsity pattern of $|A_{\text{wiod}} - A_{\text{exiobase}}|$ (2014)

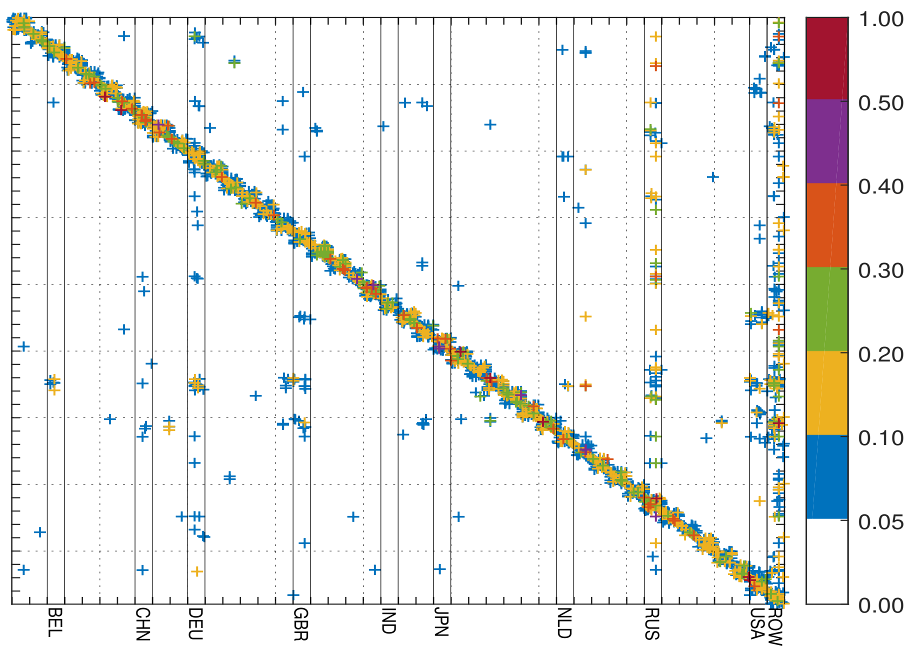

Figure 97: Multiplying coefficient $m_{(0-\infty)}$ (Exiobase 2014)

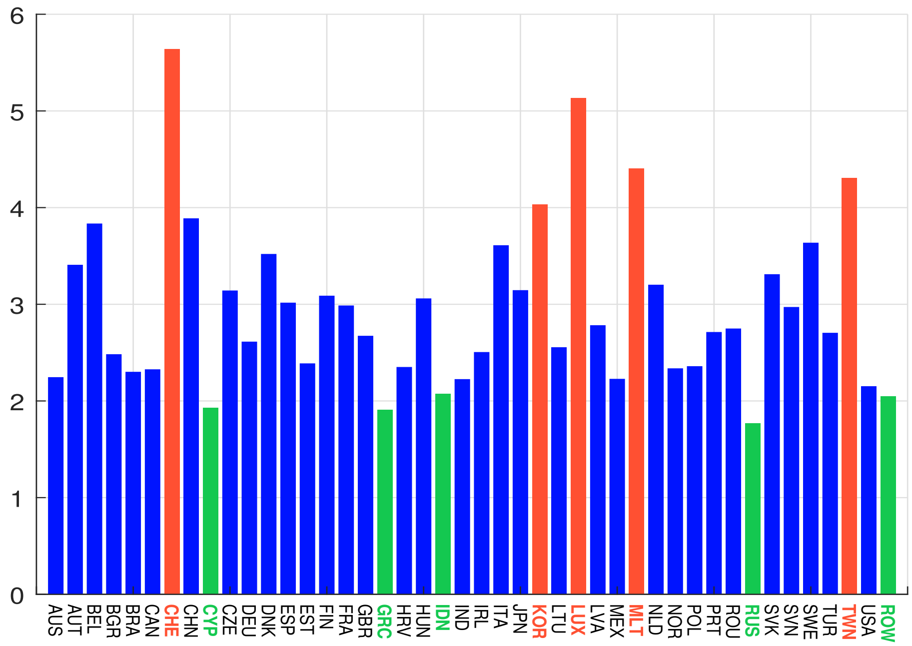

Figure 98: Multiplying coefficient $m_{(0-\infty)}$ (Exiobase 2022)

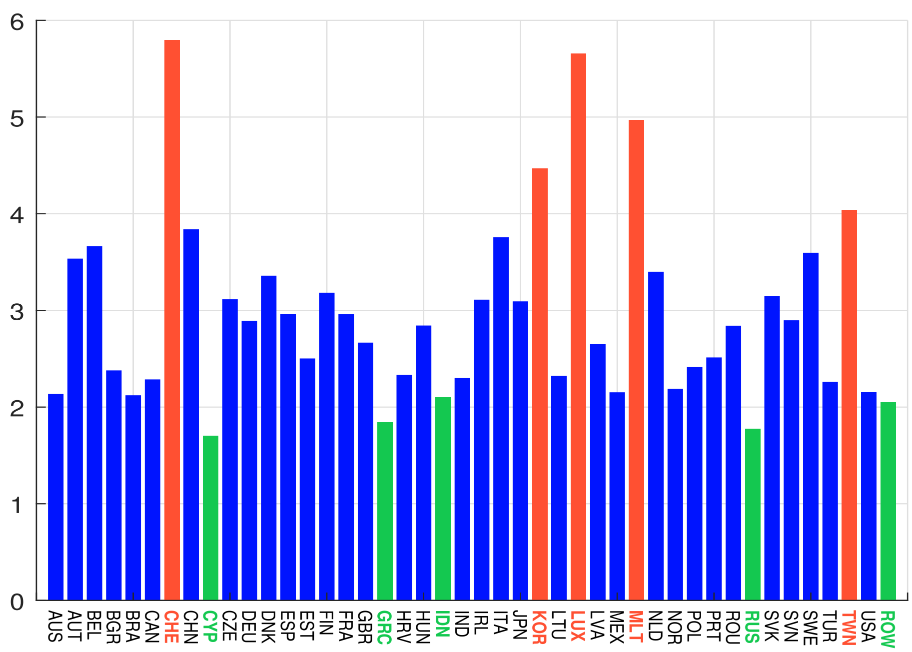

Figure 99: Sankey diagram of *Manufacture of computer, electronic and optical products* in the USA (WIOD 2014)

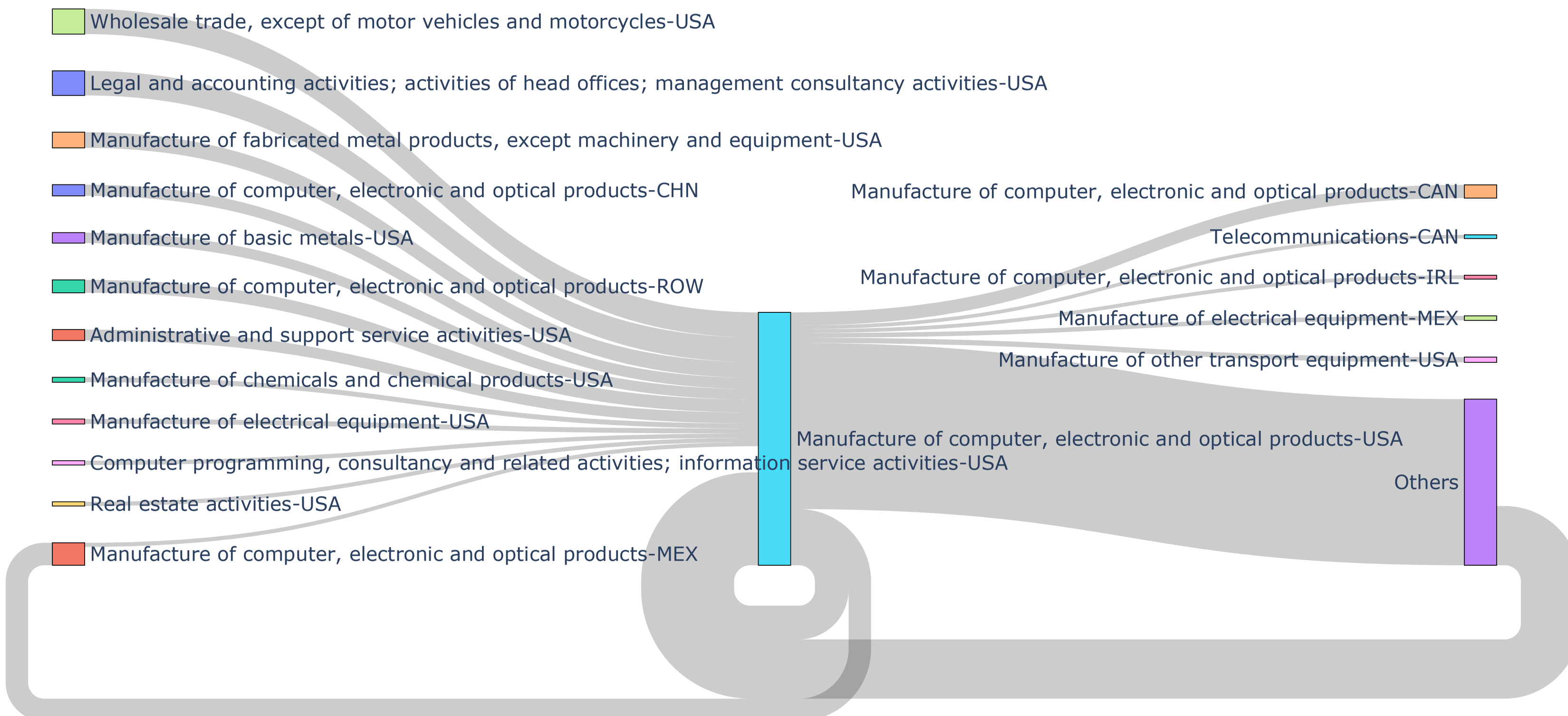

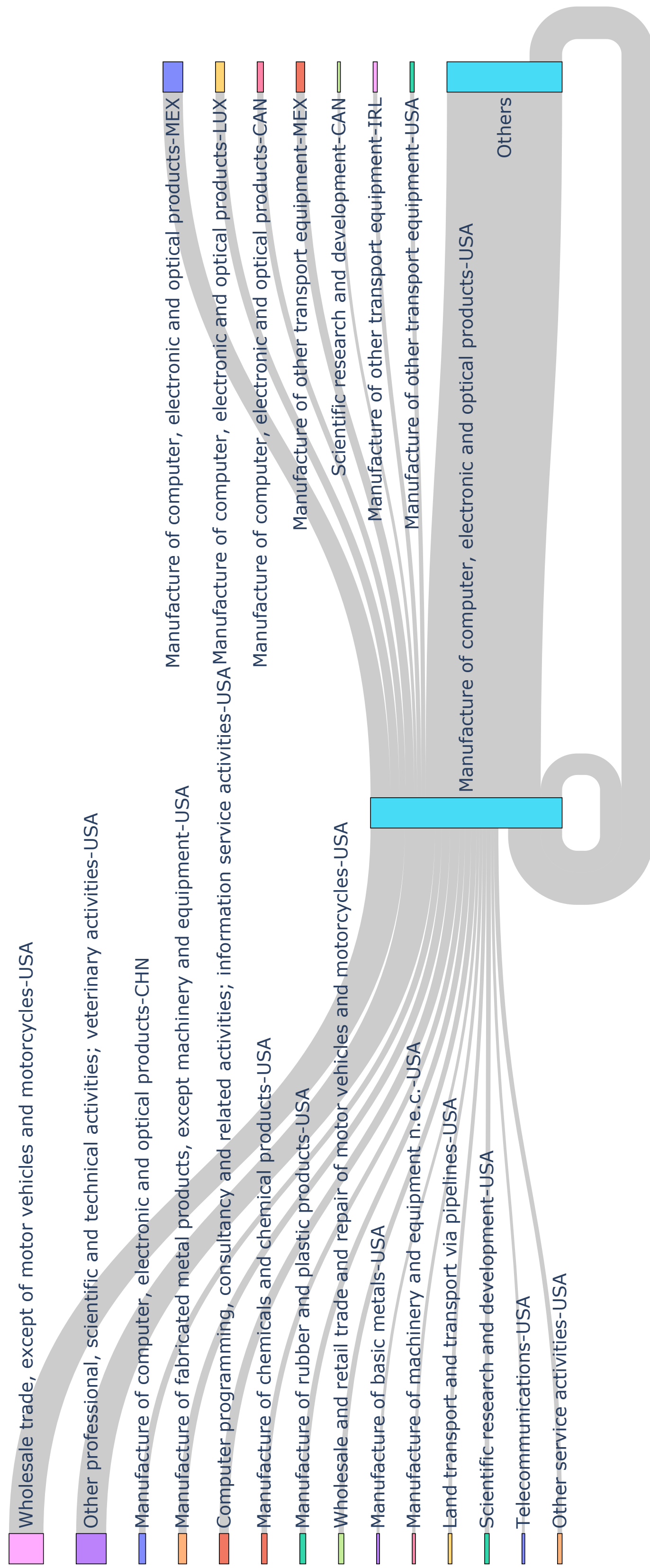

Figure 100: Sankey diagram of *Manufacture of computer, electronic and optical products* in the USA (Exiobase 2014)

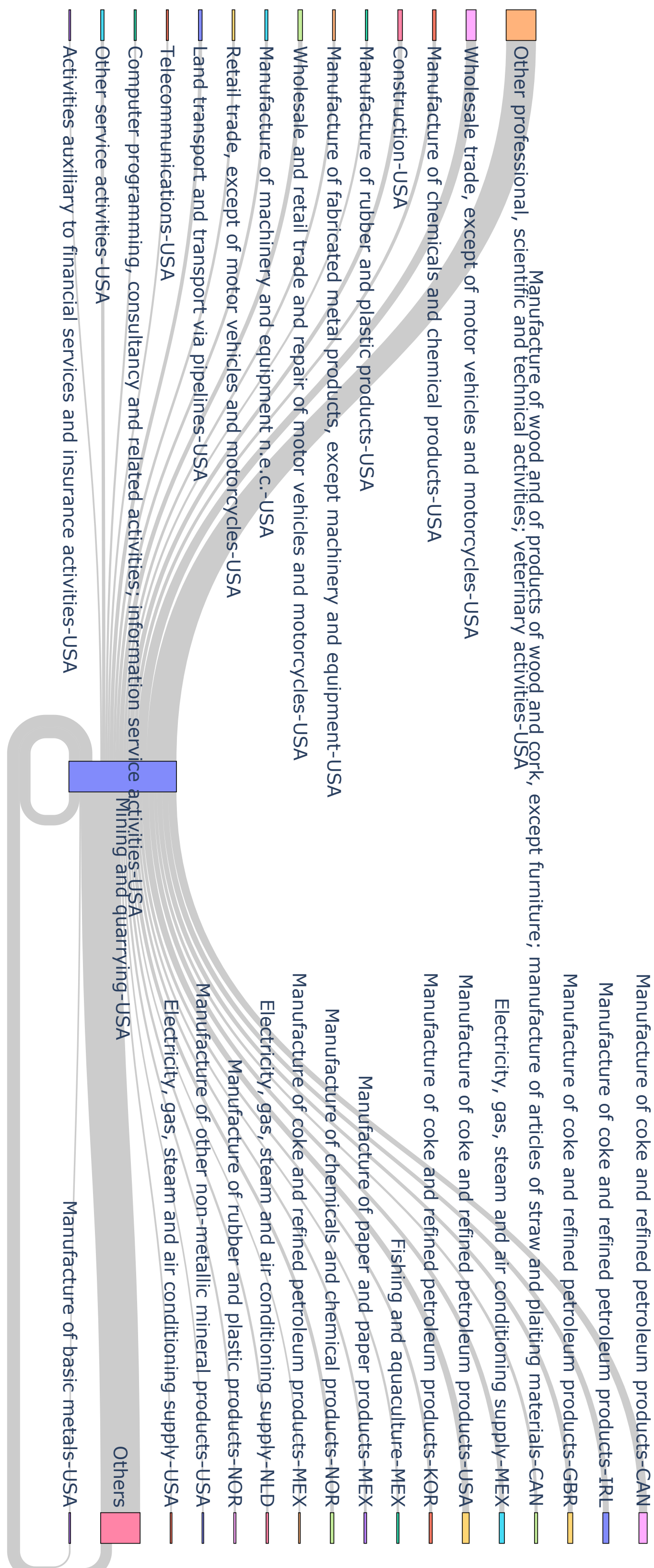

Figure 101: Sankey diagram of *Manufacture of computer, electronic and optical products* in the USA (Exiobase 2022)

Figure 102: Multiplying coefficients (country-sector analysis, WIOD 2014)

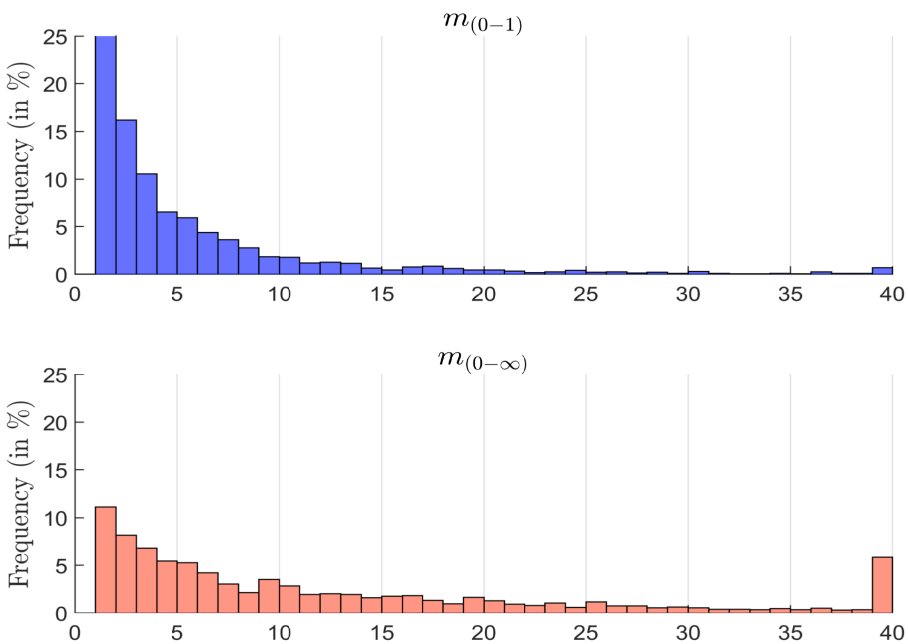

Figure 103: Multiplying coefficients (country-sector analysis, Trucost 2021)

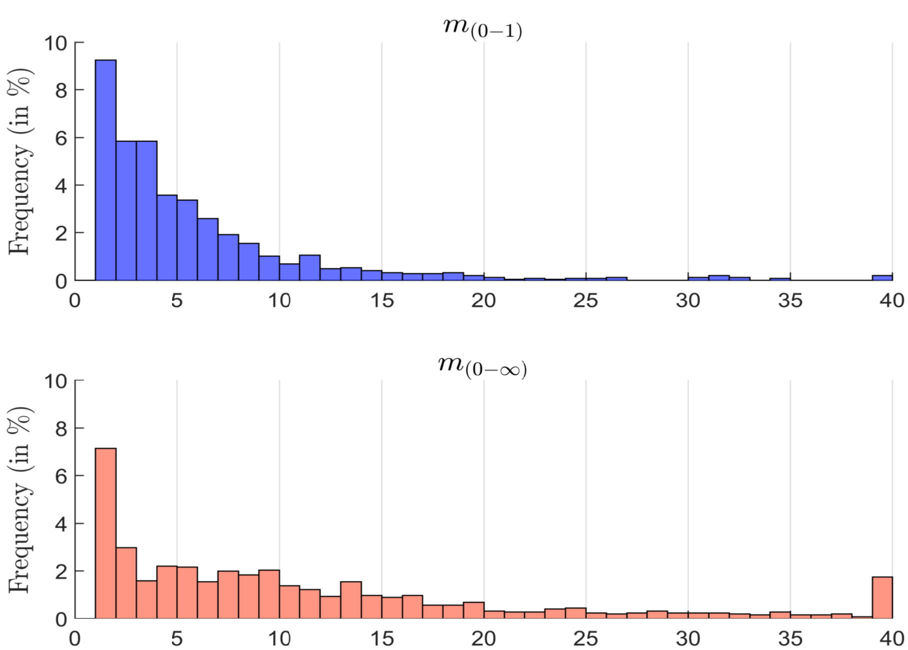

Figure 104: Breakdown of the portfolio intensity per GICS sector (MSCI World index, May 2023)

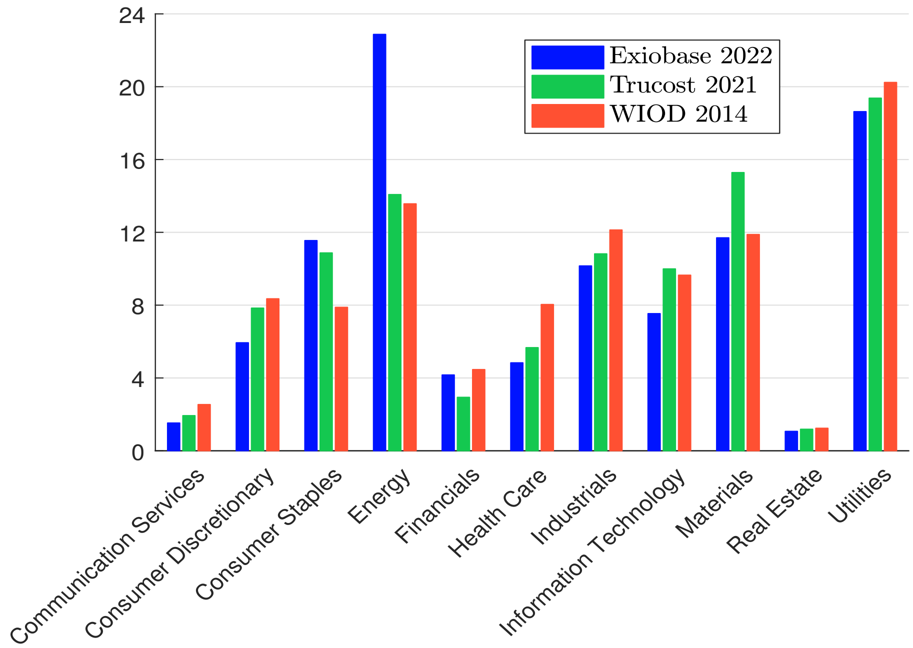

Figure 105: Cumulative distribution function of pass-through rates

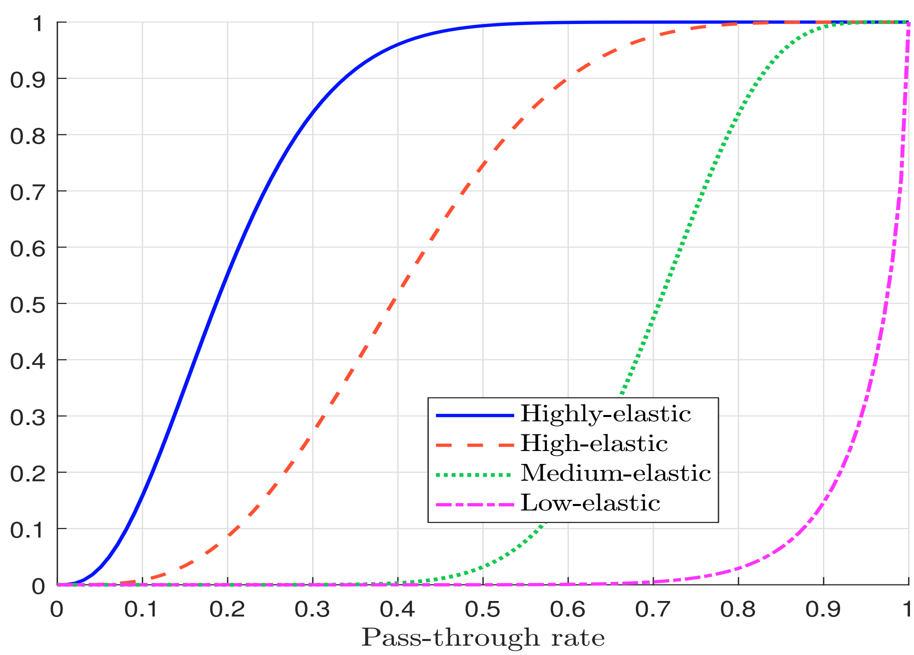

Figure 106: Cost multiplier (global analysis, uniform taxation, WIOD 2014)

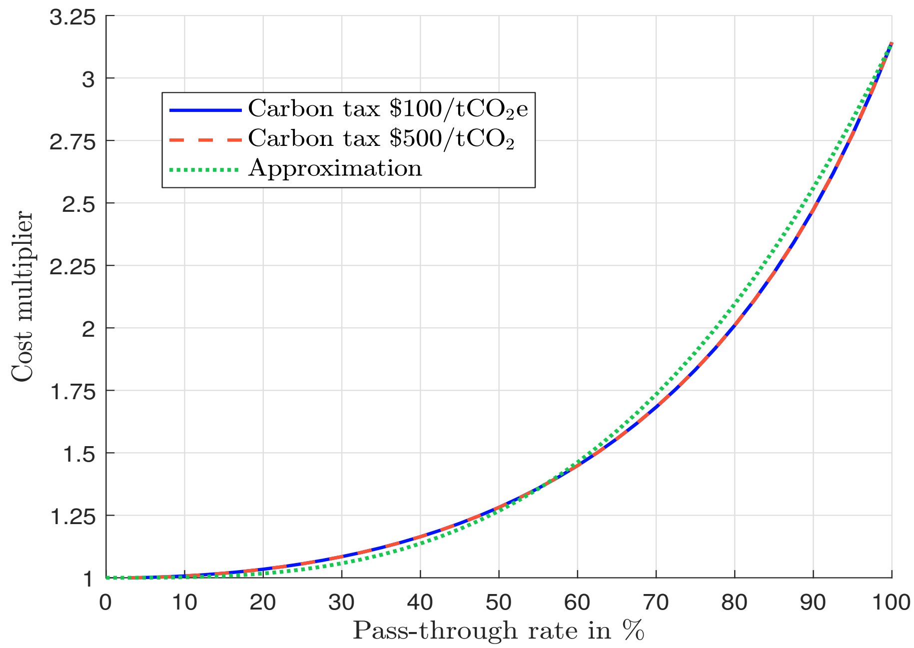

Figure 107: Distribution of country inflation rates in % (global analysis, uniform taxation, Exiobase 2022)

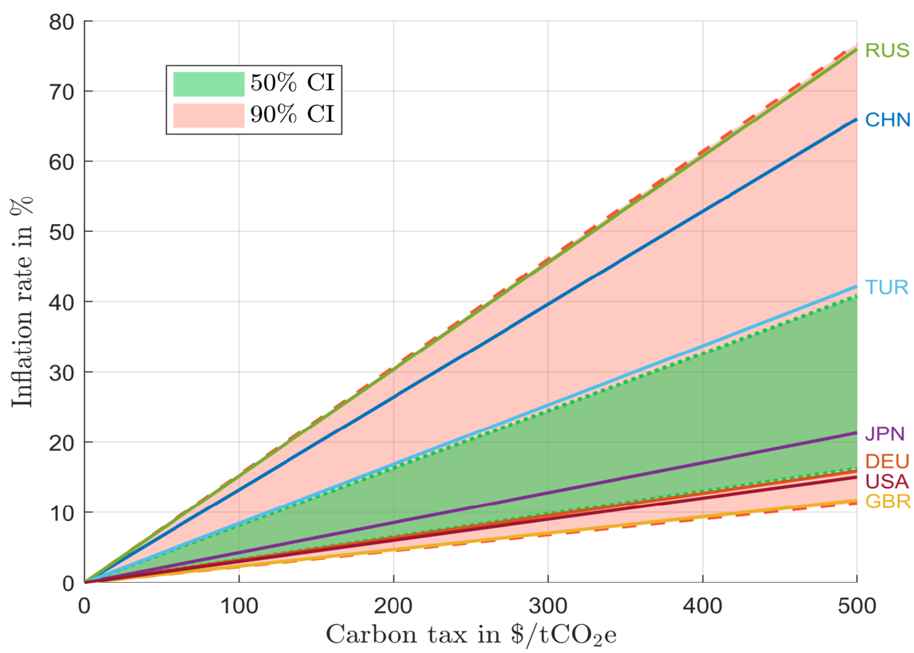

Figure 108: Distribution of country inflation rates in % (global analysis, uniform taxation, WIOD 2014)

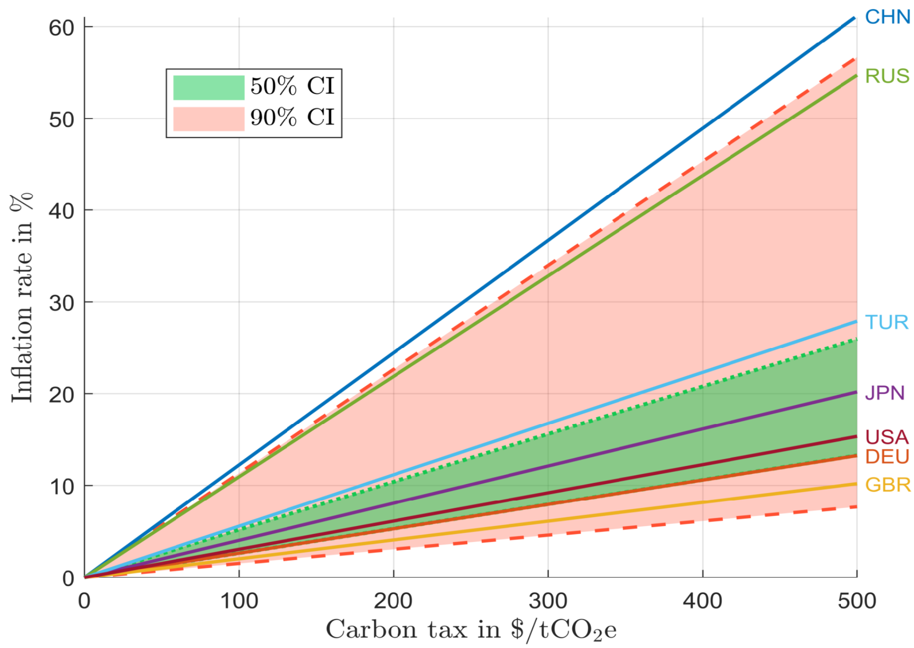

Figure 109: Contribution of the direct emissions in % (global analysis, uniform taxation, $\boldsymbol{\tau} = \$100/tCO_2e$, $\boldsymbol{\phi} = 100\%$, Exiobase 2022)

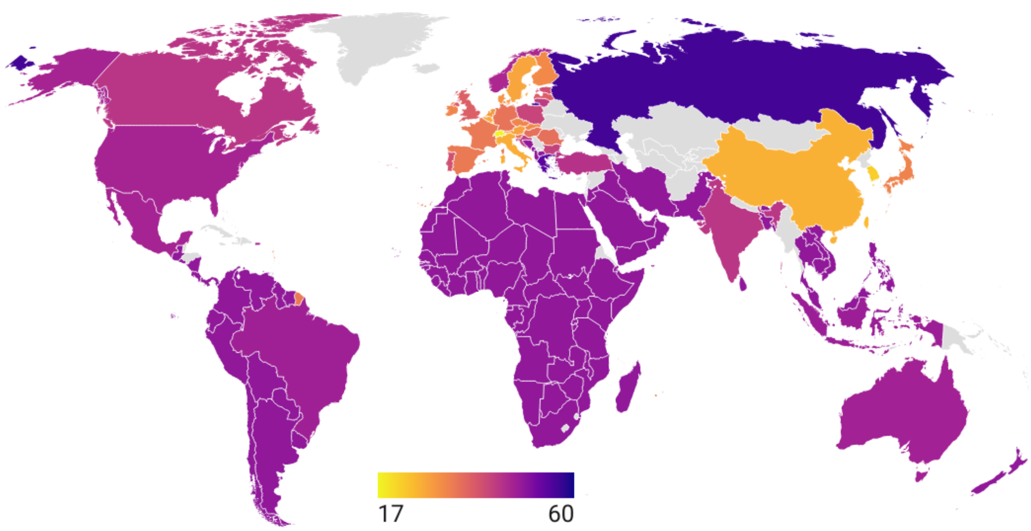

Source: Author's calculations (created by Datawrapper).

Figure 110: Production inflation rate in % explained by the direct emissions (global analysis, uniform taxation, $\tau = \$100/tCO_2e$, $\phi = 100\%$, Exiobase 2022)

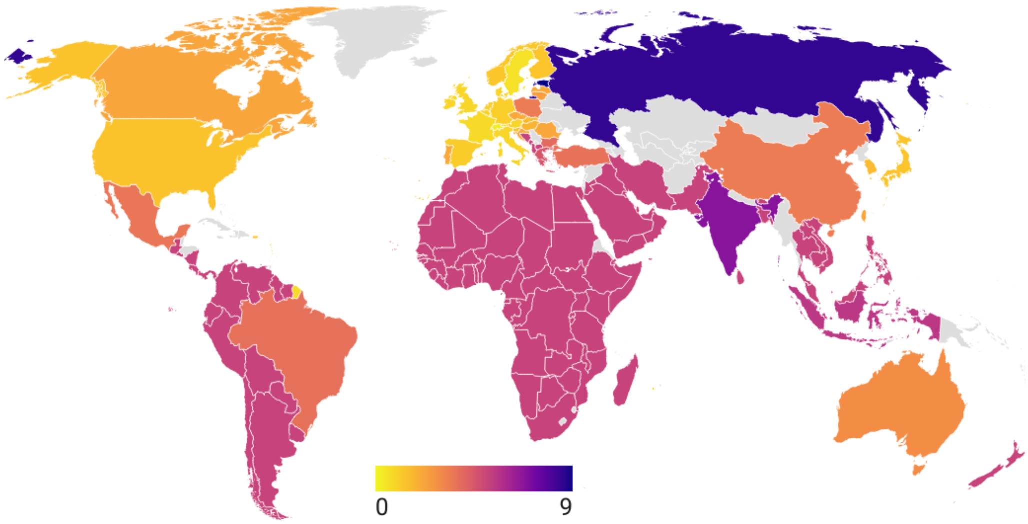

Source: Author's calculations (created by Datawrapper).

Figure 111: Production inflation rate in % explained by the global value chain (global analysis, uniform taxation, $\tau = \$100/tCO_2e$, $\phi = 100\%$, Exiobase 2022)

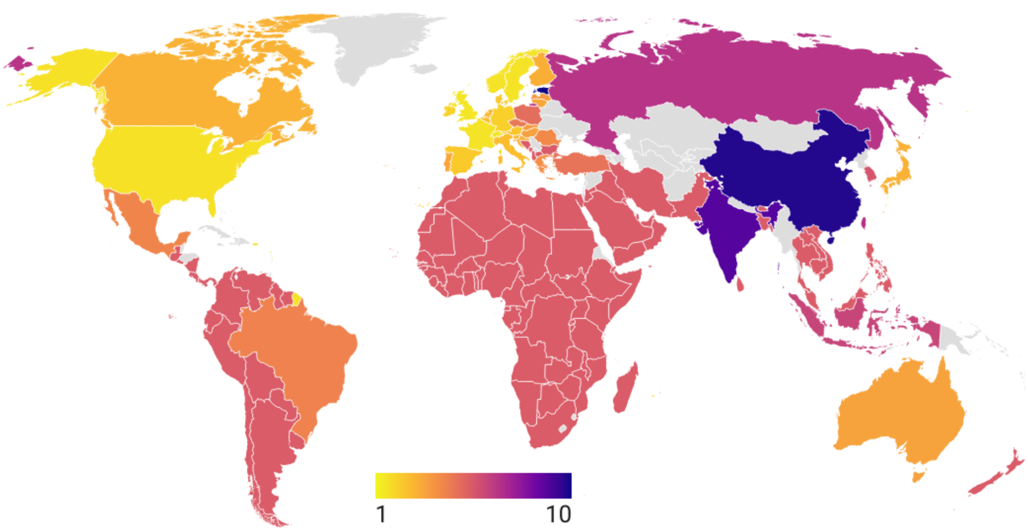

Source: Author's calculations (created by Datawrapper).

Figure 112: Cost multiplier (global analysis, differentiated taxation, Exiobase 2022)

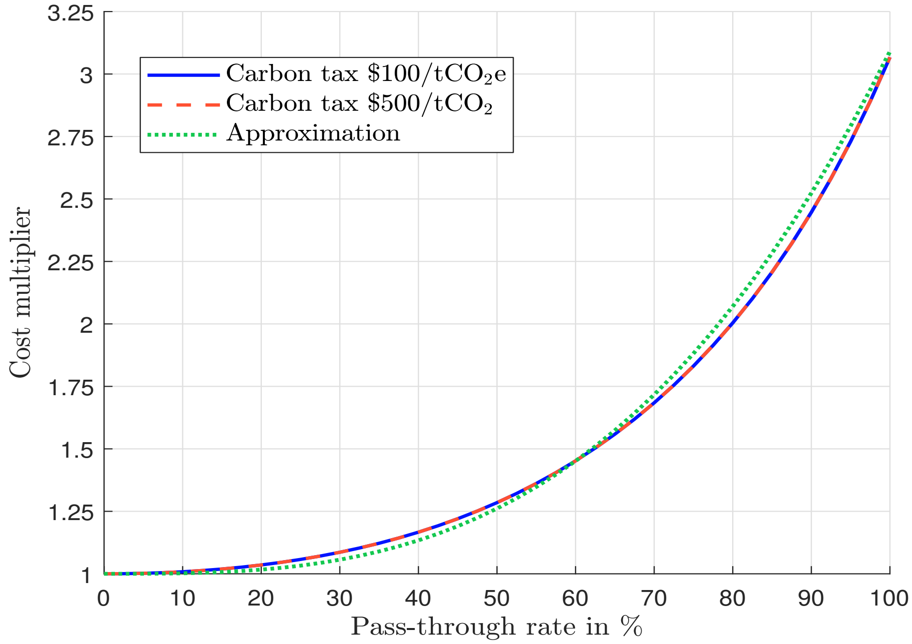

Figure 113: Cost breakdown (EU, uniform taxation, $\phi = 50\%$, Wiod 2014)

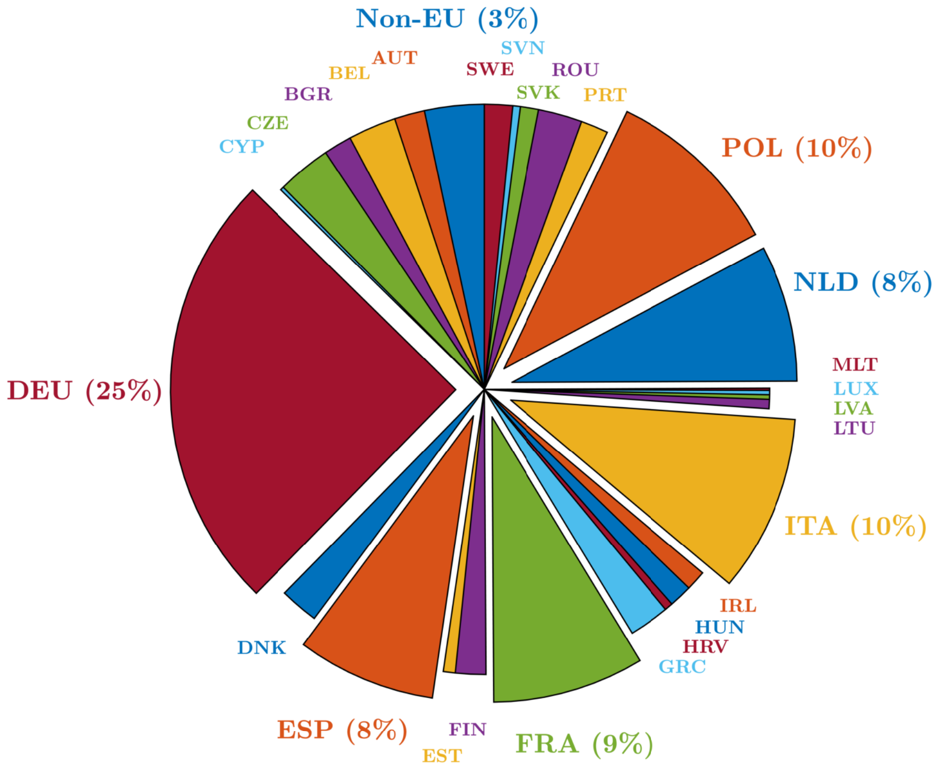

Figure 114: Cost breakdown (EU, uniform taxation, $\phi = 100\%$, Wiod 2014)

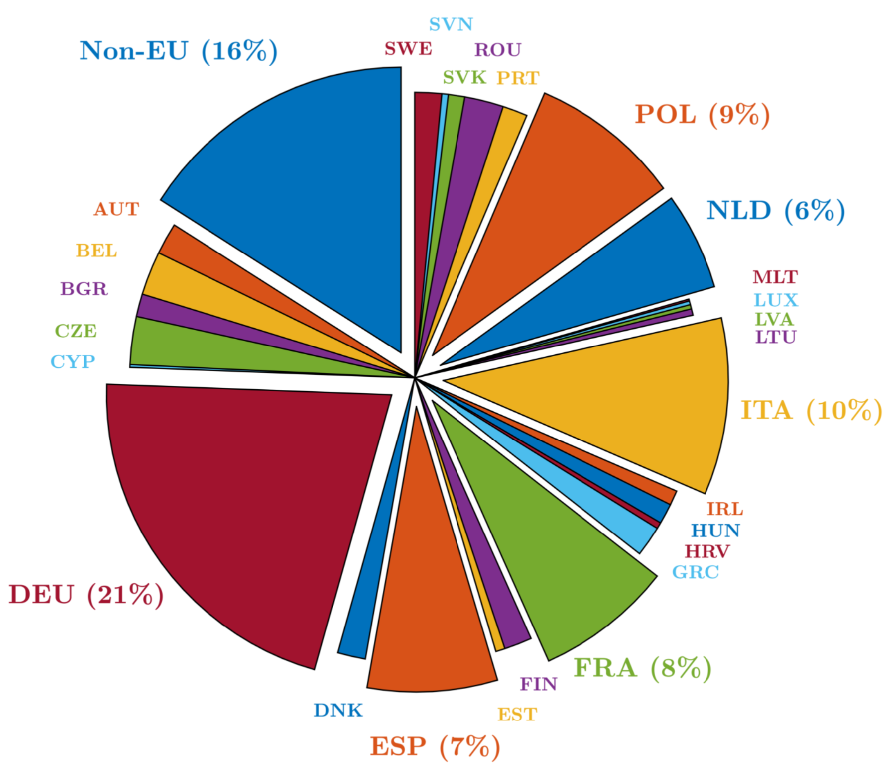

Figure 115: Directed graph (matrix #2)

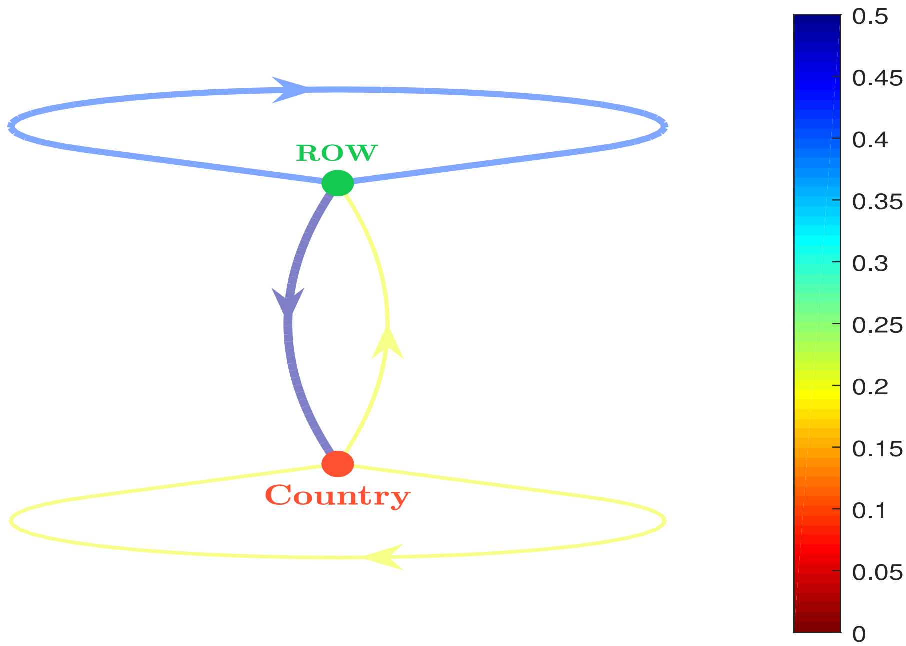

Figure 116: Impact of the k^{th} tier on the directed graph (matrix #2)

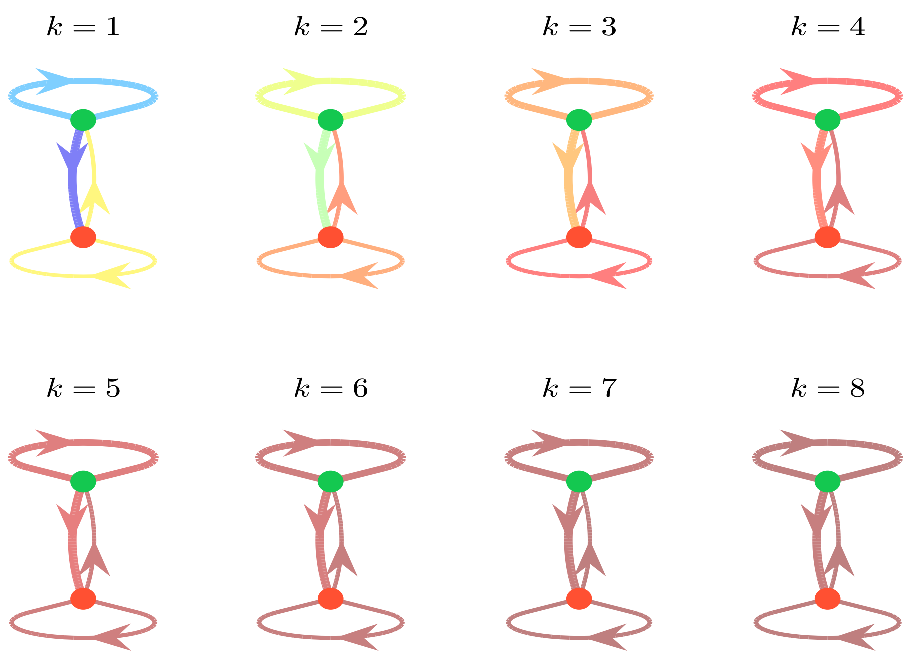

Figure 117: Directed graph (matrix #3)

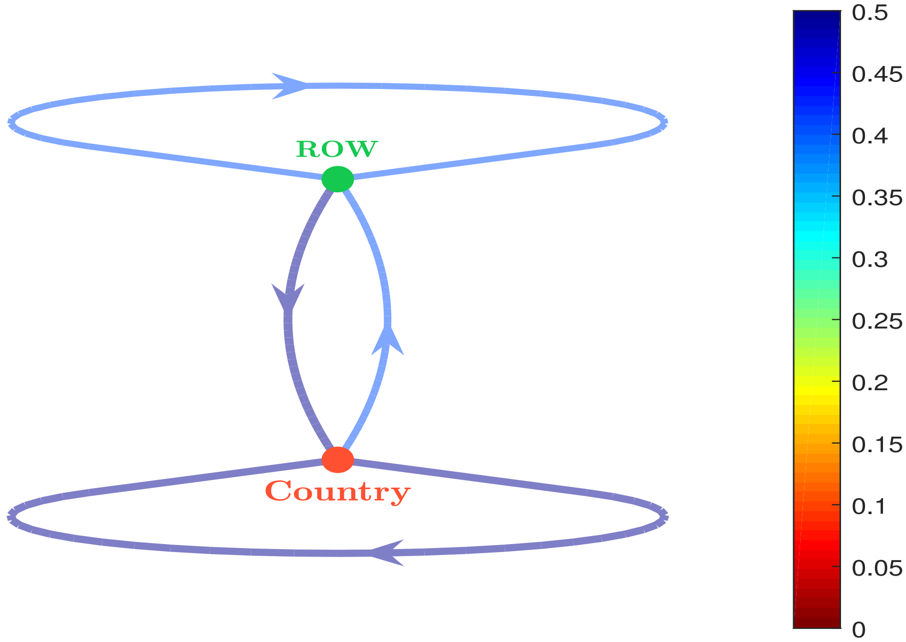

Figure 118: Impact of the k^{th} tier on the directed graph (matrix #3)

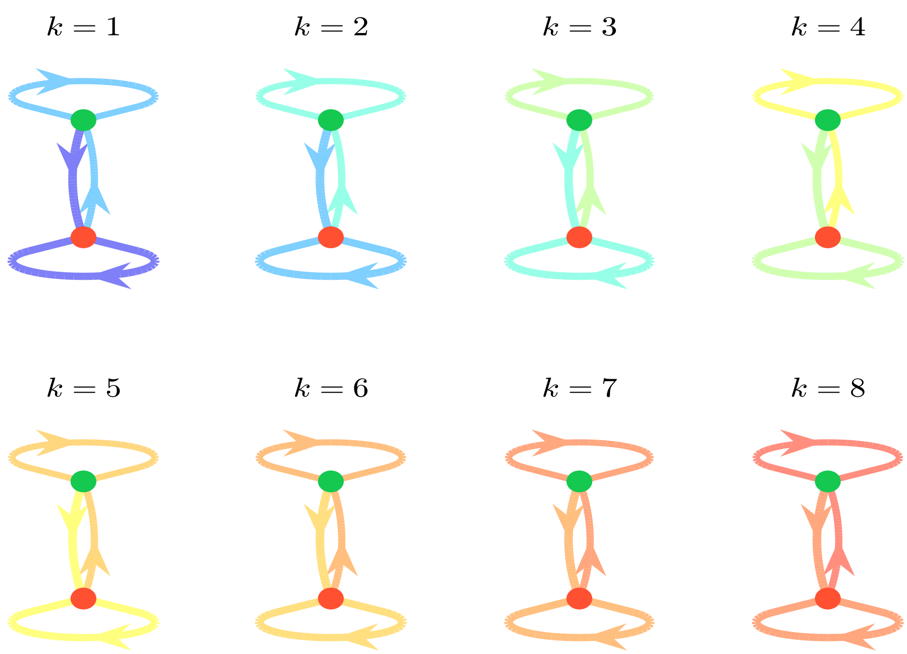

Figure 119: World economic cost in \$ tn (global analysis, stochastic pass-through, Exiobase 2022)

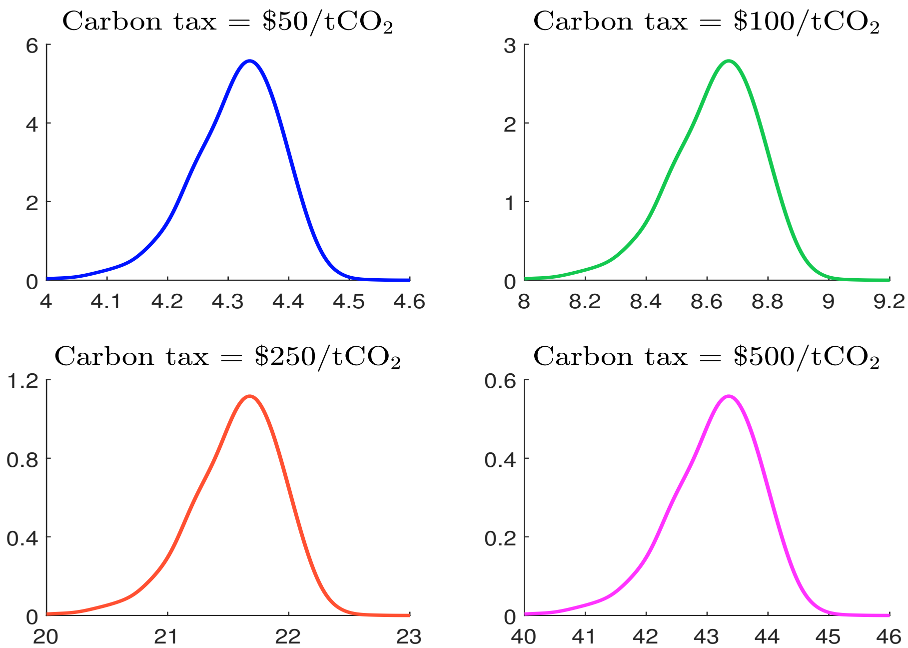

Figure 120: World economic cost in % of GDP (global analysis, stochastic pass-through, Exiobase 2022)

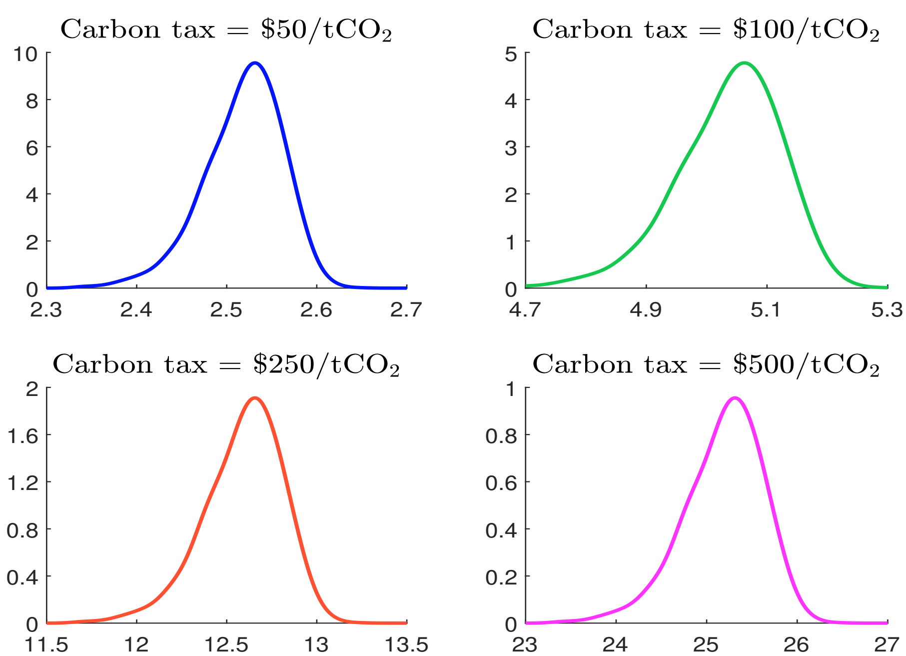

Figure 121: World PPI inflation rate in % (global analysis, stochastic pass-through, Exiobase 2022)

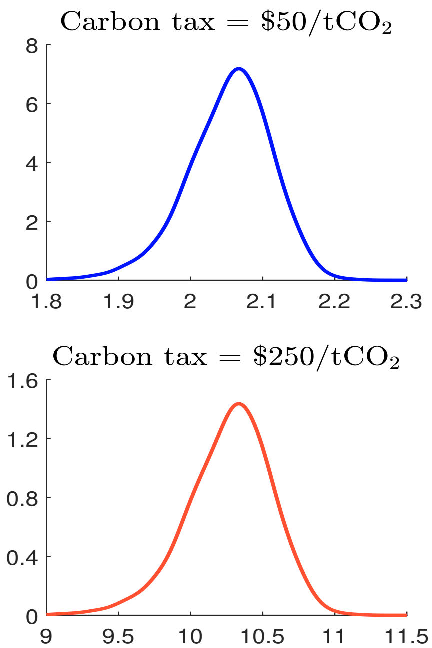

Figure 122: World CPI inflation rate in % (global analysis, stochastic pass-through, Exiobase 2022)

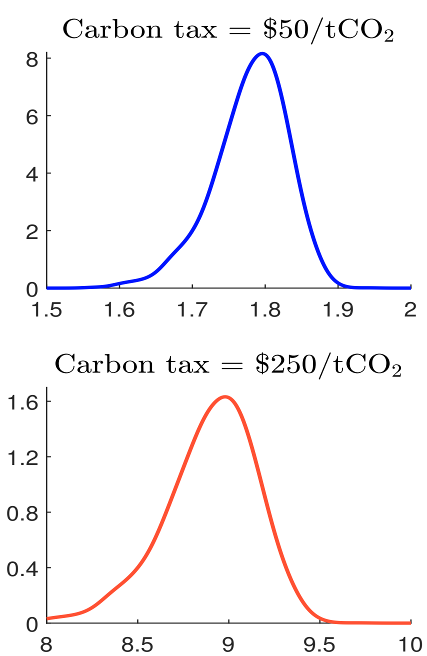

Figure 123: Probability density function of earnings' shocks (global analysis, $\boldsymbol{\tau}$ = \$100/tCO$_2$e, stochastic pass-through and elasticity, Gaussian copula, ρ = 70%, Exiobase 2022)

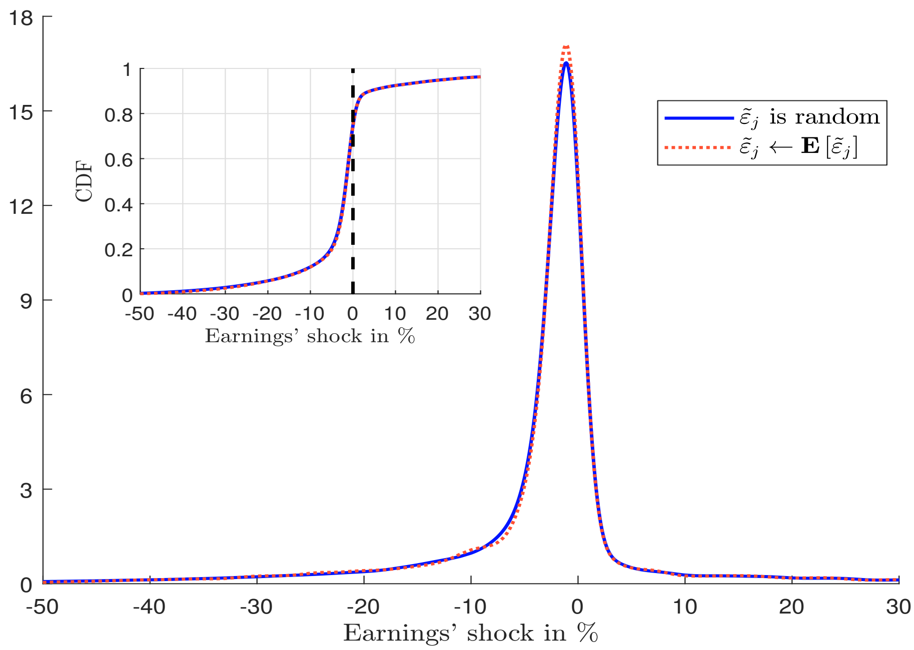

Figure 124: Expected shortfall at the 99% confidence level (global uniform taxation, $\boldsymbol{\tau}$ = \$100/tCO$_2$e, stochastic pass-through rate, Gaussian copula, Exiobase 2022, MSCI World, May 2023)

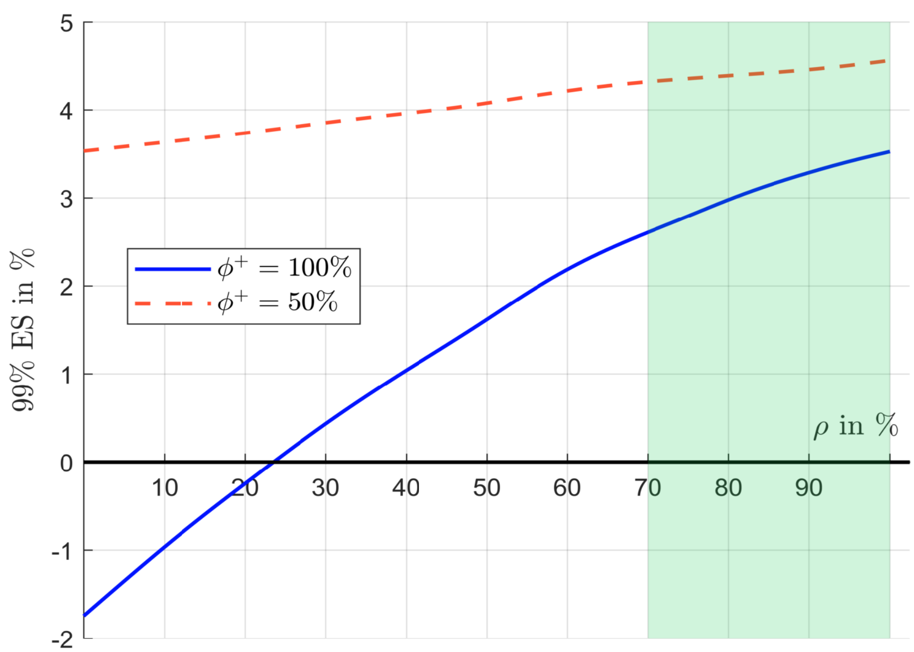

B.2 Tables

Table 45: List of countries/regions (WIOD 2014)

No.	ISO	Name	No.	ISO	Name
$\mathcal{C}_1$	AUS	Australia	$\mathcal{C}_2$	AUT	Austria
$\mathcal{C}_3$	BEL	Belgium	$\mathcal{C}_4$	BGR	Bulgaria
$\mathcal{C}_5$	BRA	Brazil	$\mathcal{C}_6$	CAN	Canada
$\mathcal{C}_7$	CHE	Switzerland	$\mathcal{C}_8$	CHN	China
$\mathcal{C}_9$	CYP	Cyprus	$\mathcal{C}_{10}$	CZE	Czech Republic
$\mathcal{C}_{11}$	DEU	Germany	$\mathcal{C}_{12}$	DNK	Denmark
$\mathcal{C}_{13}$	ESP	Spain	$\mathcal{C}_{14}$	EST	Estonia
$\mathcal{C}_{15}$	FIN	Finland	$\mathcal{C}_{16}$	FRA	France
$\mathcal{C}_{17}$	GBR	United Kingdom	$\mathcal{C}_{18}$	GRC	Greece
$\mathcal{C}_{19}$	HRV	Croatia	$\mathcal{C}_{20}$	HUN	Hungary
$\mathcal{C}_{21}$	IDN	Indonesia	$\mathcal{C}_{22}$	IND	India
$\mathcal{C}_{23}$	IRL	Ireland	$\mathcal{C}_{24}$	ITA	Italy
$\mathcal{C}_{25}$	JPN	Japan	$\mathcal{C}_{26}$	KOR	Republic of Korea
$\mathcal{C}_{27}$	LTU	Lithuania	$\mathcal{C}_{28}$	LUX	Luxembourg
$\mathcal{C}_{29}$	LVA	Latvia	$\mathcal{C}_{30}$	MEX	Mexico
$\mathcal{C}_{31}$	MLT	Malta	$\mathcal{C}_{32}$	NLD	Netherlands
$\mathcal{C}_{33}$	NOR	Norway	$\mathcal{C}_{34}$	POL	Poland
$\mathcal{C}_{35}$	PRT	Portugal	$\mathcal{C}_{36}$	ROU	Romania
$\mathcal{C}_{37}$	RUS	Russian Federation	$\mathcal{C}_{38}$	SVK	Slovakia
$\mathcal{C}_{39}$	SVN	Slovenia	$\mathcal{C}_{40}$	SWE	Sweden
$\mathcal{C}_{41}$	TUR	Turkey	$\mathcal{C}_{42}$	TWN	Taiwan
$\mathcal{C}_{43}$	USA	United States of America	$\mathcal{C}_{44}$	ROW	Rest-of-the-world

Table 46: List of industries/sectors (WIOD 2014)

No.	Name
$\mathcal{S}_1$	Accommodation and food service activities
$\mathcal{S}_2$	Activities auxiliary to financial services and insurance activities
$\mathcal{S}_3$	Activities of extraterritorial organizations and bodies
$\mathcal{S}_4$	Activities of households as employers; undifferentiated goods- and services-producing activities of households for own use
$\mathcal{S}_5$	Administrative and support service activities
$\mathcal{S}_6$	Advertising and market research
$\mathcal{S}_7$	Air transport
$\mathcal{S}_8$	Architectural and engineering activities; technical testing and analysis
$\mathcal{S}_9$	Computer programming, consultancy and related activities; information service activities
$\mathcal{S}_{10}$	Construction
$\mathcal{S}_{11}$	Crop and animal production, hunting and related service activities
$\mathcal{S}_{12}$	Education
$\mathcal{S}_{13}$	Electricity, gas, steam and air conditioning supply
$\mathcal{S}_{14}$	Financial service activities, except insurance and pension funding
$\mathcal{S}_{15}$	Fishing and aquaculture
$\mathcal{S}_{16}$	Forestry and logging
$\mathcal{S}_{17}$	Human health and social work activities
$\mathcal{S}_{18}$	Insurance, reinsurance and pension funding, except compulsory social security
$\mathcal{S}_{19}$	Land transport and transport via pipelines
$\mathcal{S}_{20}$	Legal and accounting activities; activities of head offices; management consultancy activities
$\mathcal{S}_{21}$	Manufacture of basic metals
$\mathcal{S}_{22}$	Manufacture of basic pharmaceutical products and pharmaceutical preparations
$\mathcal{S}_{23}$	Manufacture of chemicals and chemical products
$\mathcal{S}_{24}$	Manufacture of coke and refined petroleum products
$\mathcal{S}_{25}$	Manufacture of computer, electronic and optical products
$\mathcal{S}_{26}$	Manufacture of electrical equipment
$\mathcal{S}_{27}$	Manufacture of fabricated metal products, except machinery and equipment
$\mathcal{S}_{28}$	Manufacture of food products, beverages and tobacco products
$\mathcal{S}_{29}$	Manufacture of furniture; other manufacturing
$\mathcal{S}_{30}$	Manufacture of machinery and equipment n.e.c.
$\mathcal{S}_{31}$	Manufacture of motor vehicles, trailers and semi-trailers
$\mathcal{S}_{32}$	Manufacture of other non-metallic mineral products
$\mathcal{S}_{33}$	Manufacture of other transport equipment
$\mathcal{S}_{34}$	Manufacture of paper and paper products
$\mathcal{S}_{35}$	Manufacture of rubber and plastic products
$\mathcal{S}_{36}$	Manufacture of textiles, wearing apparel and leather products
$\mathcal{S}_{37}$	Manufacture of wood and of products of wood and cork, except furniture; manufacture of articles of straw and plaiting materials
$\mathcal{S}_{38}$	Mining and quarrying
$\mathcal{S}_{39}$	Motion picture, video and television programme production, sound recording and music publishing activities; programming and broadcasting activities
$\mathcal{S}_{40}$	Other professional, scientific and technical activities; veterinary activities
$\mathcal{S}_{41}$	Other service activities
$\mathcal{S}_{42}$	Postal and courier activities
$\mathcal{S}_{43}$	Printing and reproduction of recorded media
$\mathcal{S}_{44}$	Public administration and defence; compulsory social security
$\mathcal{S}_{45}$	Publishing activities
$\mathcal{S}_{46}$	Real estate activities
$\mathcal{S}_{47}$	Repair and installation of machinery and equipment
$\mathcal{S}_{48}$	Retail trade, except of motor vehicles and motorcycles
$\mathcal{S}_{49}$	Scientific research and development
$\mathcal{S}_{50}$	Sewerage; waste collection, treatment and disposal activities; materials recovery; remediation activities and other waste management services
$\mathcal{S}_{51}$	Telecommunications
$\mathcal{S}_{52}$	Warehousing and support activities for transportation
$\mathcal{S}_{53}$	Water collection, treatment and supply
$\mathcal{S}_{54}$	Water transport
$\mathcal{S}_{55}$	Wholesale and retail trade and repair of motor vehicles and motorcycles
$\mathcal{S}_{56}$	Wholesale trade, except of motor vehicles and motorcycles

Table 47: Density metrics of the matrix A (WIOD 2014)

Country	max $A_{i,j}(\Omega)$				$\#\left\{A_{i,j}(\Omega) \geq 10\%\right\}$			
	$\mathcal{D}_A(\mathcal{C})$	$\mathcal{O}_A(\mathcal{C})$	$\mathcal{R}_A(\mathcal{C})$	$\mathcal{C}_A(\mathcal{C})$	$\mathcal{D}_A(\mathcal{C})$	$\mathcal{O}_A(\mathcal{C})$	$\mathcal{R}_A(\mathcal{C})$	$\mathcal{C}_A(\mathcal{C})$
AUS	0.31	0.44	0.11	0.22	8	12	1	2
AUT	0.37	0.25	0.07	0.34	18	9	0	4
BEL	0.24	0.26	0.20	0.09	11	10	2	0
BGR	0.31	0.19	0.08	0.34	12	12	0	6
BRA	0.30	0.36	0.03	0.09	16	12	0	0
CAN	0.34	0.38	0.09	0.23	9	10	0	5
CHE	0.49	0.18	0.07	0.08	20	16	0	0
CHN	0.44	0.47	0.15	0.09	20	30	2	0
CYP	0.17	0.44	0.12	0.30	6	18	2	5
CZE	0.32	0.33	0.05	0.18	24	12	0	3
DEU	0.23	0.34	0.20	0.10	15	15	7	0
DNK	0.30	0.48	0.06	0.18	10	12	0	3
ESP	0.38	0.22	0.21	0.40	18	16	2	1
EST	0.25	0.25	0.09	0.09	9	14	0	0
FIN	0.28	0.29	0.08	0.13	12	12	0	1
FRA	0.38	0.33	0.08	0.22	17	6	0	1
GBR	0.37	0.29	0.14	0.14	18	9	2	2
GRC	0.20	0.39	0.09	0.44	4	32	0	1
HRV	0.25	0.33	0.02	0.14	7	28	0	2
HUN	0.21	0.38	0.04	0.27	8	7	0	3
IDN	0.46	0.38	0.07	0.09	9	20	0	0
IND	0.26	0.32	0.06	0.44	13	17	0	2
IRL	0.40	0.12	0.06	0.23	6	2	0	4
ITA	0.33	0.22	0.10	0.22	17	14	1	1
JPN	0.40	0.36	0.06	0.34	16	17	0	4
KOR	0.35	0.29	0.12	0.44	16	19	1	2
LTU	0.20	0.18	0.07	0.30	11	6	0	2
LUX	0.33	0.28	0.24	0.20	5	2	1	13
LVA	0.38	0.30	0.04	0.13	11	16	0	1
MEX	0.23	0.45	0.06	0.14	7	23	0	4
MLT	0.35	0.17	0.01	0.24	9	10	0	6
NLD	0.21	0.29	0.10	0.13	11	10	0	1
NOR	0.29	0.46	0.18	0.07	7	13	3	0
POL	0.26	0.35	0.08	0.19	15	9	0	1
PRT	0.49	0.21	0.01	0.51	20	15	0	2
ROU	0.18	0.21	0.03	0.26	3	9	0	2
RUS	0.23	0.18	0.30	0.07	9	15	9	0
SVK	0.38	0.39	0.04	0.23	15	13	0	3
SVN	0.31	0.21	0.03	0.11	13	7	0	1
SWE	0.18	0.24	0.06	0.15	9	11	0	2
TUR	0.46	0.29	0.15	0.12	12	10	1	1
TWN	0.40	0.28	0.03	0.36	19	24	0	4
USA	0.28	0.38	0.23	0.09	12	10	16	0
ROW	0.40	0.63	0.51	0.10	18	22	45	0
Total	0.49	0.63	0.51	0.51	544	602	95	95

Table 48: Density metrics of the matrix A (Exiobase 2014)

Country	$\max A_{i,j}(\Omega)$				$\#\left\{A_{i,j}(\Omega) \geq 10\%\right\}$			
	$\mathcal{D}_A(\mathcal{C})$	$\mathcal{O}_A(\mathcal{C})$	$\mathcal{R}_A(\mathcal{C})$	$\mathcal{C}_A(\mathcal{C})$	$\mathcal{D}_A(\mathcal{C})$	$\mathcal{O}_A(\mathcal{C})$	$\mathcal{R}_A(\mathcal{C})$	$\mathcal{C}_A(\mathcal{C})$
AUS	0.27	0.44	0.06	0.49	10	25	0	1
AUT	0.61	0.22	0.08	0.64	16	9	0	2
BEL	0.27	0.31	0.05	0.15	14	14	0	2
BGR	0.22	0.28	0.11	0.31	9	12	1	4
BRA	0.25	0.56	0.05	0.17	12	16	0	1
CAN	0.25	0.91	0.13	0.19	12	17	2	3
CHE	0.39	0.62	0.03	0.34	18	17	0	3
CHN	0.48	0.36	0.12	0.22	18	27	1	1
CYP	0.33	0.31	0.01	0.16	9	14	0	2
CZE	0.36	0.34	0.05	0.33	21	16	0	3
DEU	0.27	0.37	0.12	0.14	16	13	3	2
DNK	0.38	0.75	0.05	0.14	8	21	0	1
ESP	0.34	0.27	0.13	0.47	17	16	1	2
EST	0.37	0.40	0.02	0.18	15	14	0	5
FIN	0.27	0.32	0.04	0.42	13	12	0	1
FRA	0.34	0.40	0.09	0.42	14	12	0	2
GBR	0.37	0.35	0.15	0.19	13	13	3	2
GRC	0.31	0.33	0.10	0.58	10	19	0	4
HRV	0.45	0.28	0.01	0.29	6	9	0	2
HUN	0.21	0.41	0.07	0.39	5	10	0	4
IDN	0.29	0.49	0.04	0.11	10	19	0	3
IND	0.33	0.32	0.03	0.56	16	20	0	1
IRL	0.35	0.28	0.03	0.14	12	16	0	5
ITA	0.27	0.37	0.09	0.53	16	18	0	2
JPN	0.50	0.42	0.05	0.53	16	18	0	1
KOR	0.46	0.56	0.11	0.58	22	27	1	2
LTU	0.24	0.23	0.23	0.30	10	10	1	3
LUX	0.33	0.59	0.01	0.37	6	15	0	17
LVA	0.51	0.50	0.03	0.28	11	13	0	7
MEX	0.26	0.49	0.10	0.22	6	20	1	6
MLT	0.49	0.64	0.01	0.75	15	8	0	12
NLD	0.33	0.39	0.15	0.27	13	10	1	3
NOR	0.48	0.90	0.37	0.07	9	8	6	0
POL	0.32	0.29	0.06	0.46	14	10	0	1
PRT	0.43	0.27	0.01	0.49	16	14	0	3
ROU	0.34	0.32	0.04	0.42	11	11	0	1
RUS	0.31	0.99	0.56	0.14	14	14	30	1
SVK	0.39	0.36	0.03	0.56	14	11	0	1
SVN	0.34	0.17	0.03	0.05	12	9	0	0
SWE	0.20	0.27	0.03	0.30	5	15	0	4
TUR	0.42	0.45	0.09	0.17	11	22	0	1
TWN	0.57	0.36	0.02	0.45	22	21	0	4
USA	0.31	0.63	0.22	0.17	15	23	12	2
ROW	0.23	0.47	0.75	0.08	10	8	64	0
Total	0.61	0.99	0.75	0.75	562	666	127	127

Table 49: Density metrics of the matrix A (Exiobase 2022)

Country	$\max A_{i,j}(\Omega)$				$\#\left\{A_{i,j}(\Omega) \geq 10\%\right\}$			
	$\mathcal{D}_A(\mathcal{C})$	$\mathcal{O}_A(\mathcal{C})$	$\mathcal{R}_A(\mathcal{C})$	$\mathcal{C}_A(\mathcal{C})$	$\mathcal{D}_A(\mathcal{C})$	$\mathcal{O}_A(\mathcal{C})$	$\mathcal{R}_A(\mathcal{C})$	$\mathcal{C}_A(\mathcal{C})$
AUS	0.29	0.54	0.05	0.34	11	23	0	1
AUT	0.63	0.26	0.06	0.63	16	10	0	1
BEL	0.26	0.31	0.23	0.13	12	14	1	1
BGR	0.21	0.30	0.03	0.12	9	11	0	3
BRA	0.25	0.44	0.05	0.12	12	17	0	1
CAN	0.23	0.92	0.09	0.18	10	15	0	5
CHE	0.37	0.63	0.09	0.25	13	12	0	1
CHN	0.46	0.37	0.12	0.14	19	28	4	1
CYP	0.42	0.39	0.00	0.21	14	21	0	6
CZE	0.35	0.34	0.03	0.31	19	17	0	3
DEU	0.28	0.38	0.11	0.13	16	12	1	2
DNK	0.33	0.66	0.05	0.18	6	18	0	1
ESP	0.44	0.45	0.13	0.42	14	16	1	1
EST	0.31	0.43	0.05	0.15	11	15	0	1
FIN	0.29	0.36	0.03	0.35	15	11	0	1
FRA	0.38	0.40	0.09	0.48	14	11	0	3
GBR	0.32	0.30	0.17	0.18	14	13	4	3
GRC	0.29	0.30	0.03	0.53	11	19	0	2
HRV	0.48	0.28	0.02	0.32	6	16	0	1
HUN	0.21	0.38	0.06	0.18	6	9	0	4
IDN	0.31	0.54	0.02	0.13	9	21	0	2
IND	0.33	0.33	0.07	0.34	16	16	0	1
IRL	0.38	0.32	0.21	0.17	9	12	5	6
ITA	0.27	0.30	0.07	0.63	17	16	0	1
JPN	0.54	0.43	0.05	0.31	17	19	0	2
KOR	0.43	0.68	0.04	0.42	20	26	0	1
LTU	0.30	0.23	0.05	0.17	10	11	0	1
LUX	0.30	0.57	0.16	0.36	7	10	1	9
LVA	0.58	0.49	0.01	0.17	10	17	0	5
MEX	0.30	0.51	0.05	0.24	6	24	0	7
MLT	0.58	0.46	0.01	0.75	15	12	0	18
NLD	0.26	0.37	0.10	0.24	12	11	0	4
NOR	0.54	0.88	0.18	0.08	10	14	3	0
POL	0.41	0.27	0.03	0.26	12	9	0	2
PRT	0.42	0.29	0.02	0.40	15	13	0	2
ROU	0.22	0.42	0.02	0.33	11	10	0	2
RUS	0.43	0.99	0.35	0.14	16	18	12	1
SVK	0.36	0.28	0.03	0.29	12	14	0	2
SVN	0.28	0.17	0.05	0.08	12	9	0	0
SWE	0.19	0.29	0.04	0.21	4	16	0	4
TUR	0.41	0.35	0.05	0.10	9	21	0	0
TWN	0.47	0.33	0.01	0.28	22	23	0	4
USA	0.33	0.68	0.24	0.15	14	27	16	1
ROW	0.21	0.44	0.75	0.10	12	7	70	1
Total	0.63	0.99	0.75	0.75	545	684	118	118

Table 50: Decomposition of the direct + indirect carbon emissions (WIOD 2014)

Country	Direct		First-tier		Indirect		Total
	$MtCO_2e$	%	$MtCO_2e$	%	$MtCO_2e$	%	$MtCO_2e$
AUS	365	33.9	270	25.1	711	66.1	1 076
AUT	44	24.9	40	22.8	131	75.1	175
BEL	72	22.4	83	25.9	249	77.6	321
BGR	43	41.0	29	27.4	62	59.0	105
BRA	494	37.9	341	26.1	809	62.1	1 304
CAN	467	41.1	257	22.7	667	58.9	1 134
CHE	26	13.9	40	21.4	161	86.1	187
CHN	9 946	25.6	9 076	23.4	28 896	74.4	38 842
CYP	5	36.6	4	27.5	9	63.4	15
CZE	82	34.5	55	23.3	155	65.5	237
DEU	676	36.1	453	24.2	1 196	63.9	1 872
DNK	63	40.3	31	20.0	94	59.7	157
ESP	207	30.4	153	22.4	475	69.6	682
EST	19	43.9	11	26.5	24	56.1	42
FIN	45	29.9	38	25.5	105	70.1	150
FRA	230	28.7	169	21.0	574	71.3	804
GBR	364	33.7	243	22.6	714	66.3	1 078
GRC	64	44.1	36	24.8	82	55.9	146
HRV	13	40.0	8	23.5	20	60.0	33
HUN	35	31.5	26	23.3	75	68.5	110
IDN	470	40.9	295	25.7	678	59.1	1 148
IND	2 041	39.8	1 517	29.6	3 092	60.2	5 134
IRL	32	31.2	25	24.4	71	68.8	104
ITA	259	27.2	215	22.5	693	72.8	952
JPN	1 122	32.1	848	24.2	2 379	67.9	3 502
KOR	618	27.7	515	23.1	1 611	72.3	2 229
LTU	15	39.6	9	22.3	23	60.4	38
LUX	7	20.4	7	20.9	26	79.6	33
LVA	7	26.8	6	23.3	19	73.2	25
MEX	399	44.0	243	26.7	509	56.0	908
MLT	3	33.2	2	23.2	7	66.8	10
NLD	224	41.3	106	19.5	319	58.7	543
NOR	46	37.5	24	19.5	77	62.5	123
POL	270	39.1	185	26.7	421	60.9	691
PRT	41	32.6	29	22.7	85	67.4	126
ROU	66	35.1	48	25.4	122	64.9	187
RUS	1 525	41.2	1 088	29.4	2 175	58.8	3 700
SVK	28	31.7	18	20.0	61	68.3	90
SVN	11	33.1	9	24.9	23	66.9	35
SWE	42	25.7	37	22.6	122	74.3	164
TUR	271	32.5	221	26.5	564	67.5	834
TWN	294	29.3	243	24.2	711	70.7	1 006
USA	4 343	45.7	2 334	24.6	5 156	54.3	9 499
ROW	6 977	31.4	5 396	24.3	15 231	68.6	22 208
Total	32 377	31.8	24 781	24.4	69 385	68.2	101 762

Table 51: Decomposition of the direct + indirect carbon emissions (Exiobase 2014)

Country	Direct		First-tier		Indirect		Total
	$MtCO_2e$	%	$MtCO_2e$	%	$MtCO_2e$	%	$MtCO_2e$
AUS	635	44.5	366	25.7	791	55.5	1 426
AUT	72	29.3	61	24.8	173	70.7	245
BEL	89	26.1	87	25.6	252	73.9	340
BGR	51	40.3	40	32.3	75	59.7	126
BRA	1 065	43.5	723	29.5	1 386	56.5	2 451
CAN	651	43.0	397	26.2	864	57.0	1 514
CHE	37	17.7	51	24.8	171	82.3	207
CHN	11 462	25.7	11 160	25.1	33 088	74.3	44 550
CYP	12	51.8	6	24.2	11	48.2	23
CZE	111	31.8	93	26.6	238	68.2	349
DEU	814	38.3	557	26.2	1 313	61.7	2 127
DNK	63	28.4	58	26.2	160	71.6	223
ESP	272	33.1	221	26.9	549	66.9	821
EST	23	41.9	16	29.5	31	58.1	54
FIN	67	32.4	63	30.3	140	67.6	207
FRA	349	33.5	271	26.0	693	66.5	1 042
GBR	478	37.4	315	24.7	800	62.6	1 277
GRC	150	52.3	78	27.2	136	47.7	286
HRV	19	42.5	13	29.8	26	57.5	45
HUN	47	32.7	44	30.2	98	67.3	145
IDN	800	48.2	473	28.5	858	51.8	1 658
IND	2 895	44.9	1 833	28.5	3 548	55.1	6 443
IRL	65	39.9	41	25.2	98	60.1	163
ITA	331	27.7	343	28.7	865	72.3	1 196
JPN	1 239	31.8	1 080	27.7	2 659	68.2	3 899
KOR	615	24.8	653	26.3	1 868	75.2	2 484
LTU	19	39.1	17	33.8	30	60.9	49
LUX	9	19.5	11	23.7	37	80.5	46
LVA	14	35.9	10	27.3	24	64.1	38
MEX	558	44.9	334	26.8	686	55.1	1 244
MLT	3	22.7	3	25.6	10	77.3	13
NLD	185	31.2	187	31.7	407	68.8	592
NOR	79	42.8	43	22.9	106	57.2	186
POL	342	42.4	231	28.6	465	57.6	807
PRT	68	36.9	51	27.6	116	63.1	184
ROU	80	36.4	66	30.1	140	63.6	220
RUS	1 827	56.5	792	24.5	1 405	43.5	3 233
SVK	33	30.2	30	27.4	77	69.8	111
SVN	13	33.6	10	25.3	26	66.4	40
SWE	51	27.5	53	28.7	134	72.5	184
TUR	427	37.0	346	30.0	727	63.0	1 154
TWN	252	23.2	286	26.3	835	76.8	1 088
USA	4 933	46.4	2 966	27.9	5 688	53.6	10 621
ROW	9 436	48.8	5 044	26.1	9 898	51.2	19 334
Total	40 740	36.2	29 522	26.3	71 704	63.8	112 444

Table 52: Decomposition of the direct + indirect carbon emissions (Exiobase 2022)

Country	Direct		First-tier		Indirect		Total
	$MtCO_2e$	%	$MtCO_2e$	%	$MtCO_2e$	%	$MtCO_2e$
AUS	731	46.8	402	25.8	830	53.2	1 560
AUT	74	28.3	65	24.6	188	71.7	262
BEL	98	27.3	91	25.4	260	72.7	358
BGR	55	42.0	42	32.0	75	58.0	130
BRA	1 136	47.1	699	29.0	1 274	52.9	2 410
CAN	682	43.7	419	26.9	878	56.3	1 560
CHE	41	17.3	61	25.2	199	82.7	240
CHN	13 908	26.1	13 553	25.4	39 463	73.9	53 371
CYP	15	58.8	5	21.8	10	41.2	25
CZE	130	32.1	109	27.0	275	67.9	405
DEU	747	34.6	553	25.6	1 415	65.4	2 162
DNK	58	29.8	53	27.5	137	70.2	194
ESP	284	33.7	229	27.2	558	66.3	841
EST	229	40.0	201	35.0	344	60.0	573
FIN	67	31.4	63	29.4	147	68.6	214
FRA	361	33.8	276	25.8	708	66.2	1 069
GBR	411	37.5	270	24.6	685	62.5	1 097
GRC	157	54.2	75	25.8	132	45.8	289
HRV	22	42.9	16	30.7	29	57.1	51
HUN	61	35.2	48	27.8	113	64.8	174
IDN	1 145	47.6	730	30.3	1 261	52.4	2 406
IND	4 222	43.5	2 733	28.1	5 488	56.5	9 709
IRL	91	32.1	70	24.6	192	67.9	283
ITA	343	26.6	366	28.4	945	73.4	1 288
JPN	1 242	32.3	1 053	27.4	2 600	67.7	3 842
KOR	690	22.4	799	25.9	2 392	77.6	3 083
LTU	21	43.0	16	31.8	28	57.0	50
LUX	12	17.7	17	25.4	54	82.3	66
LVA	14	37.7	9	24.1	23	62.3	37
MEX	746	46.5	427	26.6	860	53.5	1 605
MLT	2	20.1	3	27.8	8	79.9	10
NLD	184	29.4	188	30.1	442	70.6	626
NOR	82	45.7	42	23.5	98	54.3	181
POL	395	41.4	266	27.9	559	58.6	954
PRT	89	39.8	61	27.1	135	60.2	224
ROU	87	35.2	77	30.9	161	64.8	248
RUS	2 334	56.3	1 051	25.3	1 813	43.7	4 147
SVK	38	31.7	32	27.2	81	68.3	118
SVN	16	34.5	13	27.5	30	65.5	46
SWE	53	27.8	52	27.0	139	72.2	192
TUR	547	44.2	345	27.8	691	55.8	1 238
TWN	302	24.7	309	25.4	918	75.3	1 220
USA	5 027	46.4	2 988	27.6	5 804	53.6	10 832
ROW	11 394	48.8	6 259	26.8	11 949	51.2	23 343
Total	48 343	36.4	35 134	26.5	84 391	63.6	132 734

Table 53: Estimated parameters of the multiplying coefficient ($k = 1$)

	Country		Sector	
	Cluster #1	Cluster #2	Cluster #1	Cluster #2
$\hat{\mu}_{\mathcal{C}_j}$ / $\hat{\mu}_{\mathcal{S}_k}$	−0.55	−0.49	0.48	1.76
$\hat{\sigma}_{\mathcal{C}_j}$ / $\hat{\sigma}_{\mathcal{S}_k}$	0.47	0.48	1.05	1.07

Table 54: Estimated Mean and standard deviation of the multiplying coefficient ($k = 1$)

		$\hat{\mu}_{(0-k)}$		$\hat{\sigma}_{(0-k)}$	
	Country	Cluster #1	Cluster #2	Cluster #1	Cluster #2
Sector	Cluster #1	2.81	2.94	3.02	3.23
	Cluster #2	7.48	7.93	10.83	11.57

Table 55: Estimated parameters of the multiplying coefficient ($k = \infty$)

	Country		Sector	
	Cluster #1	Cluster #2	Cluster #1	Cluster #2
$\hat{\mu}_{\mathcal{C}_j}$ / $\hat{\mu}_{\mathcal{S}_k}$	−0.17	−0.04	0.83	2.40
$\hat{\sigma}_{\mathcal{C}_j}$ / $\hat{\sigma}_{\mathcal{S}_k}$	0.67	0.69	1.11	1.09

Table 56: Estimated Mean and standard deviation of the multiplying coefficient ($k = \infty$)

		$\hat{\mu}_{(0-k)}$		$\hat{\sigma}_{(0-k)}$	
	Country	Cluster #1	Cluster #2	Cluster #1	Cluster #2
Sector	Cluster #1	5.53	6.14	9.52	10.80
	Cluster #2	22.75	25.66	45.73	51.85

Table 57: Direct + indirect carbon intensities of GICS sectors (MSCI World index, May 2023)

Sector	Exiobase 2022	Trucost 2021	WIOD 2014
Communication Services	66	78	102
Consumer Discretionary	168	209	219
Consumer Staples	437	387	277
Energy	1 373	796	757
Financials	83	55	83
Health Care	108	120	167
Industrials	276	277	307
Information Technology	110	138	131
Materials	791	973	747
Real Estate	128	134	138
Utilities	1 872	1 833	1 889
MSCI World	299	281	278

Table 58: Literature review on sector pass-through rates

Sector	Product	Estimate	Source
Aluminum	Aluminium	9 – 20%	McKinsey and Ecofys (2006); Vivid Economics (2014)
Agriculture	Malt	84 – 100%	Vivid Economics (2014)
Cement	Clinker	35 – 40%	De Bruyn *et al.* (2015); Cludius *et al.* (2020)
	Concrete	80%	Ganapati *et al.* (2020)
	Lime	73 – 96%	Vivid Economics (2014); Ganapati *et al.* (2020)
	Portland cement	73 – 100%	Demailly and Quirion (2006); Alexeeva-Talebi (2010); De Bruyn *et al.* (2015); Cludius *et al.* (2020)
	Total cement	20 – 40%	Ponssard and Walker (2008); De Bruyn *et al.* (2015); Cludius *et al.* (2020)
Ceramics	Bricks (heavy clay)	30 – 40%	Oberndorfer *et al.* (2010)
	Ceramic goods	92 – 100%	Oberndorfer *et al.* (2010); Vivid Economics (2014)
Chemicals	Ethylene	100%	Oberndorfer *et al.* (2010)
	Other basic inorganic chemicals	10%	Alexeeva-Talebi (2010)
	Perfumes and toilet preparations	0%	Alexeeva-Talebi (2010)
	Plastics in primary forms	42%	Alexeeva-Talebi (2010)
	Polyethylene (PE) and Polyvinylchloride (PVC)	32 – 100%	Alexeeva-Talebi (2010); De Bruyn *et al.* (2010a); Oberndorfer *et al.* (2010); Cludius *et al.* (2020)
	Polystyrene (PS)	33%	De Bruyn *et al.* (2010a)
	Propylene oxide	100%	De Bruyn *et al.* (2015)
	Dyes and pigments	37%	Alexeeva-Talebi (2010)
	Rubber	75%	Alexeeva-Talebi (2010)

Source: Sautel *et al.* (2022, pages 30-31) & Author's research.

Table 59: Literature review on sector pass-through rates

Sector	Product	Estimate	Source
Fertiliser	Ammonia and ammonium nitrate	16 – 100%	Alexeeva-Talebi (2010); Oberndorfer *et al.* (2010); Vivid Economics (2014); De Bruyn *et al.* (2015); Cludius *et al.* (2020)
	Nitrogen	15 – 100%	Alexeeva-Talebi (2010); Oberndorfer *et al.* (2010); Vivid Economics (2014); De Bruyn *et al.* (2015); Cludius *et al.* (2020)
Glass	Container glass	20 – 100%	Oberndorfer *et al.* (2010); Vivid Economics (2014); De Bruyn *et al.* (2015); Cludius *et al.* (2020)
	Glass fibres	27%	Alexeeva-Talebi (2010)
	Hollow glass and others	20 – 100%	Alexeeva-Talebi (2010); Oberndorfer *et al.* (2010); De Bruyn *et al.* (2015); Cludius *et al.* (2020)
Refineries	Diesel	40 – 350%	Oberndorfer *et al.* (2010); De Bruyn *et al.* (2010b, 2015); Cludius *et al.* (2020)
	Gasoil	36 – 100%	Oberndorfer *et al.* (2010); De Bruyn *et al.* (2015); Cludius *et al.* (2020); Ganapati *et al.* (2020)
	Petrol	50 – 500%	McKinsey and Ecofys (2006); De Bruyn *et al.* (2010a); Alexeeva-Talebi (2011); Oberndorfer *et al.* (2010); Cludius *et al.* (2020)
Power generation	Off-peak power	60 – 90%	Sijm *et al.* (2006)
	Peak power	64 – 117%	Sijm *et al.* (2006)
Pulp and paper	Boxes and plywood	89 – 142%	Vivid Economics (2014); Ganapati *et al.* (2020)
	Household and toilet paper	38 – 86%	Alexeeva-Talebi (2010); Vivid Economics (2014)
	Printing	78 – 94%	Vivid Economics (2014)
Steel	Basic oxygen furnace	6%	McKinsey and Ecofys (2006)
	Electric air furnace	66%	McKinsey and Ecofys (2006)
	Flat steel	55 – 120%	De Bruyn *et al.* (2010b, 2015); Cludius *et al.* (2020)
	Long steel	66 – 81%	McKinsey and Ecofys (2006); Vivid Economics (2014)

Source: Sautel *et al.* (2022, pages 30-31) & Author's research.

Table 60: Classification of sectors into pass-through types

No.	Type	Sector
1	highly-elastic	Air transport ($\mathcal{S}_7$); Crop and animal production, hunting and related service activities ($\mathcal{S}_{11}$); Manufacture of chemicals and chemical products ($\mathcal{S}_{23}$); Manufacture of other non-metallic mineral products ($\mathcal{S}_{32}$); Manufacture of paper and paper products ($\mathcal{S}_{34}$); Water transport ($\mathcal{S}_{54}$)
2	high-elastic	Accommodation and food service activities ($\mathcal{S}_1$); Manufacture of basic pharmaceutical products and pharmaceutical preparations ($\mathcal{S}_{22}$); Manufacture of food products, beverages and tobacco products ($\mathcal{S}_{28}$); Manufacture of furniture; other manufacturing ($\mathcal{S}_{29}$); Manufacture of textiles, wearing apparel and leather products ($\mathcal{S}_{36}$); Retail trade, except of motor vehicles and motorcycles ($\mathcal{S}_{48}$)
3	medium-elastic	Activities auxiliary to financial services and insurance activities ($\mathcal{S}_2$); Administrative and support service activities ($\mathcal{S}_5$); Advertising and market research ($\mathcal{S}_6$); Architectural and engineering activities; technical testing and analysis ($\mathcal{S}_8$); Computer programming, consultancy and related activities; information service activities ($\mathcal{S}_9$); Construction ($\mathcal{S}_{10}$); Financial service activities, except insurance and pension funding ($\mathcal{S}_{14}$); Forestry and logging ($\mathcal{S}_{16}$); Legal and accounting activities; activities of head offices; management consultancy activities ($\mathcal{S}_{20}$); Manufacture of computer, electronic and optical products ($\mathcal{S}_{25}$); Manufacture of electrical equipment ($\mathcal{S}_{26}$); Manufacture of fabricated metal products, except machinery and equipment ($\mathcal{S}_{27}$); Manufacture of machinery and equipment n.e.c. ($\mathcal{S}_{30}$); Manufacture of motor vehicles, trailers and semi-trailers ($\mathcal{S}_{31}$); Manufacture of other transport equipment ($\mathcal{S}_{33}$); Manufacture of rubber and plastic products ($\mathcal{S}_{35}$); Manufacture of wood and of products of wood and cork, except furniture; manufacture of articles of straw and plaiting materials ($\mathcal{S}_{37}$); Motion picture, video and television programme production, sound recording and music publishing activities; programming and broadcasting activities ($\mathcal{S}_{39}$); Other professional, scientific and technical activities; veterinary activities ($\mathcal{S}_{40}$); Postal and courier activities ($\mathcal{S}_{42}$); Printing and reproduction of recorded media ($\mathcal{S}_{43}$); Publishing activities ($\mathcal{S}_{45}$); Repair and installation of machinery and equipment ($\mathcal{S}_{47}$); Scientific research and development ($\mathcal{S}_{49}$); Telecommunications ($\mathcal{S}_{51}$); Warehousing and support activities for transportation ($\mathcal{S}_{52}$); Water collection, treatment and supply ($\mathcal{S}_{53}$); Wholesale trade, except of motor vehicles and motorcycles ($\mathcal{S}_{56}$)
4	low-elastic	Activities of extraterritorial organizations and bodies ($\mathcal{S}_3$); Activities of households as employers; undifferentiated goods- and services-producing activities of households for own use ($\mathcal{S}_4$); Education ($\mathcal{S}_{12}$); Electricity, gas, steam and air conditioning supply ($\mathcal{S}_{13}$); Fishing and aquaculture ($\mathcal{S}_{15}$); Human health and social work activities ($\mathcal{S}_{17}$); Insurance, reinsurance and pension funding, except compulsory social security ($\mathcal{S}_{18}$); Land transport and transport via pipelines ($\mathcal{S}_{19}$); Manufacture of basic metals ($\mathcal{S}_{21}$); Manufacture of coke and refined petroleum products ($\mathcal{S}_{24}$); Mining and quarrying ($\mathcal{S}_{38}$); Other service activities ($\mathcal{S}_{41}$); Public administration and defence; compulsory social security ($\mathcal{S}_{44}$); Real estate activities ($\mathcal{S}_{46}$); Sewerage; waste collection, treatment and disposal activities; materials recovery; remediation activities and other waste management services ($\mathcal{S}_{50}$); Wholesale and retail trade and repair of motor vehicles and motorcycles ($\mathcal{S}_{55}$)

Table 61: Sector allocation in % of the market portfolio (global uniform taxation, Exiobase 2022, MSCI World, May 2023)

Sector	w_i^-	$\phi = 0\%$		$\phi = 100\%$	
		$\tau = 100$	$\tau = 500$	$\tau = 100$	$\tau = 500$
Communication Services	7.3	7.68	8.3	6.89	5.6
Consumer Discretionary	10.7	11.09	11.6	10.04	8.1
Consumer Staples	7.3	7.58	7.8	6.99	6.0
Energy	4.6	3.94	1.4	6.94	13.8
Financials	12.7	13.12	13.5	11.89	9.5
Health Care	13.2	13.76	14.7	12.68	11.3
Industrials	10.4	10.35	10.1	10.09	9.3
Information Technology	24.4	25.53	27.4	22.87	18.4
Materials	4.1	3.35	2.0	4.76	6.8
Real Estate	2.4	2.48	2.6	2.24	1.8
Utilities	2.9	1.11	0.6	4.60	9.4

Amundi Institute
ASSET MANAGEMENT

Working Paper
July 2023

Important Information

Date of first use: 03 July 2023.

Document issued by Amundi Asset Management, "société par actions simplifiée"- SAS with a capital of €1,143,615,555 - Portfolio manager regulated by the AMF under number GP04000036 – Head office: 91-93 boulevard Pasteur – 75015 Paris – France – 437 574 452 RCS Paris – www.amundi.com

Photo credit: iStock by Getty Images - monsitj